



Norwegian University of
Science and Technology

Development, Building and Competing with a New Car in Shell Eco-marathon

Bård Dagestad Carlsen
Odin Jul Oma

Master of Science in Mechanical Engineering

Submission date: June 2017

Supervisor: Knut Einar Aasland, MTP

Norwegian University of Science and Technology
Department of Mechanical and Industrial Engineering

Preface

This report presents the work done by a team of two master students at department of mechanical and industrial engineering and 23 other volunteers, who developed and built a new car for the Shell Eco-marathon competition held in London May 25-28th 2017. The work began in September 2016. This report mainly presents the development and production of the vehicle from January to May 2017. The initial development of the vehicle can be found the project thesis of Carlsen and Oma (2016). This report focuses mainly on the mechanical aspects of the vehicle's development, as it is the field of study of the authors. It has been written with future teams in mind.

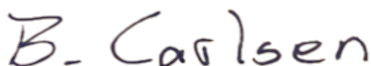
We want to thank our supervisor Knut Aasland and the institute for the opportunity to do this kind of a master project. It has significantly boosted our knowledge of engineering development processes and practical know-how of production processes. The project would also not have been possible without the funding from sponsors, which we would like to thank. Our highest gratitude goes to our main sponsor DNV GL and Kristina Dahlberg.

We also want to thank the staff at the institute for their guidance and contribution throughout this project. We would in particular express gratitude to:

Natalia Trotsenko, Cecilia Haskins, Per-Erik Heksem, Børge Holen, Emil Kulbotten, Roar Munkebye and Eyvinn Høvring Mikkelsen.

Trondheim, June 2017

Bård Dagestad Carlsen, Product Development and Materials Engineering



Odin Jul Oma, Product Development and Materials Engineering



Abstract

This Master's thesis is the continuation of the project thesis by Carlsen and Oma (2016). It describes the work that has been done in order to participate with a new car in Shell Eco-marathon in May of 2017.

A new UrbanConcept vehicle has been developed with the goal of a top 3 place in the Battery Electric category. The vehicle was made as a base for later teams to improve, and the thesis includes advises for next year. The thesis describes the development and production of the major mechanical subsystems of the car. Among the achievement are:

- A chassis built in carbon fibre reinforced polymer weighing 35 kg, and with a theoretical drag coefficient of 0.14.
- Lightweight aluminium suspensions produced by CNC-milling, with air shock absorbers on all wheels.

It also contains non-technical aspects of the project, such as project management. Unfortunately, the ambitions of the team proved to be too high and the vehicle ended up without a valid result in the competition.

Sammendrag

Denne masteroppgaven bygger videre på prosjektoppgaven skrevet av Carlsen og Oma (2016). Den beskriver arbeidet som er blitt gjort for å kunne delta med en ny bil i Shell Eco-marathon i mai 2017.

En ny UrbanConcept bil har blitt utviklet med mål om en topp 3 plassering i kategorien Battery Electric. Bilen er laget som et utgangspunkt for senere team å forbedre, og avhandlingen inneholder råd til neste år. Avhandlingen beskriver utviklingen og produksjonen av de viktigste mekaniske delsystemene til bilen. Noen resultater er:

- Chassis produsert i karbonfiberforsterket polymer som veier 35 kg og har en teoretisk dragkoeffisient på 0,14.
- Lette hjuloppheng av aluminium produsert med CNC-fresing, og med luftdempere på alle hjul.

Den inneholder også ikke-tekniske aspekter av prosjektet, som prosjektledelse. Dessverre viste det seg at teamet hadde for høye ambisjoner, og bilen endte uten et gyldig resultat i konkurransen.

Problem description

Development, Building and Competing with a New Car in Shell Eco-marathon

Based on the candidates' work in the project paper, a new car is to be developed and built to compete in the 2017 edition of Shell Eco-marathon.

The project consists of:

- Complete development of all components of the car, such that it is ready to be built.
- Build the car.
- Testing of sub-components and the entire car.
- Organizing the participation of the competition in London.
- Compete in London.
- Summarize the results, knowledge gained and what to improve for the next year's competition.

During the project, work must be done to sustain good relations with sponsors, both main sponsor DNV GL and smaller sponsors which we are dependent of regarding funds, production assistance and acquiring necessary materials.

Our contact person at DNV GL is Kristina Dahlberg.

Table of Contents

1	Introduction	11
1.1	DNV GL Fuel Fighter 2017.....	11
1.2	About Shell Eco-marathon 2017	12
1.3	The team	14
1.3.1	Recruitment.....	14
1.3.2	Team structure	15
1.3.3	Advises for later teams	16
1.4	Scope	16
1.5	Sponsors	17
2	Product requirements.....	18
3	Chassis	22
3.1	Aerodynamic design.....	22
3.2	Monocoque	24
3.2.1	Deciding CFRP layup with FEM software	24
3.3	Mesh	26
3.4	Properties of the CFRP fabric.....	27
3.5	Initial analysis.....	28
3.5.1	Buckling analysis.....	31
3.6	Selection of core material	32
3.7	Final layup.....	33
3.8	Mould	35
3.9	Mould production	35
4	Monocoque production	39
4.1	Process.....	39
4.2	Door.....	42
4.3	Upper body	43
4.4	Motor compartment cover	45
4.5	Bulkhead.....	46
4.6	Lower body.....	48
4.7	Production diary	51
5	Monocoque assembly.....	52

6	Steering	56
6.1	Choosing steering system.....	56
6.2	King pin steering mechanism.....	58
6.3	Rack-and-pinion steering optimization.....	59
6.3.1	Rack-and-pinion geometry.....	59
6.4	Further optimizing.....	62
7	Front suspension	67
7.1	Parameters of driving performance.....	67
7.2	Front suspension systems.....	69
7.3	Choosing front suspension system.....	71
7.4	Design for production.....	73
8	Rear suspension	77
9	Powertrain	81
9.1	Powertrain jig.....	81
9.2	Drivetrain.....	82
9.3	Production of pulleys for the belt drive.....	84
9.4	Motors.....	86
9.5	Selection of gear ratio.....	89
10	Windows	90
10.1	Production method.....	91
10.2	Moulds.....	93
10.3	Production.....	94
10.4	Result.....	97
11	Interior	98
11.1	Steering wheel.....	98
11.2	Control panel.....	102
11.3	Seat.....	102
11.4	Other interior.....	103
12	Other subsystems	105
12.1	Door mechanism.....	105
12.2	Compartment cover.....	105
12.3	Head and rear lights.....	106

12.4	Electronics.....	106
13	Conclusion	107
13.1	SEM Summarized	107
13.1.1	Arrival and technical inspection	107
13.1.2	Competition day 1	107
13.1.3	Competition day 2	108
13.2	Travel advises.....	109
13.3	Project management	109
13.4	Vehicle improvements.....	110
13.5	Final remarks.....	112
14	References	113
15	Appendix	114
15.1	Appendix A: Steering optimization.....	114
15.1.1	Racket error optimization	114
15.1.2	Racket error plotting	117
15.1.3	Ideal turning angles	118
15.2	Appendix B: Motor efficiency plots.....	119
15.3	Appendix C: Motor datasheets.....	123
15.3.1	Maxon RE50.....	123
15.3.2	Maxon RE65.....	124
15.3.3	BMS documentation	125
15.3.4	Motor controller documentation.....	130
15.4	Appendix D: Off-track award applications	136
15.4.1	Design award application	136
15.4.2	Design award application	143
15.5	Appendix E: Project paper	155

List of figures

Figure 1: DNV GL Fuel Fighter at SEM 2017.....	11
Figure 2: Left: A selection of vehicles at SEM 2017. Right: Participants as SEM 2017 ...	12
Figure 3: Upper row: Prototype vehicles. Bottom row: UrbanConcept vehicles	13
Figure 4: Track of 2017	13
Figure 5: The team at the revealing of the car	14
Figure 6: CAD model of final design	22
Figure 7: Monocoque model in Abaqus	24
Figure 8: Using beam elements to represent the suspension	24
Figure 9: Meshed monocoque	26
Figure 10: Sandwich structure:.....	28
Figure 11: Deformations under load case max.	30
Figure 12: Composite failure with Tsai Wui criterion.....	31
Figure 13: Risk of buckling in lower door corner	32
Figure 14: locations of areas reinforced with additional 0/90 plies.....	33
Figure 15: Arrangement of core material	34
Figure 16: Modified wheel wells.....	35
Figure 17: CAD-geometry used CNC mill the upper body mould.....	36
Figure 18: CAD-geometry used to CNC mill the lower body mould.....	36
Figure 19: CAD-geometry used to CNC-mill the door mould	37
Figure 20: Production of moulds at Eker design. Epoxy paste is used to give the moulds a hard surface	38
Figure 21: Vacuum infusion process	39
Figure 22: Consumables	41
Figure 23: Left: Carbon fibre lay-up. Right: Door out of mould.....	42
Figure 24: Infusion of door.....	42
Figure 25: Coated top mould	43
Figure 26: Left: Core material. Right: Peel ply and flow mesh.....	44
Figure 27: Placement of inlet and outlets	44
Figure 28: Process of cover production	45
Figure 29: Left: Inserts in core material. Right: Covered with peel ply	46
Figure 30: Layers in bulkhead production.....	47
Figure 31: Bulkhead infusion	47
Figure 32: Lower mould.....	48
Figure 33: Inlet and outlets in bottom mould	48
Figure 34: Core material in lower body.....	49
Figure 35: Voids that gather resin	50
Figure 36: Left: Dry spot on wheel arch. Top right: Dry spot on right side. Bottom right: Accumulation of resin in the edge	50
Figure 37: Left: Remains of mould on body. Right: Applying resin to dry spot.....	52
Figure 38: Grinding excess resin and trimming body	53

Figure 39:Joining of body.....	54
Figure 40:Grinding flanges off and plastering joint line	54
Figure 41: Clockwise from upper left: Bulkhead template, rough cut, fine grinding, bulkhead in lower body	55
Figure 42: True rolling conditions.....	56
Figure 43: Ackerman geometry	57
Figure 44: Centre pivoted steering	57
Figure 45: Rack-and-pinion steering system	59
Figure 46: Rack-and-pinion geometry. Initial zero toe condition	59
Figure 47: Rack-and-pinion geometry. Inner wheel angle	60
Figure 48: Rack-and-pinion geometry. Outer wheel angle.....	61
Figure 49:Tie-rod at an angle	61
Figure 50: Calculated mean of racket error through the London track of 2017	62
Figure 51: Required racket to meet turning radius requirement of 6 m.....	63
Figure 52: Mean racket error, where configurations exceeding the max travel of the racket are removed	63
Figure 53: Detailed contour plot of the mean racket error	64
Figure 54: Obtain relation of inner and outer wheel angle, racket offset 120mm	65
Figure 55: Outer wheel angle error (difference from ideal angle). Fixed Racket offset: 120mm.....	65
Figure 56: Camber angle	67
Figure 57: Kingpin inclination	67
Figure 58: Caster angle.....	68
Figure 59: Toe in/out	68
Figure 60: 4 common front suspension systems (Longhurst, 2017), (Simionesci,2008) ...	69
Figure 61: Fox Float R air shock absorber	71
Figure 62: Early designs	73
Figure 63: FEM-model. Support and forces on front suspension.....	74
Figure 64: Von Mises Plot - front suspension	75
Figure 65: Deformation plot - front suspension	75
Figure 66: Final design of the wishbones and the steering knuckle	76
Figure 67: Front suspension with all parts (wishbones, steering knuckle, steering arm, wheel hub, brake disc, brake calliper, shock absorber).....	76
Figure 68: Top row: Early version - Bottom row: Final version	77
Figure 69: Top row: 3D-print, Motor mount and Bulkhead mount. Bottom row: Milled rear suspension.....	78
Figure 70: FEM-model. Support and forces on rear suspension	79
Figure 71: Von Mises Plot - rear suspension.....	80
Figure 72: Deformation plot - rear suspension	80
Figure 73: Powertrain jig, front view	81
Figure 74: Powertrain jig, back view.....	82
Figure 75: Drivetrain alternatives.....	83
Figure 76: Nylon pulleys	85

Figure 77: Pulley rims	86
Figure 78: Maxon brushed DC motor.....	86
Figure 79: Efficiency plot of Maxon RE50	88
Figure 80: Efficiency plot of Maxon RE65	89
Figure 81: Drape forming	91
Figure 82: Vacuum forming	91
Figure 83: Bubble forming	92
Figure 84: Pressure forming	92
Figure 85: CAD models of window moulds.....	93
Figure 86: Window moulds	94
Figure 87: Bubbles in the Lexan.....	94
Figure 88: Left: Broken vacuum box. Right: Oven.....	95
Figure 89: Forming of left side window	95
Figure 90: Front window forming	96
Figure 91: Motor compartment window.....	96
Figure 92: Rear light windows	97
Figure 93: Window flanges	97
Figure 94: Early prototypes. Ruler acts as levers.	98
Figure 95: Larger radius on the inside of the left (for us) than right grip.....	99
Figure 96: Production of steering wheel.....	100
Figure 97: Finished steering wheel.....	101
Figure 98: Control panel.....	102
Figure 99: Seat.....	102
Figure 100: Luggage holder	103
Figure 101: Interior.....	104
Figure 102: Motor compartment cover mechanism.....	105
Figure 103: Weight of vehicle components.....	111
Figure 104: Laminar vs turbulent flow.....	111

List of tables

Table 1: SEM off-track awards.....	14
Table 2: Team members	15
Table 3: Sponsors	17
Table 4: Monocoque requirements	18
Table 5: Front suspension requirements	19
Table 6: Rear suspension requirements	19
Table 7: Motor requirements	20
Table 8: Window requirements	20
Table 9: Steering wheel requirements	21
Table 10: Loads for FEM-simulation	25
Table 11: Element composition of the mesh	26
Table 12: CFRP composite properties.....	27
Table 13: Diab Divinycell® core material properties	32
Table 14: CFRP Layup for the monocoque.....	33
Table 15: Variables in rack-and-pinion model	60
Table 16: Rack-and-pinion parameters.....	62
Table 17: Improved rack-and-pinion parameters	64
Table 18: Suspension systems	70
Table 19: Suspension variables	71
Table 20: Gear comparison.....	84

1 Introduction



Figure 1: DNV GL Fuel Fighter at SEM 2017

1.1 DNV GL Fuel Fighter 2017

The DNV GL Fuel Fighter 2017 project started in August 2016 with the students who should write their project paper about it. After a new team had been recruited it was decided that a new battery powered car should be built. This thesis summarizes the project of developing and building a new car, and competing with it in the Shell Eco-marathon (SEM). The technical chapters are mainly about the mechanical work, as it is the field of the authors. During development of the car, we have considered different solutions to most aspects of our car. To avoid making the thesis too comprehensive, the alternative solutions for several areas of the car are not presented.

1.2 About Shell Eco-marathon 2017



Figure 2: Left: A selection of vehicles at SEM 2017. Right: Participants at SEM 2017

Shell Eco-marathon is a unique competition that challenges students around the world to design, build and drive the most energy-efficient car. With three annual events in Asia, Americas and Europe, student teams take to the track to see who goes further on the least amount of fuel. (Shell, 2016a)

Shell Eco-marathon was arranged for the first time in 1939. The European version started in 1985 and has been held every year since. The European version of SEM 2017 was held in Queen Elizabeth Park, London, UK on May 25-28th. 171 teams from 29 different countries participated. The Norwegian University of Science and Technology (NTNU) has been represented by a team in the competition every year since 2008. SEM is split into two vehicle classes;

- Prototype, which focuses on maximum efficiency
- UrbanConcept, which encourages a more practical design.

A selection of vehicles can be seen in Figure 3. The UrbanConcept vehicles are meant to inspire people into choosing a greener car in their personal life. They are therefore larger than the prototypes and have additional regulations, e.g. the need for a window wiper and luggage room. The SEM rulebook states the regulations the vehicles must adhere to.

In the two classes, the vehicles are again split into three separate energy categories.

1. Internal combustion
2. Hydrogen
3. Battery Electric

The internal combustion engines are allowed to run on gasoline, diesel, ethanol, GtL or CNG (methane). They are ranked by calculating the fuel used into the equivalent consumption of gasoline. In the Battery Electric category, the batteries must be Lithium-based.

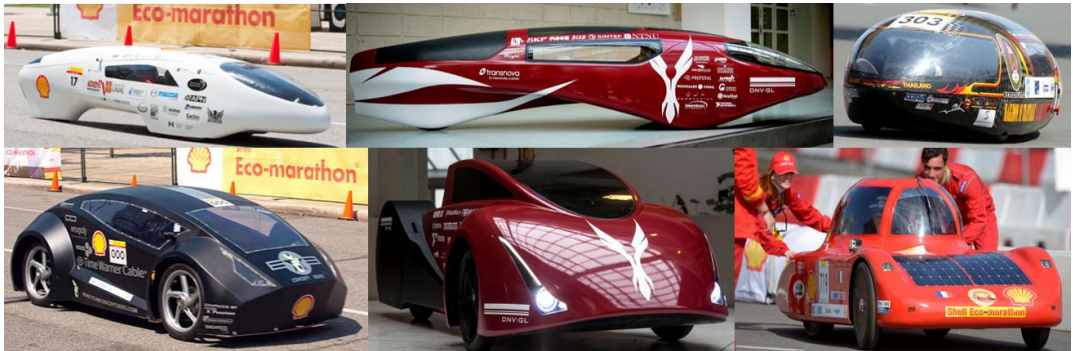


Figure 3: Upper row: Prototype vehicles. Bottom row: UrbanConcept vehicles

The challenge is to complete 10 laps on a 1.659m track within 39 minutes, which gives an avg. speed of approximate 25 km/h. The track includes a hill, and the UrbanConcept vehicles must make a full stop each lap.



Figure 4: Track of 2017

Off-track prizes are also awarded at SEM. They are the Communications Award, Vehicle Design Award Prototype, Vehicle Design Award UrbanConcept, Technical Innovation Award, Safety Award, and Perseverance and Spirit of the event Award.

Table 1: SEM off-track awards

SHELL ECO-MARATHON OFF-TRACK AWARD	ASIA/AMERICAS	EUROPE
Communications Award	\$3,000	€2,500
Vehicle Design Award Prototype	\$3,000	€2,500
Vehicle Design Award UrbanConcept	\$3,000	€2,500
Technical Innovation Award	\$3,000	€2,500
Safety Award	\$3,000	€2,500
Perseverance and Spirit of the event Award	\$3,000	€2,500

1.3 The team

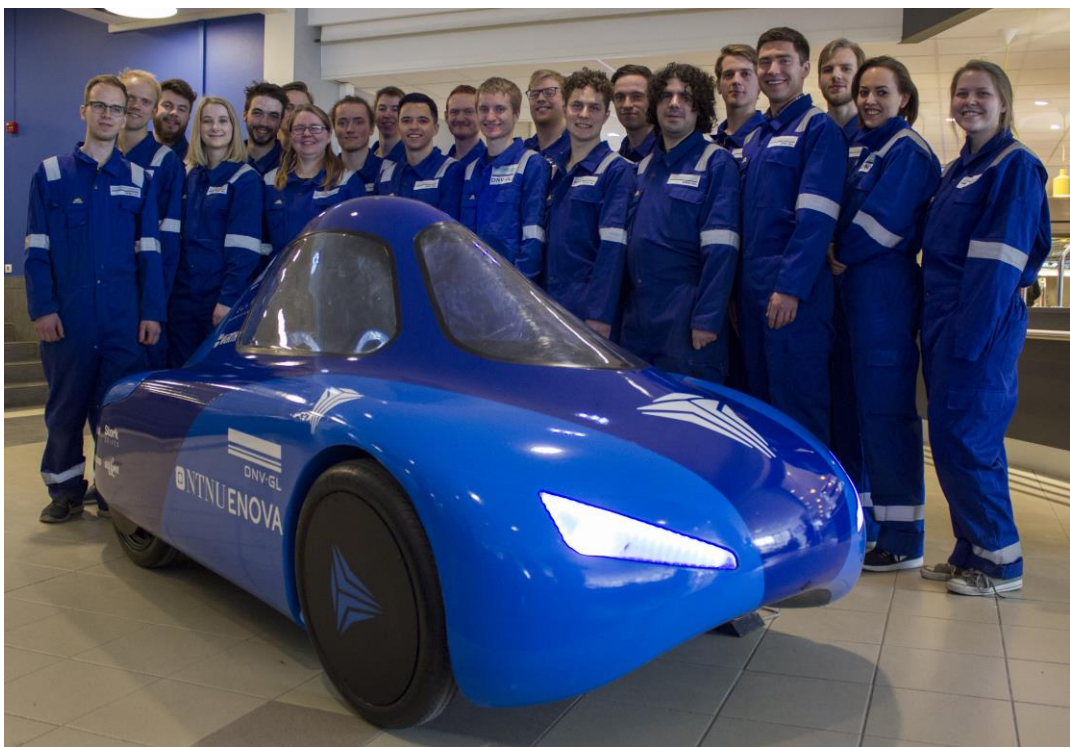


Figure 5: The team at the revealing of the car

1.3.1 Recruitment

The team is new this year and consists of 25 people. The two in management are writing their Master's thesis about the project while the rest are volunteers. The members were interviewed and chosen by the management. We had a recruitment period in early September. After selecting the wanted persons, the team counted 18 people in the first semester. More about the recruitment process can be read in Appendix E: Project paper. After the first semester, we identified areas we wanted to recruit to, and new members were recruited in January. There was also one exchange student who left at Christmas.

1.3.2 Team structure

Table 2: Team members

MANAGEMENT	
Bård Dagestad Carlsen <i>Project manager</i>	Odin Jul Oma <i>Technical Manager</i>
SUPPORT	
Anne-Maren Karlberg <i>PR & Reserve Driver</i>	Renate Molvik <i>PR</i>
Serya Raisi* <i>Logistics</i>	Brage Halvorsen** <i>Systems Engineering</i>
MECHANICAL	
Kjell Sverre Høvik Bergum <i>Mechanical Team Leader</i>	Sivert Rød Hatletveit <i>Driver</i>
Espen Halvorsen Verpe	Espen Braastad
Josefine Caroline Stokke Haugom	Thomas Hybertsen
Mirko Indumi	Håvard Vestad*
Veronika Næss*	Kjetil Vasstein*
ELECTRICAL	
Jørgen Jackwitz <i>Electrical Team Leader</i>	
Kristoffer Rakstad Solberg	Marius Strand Ødven
Ole Sivert Otterholm	Ola Lium
Jan Fijalkowski	Sondre Ninive Andersen*
Vlad Tamas*	Amund Marton*

*Recruited in January 2017.

**Recruited in February 2017.

The team members are from the following studies:

- Mechanical Engineering
- Industrial Cybernetics
- Marine Technology
- Cybernetics and Robotics
- Computer Science
- Creative Marketing Communication
- Media Com. And Information Technology
- Petroleum Geosciences and Engineering

A large proportion is from mechanical engineering.

1.3.3 Advises for later teams

There should be a deputy project manager who can aid the project manager. Tasks may include organizing regular team meetings, be responsible for recruitment, arrange social event, and management tasks. We focused more on recruiting people from cybernetics and were unsuccessful in recruiting people from electrical engineering. There should also be members from this study. We recruited the systems engineer too late. This role should be filled from the start. Associate Professor Cecilia Haskins can help with this. One thing to have in mind when recruiting is the mix of members at different years in their study. It is common to study abroad in the 4th year, which results in few applicants from this year and 3rd graders being less likely to continue in the team. 4th grades are also less likely to continue as they want to focus on their Master's thesis in their 5th year. Some 1st and/or 2nd graders should be recruited to have a continuity in the project over the years.

1.4 Scope

The 2017 project wanted a stronger focus on the objective of SEM, energy efficiency, than the previous DNV GL Fuel Fighter car had. The 2017 project was about developing and building a new car to compete in the Battery Electric category of the UrbanConcept class. We were aware that building a new car and changing energy category was an ambitious task and a major challenge, but we felt that they were decisions that had to be made. The key decisions about the project were made in the autumn and the reasoning can be read in the project paper. The vision and mission of the project were defined as follows:

VISION

To focus on innovation towards a sustainable future – To learn, improve and challenge how we perceive today's transportation possibilities.

MISSION

To develop and build an ultra-energy-efficient car and demonstrate its performance in the Shell Eco-marathon.

The car is built to serve as a base for later teams to optimize for a winning chance. This year we had the ambition of top 3 in our category. In addition to energy-efficiency competition, we wanted to compete for the off-track awards. A team is allowed to apply for two of the off-track awards, and we chose the Communications Award and the Design Award. Solid financial management was also in our scope, as it is important to stick to the budget.

1.5 Sponsors

Table 3: Sponsors

SPONSOR	CONTRIBUTION
DNV GL	The main sponsor of the project. Financial contribution of NOK 400 000. Also provided ambassador for the car and media coverage. Held the DNV GL Technology Qualification course for the team in November.
NTNU	Staff support. Provided an office, a workshop and computers. Produced several components. The principal's office also contributed financially.
Enova	Financial
Eker Design	Reduced price on milling of vehicle moulds.
High Performance Composites	Let us their facilities for free to produce the monocoque parts. Staff support. Materials at cost.
Würth	Tool wagon incl. tools.
Elefun	50 % off batteries and other electrical components.
Speedoptions	Discount on brake components.
Stork Drives	Discount on motors.
Skilt & print	Discount on wrapping of car, roll-up and stickers.
Diab	Core material
Trondheim Stål AS	Helped manufacturing the pulleys in the powertrain, using their water jet machine.
VINK AS	Provided us with nylon plates for the powertrain.

2 Product requirements

These tables of product requirements presented below does not cover all the requirements for the vehicle. A complete list of requirements would be too comprehensive. We have focused on the requirements of the parts that are discussed in the thesis, as they are the most relevant. Many of the must-haves are stipulated by the Shell rulebook. The Shell rulebook and practical considerations can be seen as the requirements for the areas of the car not presented below.

Table 4: Monocoque requirements

Monocoque

		Must	Should
1	Production requirements		
1.1	Number of parts/moulds	<20	<10
1.2	Manufacturing time parts		<40 hours
1.3	Assembly time		<30 hours
1.4	Maximum total cost	<300 000 NOK	<200 000 NOK
2	Functional requirements		
2.1	Max displacement	5 mm	
2.2	Coefficient of drag	<0.30	<0.15
2.3	Field of view at driver position	180 degrees	
2.4	Wheel size fitting in wheel well	17 inches	
2.5	Wheel well depth	<300 mm	
2.6	Load on wheel wells	1000 N	1500 N
2.7	Load on roof	700 N	1000 N
2.8	Fatigue life under load	>100 hours	>1000 hours
3	Physical properties		
3.1	Height	>1000 mm	1020 mm
3.2	Width	1200-1300 mm	1220 mm
3.3	Weight	<40 kg	<25 kg
3.4	Length	2200-3500 mm	
3.5	Fixed roof	X	
3.6	Door size (vertical plane)	>800x500 mm	805x505 mm
4	Requirements from surroundings		
4.1	Operational temperatures	0-50 °C	
4.2	Waterproof	IP44	

Table 5: Front suspension requirements

Front suspension

		Must	Should
5	Production requirements		
5.1	Can be CNC-milled from 50 mm aluminium plate	X	
5.2	Single fixture milling (one side milling)		X
5.3	Maximum total cost	<30 000 NOK	<10 000 NOK
6	Functional requirements		
6.1	Camber angle	>0°	1.5-2°
6.2	Minimum wheel turning	<15°	>16°
6.3	Adjustable ground clearance	>100 mm	100-130 mm
6.4	Shock absorber allowed displacement	>30 mm	>40 mm
6.5	Scrub radius		5-20 mm
6.6	King pin inclination		2-4°
6.7	Fatigue life under load	>100 hours	>1000 hours
6.8	Corrosion resistance in humid environment	>100 hours	>1000 hours

Table 6: Rear suspension requirements

Rear suspension

		Must	Should
7	Production requirements		
7.1	Made from 30 mm aluminium plates	X	
7.2	Single fixture milling (one side milling)		X
7.3	Maximum cost	<30 000 NOK	<10 000 NOK
8	Functional requirements		
8.1	Adjustable ground clearance	>100mm	100-130mm
8.2	Adjustable belt tensioning		X
8.3	Shock absorber allowed displacement	>30mm	>40mm
8.4	Fatigue life under load	>100 hours	>1000 hours
8.5	Corrosion resistance in humid environment	>100 hours	>1000 hours
8.6	Camber angle		0°

Table 7: Motor requirements

Motor

		Must	Should
9	General requirements		
9.1	Brushed DC-motor	X	
9.2	Rated voltage		48 V
9.3	Rated power	100-400 W	150-300 W
9.4	Rated speed	0-5000 RPM	
9.5	Efficiency	>80 %	>90 %
10	Physical requirements		
10.1	Weight	<3 kg	<1 kg
11	Requirements from surroundings		
11.1	Operational temperatures	10-40 °C	
11.2	Waterproof	IP44	

Table 8: Window requirements

Windows

		Must	Should
12	Production requirements		
12.1	Made of a material that won't shatter into sharp shards	X	
12.2	Maximum cost	<25 000 NOK	<10 000 NOK
13	Functional requirements		
13.1	See-through	X	
13.2	Distortion	Minor	None
13.3	Tinted		X

Table 9: Steering wheel requirements

Steering wheel

		Must	Should
14	Production requirements		
14.1	Maximum cost [NOK]	< 8000 NOK	< 2000 NOK
15	Functional requirements		
15.1	Uses a turning motion	X	
15.2	Steering wheel or sections of a wheel	X	
15.3	Diameter of wheel	≥ 25 cm	
15.4	Quick release		X
15.5	Dead man's safety device	X	
15.6	Weight	<2 kg	<1 kg
15.7	Throttle	X	
15.8	Indicator buttons	X	
15.9	Horn button	X	
15.10	Cruise control button		X
15.11	Windscreen wiper control		X

3 Chassis

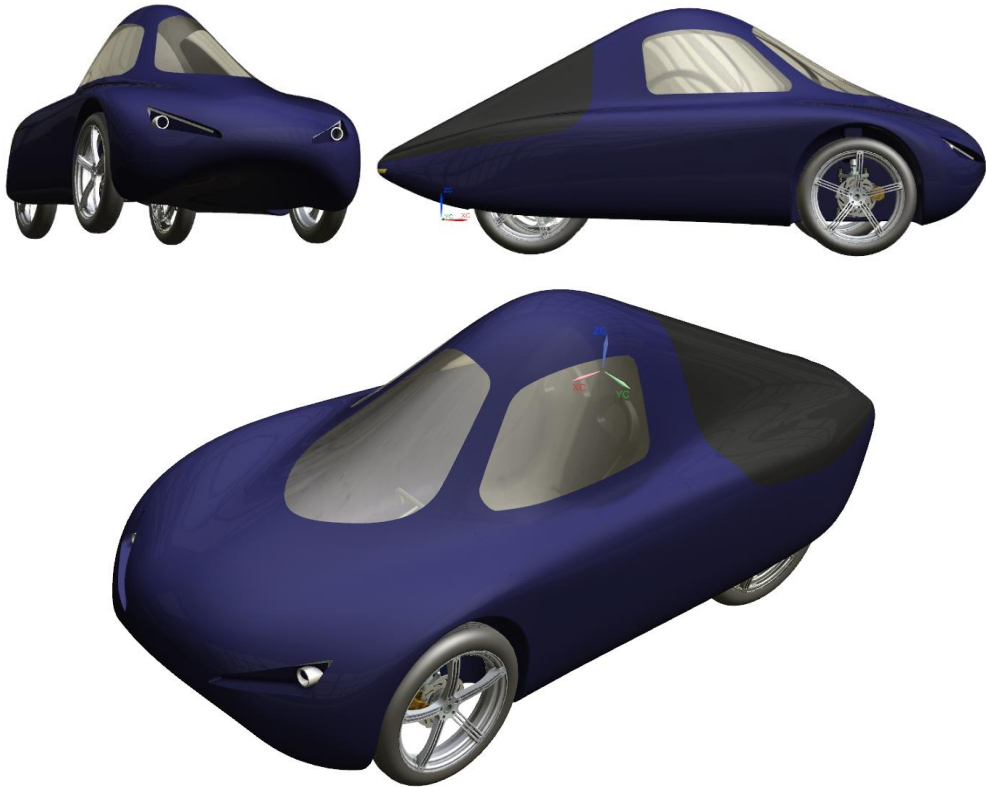


Figure 6: CAD model of final design

3.1 Aerodynamic design

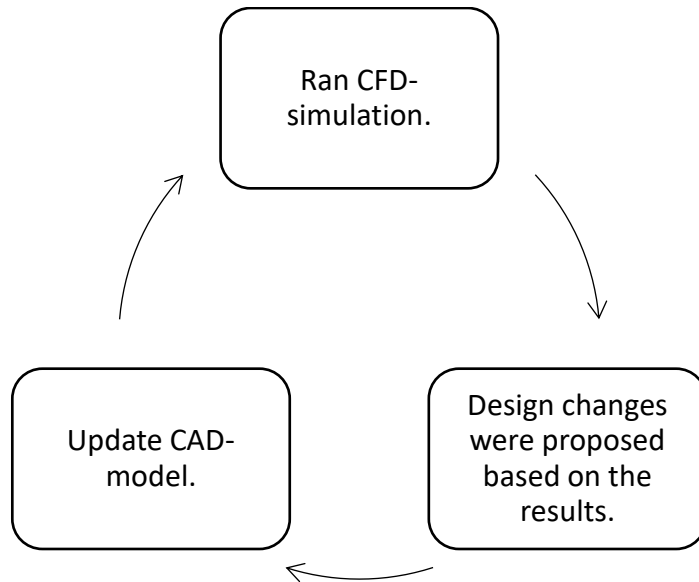
The design of the chassis was finalized in the autumn semester. The work is described in detail in the project thesis. A summary of the work follows:

Goal: Design a one-person car with the lowest aerodynamic drag possible, while still being a good looking and convenient city car; easy to go in and out, a comfortable seat and luggage space.

Method:

- Workshop with sketching designs. The team was urged to draw freely and unrestricted.
- CAD models were made based on the sketched most liked.
- A reference CAD model of the minimum size requirements was made to guide the vehicle designs.

- CFD-simulations were performed on the candidates. The design that possessed the best aerodynamics properties become the chosen design.
- The design went through a cyclic improvement process until convergence:



Properties of final design:

- CFD-simulated drag coefficient of 0.138
- Front wheel wells for double wishbone steering
- No wheel wells in the back to save weight. Back suspension will be mounted directly to the bulkhead.
- Design for being produced as a monocoque: the skin of the structure supporting the loads, with no internal frame structure.

3.2 Monocoque

3.2.1 Deciding CFRP layup with FEM software

This section the dimensioning work of the monocoque. The goal was get the lowest body weight possible while having very low risk of:

- Composite failure
- Buckling failure
- Too high deformations, impacting the driving performance

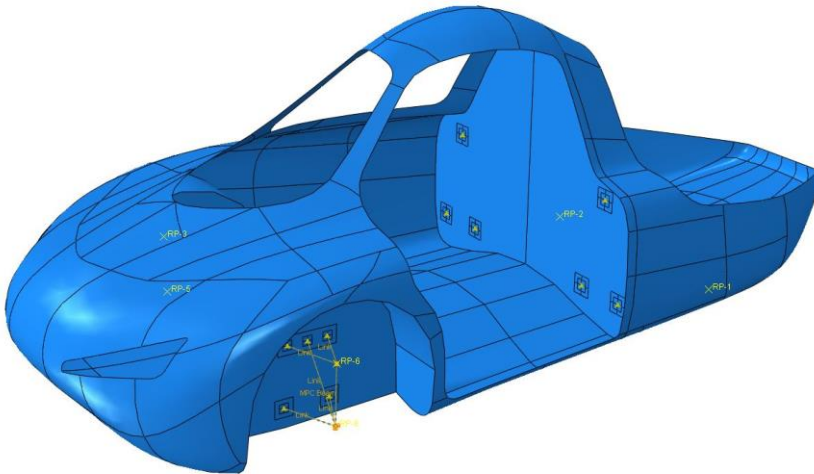


Figure 7: Monocoque model in Abaqus

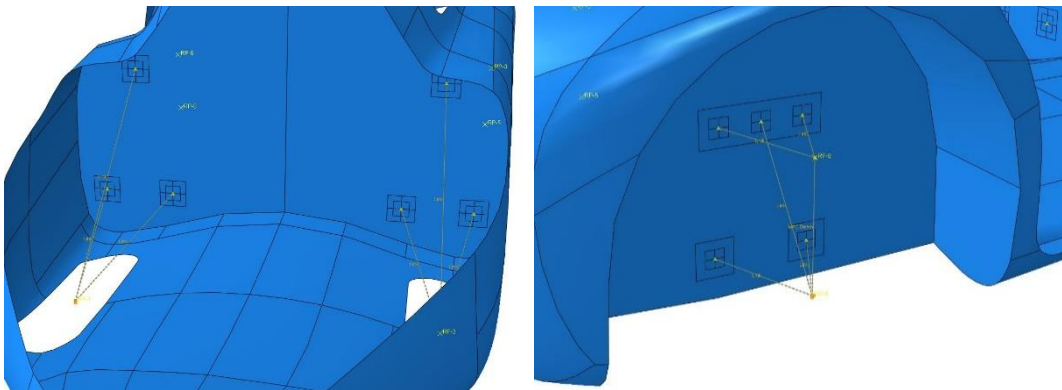


Figure 8: Using beam elements to represent the suspension

The geometry of the monocoque was imported to Abaqus as a sheet model. CFRP plies could then be applied to the sheet bodies, allowing us to vary the number of plies and direction and core thickness to the different regions of the chassis body. Geometry idealizing was applied to the wheel wells, as the rounded edge would give bad mesh quality.

The suspensions were modelled onto the car as infinite stiff beam elements with rotation joints; see Figure 8. The structure’s support was defined in the lower nodes of the “beam”-suspensions. The “beam”-suspensions will provide the correct reaction forces between the suspensions and the connection points in the monocoque when load is applied to the chassis body.

Loads were defined to simulate the forces acting on the car in a race situation. Suggested braking and cornering loads from the project thesis were considered too conservative, and were adjusted downwards:

- **The brake force** was originally set to 1G deceleration with safety factor 2, effectively 2G. Tyre friction is about 1.2 maximum, and down to 0.6 with no anti-block system (Lambourn and Wesley, 2010). Since we have no anti-block system, and generally stiff tyres – it can be certain that the coefficient will not surpass 1, which physically limits the deceleration to 1G:

$$F_{brake} = \mu N$$

$$m a_{brake} = N = mg \Rightarrow a_{brake} = g \quad (1)$$

Hence, the safety factor was removed.

- **The cornering force** was updated after examination the track. The suggested cornering force originated from assuming the vehicle will do a high-speed turn with the lowest turning radius it is capable of. However, it will not be necessary to turn that sharply in the race – the force was adjusted to 900 N.

Table 10: Loads for FEM-simulation

Load type	Force
1. Gravity load	$9.81 \text{ m/s}^2 \cdot \text{mass}$
2. Driver +equipment weight	1000N
3. Driver + equipment weight 2.6 safety factor	2600N
4. Cornering	900N
5. Breaking	1550N
6. Climbing in: Driver’s weight concentrated in door opening.	800N
7. Force on the roof (Rulebook req.)	1000N

3.3 Mesh

The model was meshed with the highest number possible of square shell elements. Concerning shell elements, triangular elements should generally be avoided due to its properties of constant bending and membrane strain approximation (Dassault-Systèmes, 2014) which can result with too high stiffness of the structure. There was done extensive effort in mesh refinement to reduce the number of triangular elements to a minimum.

The final mesh shown in Figure 9 has the following element composition:

Table 11: Element composition of the mesh

Element	Abaqus code	Count	Percentage
Quadratic quadrilateral	S8R	42 740	91.5%
Linear quadrilateral	S4R	3234	6.9%
Quadratic triangular	STR165	623	1.3%
Linear triangular	S3	131	0.3%

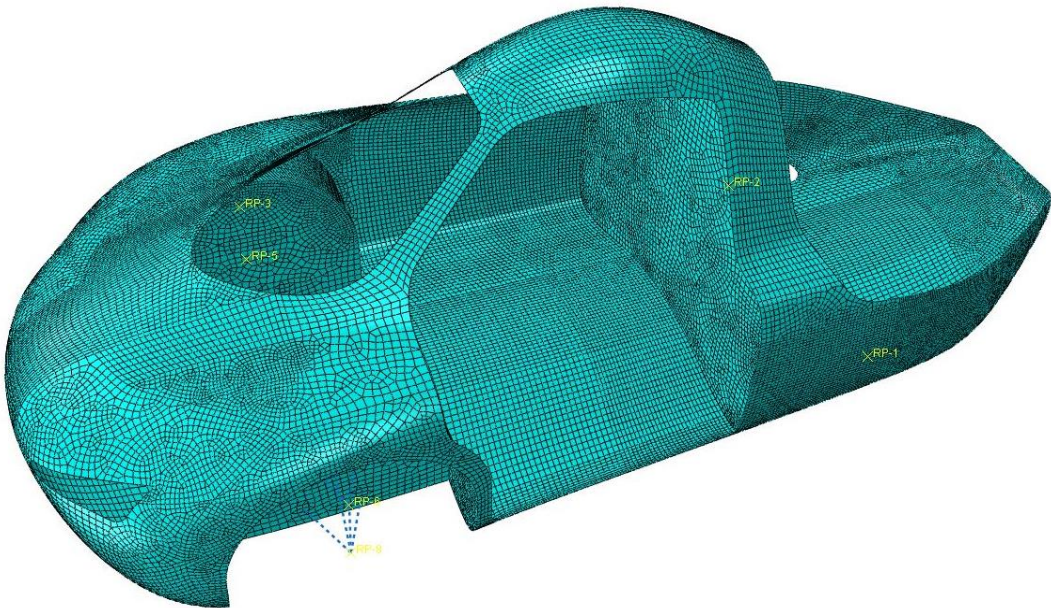


Figure 9: Meshed monocoque

3.4 Properties of the CFRP fabric

The carbon fibre fabric is a pre-stitched two-ply -45/45 fabric, consequently restricting the layup selection to be a multiplier of this fabric. In Table 12 the composition of the fabric is presented. It can be seen that the fabric contains a small amount of glass fibre, which are only used for stitching the fabric together.

Table 12: CFRP composite properties

CONSTRUCTION	AREAL-WEIGHT [g/m ²]	TOLERANCE [+/-%]	MATERIAL
<i>upper side</i>			
45 °	200	5	TORAY T700SC F0E 12K
0 °	1	5	E-glass 34 TEX
90 °	1	5	E-glass 68 TEX
-45 °	200	5	TORAY T700SC FOE 12K
<i>lower side</i>			
STITCHING:	6 g/m ²	+/- 1 g/m ²	PES 76 dtex

Stitching pattern:	tricot	Gauge:	5,0
Width:	1.270 mm		
Total areal weight:	408 g/m ²	Total Tolerance:	5,2 %

COMPOSITE PROPERTIES *

Tensile Strength	370 ksi	2,550 MPa	ASTM D-3039
Tensile Modulus	20.0 Msi	135 GPa	ASTM D-3039
Tensile Strain	1.7 %	1.7 %	ASTM D-3039
Compressive Strength	215 ksi	1,470 MPa	ASTM D-695
Flexural Strength	245 ksi	1,670 MPa	ASTM D-790
Flexural Modulus	17.5 Msi	120 GPa	ASTM D-790
ILSS	13 ksi	9 kgf/mm ²	ASTM D-2344
90° Tensile Strength	10.0 ksi	69 MPa	ASTM D-3039

* Toray 250°F Epoxy Resin. Normalized to 60% fiber volume.

3.5 Initial analysis

The basis of the layup is a “thick core, thin skin” design, which is the common practice in composite manufacturing. Light core material is used to offset the outer skin from the centre plane. The sandwich structure gains stiffness with increasing distance between the outer skin layers. This can be explained by elementary beam theory, where the curvature of a beam is given by,

$$\kappa = \frac{M}{EI} \quad (2)$$

Increasing second moment of area would decrease the curvature of the beam.

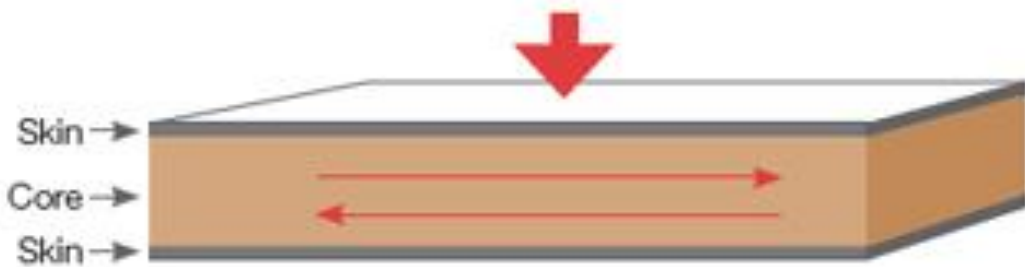


Figure 10: Sandwich structure:

However, the curved shape of the monocoque means the core plates must be cut when the curvature is above how much the core can be bent. The gap in these cuts will be filled with epoxy in the vacuum infusion process. The core plates should therefore not be any thicker than necessary.

Initial experimenting with the layup gave good results with 4mm in general core thickness, and 8mm thickness in the floor. The bulkhead is a flat surface, which means there will not be cuts or gaps in its core material. A comfortable thickness of 15mm was chosen.

The next step involved revealing any weak areas of the design, which would be especially at risk of composite failure.

The car must be dimensioned to withstand the toughest load case without failure. This would be a combination of:

- Gravity (load 1)
- Driving over a bump (load 3)
- Cornering or avoided obstacle by turning (load 4)
- Breaking (load 5)

From here on referred as “load case max”.

The monocoque was well within the limit of Tsai Wui criterion, even with only one sheet of Saertex fabric on each side of the core. The criterion creates a polynomial interaction between the failure strength parameters of the composite. If the function reaches 1, the criterion predicts failure. However, the deformations were too high. Further work had to be done with the layup to address the certain issues:

- Door opening deformations preventing the door to stay in place.
- Front wheel well deformation causing undesired effects on the front wheel dynamics.
- Propagated deformation of the tail causing the back wheels to crash with the sidewalls while cornering.

Improving stiffness

It was experimented with adding thicker core in the areas with too much deformation; around the door opening, the right sidewall of the tail and the front windows frame. This increased stiffness greatly, and with additional symmetric pair of 0/90 plies, the deformations became sufficiently low. The same layer addition was applied to the separation wall and its surrounding sidewall, which also gave sufficient reduction of deformation. It can be noted that the chosen layup (0/90/-45/45/C/-45/45/90/0) in these reinforced areas makes the composite Quasi-isotropic, meaning the properties become similar to an isotropic material, having equal strength, and stiffness in all directions. The resulting deformations of the monocoque with the final layup under “load case max” are presented in Figure 11.

Deformation analysis of the final layup

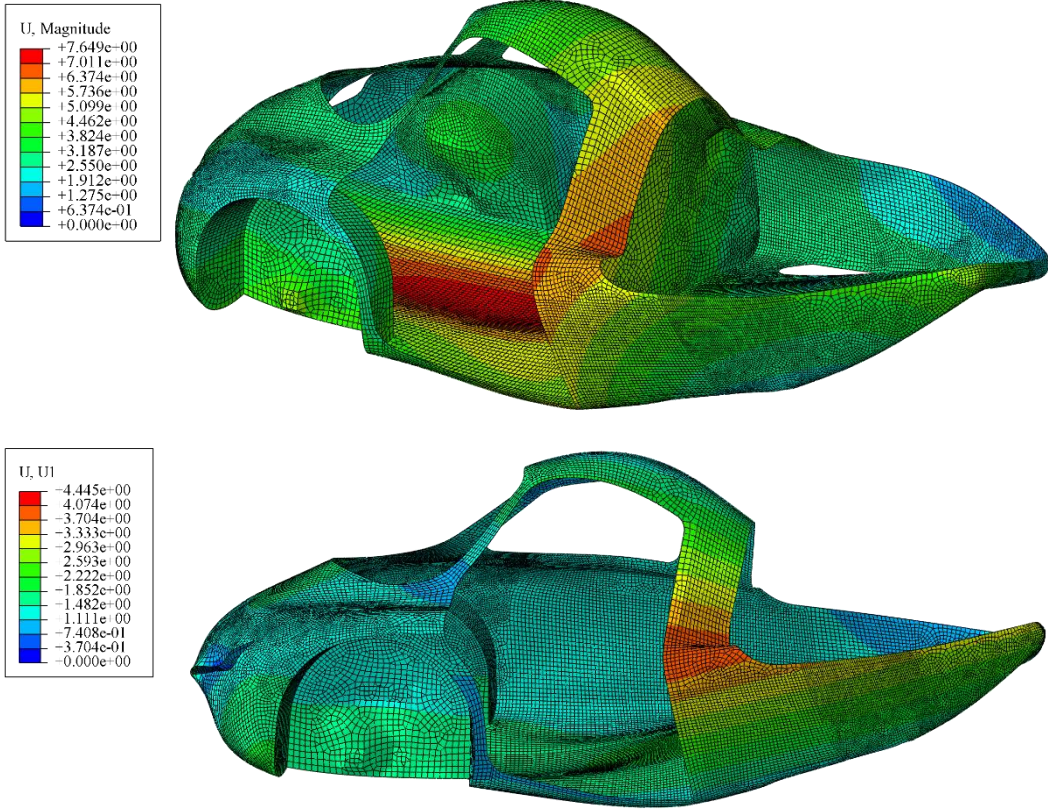


Figure 11: Deformations under load case max.

Tsai Wui criterion analysis of the final layup

The most exposed areas have a value below 0.2, which means the safety factor is above 5. The maximum point of 0.3 is an isolated extremum, and may be neglected. The risk of composite failure can be considered as very low.

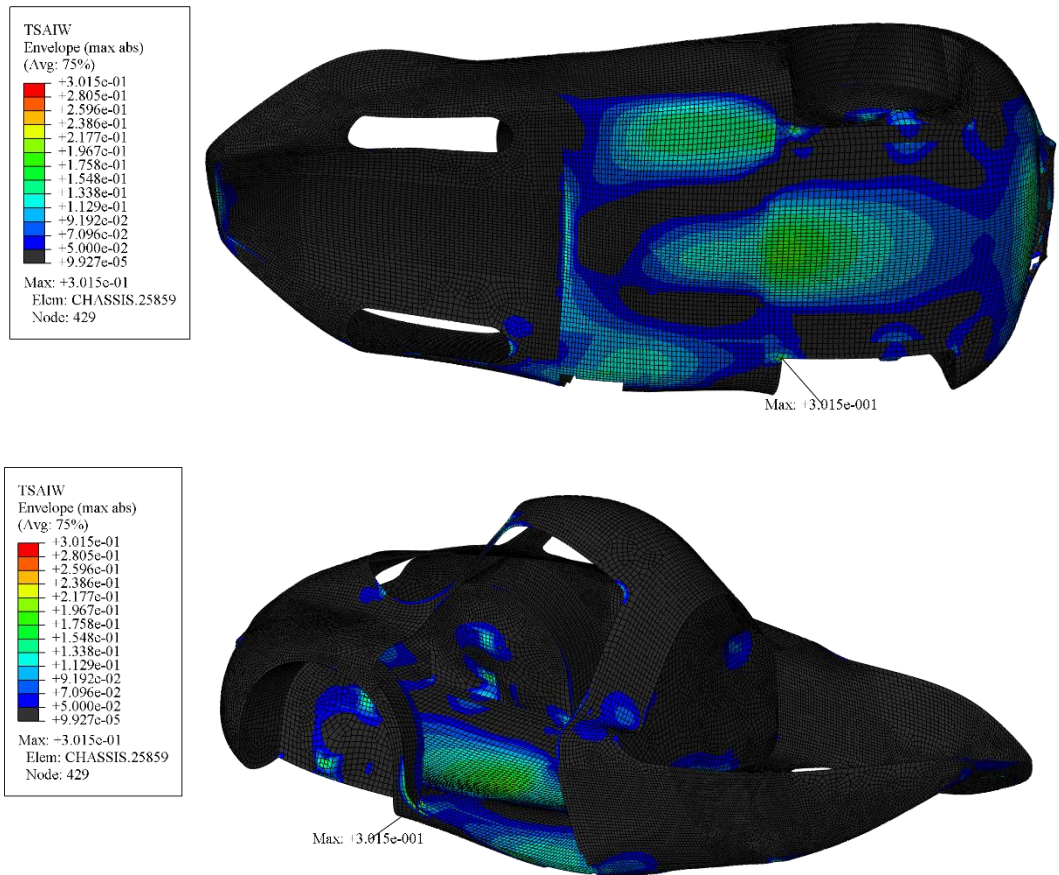


Figure 12: Composite failure with Tsai Wui criterion.

3.5.1 Buckling analysis

Even though the chance of a direct composite failure is unlikely, there could be a risk of local buckling. The thin composite skin of the monocoque makes it exposed to buckling if the local stress in compression. Instability in the structure cause a sudden side movement, which may give local composite failure that propagating to total failure. Also, buckling of less severity could yet be causing delamination, weakening the composite toughness (Lee and Park, 2007).

The analysis predicted buckling to occur at the door opening if the loads were multiplied by 1.17. Even though the analysis predicts the structure will hold for our force requirements,

there were addressed concerns to the risk of higher shock forces than calculated and error in FEM analysis. Buckling is a rather brutal and rapid failure mode. It was decided to find a solution to reduce the risk of buckling in this area. Increasing the core thickness to 30 mm in the corner of the door opening raised the safety factor to 3, which felt much more comfortable and with minimum weight gain.

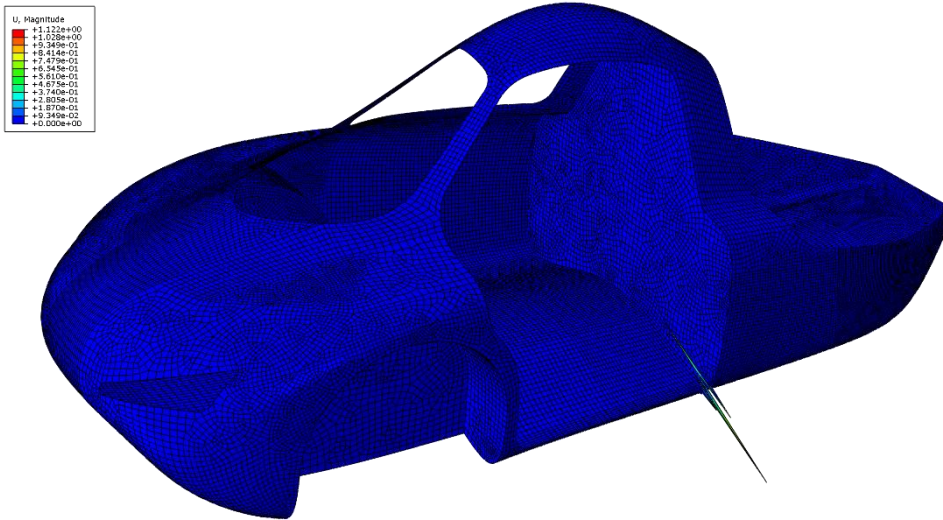


Figure 13: Risk of buckling in lower door corner

3.6 Selection of core material

It was decided to use DIAB as our provider of core material. The range of core densities and their properties in their series Divinycell® are shown in Table 13. The recommendation from DIAB was to use H45 in our application. Running analysis with different core densities confirmed H45 to be sufficient. Denser cores only gave slightly better overall stiffness, while adding more weight.

Table 13: Diab Divinycell® core material properties

Property	Test Procedure	Unit		H35	H45	H60	H80	H100	H130	H200	H250
Compressive Strength ¹	ASTM D 1621	MPa	Nominal	0.5	0.6	0.9	1.4	2.0	3.0	5.4	7.2
			Minimum	0.3	0.5	0.7	1.15	1.65	2.4	4.5	6.1
Compressive Modulus ¹	ASTM D1621-B-73	MPa	Nominal	40	50	70	90	135	170	310	400
			Minimum	29	45	60	80	115	145	265	350
Tensile Strength ¹	ASTM D 1623	MPa	Nominal	1.0	1.4	1.8	2.5	3.5	4.8	7.1	9.2
			Minimum	0.8	1.1	1.5	2.2	2.5	3.5	6.3	8.0
Tensile Modulus ¹	ASTM D 1623	MPa	Nominal	49	55	75	95	130	175	250	320
			Minimum	37	45	57	85	105	135	210	260
Shear Strength	ASTM C 273	MPa	Nominal	0.4	0.56	0.76	1.15	1.6	2.2	3.5	4.5
			Minimum	0.3	0.46	0.63	0.95	1.4	1.9	3.2	3.9
Shear Modulus	ASTM C 273	MPa	Nominal	12	15	20	27	35	50	73	97
			Minimum	9	12	16	23	28	40	65	81
Shear Strain	ASTM C 273	%	Nominal	9	12	20	30	40	40	45	45
Density	ISO 845	kg/m ³	Nominal	38	48	60	80	100	130	200	250

3.7 Final layup

Table 14: CFRP Layup for the monocoque

<i>Ply #</i>	<i>Material</i>	<i>Dir.</i>	<i>Thick.[mm]</i>	<i>Location</i>
3/4	CF	0/90	0.4	Door frame, front window frame, wheel wells, firewall
1/2	CF	-45/45	0.4	Whole body
5	Core	-	4	Front, tail, roof
6	Core	-	8	Floor
7	Core	-	15	Front window and door frame, firewall
8	Core	-	15	Door opening corner
9	Dense-core	-	15	Suspension fastening points
10/11	CF	-45/45	0.4	Whole body
12/13	CF	0/90	0.4	Door frame, front window frame, wheel wells, firewall

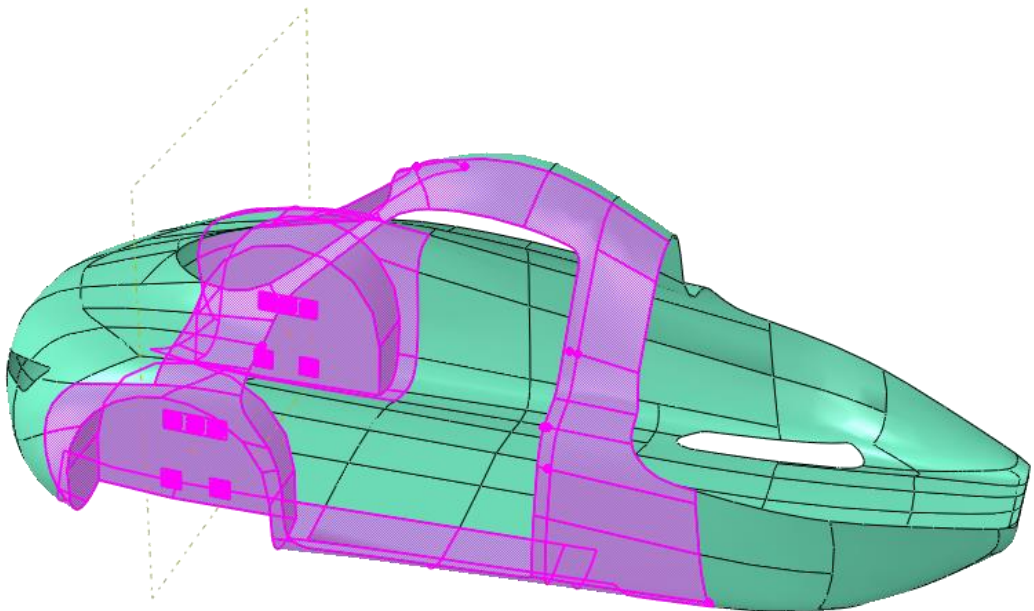
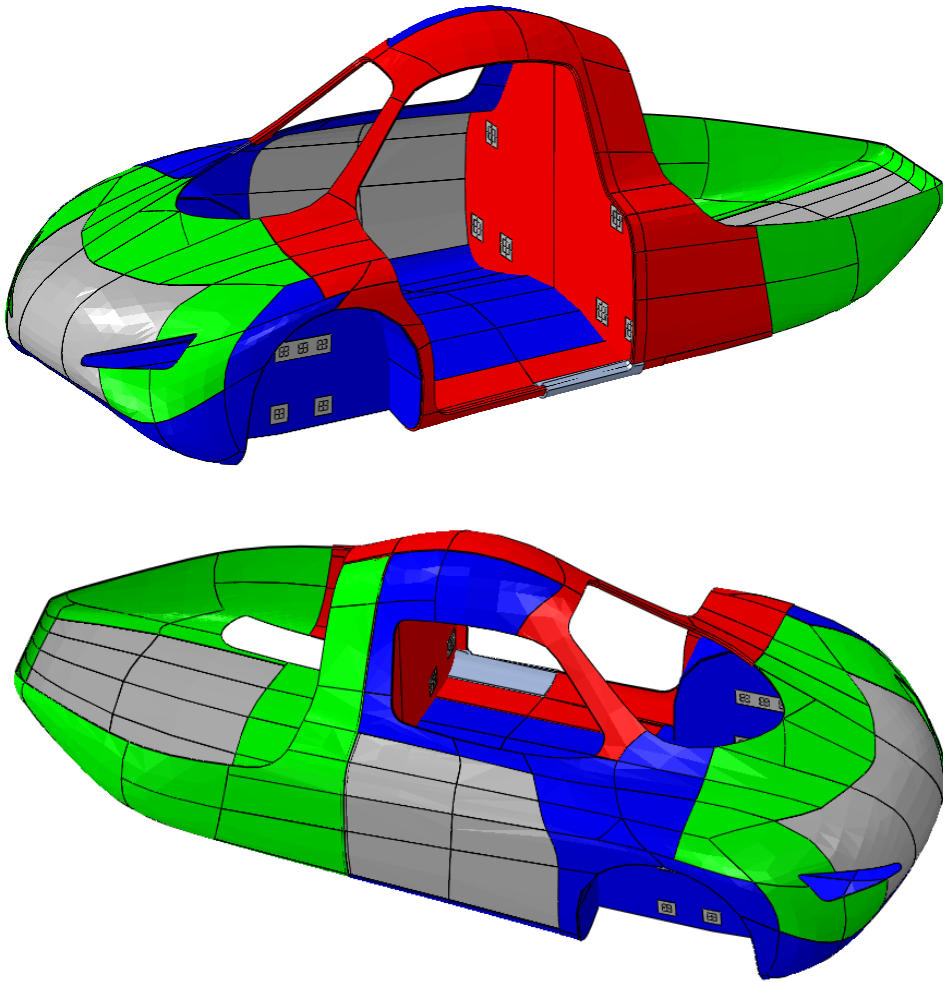


Figure 14: locations of areas reinforced with additional 0/90 plies



Green	4mm
Blue	8mm
Red	15mm
Door corner	30mm

Figure 15: Arrangement of core material

Achievable weight of monocoque

Mass of layup (Abaqus)	14.1 kg
Core material epoxy absorption ¹ ~ 1.1 – 1.6 kg/m ²	7.2 - 10.5 kg
Minimum total mass	21.3 - 24.6 kg

¹ Estimate from DIAB Norway

3.8 Mould

When choosing which type of mould to use, closed moulds were quickly discarded due to the required size, complexity and cost. We used an open mould. One disadvantage of open moulds is that only one surface of the product will be finished and smooth. This is because the other surface will not be in contact with the open mould surface (Akovali, 2001). The open mould surface is also required to be very smooth to get a smooth product finish. Since we wanted the outside of our car to be the smooth surface, it needed to be in contact with the mould. We therefore decided to use negative (female) moulds.

3.9 Mould production

We wanted to use few moulds to produce the mould to get a continuous and smooth body shape to gain the best possible aerodynamic properties. The body must at least be cut in two to make it possible to get the part of the mould. The most natural option was to cut the body horizontally. A vertical split would be a cut through an area with high strain energy, as can be seen from the Abaqus results. This is not ideal for a weaker patched area. Secondly, the moulds would need depth of half the car's length. Also not ideal, as you must manually dive into the mould, and precisely form with your hands the carbon fibre fabric to the mould.

Some modifications had to be done to the design to allow mould production. The moulds need to have a slip angle of at least 1° to be able to get the finished part out of the mould. The wheel wells had to be modified as shown in Figure 16. The change has minimal influence on the structural rigidity. However, it has a negative effect on the aerodynamics. The initial design can be achieved by constructing the missing part at the composite lab at NTNU, and attaching it. It was scheduled on the lower priority list, but in the end with did not have time to make these.

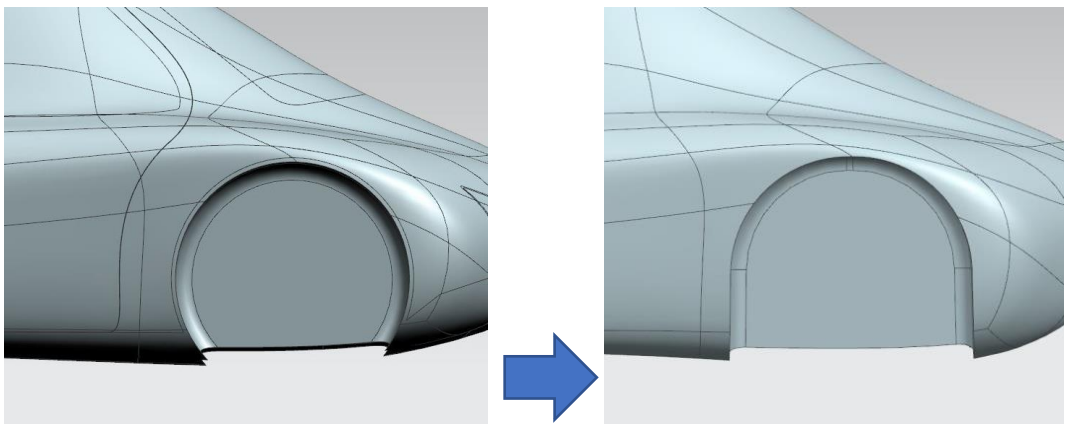


Figure 16: Modified wheel wells

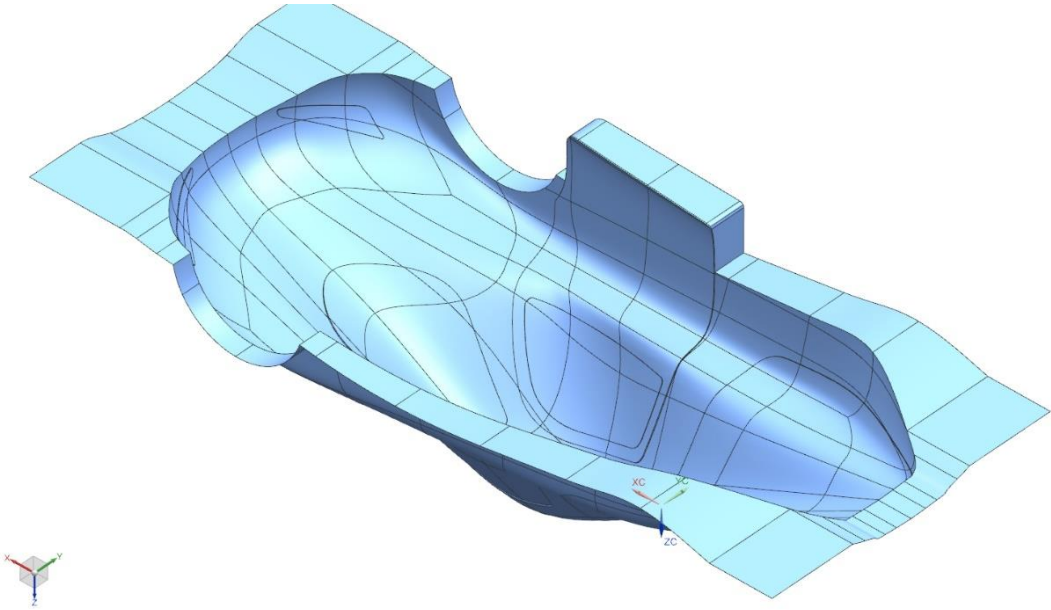


Figure 17: CAD-geometry used CNC mill the upper body mould

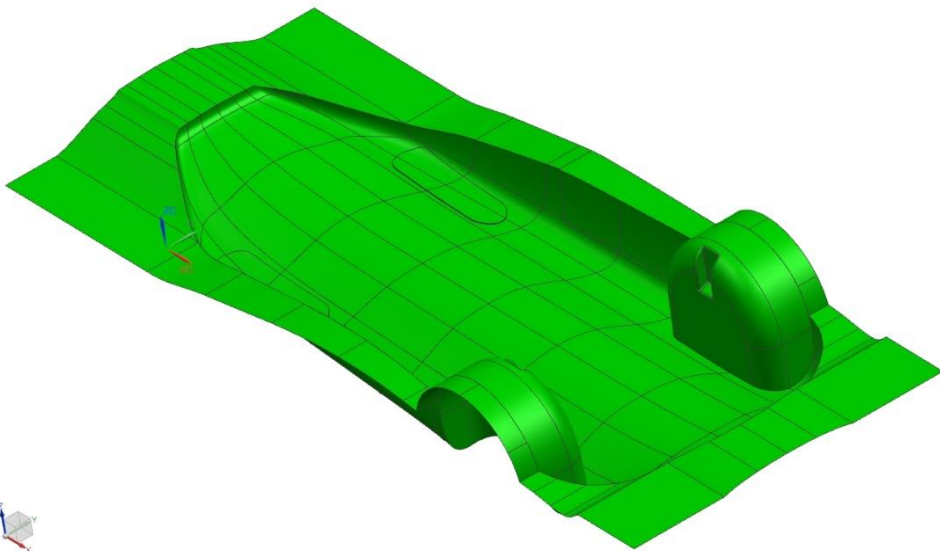


Figure 18: CAD-geometry used to CNC mill the lower body mould

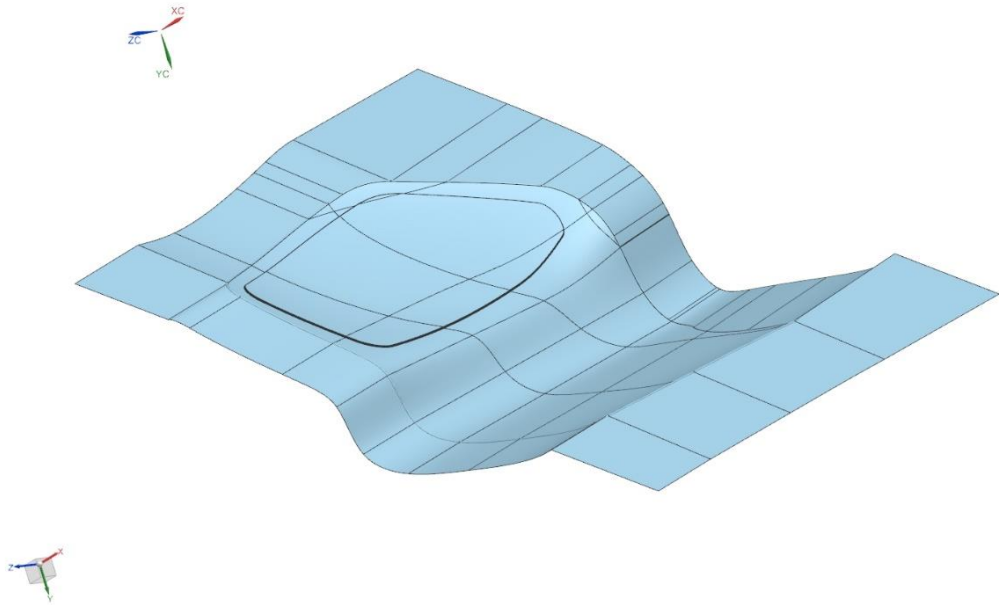


Figure 19: CAD-geometry used to CNC-mill the door mould

Initially the plan was to use the upper body mould also for production of the door. The door has a slightly overhang, which means it must be milled with 4-axis. Eker design reported back to us that they preferably would like to run a 3-axis code for the milling. Preparing a 4-axis program would be more time consuming, and could result with a higher bill. Fortunately, we had acquired enough foam material to make a separate mould for the door.

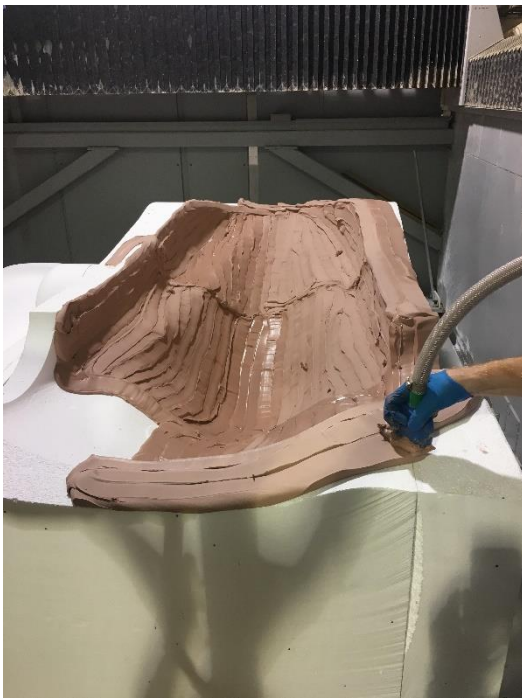
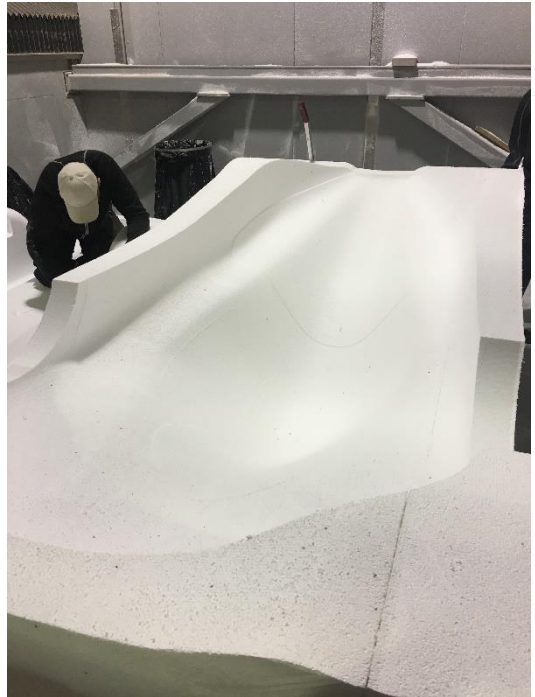
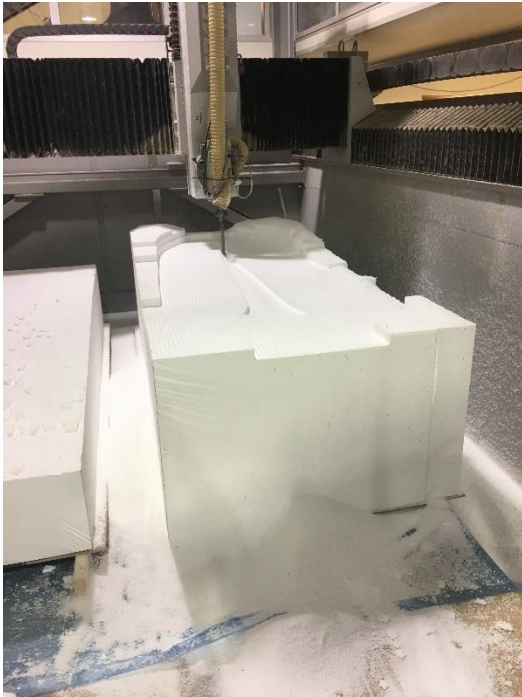


Figure 20: Production of moulds at Eker design. Epoxy paste is used to give the moulds a hard surface

4 Monocoque production

4.1 Process

After contacting companies in Norway and exploring our possibilities for different methods for production, we opted to use vacuum infusion (illustrated in Figure 21). Materials are laid dry into the mould and the vacuum is applied before the resin (Van Paepegem, 2014). The vacuum drives the resin into the laminate. The vacuum is achieved by covering the mould with a flexible, non-adhering polymeric sheet, and pumping out the air. In traditional hand lay-up, the laminate is wet by brushes, rollers or other means. It can then be put under vacuum to improve the fibre-to-resin ratio. By wetting through infusion, the fibre-to-resin ratio will be even better. A higher ratio lowers weight, increases strength, and maximizes the properties of fibre and resin (Van Paepegem, 2014). The resin is a mixture of an epoxy and a hardener. This resin is applied in a viscous form and through curing it transforms into a hardened rigid state. The curing may take days with larger products, but can be accelerated by applying heat.

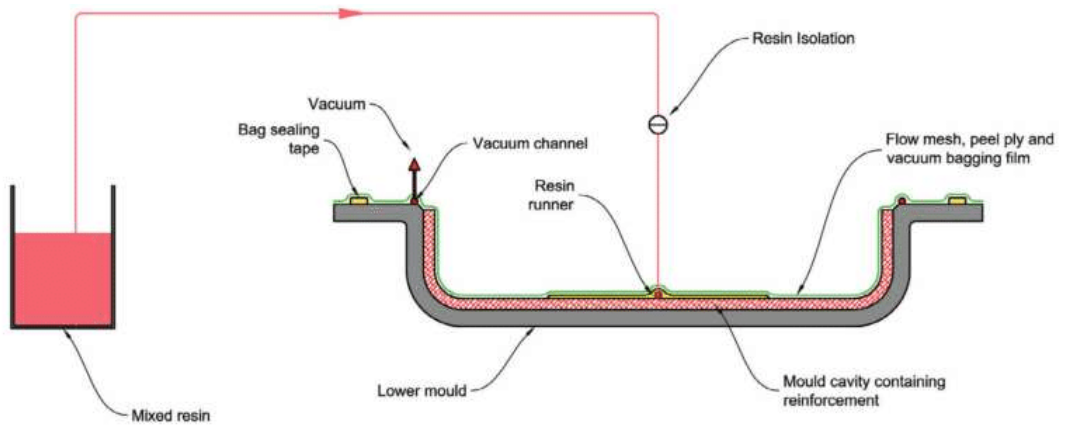


Figure 21: Vacuum infusion process

The production of the carbon fibre parts for the monocoque was done at High Performance Composites (HPC). A few team members travelled there to make the parts, and was guided through the work by the owner of HPC, Paal Feduik.

For the production of our parts, the steps of the process were as follows:

1. Coating the moulds to get a smooth surface. This had already been done when we arrived at HPC.
2. Apply a release wax on the mould to make it easier to remove the part when finished. The wax was applied, wiped even and set to dry for 15 min. This was done three times with the final layer set to dry for 30 minutes.
3. Mask around the form with a sealant tape. It was placed at a distance from the edges such that the parts could have flanges. By placing the tape this early in the process we make sure that the surface is clean for a secure seal. It also acts as a guide through the lay-up process.
4. The lay-up of the carbon fibre fabric. The sheets of fabric were laid with an overlap of a couple of centimetres to ensure continuous fibre. A few millimetres would have been enough, but would have required a much more meticulous work. A spray adhesive was used to get the fabric to stick to the moulds. The use had to be spartan or else it could saturate the fabric. Core material was placed where needed and covered by the final layer(s) of carbon fibre fabric.
5. Everything was covered in peel ply. Peel ply is necessary to prevent flow mesh, spiral tubing and other parts to stick to the fibre.
6. Resin infusion mesh, also called flow mesh, was put on top of the peel ply. The mesh assists the flow of resin across and throughout the laminate during the infusion process. The mesh stops some centimetres from the outlet, as we want the resin to slow down before being sucked out.
7. Spiral tubing was placed around the edge of the mould with tee connectors where the outlets should be. The spiral tubing allows for easy flow of resin such that when the resin reach the tube at the edges it goes to the outlets. A length of spiral tube with a tee connector is also placed where the resin inlet should be. It is desired to have the inlet at a low point and outlet at a higher point. Larger moulds require multiple outlets such that the resin can cover the entire product. The tee connector guides the resin flow from the spiral to the vacuum tube (or the opposite direction).
8. Everything is covered with a vacuum bag. It is important the bag is of a sufficient size to put a pressure on all areas of the mould during infusion. To ensure it reaches all areas it is wise to assist in positioning the bag when the vacuum is created.
9. Vacuum tubes are placed on the tee connectors and connected to the vacuum pump. The inlet tube gets clamped and the vacuum is created.
10. The pump is turned off, outlet tube(s) are clamped and the set-up is checked for leaks.
11. The infusion process where the resin goes into the laminate. The resin gets sucked from a bucket into the part. At the outlet end, there is a catch pot to prevent resin going into the pump.
12. Curing of the part.
13. The consumables are removed such that only the carbon fibre part is left.
14. The carbon fibre part is taken out of the mould.



Figure 22: Consumables

- a) Release wax – ensures easier release of the part from the mould.
- b) Spray adhesive – to prevent the fabric from sliding in the mould.
- c) Sealant tape – seals between the mould and bag, and other areas.
- d) Peel ply – needed to remove excess resin and consumables.
- e) Flow mesh – ensures resin flow under vacuum.
- f) Spiral tube – allows for easy distribution/collection of resin.
- g) Tee connector – connects spiral tube to vacuum tube.
- h) Vacuum bagging film – covers the mould so a vacuum can be created.
- i) Vacuum tube – sucks in air and/or resin.

4.2 Door

The door was a relatively simple part to produce. The layup was strips of carbon fibre fabric along the edge sandwiched between two sheets of fabric. Two lengths of spiral tube were placed at opposite ends of the mould, such that the resin travelled in one direction across the laminate.



Figure 23: Left: Carbon fibre lay-up. Right: Door out of mould

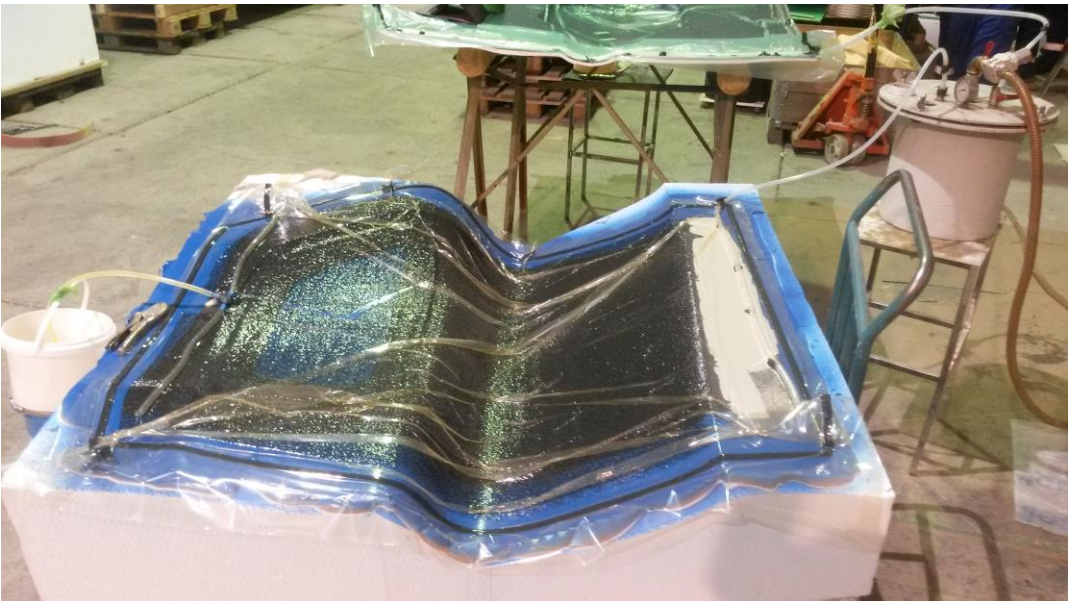


Figure 24: Infusion of door

4.3 Upper body



Figure 25: Coated top mould

The top mould had been milled such that the placements of the windows, door and compartment cover were visible. We laid the carbon fibre fabric around these. The DIAB core material had low bendability which resulted in changes to our planned lay-up, as it couldn't be placed intended. We could flex the it by heating it in an oven and shaping it in the mould. Due to this low bendability, we had to lay the core material in a cross in the roof. On other parts of the body we had to use a honeycomb core material. Honeycomb absorbs more resin and will weigh more, but allows to be able to be shaped after the curvature. Our positioning of the core material can be seen in Figure 26. The beige is the DIAB core material, while the white is honeycomb. We also used honeycomb on the bonnet, but this is covered by fabric in the picture. The DIAB also had to be drilled with small holes to allow the resin to flow through and saturate the carbon fibre under it.

The biggest deviation from our planned positioning of the core material was the cross in the roof and the use of honeycomb in the parts with strong curvature. Along with the bottom mould, we applied heat during curing to accelerate the process. This was done by covering the mould with a tarpaulin and raising the temperature with fan heaters.



Figure 26: Left: Core material. Right: Peel ply and flow mesh

In Figure 27 one can see how the resin was fed into the mould. The inlet was at the lowest point and being distributed over the mould by a spiral tube. We had to use several outlets to get the resin all over the mould, and these were positioned at the highest points.

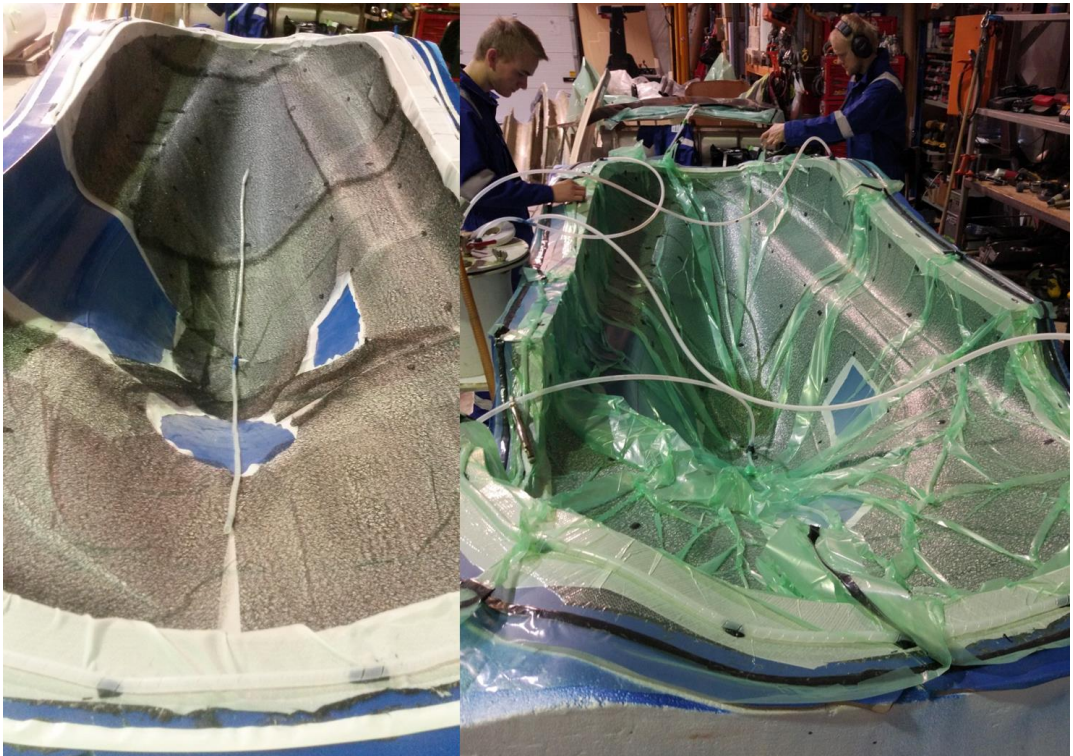


Figure 27: Placement of inlet and outlets

4.4 Motor compartment cover

The motor compartment cover was made in the top mould after the top body was removed. The production was quite similar to the door. Also here the carbon fibre fabric was layered to cover the entire surface, frame the geometry, and cover the surface again. The first layer and the frame layer can be seen in Figure 28. The resin travelled in one direction, where the inlet was at the lowest point in the mould and the outlet at the highest.



Figure 28: Process of cover production

4.5 Bulkhead

When the bulkhead was made, we decided to not produce it in its' final geometry and used a plate of core material that was larger than the finished bulkhead would be. By having excess material, we could cut and adjust the bulkhead to fit correctly once the top and bottom body had been joined during assembly. Cutting the shape of the bulkhead later would expose the core material, but that was not a problem as it would be covered once the bulkhead was inserted. It was important that the inserts in the bulkhead was placed correctly, so that the back suspension could be mounted as planned. Their position was carefully measured and cut in the core material. The inserts are of a harder, denser core material and are included so the wall won't be crushed where the suspension is mounted.



Figure 29: Left: Inserts in core material. Right: Covered with peel ply

Since the bulkhead is flat, there was no need for a mould. It could be produced on a flat surface. We used a glass table which is smooth. It was now easy to feed the laminate with resin from both sides by placing peel ply and flow mesh both on top of and below the laminate (as illustrated in Figure 30). By allowing resin to flow on both sides, we eliminated the need to drill holes in the core material, thus reducing work and the weight of resin in the holes. We laid the fabric as $-45/45$. If we were to lay it in a $0/90$ manner as planned, the fabric we used would have to be turned 45 degrees and cut in several smaller pieces. That would have resulted in overlaps, more work and wasted fabric.

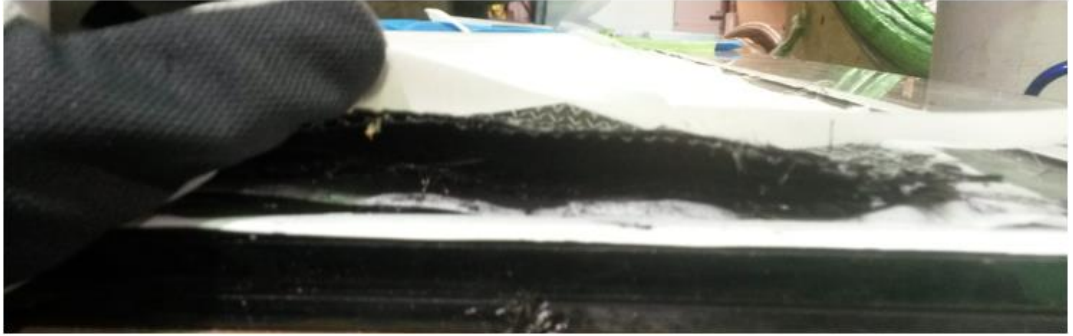


Figure 30: Layers in bulkhead production

The infusion process was simple. The resin travelled in one direction, being distributed and collected by a spiral tube at each end (see Figure 31).



Figure 31: Bulkhead infusion

4.6 Lower body



Figure 32: Lower mould

Figure 32 shows how the lower mould was covered in carbon fibre, peel ply and flow mesh. The wheel wells were the most challenging area of this part to cover. Especially the flow mesh needed many cuts to fit the geometry. To stick the flow mesh to the peel ply we used bits of sealant tape. When creating the vacuum, we also needed to position the bag such that there was a close fit all over the mould. The resin inlet was positioned in the middle of the mould with a length of spiral tube to assist the distribution. The outlets were on top of each wheel arch and in the back.

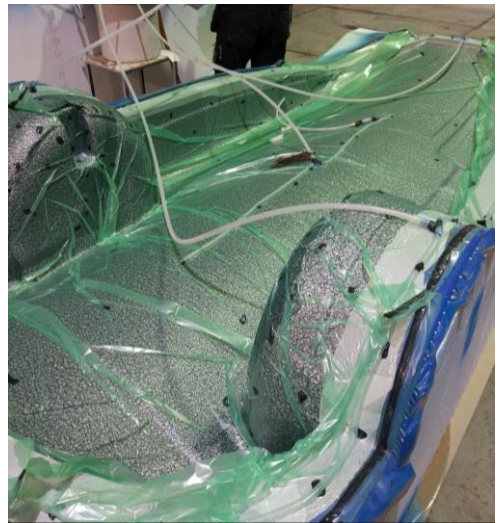


Figure 33: Inlet and outlets in bottom mould



Figure 34: Core material in lower body

The lower body was the part which required the most use of core material. Also here we had some deviations from our plan. As can be seen in Figure 34 we had to switch from DIAB core to honeycomb core in the rear and over the wheel arches. The honeycomb is the same as used in the top part, and is 4 mm thick. The DIAB core is as previously mentioned not flexible. We therefore had to cut the plates into smaller rectangles. Due to the curvature of the floor, the rectangles are at a small angle to each other which creates tiny gaps. Together with the holes drilled in the core material, these gaps will be filled with excess resin. The frame of the floor, especially at the door side, will be subjected to larger stress. We therefore had to use thicker core material (15 mm and 20 mm) in those areas, which leads to larger voids. Examples of gaps where resin will reside can be seen in Figure 35.

Another deviation from the plan was the walls of the wheel wells. Paal Feduik advised us to not use core material and inserts, but rather use extra layers of carbon fibre fabric. Based on his 20 years of experience, he reckoned that seven layers suited us. Using many layers of fabric, one can risk that not every layer gets saturated with resin, but our result was fine. Some flaws in the part occurred during infusion. We got two dry spots, one the right wheel arch and one the right wall. Here the fabric hasn't been saturated with resin, resulting in an area with lower strength. We later saturated the areas by applying resin with brushes, and since the dry spots were in areas which weren't critical it wasn't a major problem. We can't determine for certain what caused the dry spots, but Paal suspect a small leakage of air from the mould due to older epoxy being used to cover it.



Figure 35: Voids that gather resin

We also got accumulations of resin in the edges between the wheel well and the floor which adds extra weight. Using a vacuum bag, the maximum amount of pressure supplied cannot exceed 98 kPa (Akovali, 2001). A larger pressure may have been able to create a closer fit in the edge such that less resin was collected. A larger radius in the edge would also have given a better result.



Figure 36: Left: Dry spot on wheel arch. Top right: Dry spot on right side. Bottom right: Accumulation of resin in the edge

4.7 Production diary

The trip to HPC, located in Råde near Fredrikstad, was in week 9 of 2017 (Monday Feb. 27th to Saturday Mar. 4th). This is a short summary of the work in those days.

Monday:

We drove down from Trondheim. People travelling were Bård Carlsen, Odin Oma, Kjell Sverre Bergum, Espen Verpe and Emil Kulbotten. Emil is an apprentice in the MTP workshop.

Tuesday:

Our first day at HPC. We started the day by waxing the moulds. The door was laid up, infused and set to cure. The first layer of carbon fibre was laid in the large moulds and we started cutting the core material.

Wednesday:

The core material was fitted in the top and lower body and covered by the final carbon fibre fabric.

Thursday:

The body moulds were covered with peel ply, flow mesh, tubes and vacuum film. The infusion process was done and they were set to cure. The door was removed from its mould. We started working on the bulkhead by sizing the core material and cutting holes for the inserts.

Friday:

We removed the consumables from the top and bottom body. The top part was removed from its mould. The motor compartment cover was then prepared, infused and set to cure. The bulkhead was also produced and set to cure.

Saturday:

We continued to remove consumables from the bottom part and chiselled on its mould. The bulkhead and compartment cover were finished. We tidied up, packed the trailer and departed to Trondheim.

5 Monocoque assembly

The assembly of the vehicle is a time-consuming process which was done at NTNU. When we got the carbon fibre parts to Trondheim, they needed some work before the car could be assembled. We had transported the lower body to Trondheim in its mould. This was due to the wheel wells being stuck in the mould. We had to start by chiselling the part out of the mould. Next, the residuals of the mould had to be chiselled and sanded off the part. In both the upper and lower body there were areas where excess resin had accumulated. Respectively around the core material outline and in the wheel well edges. That made us unable to rip off the peel ply in those areas. The removal of the excess resin and peel ply was a time-consuming task where we had to be careful. The work was done with a chisel and a pneumatic grinder. Some damages did unfortunately occur, but nothing critical. We also had to mend the dry spots. The method we used is a type of wet lay-up. The mixed resin was applied to the areas with brushes and pressure was put on by vacuum.



Figure 37: Left: Remains of mould on body. Right: Applying resin to dry spot

Before we assembled the car, we cut the shapes for the head lights and windows. We kept some flange for the front window. Once the car was assembled it couldn't get into the room dedicated for working on composites. When working in the room, the walls were sprayed in water to prevent carbon fibre dust to stick to them. The room was also sprayed when finished working.



Figure 38: Grinding excess resin and trimming body

To join the top and bottom part, glue was not an alternative. The walls are so thin that the surface area wouldn't suffice. The method of bonding was also restricted by the geometry near the joining line, e.g. the parts were perpendicular over the wheel arches, and also had a strong curvature in the rear. The method we chose was an overlap of carbon fibre. The fabric is flexible enough to fit along the entire line, and once cured will create a strong bond. The process of laying the carbon fibre was a wet hand lay-up. The layers of resin and carbon fibre fabric was applied manually. Resin infusion would have required a vacuum. A vacuum bag would then be required over the inside and outside of the line, and would difficult to place. The top part was aligned with the bottom and held in place by clamping the flanges, which we had kept for this purpose. We applied two layers of carbon fibre to bond the parts. The first layer had a width of approx. 7-10 cm, varying on the placement. To create a better bond between the parts, the second layer was wider. It was approx. 15-20 cm, varying on placement. Peel ply was put on top to create a similar surface texture as the inside of the parts. The resin mixture and carbon fibre used was the same as used to produce the body.



Figure 39:Joining of body

Once the curing was done, we could remove the flanges. The small gap that was in the line was sealed with plaster. It was set to dry, then sanded. We needed the entire surface of the vehicle to be smooth. This so the vinyl wrap used to colour our car would stick. We used an eccentric sander with grit sizes from P40 (on rough areas) to P240 (fine finish). We finished by going over the surface by hand with sandpaper of grit P600.



Figure 40:Grinding flanges off and plastering joint line

As the bulkhead was made as a plate we needed to cut it into its final geometry. We started by printing the outer lines in the correct scale on paper. The papers were taped together and cut along the line to show the geometry of the bulkhead. Using the paper as a guide, a template was made with the correct thickness. The placement of the bulkhead was marked in the body such that the template could be inserted and adjusted to fit the actual dimensions of the car. Using the template to check how the geometry in the parts compared to the geometry in the 3D-model, we didn't have to worry about taking excessive cuts off our

bulkhead. We could then cut our bulkhead to match the template, and just make minor adjustments when fitting it.

When fitting the bulkhead in the car we had two methods of choice:

1. Mounting the bulkhead in one part before top and bottom are jointed.
2. Fit the bulkhead in the car after the top and bottom are jointed.

We opted for method 2. The reasoning being that the bulkhead would be easier to adjust to a good fit, and that the top and bottom couldn't be joined where the bulkhead was placed if it was mounted first.

Once the top and bottom had been joined we could do the fine adjustments to fit the bulkhead inside the monocoque. The most difficult part was to get the correct angle between the sides of the bulkhead, such that there were no gaps to the roof on both sides of the bulkhead. That was an iterative process of fine cuts and inserting the bulkhead to test the fit. Once the bulkhead geometry had a good fit, it was fastened in the body. The bonding method was the same as for the top and bottom part, wet hand lay-up of carbon fibre. We applied two layers of fibre along the edge on both sides of the bulkhead.

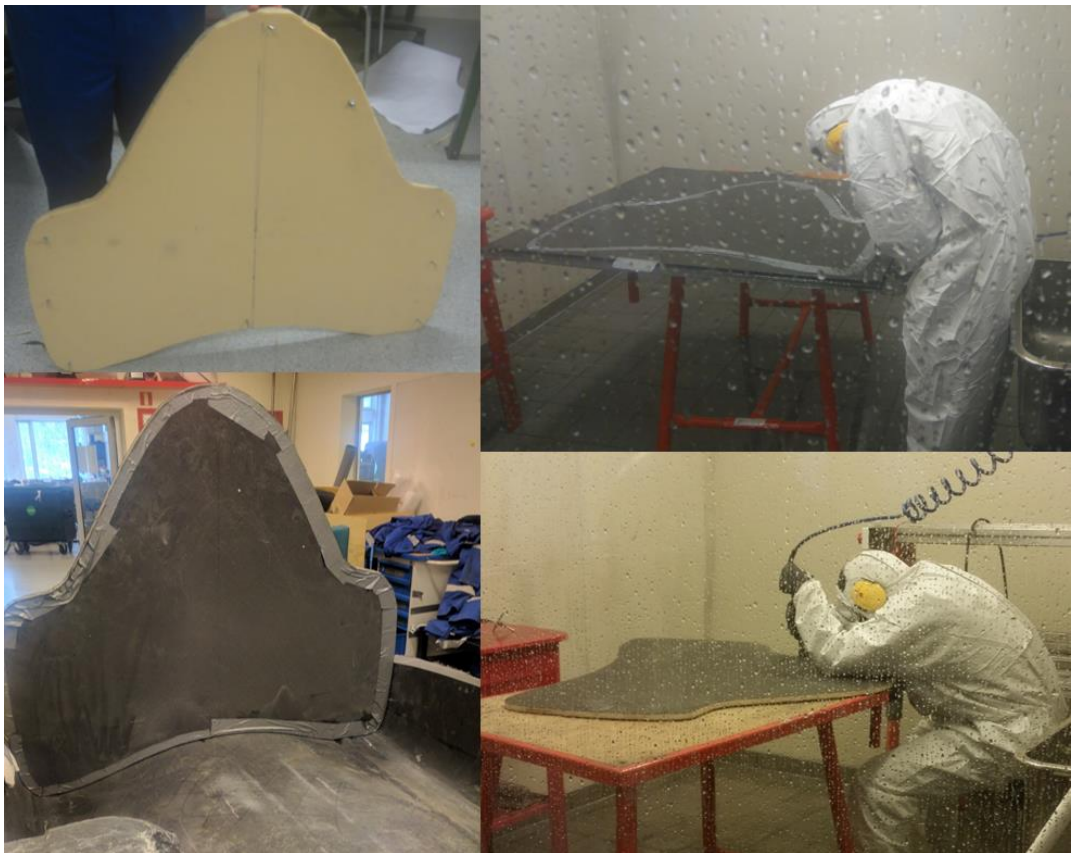


Figure 41: Clockwise from upper left: Bulkhead template, rough cut, fine grinding, bulkhead in lower body

6 Steering

6.1 Choosing steering system

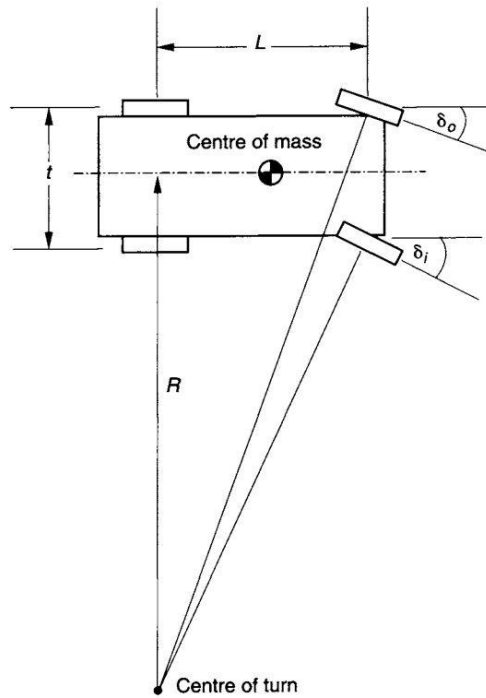


Figure 42: True rolling conditions

King pin steering

Figure 42 illustrates a vehicle with king-pin front wheel steering in a cornering manoeuvre. The king-pins are situated close to the centre of the front wheels, and are the pivot points of the steering. True rolling conditions are achieved when there is no tire scrub. Given the vehicle is turning with a radius R , the outer wheel's angle is α_0 and the inner wheel's angle is α_i . The relations between the turning radius and the angles are,

$$\tan \alpha_0 = \frac{L}{R + t/2}$$

$$\tan \alpha_i = \frac{L}{R - t/2}$$

$$\Rightarrow \alpha_0 = \cot^{-1} \left(\cot \alpha_i + \frac{t}{L} \right) \quad (3)$$

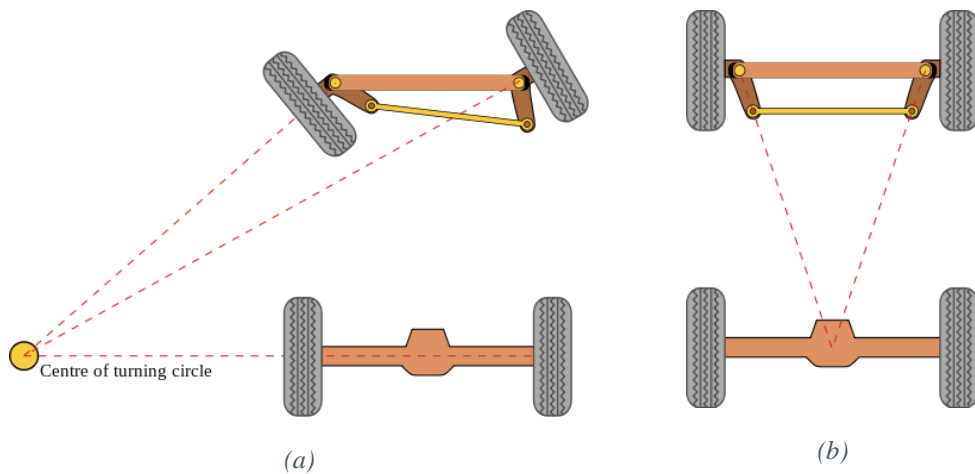


Figure 43: Ackerman geometry

Ackermann steering is a linkage arrangement improving the turning angles.

The Ackermann angle is defined by the angle between the front wheel travel direction and direction of the steering arm. An approximation to the correct Ackerman angle shown in Figure 43(b). The direction of the steering arms is set to intersect at the rear axle.

Centre pivoted steering

Another design is having the front wheels turning about a common centre point between them.

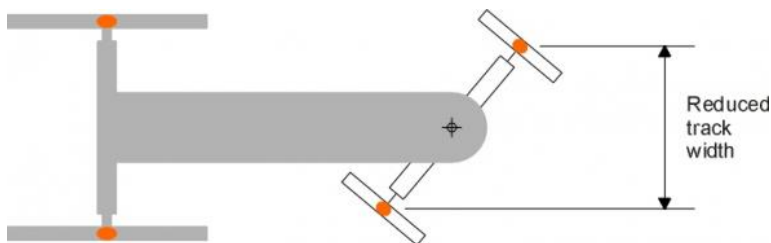


Figure 44: Centre pivoted steering

Interestingly, this arrangement provides true rolling conditions. However, several disadvantages come with the design:

- 1 Reduced track width while cornering. The car will be prone to flipping over.

- 2 Large wheel wells necessary because of the wheels' movement. Poor aerodynamic properties.
- 3 Instable steering. A force from the road (e.g. bump) will create a high moment force in the steering column because of the long pivot arms.

By these disadvantages, and mainly the negative effect on aerodynamics, it was decided that there was no point to further explore or design a centre pivoted steering system.

Rear steering, all-wheel steering

The Shell Eco-marathon rules states "Steering must be operated predominately through the front wheels". It was agreed on that it only would be risky to implement any rear steering as well. We urge future teams to pay attention if this rule change, as it would be interesting to explore rear and all-wheel steering.

To conclude, the best option was going for conventional front wheel steering with king-pins.

6.2 King pin steering mechanism

The connection between the steering wheel and wheels must be mechanical, as stated in the rulebook. This requirement is in accordance with the current Commission Delegated Regulation (EU) 2017/79, approval of motor vehicles.

The first eco-marathon cars built at NTNU used wires and pulleys in the transmission between the steering wheel and front wheels. In the report of PureChoice (2008), they wrote that the wire system was light, but that they would recommend chancing to rods, preferably CFRP rods. Mainly because of difficulty of adjusting the wheel toe and the slack in the system. Tensioning the wire for improved rigidity, provides high stress in the pulleys and their mounts – and must be dimensioned hereafter. This tension was also reported to create much friction in the system, making it hard to turn the wheel.

The team of 2014 bought "Miltera mRack 358" rack-and-pinion. It is essentially a device transferring rotation to linear movement. A rack-and-pinion steering setup is shown in Figure 45. It's an extension of the traditional Ackerman linkage. The Miltera rack has a weight of only 308 g, and the rack provides zero slack and low friction in the movement. In combination with CFRP rods, both the total weight and the rigidity of the system is hard to beat. Lastly, the tie-rods can be made easily adjustable with threaded rod-ends, making the toe adjustment very pleasant. Rack-and-pinion setup was considered superior, and we saw no reason on spending time carrying out a parallel development of a competing wire setup.

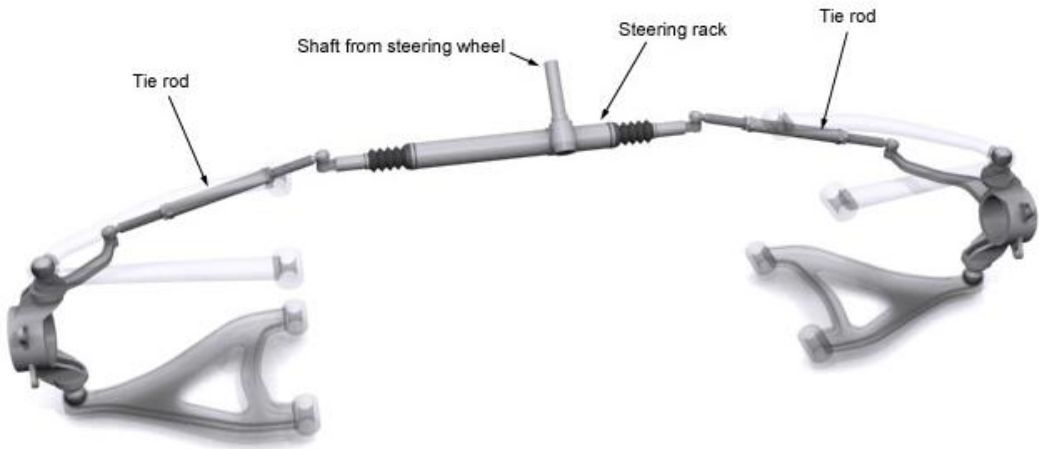


Figure 45: Rack-and-pinion steering system

6.3 Rack-and-pinion steering optimization

6.3.1 Rack-and-pinion geometry

A model of the rack-and-pinion, with parallel and straight wheels is shown in Figure 46.

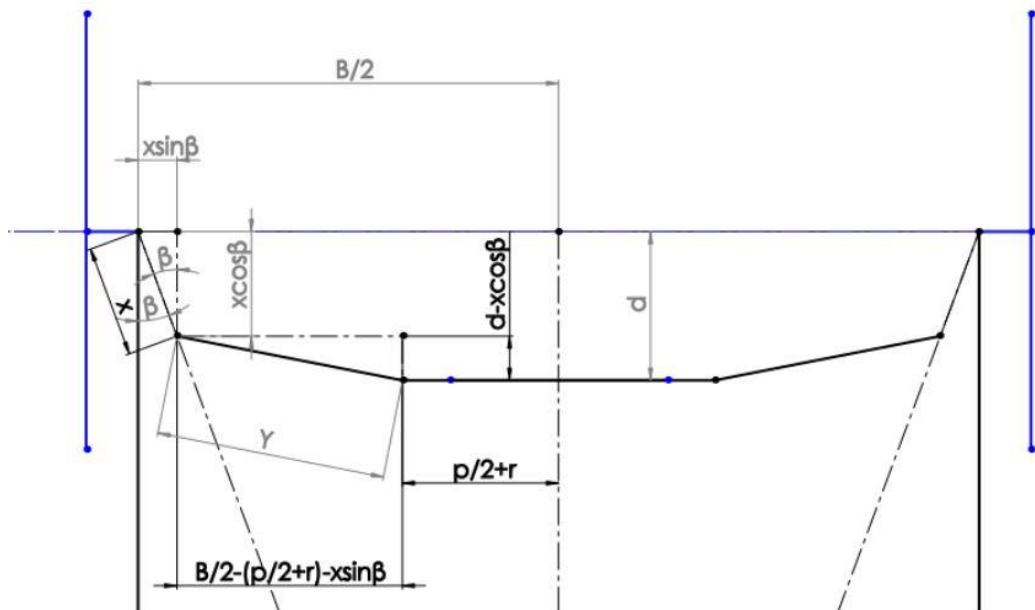


Figure 46: Rack-and-pinion geometry. Initial zero toe condition

Where the variables are:

Table 15: Variables in rack-and-pinion model

α_0	Outer wheel angle
α_i	Inner wheel angle
x	Steering arm length
γ	Tie-rod length (in top view)
p	Racket length
$p + 2r$	Distance between racket's end joints
q	Racket travel
d	Distance between centre line the of wheels to the racket
β	Ackerman angle

The geometry gives the relation:

$$\gamma^2 = \left(\frac{B-(p+2r)}{2} - x \sin \beta \right)^2 + (d - x \cos \beta)^2 \quad (4)$$

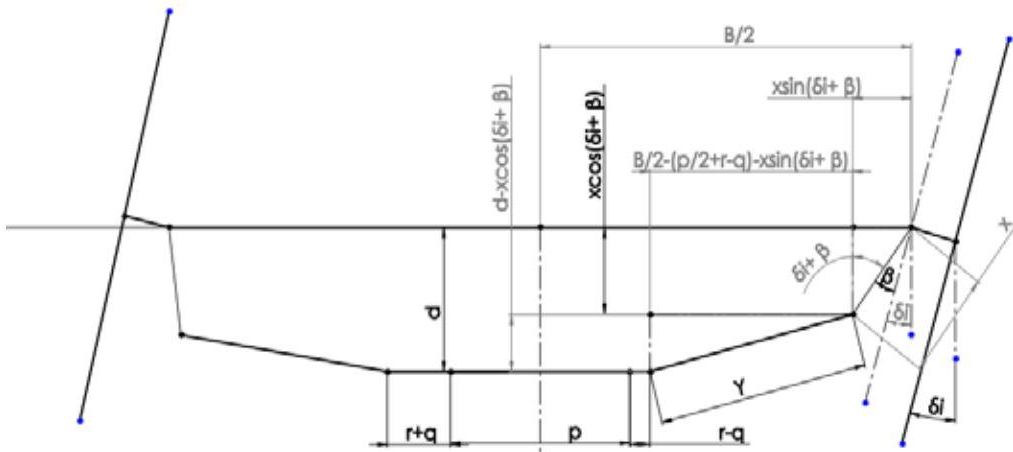


Figure 47: Rack-and-pinion geometry. Inner wheel angle

In cornering manoeuvres, the geometry in Figure 47 gives the relation:

$$\gamma^2 = \left(\frac{B}{2} - \left(\frac{P}{2} + r - q \right) - x \sin(\alpha_i + \beta) \right)^2 + (d - \cos(\alpha_i + \beta))^2 \quad (5)$$

Table 16: Rack-and-pinion parameters

Ackermann angle β	23 °
Steering arm length γ	95 mm
Racket offset d	120 mm

6.4 Further optimizing

The chosen steering parameters above was optimized to get the lowest racket travel error at the lowest turning radius (6 m). All though this gives very low error for the rest of the turning radius', a better optimization would be to get the lowest error through the corners the vehicle will encounter the most on the track in London. For this, A MATLAB Script was written. To reduce the complexity, the variables was reduced by one; the steering arm length was fixed. The spreadsheet had confirmed that this length would allow the lowest turning radius over a range of the most appropriate Ackermann angles. The script imports the track data and extract the track radius of all the increments. The racket error is calculated for each increment. Now, an indicator of the mean track travel error through the whole track can be found. This calculation was done on a range of Ackermann angles and racket offset distances. The results are presented as 3D-plots.

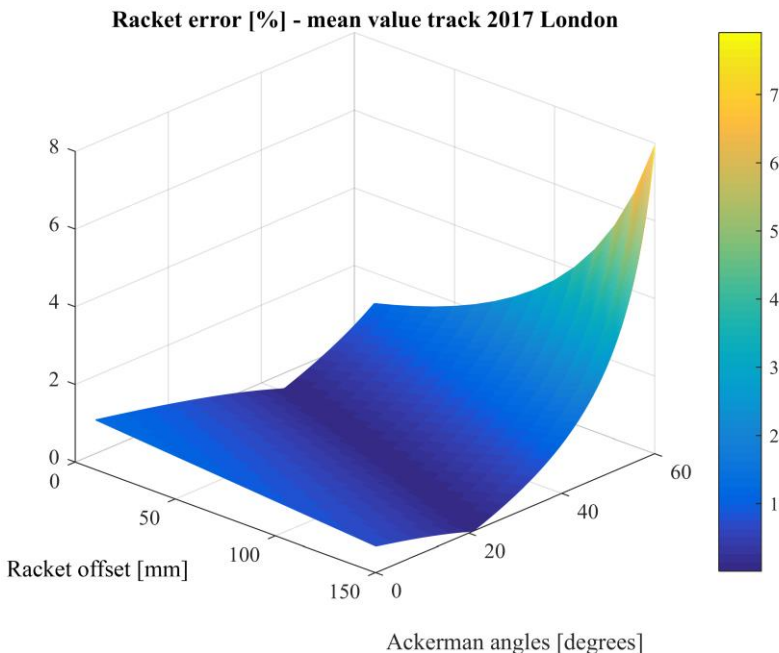


Figure 50: Calculated mean of racket error through the London track of 2017

The plot in Figure 50 clearly shows the best configurations along a valley in the surface. However, all these configurations are not necessary possible, as they may exceed the maximum travel the racket can physically do. Figure 51 displays the need rack travel of the configurations to be able perform the lowest turning radius of 6 m.

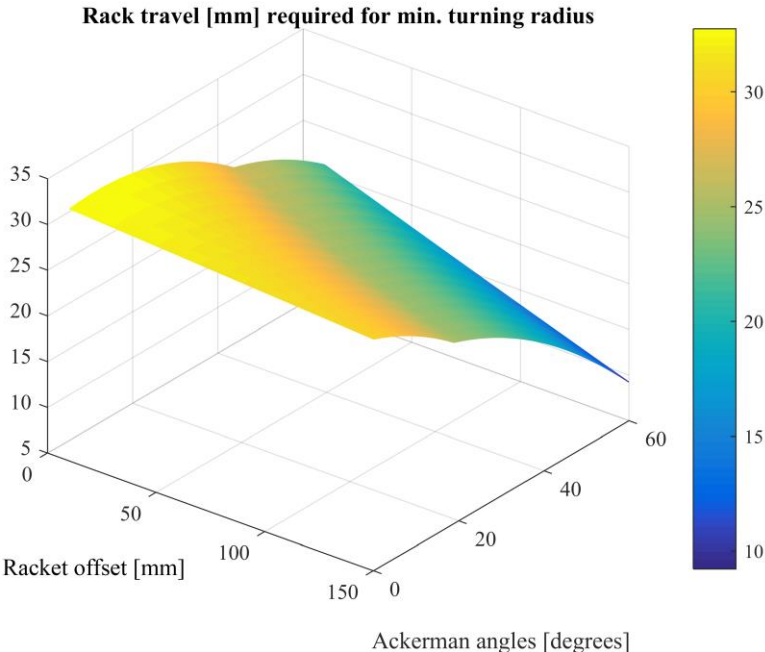


Figure 51: Required racket to meet turning radius requirement of 6 m

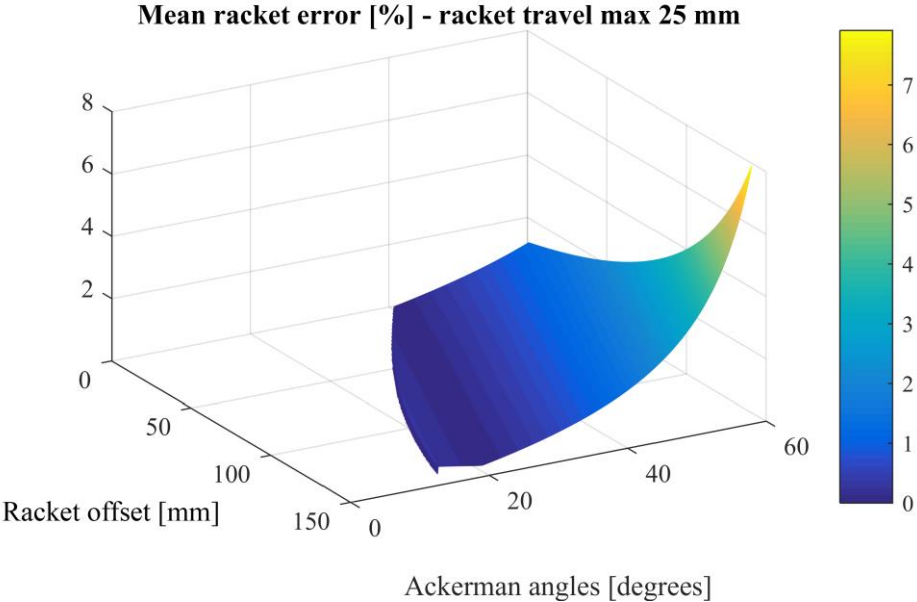


Figure 52: Mean racket error, where configurations exceeding the max travel of the racket are removed

Using the required rack travels, the configurations outside racks limitation are removed from the mean racket error plot, presented in Figure 52. Fortunately, the line of best configurations (lowest mean error) are still possible. The contour plot in Figure 53 better illustrates the exact location of this minima line. It shows that any point along minima line will give the lowest error of below 0.05. In our case, choosing an Ackermann angle in the lower range is preferred, because of the space restriction in the wheel wells. The initial racket offset of 120 mm was kept, as this would give the preferred placement of the steering column. The corresponding Ackermann angle along the minima line is 24°.

Table 17: Improved rack-and-pinion parameters

Ackermann angle β	24 °
Steering arm length γ	95 mm
Racket offset d	120 mm

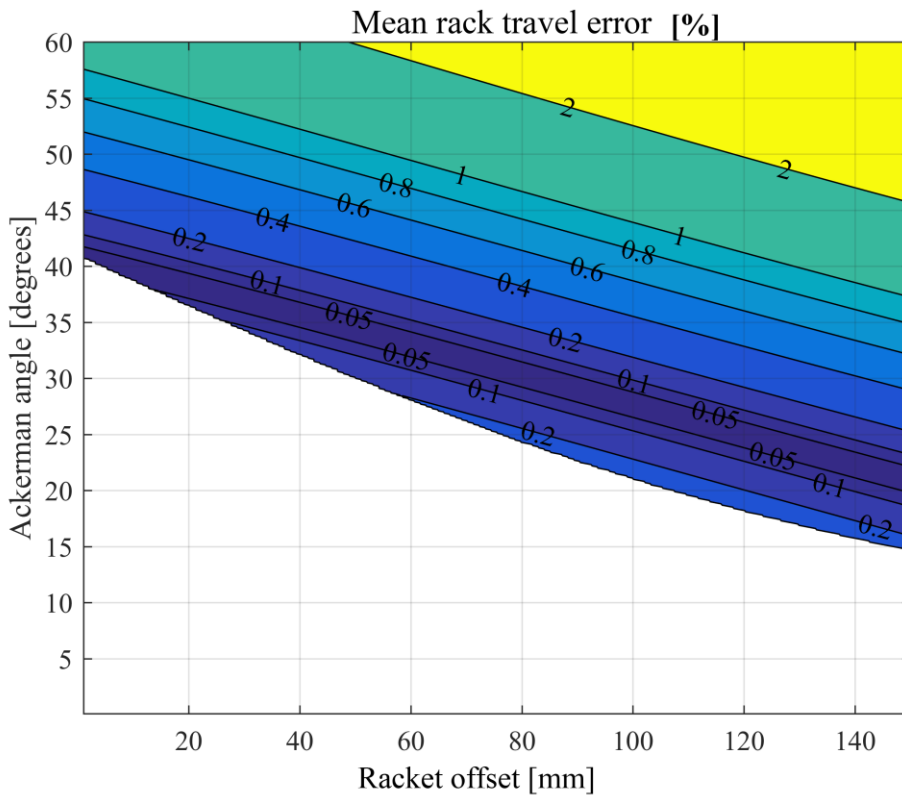


Figure 53: Detailed contour plot of the mean racket error

The inner and outer wheel angles

Figure 54 presents the relation between inner and outer wheel angle obtained by the rack-and-pinion configurations. For comparison, a stipulated line shows the ideal turning angles

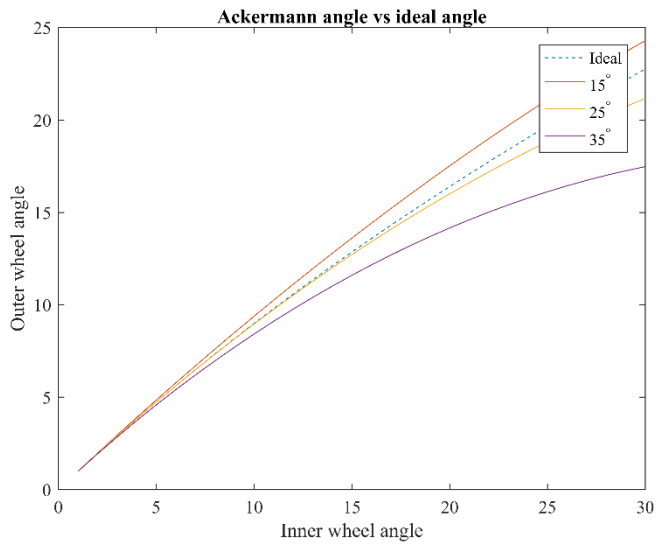


Figure 54: Obtain relation of inner and outer wheel angle, racket offset 120mm

Derived from the graph above, the difference from the ideal outer angle is shown in Figure 55.

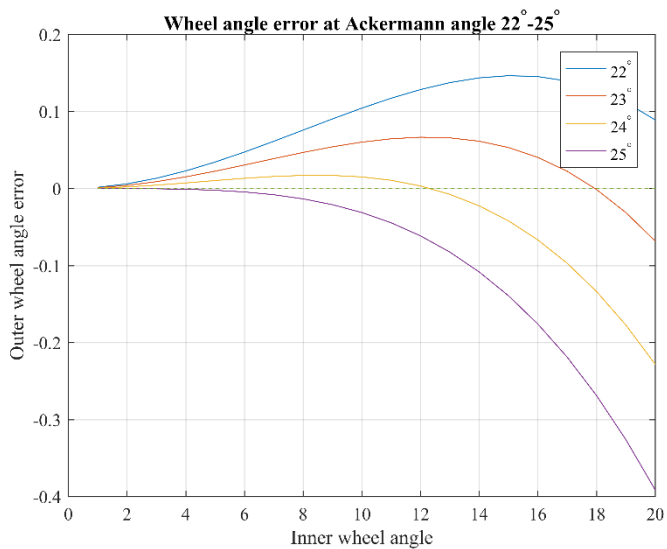


Figure 55: Outer wheel angle error (difference from ideal angle). Fixed Racket offset: 120mm

The curve of 23° Ackermann intersects the zero-line at about 18° inner wheel angle, which corresponds a turning radius of 6m. The curve of 24° Ackermann, shows a slight error at this angle, but the fit is much better at lower angles which is what our vehicle will encounter the most in the race.

7 Front suspension

7.1 Parameters of driving performance

Camber

A negative camber increased the cornering stiffness of the tire meaning better stability while turning (Meywerk, 2015). Also, with increased cornering stiffness, there will be a reduction in power loss associated with the slip angle. However, as discussed in the project thesis, the relevant speeds and turns in the Eco-marathon race will produce very small slip angle in the tyres. Further in disfavour of cambered wheels, is the fact that the wheels won't be flush with the chassis body. The overall efficiency gained from a streamlined body and optimized aerodynamic overshadows the efficiency gained with slight negative camber.

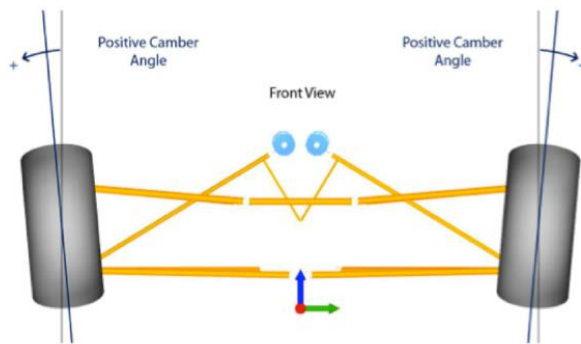


Figure 56: Camber angle

King pin inclination

This parameter is defined by angle between the steering axis and the wheel centre line, seen from the front of the vehicle. It is a parameter contribution to stable steering, and it should be positive as seen in Figure 57. Turning the wheel about the steering axis shown will lift up car slightly and a small force must be applied to the steering wheel to allow the movement. Letting go of the steering wheel and the same force pushes it back. This gives the steering a natural tendency to go back to the initial position of straight ahead.

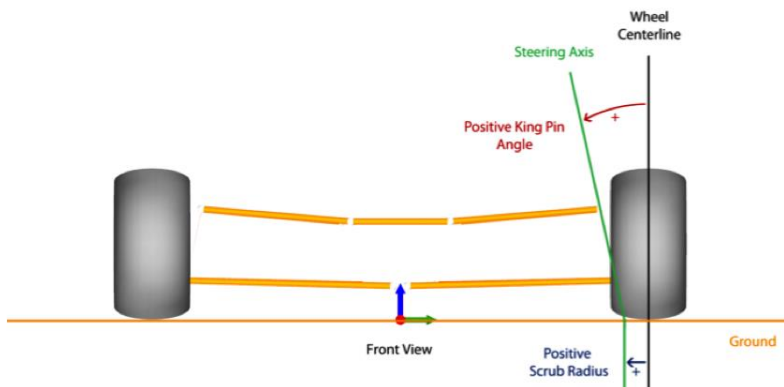


Figure 57: Kingpin inclination

Caster

The caster angle is the angle between the steering axis and wheel center line, seen from the side of the vehicle. A positive caster angle makes wheels self-center at higher speed, contributing to stable steering. The contact patch between the wheel and the ground is trailing behind the steering axis. The contact patch creates a moment force about the steering axis, if the wheel is turning – making it go back to straight line driving.

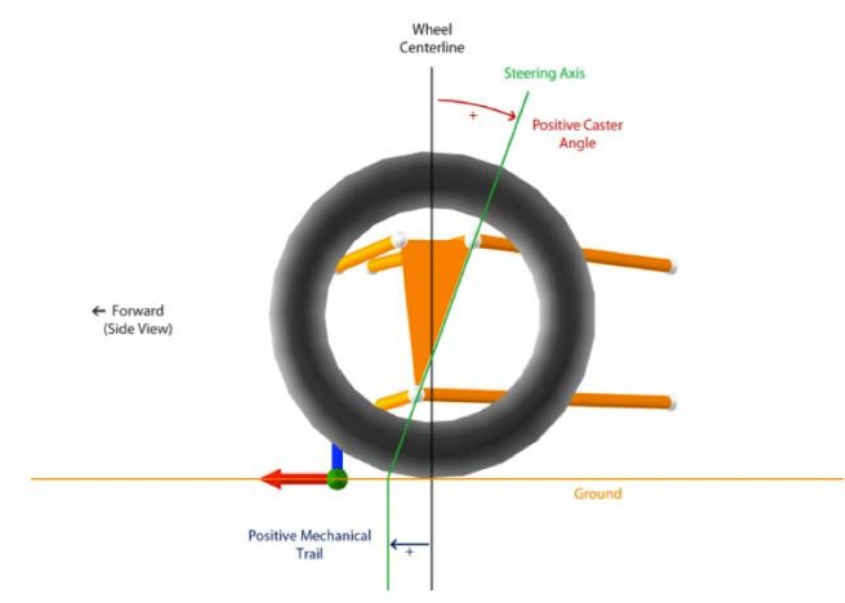


Figure 58: Caster angle

Toe in/out

With the steering in its initial position, the toe angle is defined between the direction of travel and the direction of the wheel. A positive toe angle (toe out) provides the car with better stability in high speed cornering. The obvious tire rub that will occur implies that a fuel-efficient car should have zero toe angle. The toe angle is not static, but is effected by the steering. This is discussed in the steering section.

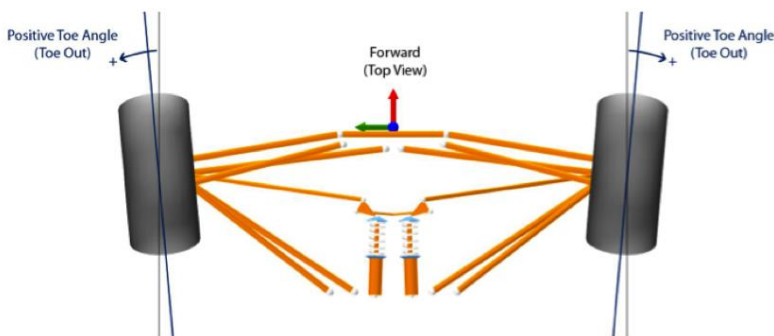


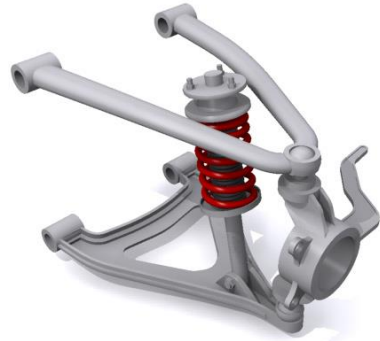
Figure 59: Toe in/out

7.2 Front suspension systems

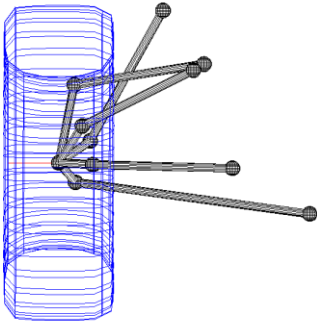
There are three main front suspension systems used on cars. This section gives a comparison of their features.



(a) MacPherson strut



(b) Double wishbone



(c) PA Simionescu 2006

(c) Multi-link



(d) Semi Multi-link

Figure 60: 4 common front suspension systems (Longhurst, 2017), (Simionescu,2008)

Table 18: Suspension systems

	MacPherson Strut	Double wishbone	Multi-link
Few parts	☑☑☑	☑☑☐	☑☐☐
Adjustability	☑☐☐	☑☑☐	☑☑☑
Complexity	☑☐☐	☑☑☐	☑☑☑
Torsion of shock absorber	Yes	No	No
Torsion of arm(s)	Yes	Yes	No

(a) **MacPherson strut** consist of few parts which reduces the risk of failure, as well as the possibility of a lightweight design. On the other hand, this design requires far more rigid shock absorber. The shock absorber in the other alternatives only experience compression force, while a MacPherson shock absorber must withstand torsion arising from brake force.

(b) **Double wishbone** introduces a second arm to support the wheel. As mentioned, this removes the moment force in the shock absorber. While braking or acceleration the wheel is hold in place by the arms.

(c) **Multi-link** is a collection term of suspensions supported by only rods and universal joints. This has the benefit that the suspension parts only have compression and tension force. The system can also be highly adjustable, and the parameters of performance can be adjusted independently. However, the adjustment is complicated. It is usually done with computer software solving the three-dimensional geometric relations. Some car suspension are a combination of double wishbone and multi-link; (d) **Semi multi-link**. In our research, we found the multi-link to be mostly advantageous in race cars and off road cars with large suspension travel. As the performance differences are smaller for stiff suspensions and due to the complexity of the system, we decided not to further investigate multi-link system for our vehicle.

7.3 Choosing front suspension system

Shock absorbers

At first, coil spring became the natural choice of shock absorber to consider, as they are common on production cars. It was calculated that an appropriate spring stiffness and travel length would be 30 N/m and 50 mm respectively. A bit too rushed, without further research, a couple of springs with the mentioned values was order. As it turns out, the weight of the delivered springs was over 350g each. Additional to the high weight, we were not satisfied with the fact that the shock absorber would have a fixed stiffness. The shock absorber should be adjustable to finely tune the stiffness vs comfort – pushing the stiffness to reduce the bouncing energy loss, while not too stiff on the expense of the driver’s comfort. Also, high stiffness gives large spikes in the dynamic forces acting on the vehicle.

Further research on suspension springs led our attention to pure air shock absorbers for mountain bikes. They offer very low weight and by adjusting the air pressure the stiffness is adjusted. Fox Float R air shock absorbers suited our requirements and with a weight per unit of only 300g, that is 50g less than just the coil spring alone. It was decided that they would be our primary choice of shock absorbers, and 4 units were ordered from the UK.



Figure 61: Fox Float R air shock absorber

Suspension systems

The table shows which variables we want adjustable:

Table 19: Suspension variables

Variable to adjust	Reason
Ground clearance	The travel, and initial position of the shock absorber is unknown.
Sideway placement of the wheel	High precision in getting the wheel in correct position. If this adjustment were fixed, error in CAD/manufacturing or minor changes may set it off position.
Camber	

Variable that can be fixed by design:

Fixed variables	Reason
Caster	Low tolerance in requirements
King-pin	

MacPherson strut consist of few parts which reduces the risk of failure and errors, as well as the possibility of a lightweight design. On the other hand, this design requires far more rigid shock absorber. The shock absorber in the other alternatives only experience compression force, while a MacPherson shock absorber must withstand torsion arising from brake force. We assume the Fox Float R air shock absorber would not be able to withstand these forces, especially not the moment. The option would have been to build a custom spring shock absorber.

Adjusting the camber and wheel position with a *MacPherson strut* required repositioning of the connection point of the shock absorber and the top of the wheel well. A rigid enough mount in the wheel well to allow the adjustment adds weight and complexity, reducing those advantages of the system. The camber and wheel positioning can be adjusted much easier with a *Double Wishbone* suspension, where it is just a matter of adjusting the length of the wishbone arms.

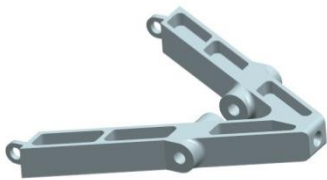
We predicted a solution with double wishbone in combination with light air shock absorbers to outperform a MacPherson setup both in weight and ease of adjustments.

7.4 Design for production

The suspension parts were going to be made with CNC-milling with 3 axes, and therefore had to design within the restriction of this production method. The personnel at the NTNU workshop are busy, and the CNC-milling can be time consuming. Some guidelines for the production with CNC-milling:

- No more complexity than needed \Rightarrow reduce production time
- Smallest radius of the geometry defines the cutting tool diameter \Rightarrow depending on overall geometry size, but above $\sim R4$ and the whole part can be made with the same cutting tool.
- Minimum top surfaces with an incline. In 3-axes, the cutting tool must cut stairs to create the incline, which again is time consuming.
- Design for single-side machining if possible. Eliminating the need to flip the workpiece. The flip and reattachment to the jig is time consuming, as well as a source of error and reduction in tolerances.
- This is not prototyping. The design should have been verified with prototyping to weed out any errors of the design. Expect several weeks for the production, which means getting the part correct at the first try is highly recommended.

The wishbones were suitable for single-side machining. The steering knuckle needed milling on both sides as it is not flat because of the king pin inclination.



(a) -over dimensioned



(b) – under dimensioned

Figure 62: Early designs

The design of the suspension parts were guided by FEM-simulations. The braking force, cornering force and the force from the weight of the car where applied to the suspension as seen in Figure 63. “Spiders”, which connect nodes of the mesh to a common point, are used to position the forces and support at the correct location in space, i.e. the forces in the contact patch between the tyre and the ground, which transfer forces to the hub.

The dimensioning parameter were the yield strength (0.2%) of 460 MPa for Aluminium 7075-T6, and deformations below “reasonable” amounts. Generally, under normal driving conditions the deformations should be low enough to not infer the driving performance parameters. However, in an emergency braking scenario, more deformation is allowed. It does not matter in that situation if the wheels are temporary bent to an inefficient position.

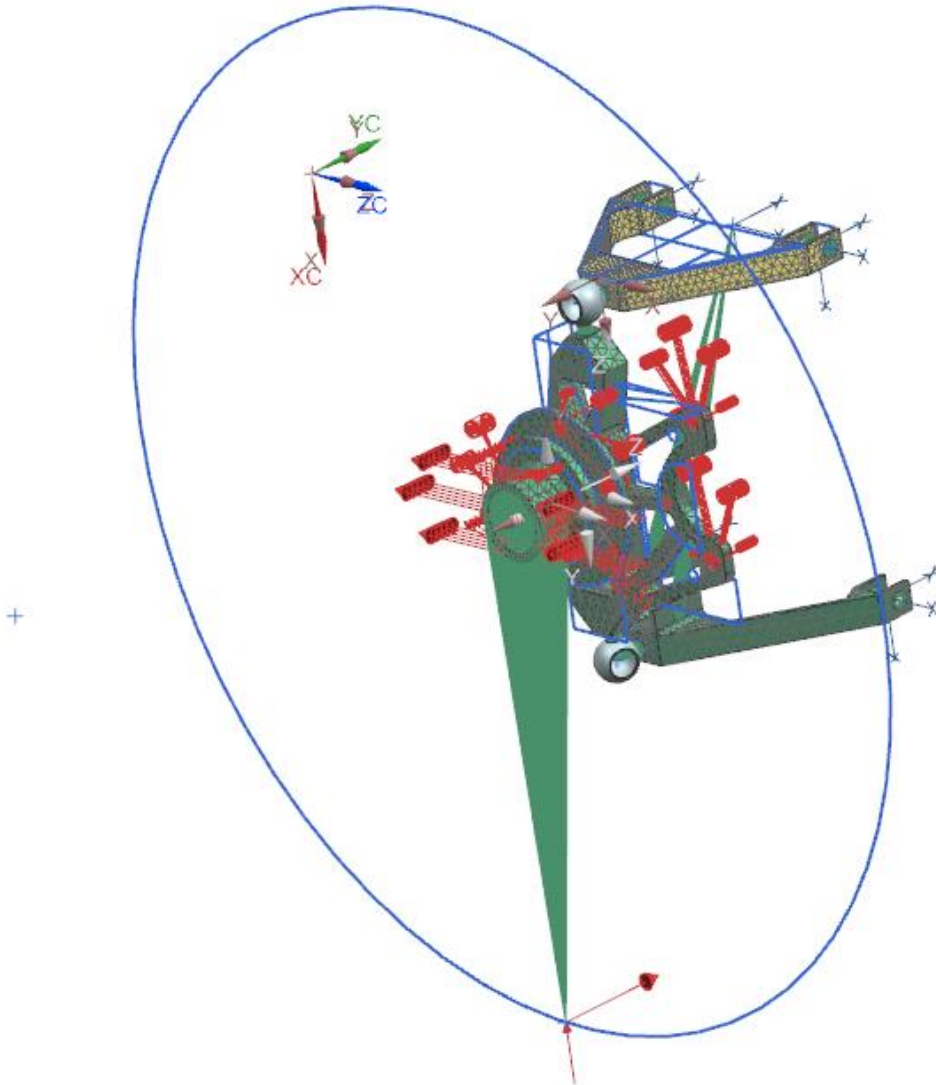


Figure 63: FEM-model. Support and forces on front suspension

The results from FEM simulation of the final design of the front suspension is presented in Figure 64 and Figure 65. The load case shown is an “all loads case” – turning, braking and weight force simultaneously. The maximum stress found is 354 MPa, which gives a safety factor of 1.3. The deformation is only up to 3.7 mm in this “all loads” case. The construction can be considered very stiff.

Frontsuspension_sim1 : Solution 1 Result
 Subcase - Static Loads 1, Static Step 1
 Stress - Elemental, Von-Mises
 Min : 0.00, Max : 353.64, Units = N/mm²(MPa)
 Deformation : Displacement - Nodal Magnitude

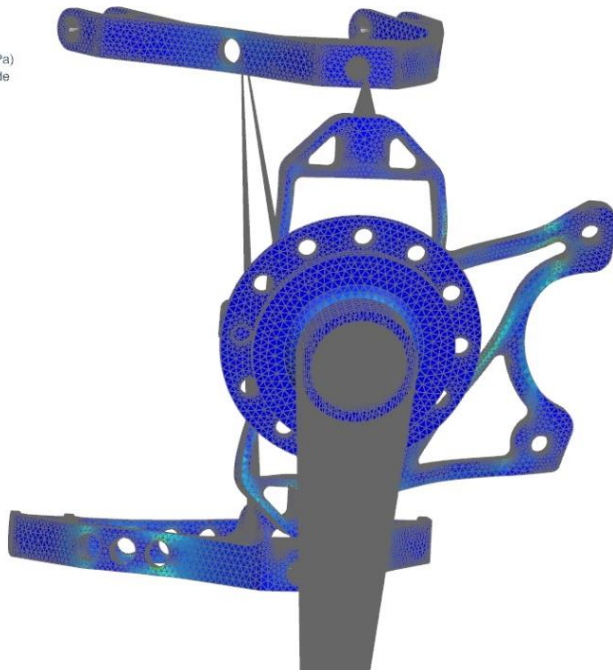


Figure 64: Von Mises Plot - front suspension

Frontsuspension_sim1 : Solution 1 Result
 Subcase - Static Loads 1, Static Step 1
 Displacement - Nodal, Magnitude
 Min : 0.000, Max : 3.705, Units = mm
 Deformation : Displacement - Nodal Magnitude

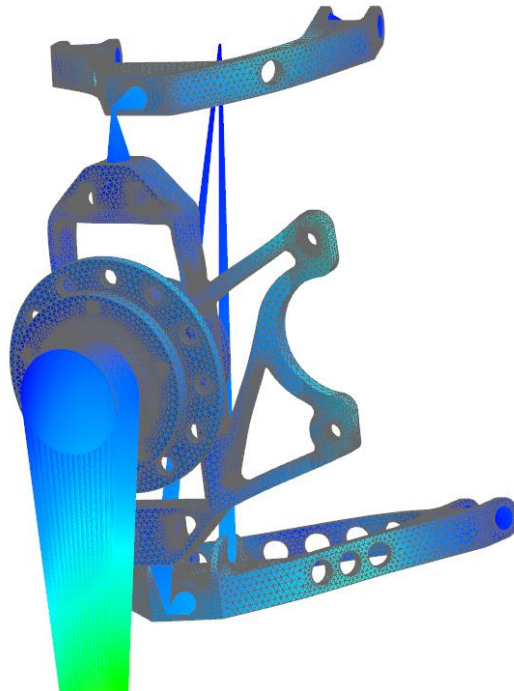


Figure 65: Deformation plot - front suspension

Special ball joints are used to connect the steering knuckle to the wishbones. The ball joints fit into a hole in the front of the wishbones. How long the ball joint sticks out can be adjusted, which will adjust the camber and the sideways wheel position.



Figure 66: Final design of the wishbones and the steering knuckle

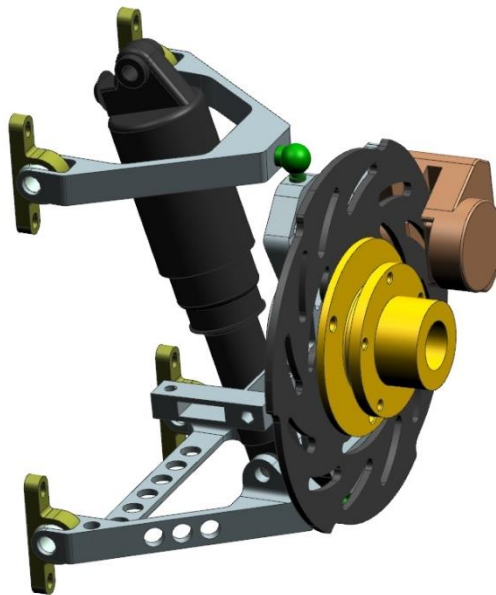


Figure 67: Front suspension with all parts (wishbones, steering knuckle, steering arm, wheel hub, brake disc, brake calliper, shock absorber)

8 Rear suspension

As described in the project report, we decided to use trailing suspension in the rear. By mounting the suspension directly into the bulkhead, we eliminated the need for rear wheel wells. In addition to the removed wheel wells, the strength needed in the floor behind the bulkhead was also reduced. These changes made the monocoque lighter, cheaper and easier to produce.

During design, there were a lot of shared considerations as with the front suspension. Both were CNC-milled in a 3-axis mill, so the same guidelines applied. The same shock absorbers were used, as they are light and adjustable. The same aluminium alloy was also used. An early model was designed to test the concept of trailing suspension (see Figure 68). This version was designed before the drivetrain concept was decided. We now wanted to mount the motor on the suspension such that it follows the movement of the wheel. This would reduce movement in the drivetrain. A problem occurring in earlier years has been that the belt has been slipping on the pulley. But the efficiency of the drivetrain will be reduced if the belt is too tight. We wanted a system where we could adjust the tension easily.

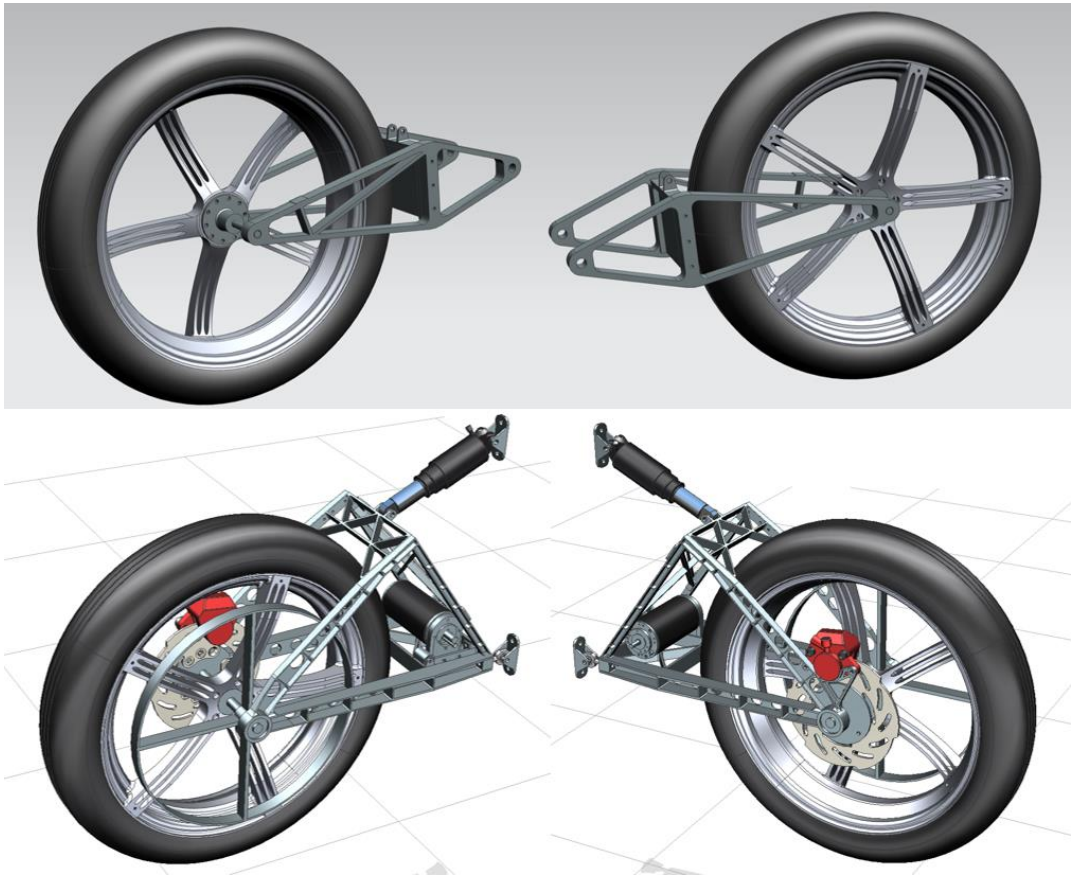
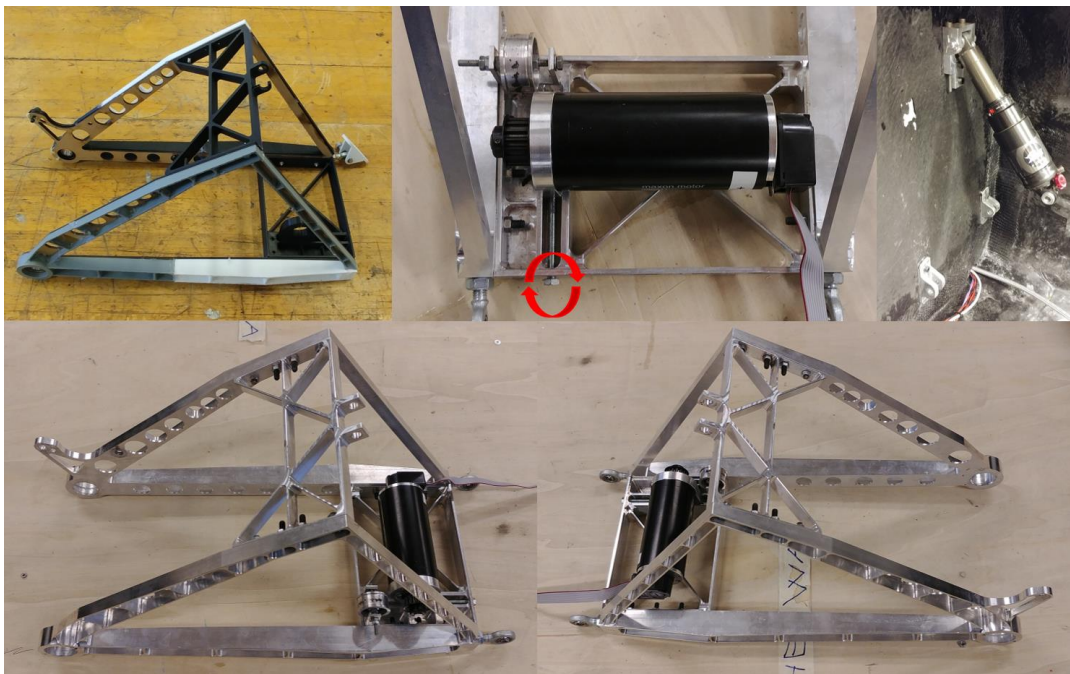


Figure 68: Top row: Early version - Bottom row: Final version

We solved this with a system where the placement of the motor was adjusted by rotating a screw (see circled area in Figure 69). By first loosening two screws on the underside, the motor could slide in the slot. The motor mount area is designed such that it accommodates both types of motor we have chosen, and could be modified if another type of motor is to be purchased later. By making the side triangles hollow/walled instead of solid, the second moment of area increases and they get stiffer. That reduces displacement. The walls could have been made taller and thinner to further increase the second moment of area, but we were advised not to as walls thinner than 1.5-2 mm easily warp while milling. They are also inclined to give a higher stiffness. The suspension was made quite tall to lift the mounting point of the shock absorber. By shifting the shock absorber into a more horizontal position, we transfer force from the shear vector to the compression vector. Thus, we reduce the stress on the bulkhead mounting elements. A disadvantage of the design is high material waste if usage can't be found of the material area inside the triangles.

We 3D-printed a model of the rear suspension before it was produced to visualize it, check the dimensions and look for any oversights. It fitted in the monocoque as intended, and the aluminium versions were produced.



*Figure 69: Top row: 3D-print, Motor mount and Bulkhead mount.
Bottom row: Milled rear suspension*

The design of the rear suspension was an iterative process using FEM-simulations and the geometry was tweaked to optimize the strength-to-weight ratio. The dimensioning parameters are the same as with the front suspension. Figure 70 shows a situation of heavy braking in a corner. “Spiders” are also used here. The red arrow represents the braking force, the yellow is the cornering force, and the blue is the weight of the car and driver.

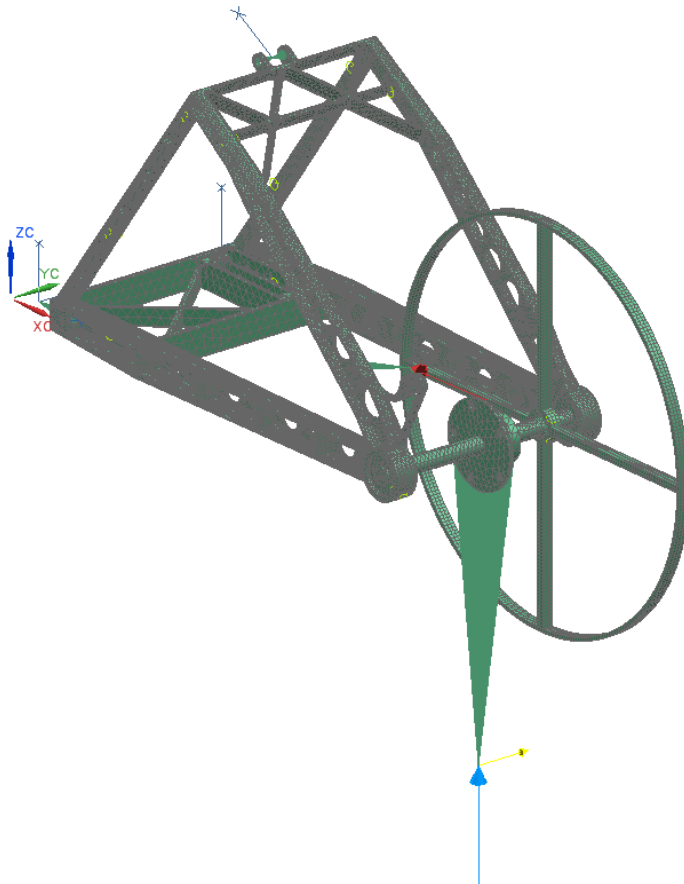


Figure 70: FEM-model. Support and forces on rear suspension

The results are presented in Figure 71 and Figure 72. The maximum stress occurs on the brake caliper mount, and is 290 MPa. That gives a safety factor of 1.59. The maximum displacement is at the contact patch between tyre and ground, and amounts to 13.3 mm. This is an acceptable value and difficult to reduce with this kind of suspension.

drivetrainAssembly_sim1 : SOL101 Result
SvingBrems, Static Step 1
Stress - Elemental, Von-Mises
Min : 0.00, Max : 290.24, Units = N/mm²(MPa)
Deformation : Displacement - Nodal Magnitude

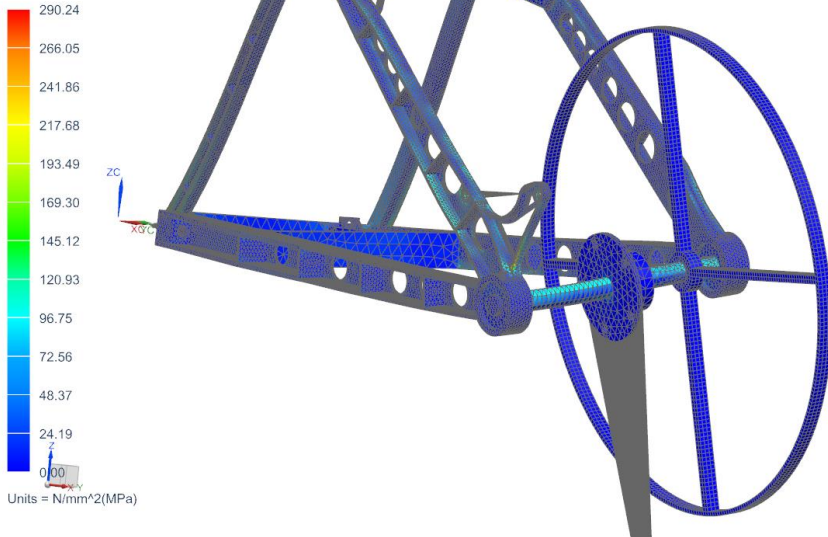


Figure 71: Von Mises Plot - rear suspension

drivetrainAssembly_sim1 : SOL101 Result
SvingBrems, Static Step 1
Displacement - Nodal, Magnitude
Min : 0.00, Max : 13.29, Units = mm
Deformation : Displacement - Nodal Magnitude

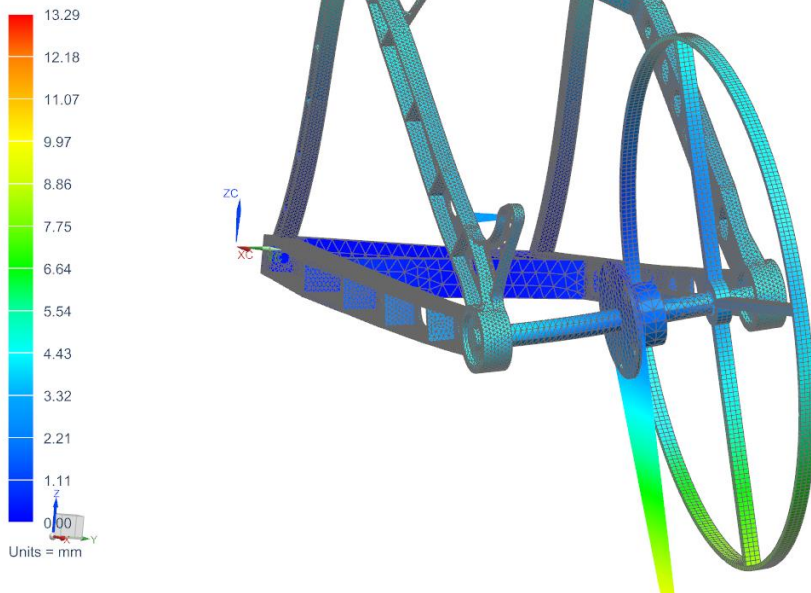


Figure 72: Deformation plot - rear suspension

9 Powertrain

The system that converts the energy in the battery to mechanical power propelling the vehicle; arguably the most important subsystem of a car. Regarding the efficiency of a car, it is also the most important variable. The car can be built light, the drag can be minimized and the wheels may roll almost without friction – which reduces the force needed to move the car. However, in the end this force must be delivered, and if the powertrain does not do that efficiently, the first mentioned properties will be irrelevant.

9.1 Powertrain jig

To be able to test the motors and drivetrain components before car is finished, it was decided to construct a powertrain jig. It is built very rigid to not allow any deformation interfering with the tests of powertrain components. Sliding plates gives the possibility of infinite number of configurations. On the second axle, a torque sensor is mounted. On the end of the axle there is a generator to apply counter force to the system. The generator was not able to produce enough braking force, so an additional friction brake of wood was installed.

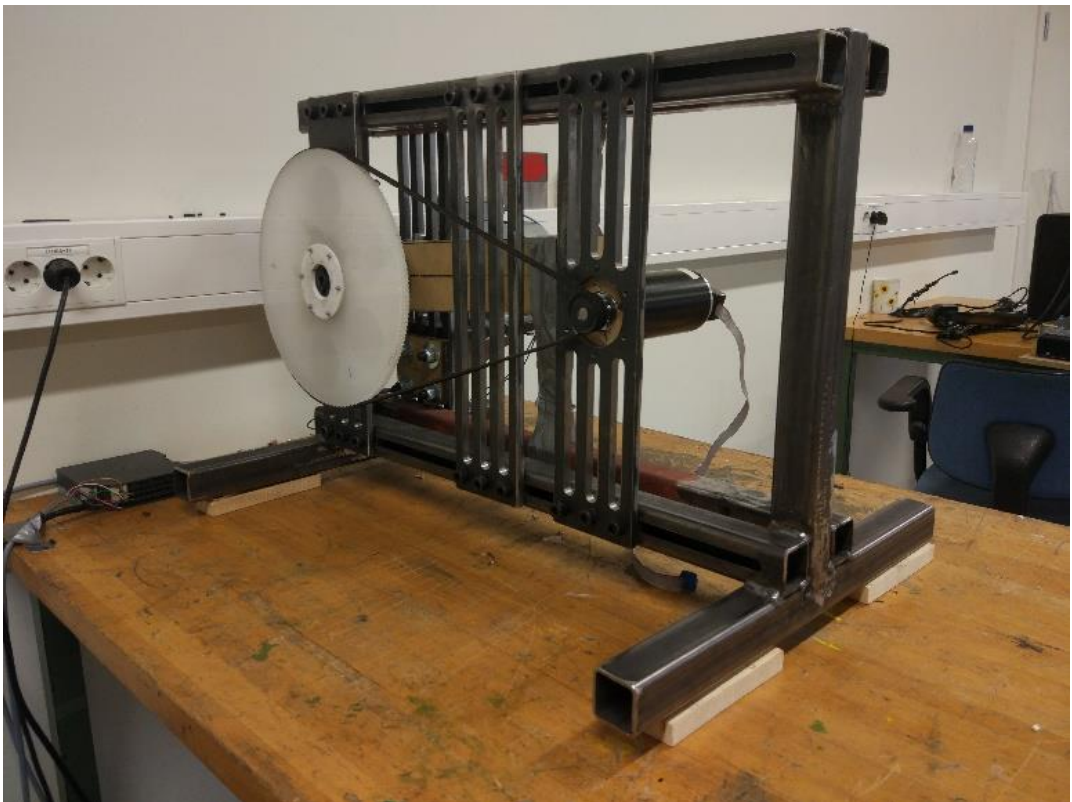


Figure 73: Powertrain jig, front view

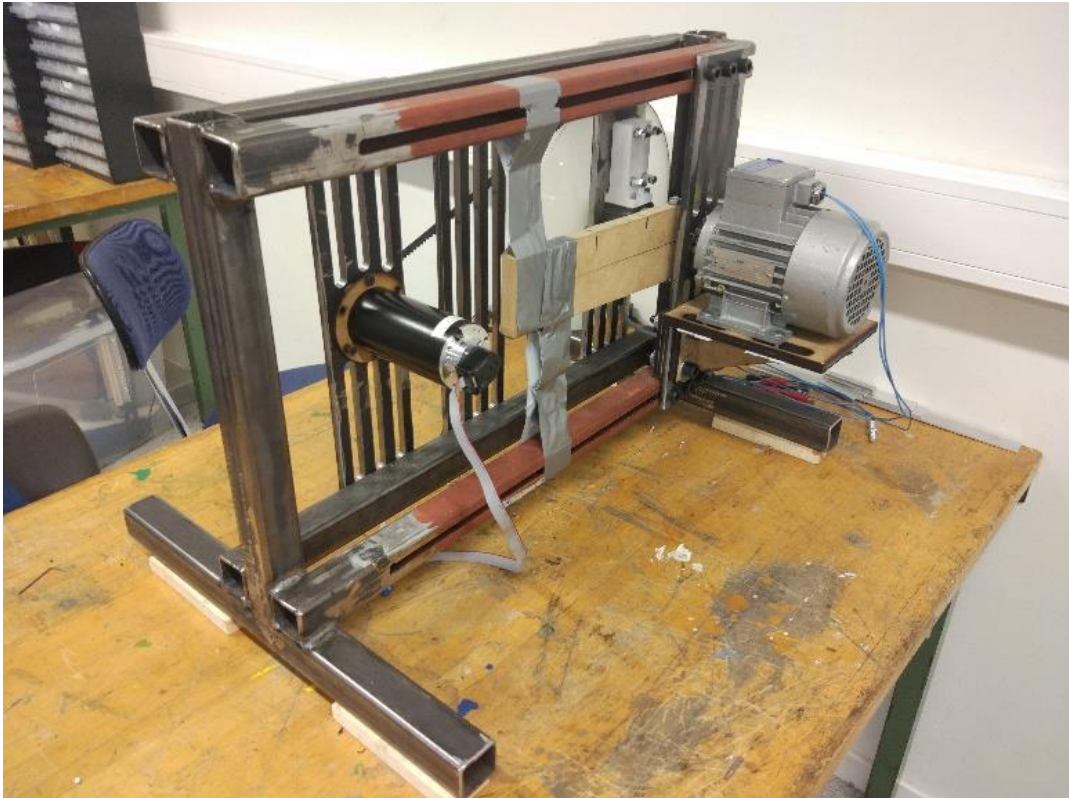


Figure 74: Powertrain jig, back view

9.2 Drivetrain

The work of the autumn semester concluded on drivetrain system being either a synchronous belt drive (Figure 75-2), or an internal gear ring setup (Figure 75-9). The discussion is continued in this section, followed by the conclusion on the selected alternative.

DRIVETRAIN CONCEPTS

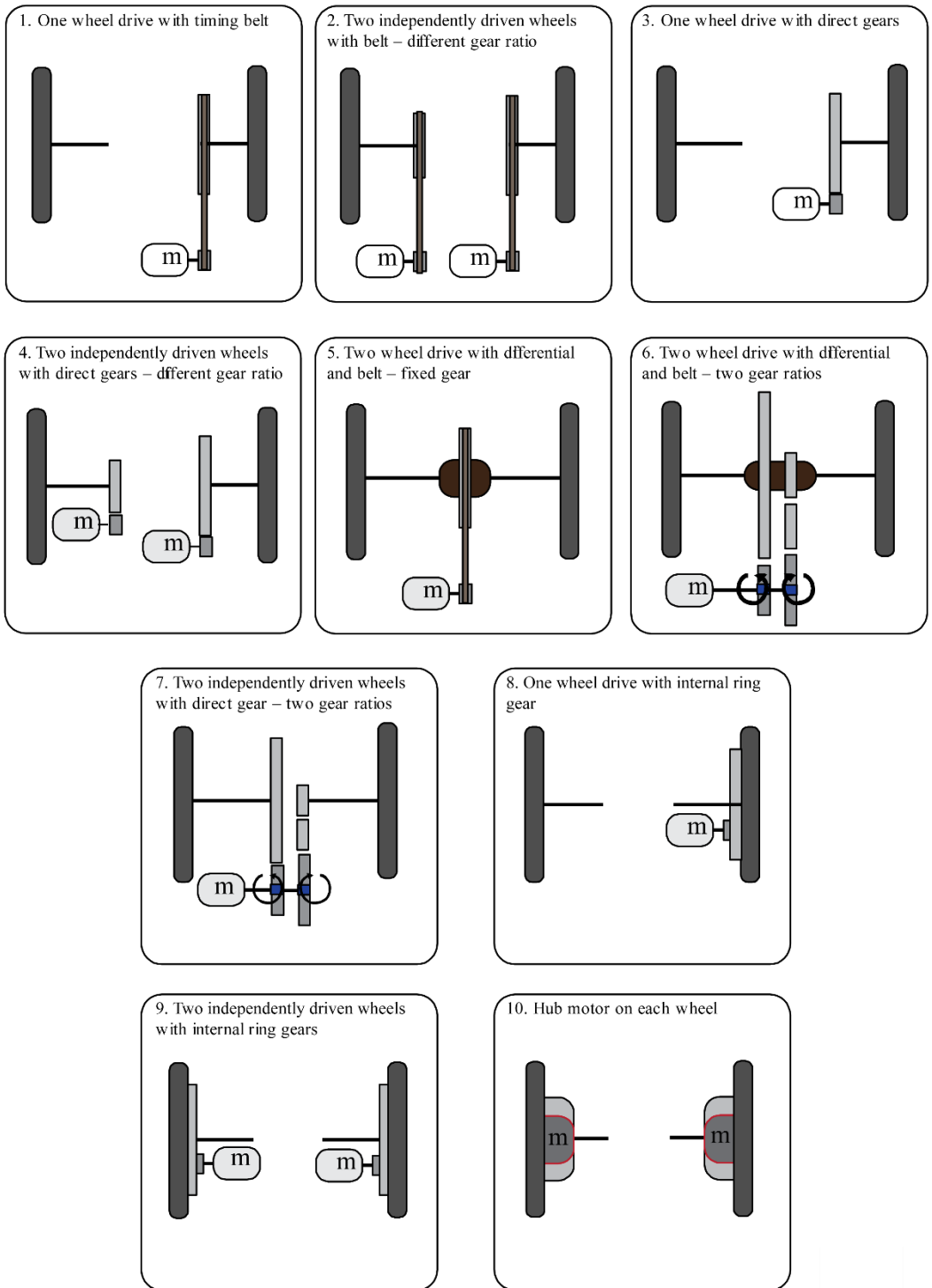


Figure 75: Drivetrain alternatives

Table 20: Gear comparison

	Internal spur gears	Synchronous belt
Efficiency	<i>Above 99%</i>	<i>98-99%</i>
Manufacturing tolerances	<i>High</i>	<i>Medium</i>
Backlash	<i>Yes</i>	<i>No</i>
Quite operation	<i>Normally, No</i>	<i>Normally, Yes</i>
Forces	<i>Conc. on single tooth</i>	<i>Spread over many teeth</i>
Vibration transfer	<i>High</i>	<i>Low</i>
Precision in positioning of parts	<i>High</i>	<i>Low</i>

Internal gears

Direct gears have the possibility of even higher efficiency than the synchronous belt. However, we saw some challenges with the direct gears:

- A precis position between the gear pairs is impossible to maintain, as the large cogwheel is situated on the wheel which deforms and bends because of the forces from the road. Thus, the requirement for perfect efficiency is not met.
- The risk of failure due to vibration transfer, which is what happened to an earlier team.

As we saw it likely that we would achieve roughly the same efficiency for both solution, the belt solution became in favour due to smoother operation and better handling of the inevitable deformation of the back suspension.

9.3 Production of pulleys for the belt drive

Initially the plan for the pulley was to cut out the pulley from an aluminium plate with Electrical discharge machining (EDM) at the Production and Quality Engineering workshop. In the design process, it was discovered that the pulley only need walls of few millimetres thickness, due to the relatively low loads. Machining this, on the other hand, would be very difficult. It was discovered that plastics would be a better suited material. The density is much lower than aluminium, while still stiff and tough enough for the intended use. The pulleys could therefore be manufactured in more convenient dimensions, while still being lighter than aluminium.

Our sponsor VINK AS provided us with nylon plates. EDM is obviously not possible on plastics. We looked into the possibility of manufacturing them with the water jet machine at Trondheim Stål. They provided us with a small test segment of the pulley. The segment was very precise, and we chose to use water jet to produce all the pulleys. The pulleys can be seen in Figure 76. Two different design were made. The first, was guided by FEM-simulation to push the limit of the design (Right pulley in Figure 76). The second a safer design, in case the FEM-simulation was very wrong. This, as we had no experience with designing mechanical parts in plastic, and reliability of FEM with plastics. Concerns were:

- Less stiffness than anticipated
- Less toughness than anticipated
- Warpage/throw

Fortunately, the FEM-analysis predicted correct, and the most extreme design proved to perform excellent. The throw after the machining was minimal, only a few millimetres could be measured. Stress test of the pulley was done in the powertrain jig, and no issues were found. We were confident that the most extreme design would hold for the loads delivered by the motor in a race situation.

There is a risk of the belt falling off the pulley. Rims were laser cut in polycarbonate plastic. The pulley, being so large, can be seen outside of the chassis when viewing the car from the side. To make the pulley blend with the wheel, it was chosen to paint the rims black and make the outer rim cover the whole pulley (Figure 77-a).

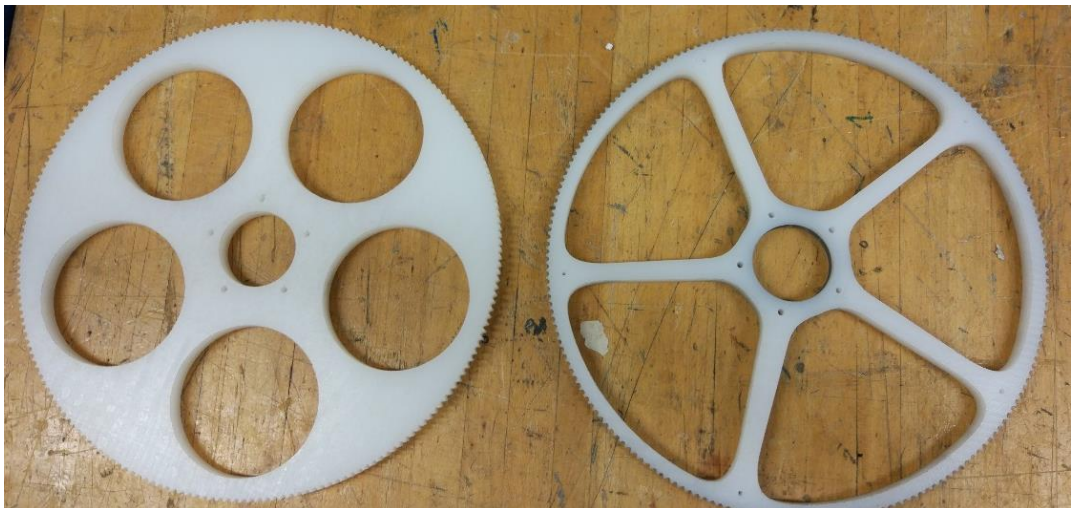


Figure 76: Nylon pulleys



(a)



(b)

Figure 77: Pulley rims

9.4 Motors

The Eco-marathon completion only allows custom built motor controllers for the battery-electric class.



Figure 78: Maxon brushed DC motor

Initially, the electrical team researched how to build a motor controller for brushless DC-motor, as we already had some of these motors in the workshop. Brushless DC-motors are becoming increasingly popular, mainly due to the advantage of their operation lifetime exceeding 10 000 hours, while brushed DC-motors could need replacement of the brushes as early as after 1000 hours. Brushes also create sparks, the brushless motor eliminates this, making them suited for operations in environments with flammable gases (Titus, 2012). Marginally higher efficiency is possible with a brushless motor, as the friction of the brushes is removed.

It was soon found out that building our own brushless motor controller was too complicated and comprehensive to have a complete and functioning prototype before SEM. It was decided to only buy brushed DC-motors and develop a motor controller for these.

Extensive web searching and looking through motor supplier's catalogues was done to find DC-motors. The specific characteristic we were looking for are presented in chapter 2: Product requirements.

Maxon Motor, a swiss premium DC-motor company, stood out for best suited motors. The many time winning prototype vehicle Pac Car II (Santin, 2007) agrees on Maxon providing most efficient motors, and specifically their brushed motors, which is found in the Pac Car

In the end, two RE50 (200W) and one RE65 (250W) were bought. Comparing their datasheet, the RE50 has the highest rated efficiency of 92%. The RE65 has efficiency peak of 88%, but the motor can provide much higher power and torque. The motors may be overloaded (doubling, or tripling the rated torque) for a certain period of time. Exceeding this time, and the motor will be overheated. RE65 has a much longer overload time period than RE50. There were three reasons to also include buying the more powerful RE65:

- Uncertainty of the RE50 being powerful enough to climb the hill.
- The RE50 could make it up the hill, but the long period of overloading while heat up the motor, where the efficiency is drastically reduced.
- Discussed later in this section, the RE65 is more efficient than RE50 when there is a need for high torque i.e. climbing the hill, and under acceleration. In the UrbanConcept class there is a complete stop each round, followed by acceleration to full speed.

Maxon motor provides documentation and motor theory through their portal Maxon Academy. They present the following formulas for the relations between RPM n , applied voltage V_m , current i and motor torque τ . The constants are found in the specific motor's datasheet.

$$n = k_n \cdot V_m \quad (8)$$

$$n = k_n \cdot V_m - K_g \cdot \tau \quad (9)$$

$$\tau = K_\tau \cdot i \quad (10)$$

Now, the electric power going into the motor can be compared to the mechanical power going out.

$$P_{in} = V \cdot i \quad (11)$$

$$P_{out} = \tau \cdot \omega = \tau \cdot \frac{\pi}{30} n \quad (12)$$

Finally, the efficiency of the motor can be calculated

$$\eta = \frac{P_{out}}{P_{in}} \quad (13)$$

A MATLAB script was made to calculate the efficiency of all operations of the motor. The results are visualised as contour plots (Figure 79Figure 80). The plots reveal the most efficient operations zone of the motors. The model may not be 100% correct to the real motor performance, but the deviation would probably not be substantial.

With the powertrain jig we hoped to confirm/correct the efficiency matrices. Unfortunately, we were not successful in obtaining meaningful results as our measurement equipment did not meet the required accuracy.

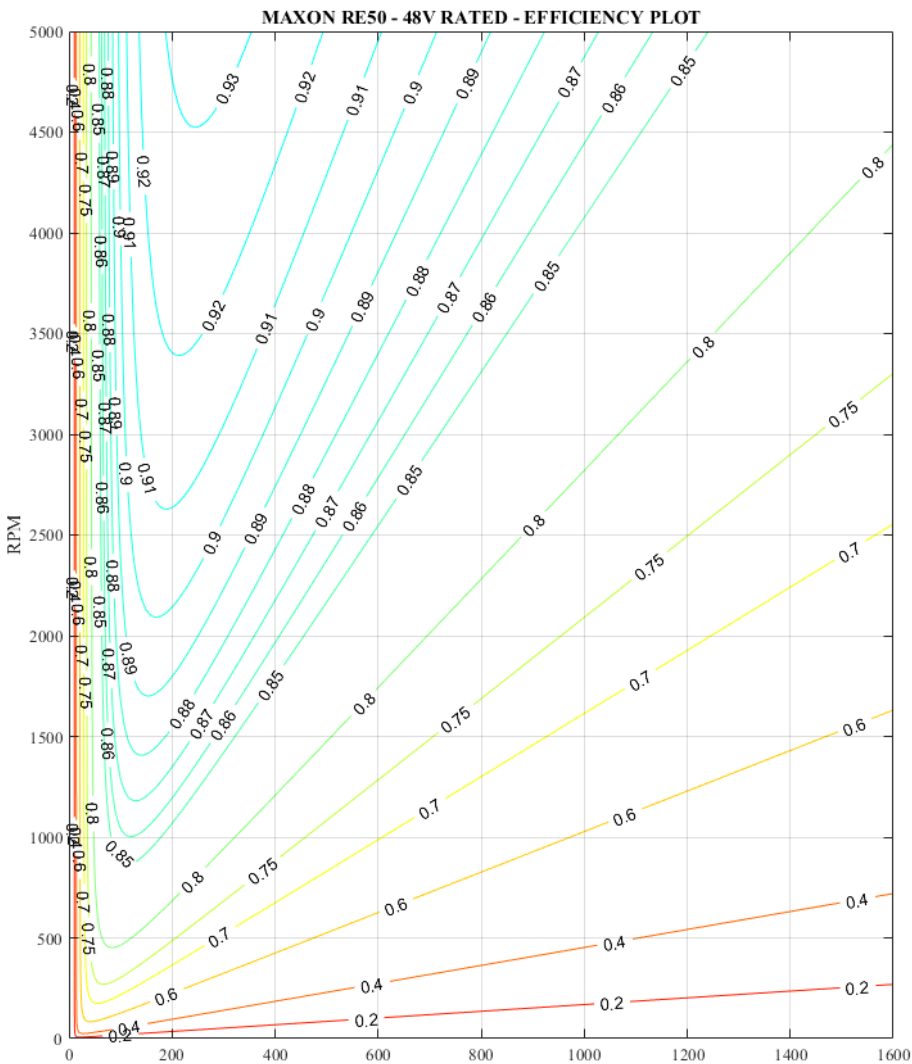


Figure 79: Efficiency plot of Maxon RE50

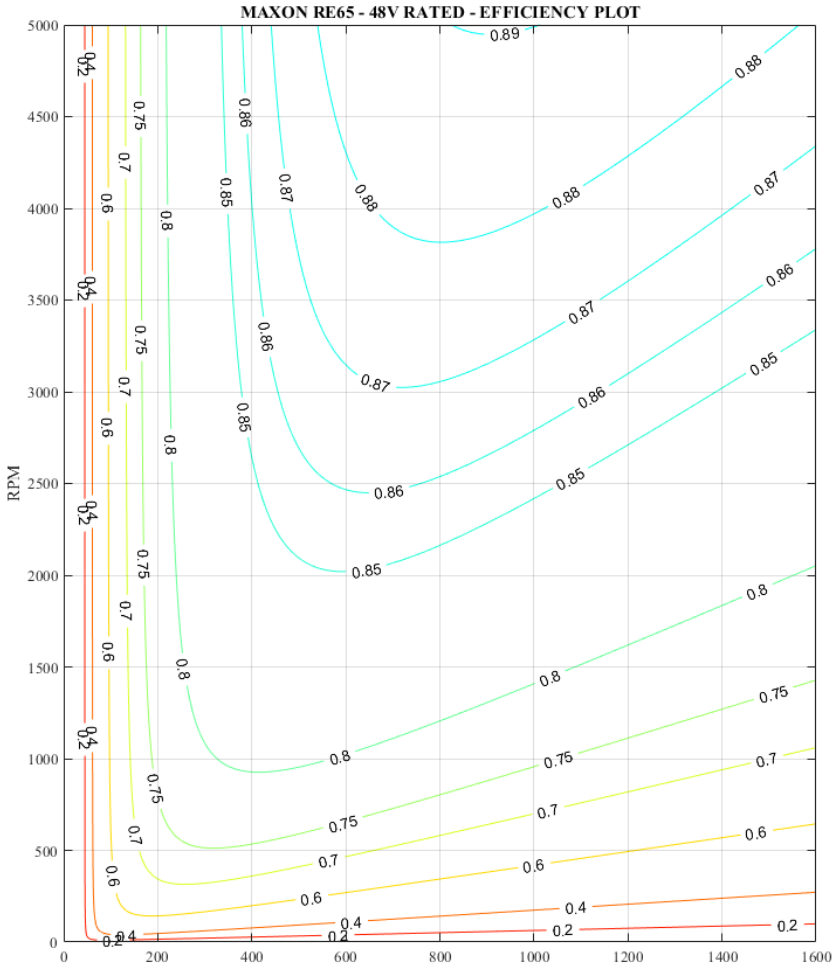


Figure 80: Efficiency plot of Maxon RE65

9.5 Selection of gear ratio

The efficiency plots show that the motors are most efficient for high RPM, therefore the gearing should be high. However, it must not be too high not allowing the desired top speed. Initially, an idea was to have one motor responsible for the lower speeds, and be geared accordingly. At the top speed limit of this motor, the second motor would take over, with a lower gear, delivering the power for the higher speeds. This way, the amount of time the motors spends at inefficient low RPM is reduced. Further investigation the idea, and it was found that the second motor responsible for the high speed, would give a very slow acceleration up to the top speed – practically never reaching it. The conclusion was that both motors must be geared for the same top speed, so the acceleration up to top speed can be done with the help from both motors. At steady state driving speed, one of the motors may be turned off, if that is more efficient. A range of small pulleys for the motors were bought to achieve a top speed in the range 30-50 km/h.

10 Windows

The rules for visibility in SEM states: “The Driver must have access to a direct arc of visibility ahead and to 90° on each side of the longitudinal axis of the vehicle. ...” (Article 28a). This must be achieved without the use of any optical or electronic devices. I.e. we need a front window and side windows. There is also a requirement for a window for visual access to a Joulemeter in the motor compartment. In addition to the formerly mentioned, we also needed windows for the front- and rear lights.

The monocoque design requires that the front- and side windows are double curved. This makes production challenging and distortion can easily occur. Distortion reduces visibility, and thus safety, and is unwanted. Tinted front- and side windows would be a beneficial feature, as it would reduce direct sunlight in the driver’s eyes and heat rise in the driver compartment. Thus, improving driver comfort and performance. As a safety precaution, the Shell Eco-marathon rules states “Windows must not be made of any material which may shatter into sharp shards. Recommended material: Polycarbonate (e.g. Lexan)” (Article 25f).

The front- and side windows were decided to have the requirements in Table 8.

The team that built the Prototype vehicle 2014 were advised by the company that made their windows, Prototal AS, to use PMMA (also known as acrylic glass or Plexiglas). The reasoning was that it would give less distortion than other materials. They were also advised to use 2 mm sheets, as thinner may lead to an unevenly stretched product. They were in doubt whether if they would get through the technical inspection at SEM as PMMA may shatter and had extra windows made of polycarbonate (PC). This year a side window on the Prototype accidentally shattered during transport. This proved that PMMA is not an acceptable material. We opted to use polycarbonate (LEXAN™) with a thickness of 2mm as recommended by Shell. The thickness was also chosen as we were unsure if a 1 mm would handle the force from the windscreen wiper.

10.1 Production method

One advantage of Lexan is that it can be thermoformed into a variety of shapes. There are several techniques for forming, which involves the basic steps of heating, forming and cooling of the sheet.

Drape forming is the simplest technique of thermoforming (illustrated in Figure 81). The sheet is placed on top of either a negative- or positive mould. They are then put in the oven where the Lexan sheet softens and shapes itself after the mould under its own weight. Drape forming won't give detailed geometry and requires that the mould won't be affected by the heat.

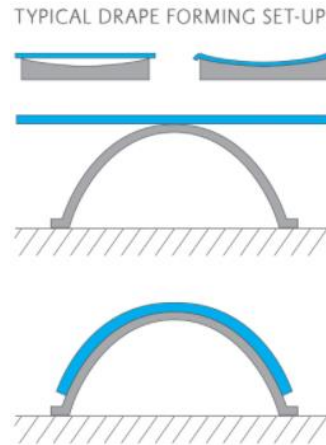


Figure 81: Drape forming

Vacuum forming (as illustrated in Figure 82) is a widely used method of thermoforming. The sheet is held in a frame and heated. After heating the sheet is placed over the mould such that the frame creates a sealed edge. A vacuum is created to remove the air between the sheet and the mould. This allows for more complex geometries than drape forming. A variation of vacuum forming is bubble forming (Figure 83). After heating, air is pumped into the sheet to create a bubble. This to avoid thinning of material with deeper moulds.

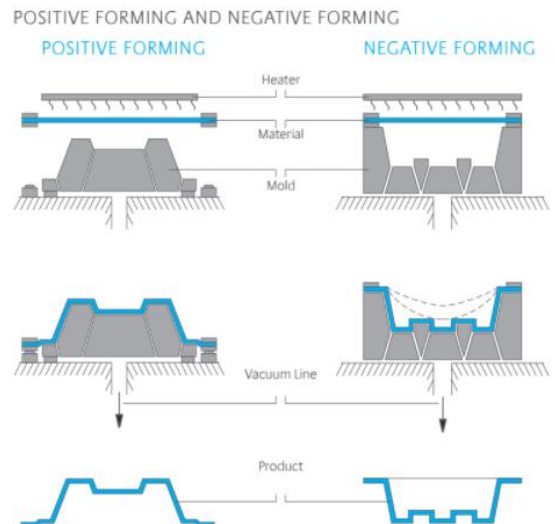


Figure 82: Vacuum forming

Pressure forming (illustrated in Figure 84) consists of the elements in vacuum forming. In addition, compressed air is applied on the positive side of the mould during forming. This is done to force the sheet closer to the mould, which results in a more detailed geometry.

We chose to use vacuum forming to make our windows. We get a better result than with drape forming and we don't need a mould that can go in the oven. We don't have easy access to a pressure forming machine, and don't need the Lexan to enhance fine features.

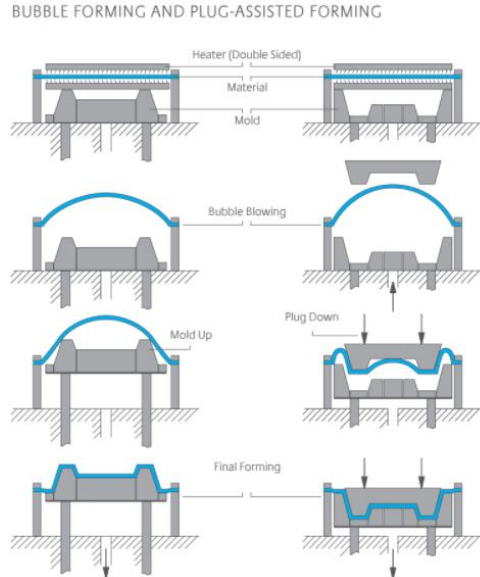


Figure 83: Bubble forming

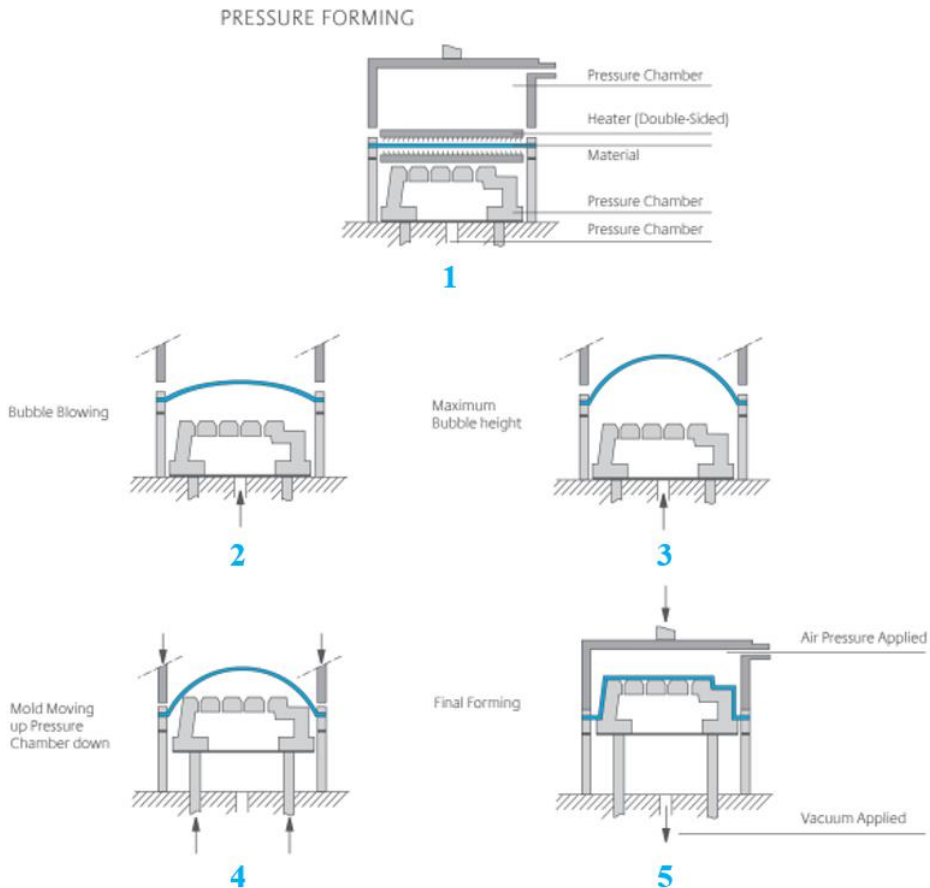


Figure 84: Pressure forming

10.2 Moulds

We needed positive moulds to make our windows. As cost was an important factor, we wanted to produce them at NTNU from affordable materials. We got access to the wood milling machine at the institute and decided to use medium-density fibreboard (MDF) as material for the moulds. MDF is not well suited to go in the oven. Since Lexan sheets cool rapidly, they must be placed over the moulds as quickly as possible once they come out of the oven during production. The finish will also be acceptable when the MDF moulds get a surface treatment.

The geometry of our window moulds was extracted from the CAD model of our car. We could not make the window moulds of casts from the vehicle mould as it was destroyed after the body had been finished. The placement of the windows for rear lights and motor compartment aren't in the model. Their size and position on the vehicle were still considered.

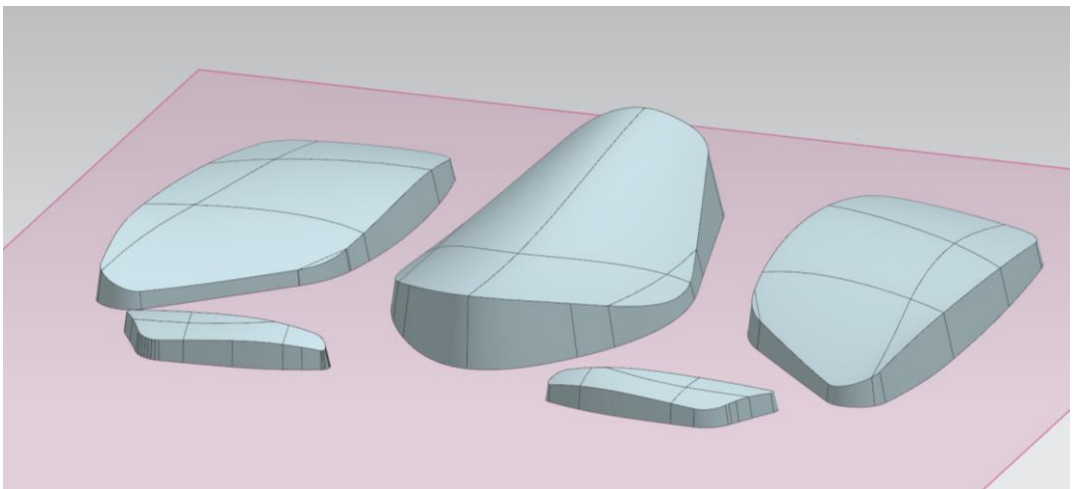


Figure 85: CAD models of window moulds

The milling machine can't do the depth of the larger moulds. The models were therefore sliced into parts of smaller depth, which were milled and assembled. We went over the surface of the moulds with sandpaper (ranging from 120 to 800 in grit size), cleaned them and coated with floor varnish. This was repeated three times, finishing on cleaning after using a fine sandpaper. The finished moulds are seen in Figure 86.



Figure 86: Window moulds

10.3 Production

Head light windows were the first we made. These were made in the Formech 686 vacuum machine in the workshop. In this we could use the bubble forming method. The machine only heats the upper side of the sheet which easily can cause bubbles in the sheet (as seen in Figure 87). Careful attention is required.

The Formech 686 is not large enough for us to make the front- and side windows in. We therefore made our own setup for vacuum forming. It was a wooden box where the top was drilled holes in and vacuum cleaners were used to suck out the air. We were unsure if two vacuum cleaners would be enough. To test, the holes were covered and the vacuum cleaners were turned on. After a few seconds the top, which was made of chipboard, broke (see Figure 88). We

then knew the setup was effective and made a new top out of MDF.



Figure 87: Bubbles in the Lexan

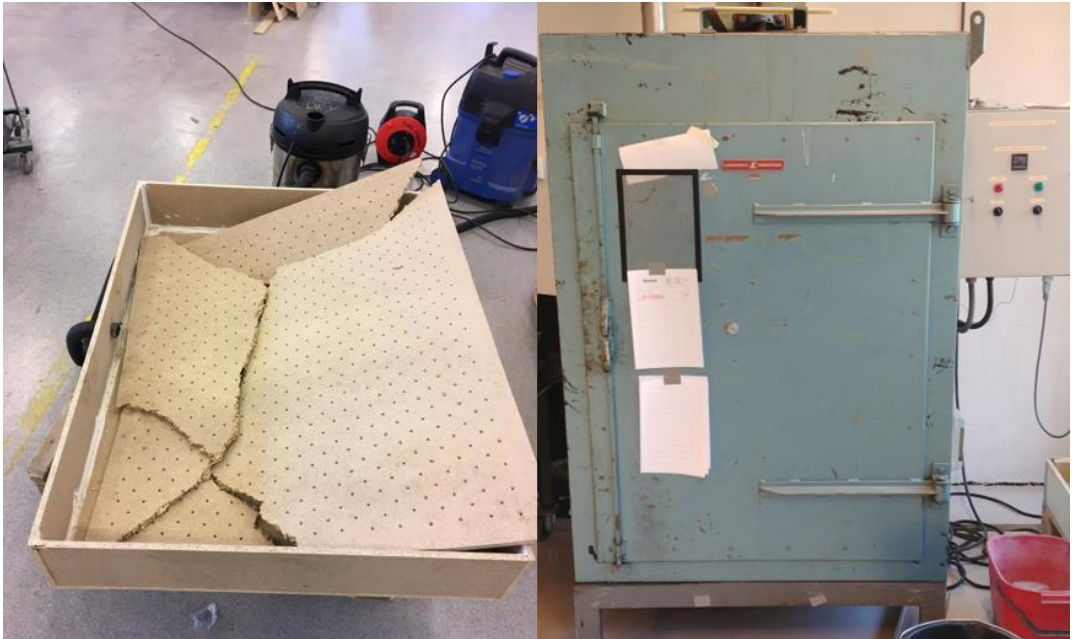


Figure 88: Left: Broken vacuum box. Right: Oven

Side windows were the first we tried on our own setup. We used the oven in Figure 88 to heat the sheets. The sheets were held in frames in the oven. To achieve vacuum, sealant tape was put on the box in where the frame was to be placed.

Normal sheet temperatures are in the process window of 170 °C-225 °C for vacuum forming. (SABIC, 2015) Ideally, the Lexan should have been pre-dried before forming to reduce the possibility of bubbles, where the temperature should be above 120 °C but not exceed 125 °C. We did not have access to a dehumidifying air circulating oven and skipped this step. The oven used was not reliable. After hours of trying to get a suitable temperature in the oven, it was set to 215-220 °C. This softened the sheets without bubbles appearing. We estimate the real temperature was about

160-170 °C as it took a long time to get the sheets soft.



Figure 89: Forming of left side window

The front window was identified as the most important window and was done last, after learning from the other. We switched to a larger oven which was more accurate. In this oven, the temperature was in the area of 180-190 °C when the Lexan was heated. The sheet softened after few minutes, much quicker than the side windows. When the window was to be formed, we didn't manage to seal the edge and create a vacuum. This was due to the frame having slightly warped (see Figure 90) and the sheet should have been bigger. The Lexan could also have been allowed to soften more, but we didn't want to risk bubbles which could quickly appear if it had been heated longer. The Lexan didn't conform to the lower parts of the mould. We thought that it had been an unsuccessful attempt, but discovered that the tension in the sheet disappeared after the window shape was cut out. It was now easy to bend the window into the correct geometry.

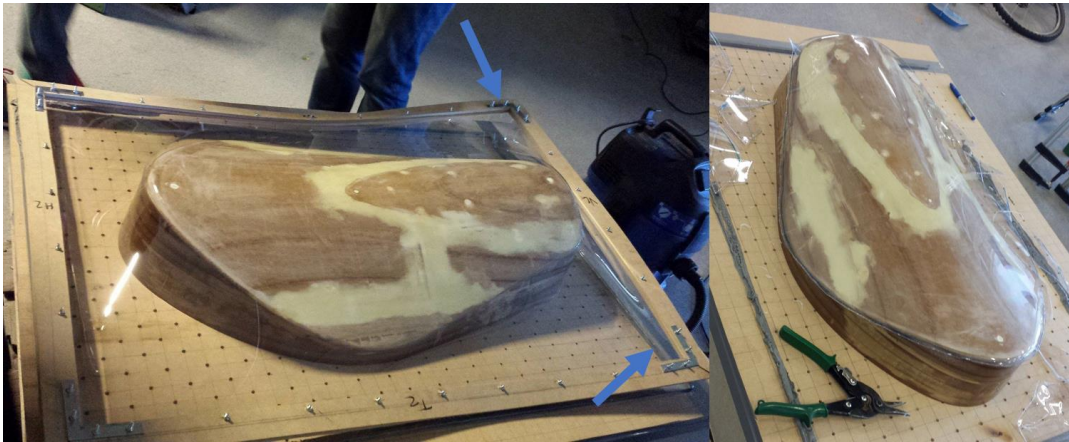


Figure 90: Front window forming

Rear light windows and motor compartment window were made after the holes for them in the monocoque had been made. The compartment window was made by cutting a sheet into a suitable size, then fitted by carefully hand shaping it using a heat gun. We extracted the geometry of the rear lights positions from the CAD-model and 3D-printed holders for the lights that had a close fit to the body. Before installing the lights in this, we used them as guides to shape the rear light windows. This also by using a heat gun.



Figure 91: Motor compartment window



Figure 92: Rear light windows

To mount the windows on the car we needed flanges. The flanges could either be on the vehicle or on the windows. We had body flanges on the front window and the door window. The reason we didn't have body flanges for the headlight windows and our right-side window was that the geometry needed for these flanges would create undercuts in the vehicle mould.

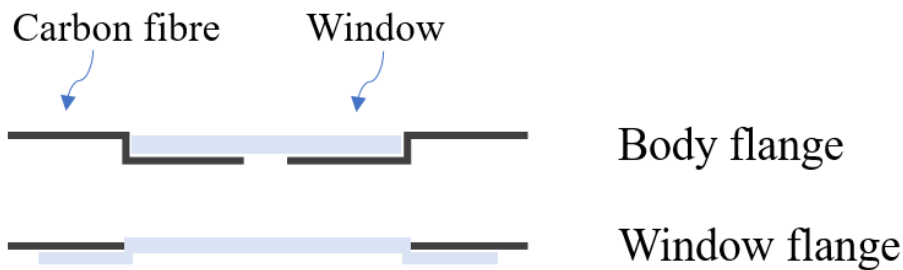


Figure 93: Window flanges

To hold the windows in place, we used Tec7 on the flanges and clamped the windows on until it had dried. The reason for using Tec7 is that it's strong, waterproof and resistant to UV rays. We didn't want the LEDs to show behind the light windows, but still needed the light to be bright. We managed this by using fine sandpaper on the windows.

10.4 Result

Due to the double curvature, we weren't able to put solar film on the windows. We also asked the company that wrapped our car if they could do it since they have experience with it, and neither they managed. Later teams should look into using PC sheets which are already tinted. The front windows turned out decent. It has got some scratches, but nothing major. We managed to form the side windows, but the sheets should have been slightly softer to get better result. They are not as smooth as the front window, and distortions show when looking in the mirrors. We would recommend that new side windows are made where the larger oven is used to have better control over the temperature. It could also be considered to go down to 1 mm thickness. If new windows are made, new frames that are less prone to warping should be made. We made our out of 2 x 6 mm MDF and they warped such that we couldn't get a sealant. Another material should be considered.

11 Interior

11.1 Steering wheel

To steer the car, the SEM rules state that it must be achieved by a system operated by two hands using a turning motion. It must be a steering wheel or section of a wheel with a diameter of at least 25 cm. It is not permitted to use steering bars, tillers, joysticks, indirect or electric systems. We are required to have a “dead man’s safety device” in our vehicle. Its function is to automatically disengage propulsion power if the driver becomes incapacitated. It can be operated by either your hands or feet. We decided that we wanted it on our steering wheel, as it would be easier than to create a foot-operated system. On the steering wheel, we had the choice between a spring-operated accelerator or an electric switch which the driver directly engages at all times during driving. With the rules in mind, we had to produce a steering wheel with our wanted design and function.

We also had the design award in mind when designing the steering wheel. Thus, we had to take into account the parameters in this award, which are aesthetics, ergonomics, technical feasibility, choice of materials and eco-friendliness. The most important for us was ergonomics. The steering wheel in last year’s car was not ergonomic, which is an unnecessary annoyance for the driver. Not just the grip has to be comfortable, but also the placement of the buttons. The driver was consulted throughout the process and gave his input on the design. The responsibility for designing the steering wheel was with the mechanical group, but they worked closely with the electrical group to facilitate their needs.

The first prototypes were made of cardboard to quickly assess the shape of the steering wheel. It was decided that it should have a diameter of 25 cm. A larger would just take more space and add weight. We wanted levers on the back. They act intuitively as the throttle and make it easy to control the speed.



Figure 94: Early prototypes. Ruler acts as levers.

We had a carbon fibre plate with room for electronics and a quick release mechanism mounted on it from two years ago. It can be seen in Figure 96. This was used as a base to save time and work. A new prototype was made to fit its geometry. Here we discovered that a larger radius on the grip felt more natural and was more comfortable. In Figure 95 one can see how the inner radius of the grip is bigger on one side than the other.

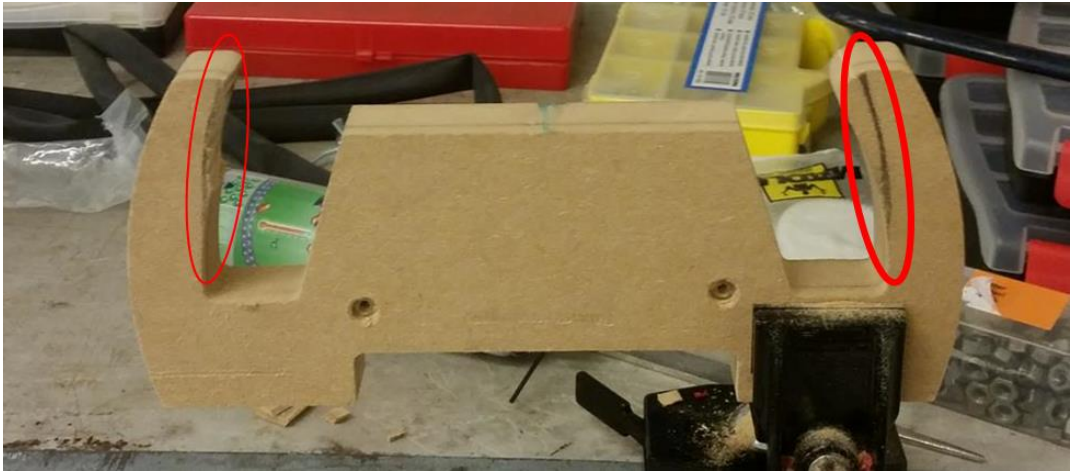


Figure 95: Larger radius on the inside of the left (for us) than right grip.

With thoughts on the design award, we opted to use wood as a material. We chose plywood which could easily be cut by laser. The laser cutter we used is a Gravograph LS1000XP. We glued together layers that had been precision cut. That allowed for hollow grips and added details. We chose to restrict the number of buttons on the steering wheel. The buttons should rather be bigger such that they are easy to operate with gloves on. A cleaner look is also more aesthetically pleasing. We decided to have two buttons on the left side for the indicator lights. On the right side, we had one button for the cruise control, one for the horn and one joystick. As the windscreen wiper also needs speed regulation, we opted not to control it from the steering wheel but rather from the control panel. The buttons are a part of the front layer, except for the joystick. That is the same type as in a PlayStation controller and acts as a multifunctional button. One intended use was to regulate the speed of the cruise control, but this was not implemented. The electronics are connected with an ethernet cable under the steering wheel. Using the laser, we also put our logo on the wheel several places. It appears as a big one on the front, on the levers and as “hinges” for the buttons.



Figure 96: Production of steering wheel

In the initial stage of prototyping, we thought of having the dead man's switch as pressure sensors on the grips such that the propulsion power got disengaged when both hands came off the steering wheel. This was changed as we found it easier to use the left lever as the dead man's switch. It is not ideal that the driver can't take his left hand off while driving, but there shouldn't be a need for it on the track. We varnished it for a rougher look. The finished product had a weight of 481 grams. The cost was also low. The plywood was free from the institute and the other components were already in our possession.



Figure 97: Finished steering wheel

11.2 Control panel

A control panel was needed for buttons we couldn't fit, or didn't want, on the steering wheel. To keep with the design theme, it was also made of varnished plywood. It includes on/off buttons for the lights, hazard warning lights, windscreen wiper, low voltage power and high voltage power. It has rotary switches for the windscreen wiper speed and the light intensity. There is also a lap time button and the mandatory emergency switch.



Figure 98: Control panel

11.3 Seat

To save time and effort we opted to reuse last year's seat. It has a low weight and is designed to be used with our seat belts. It wasn't worth making a new, but it needed a few adjustments. The major was that it had to be altered from fitting a flat floor to fit our curved floor. We also changed colour to match our car and padded it for driver comfort. The padding was cut in pieces and glued in a pattern for aesthetic reasons.



Figure 99: Seat

11.4 Other interior

When we designed our interior, we had the design award in mind. We continued with our theme of blue colours and varnished wood. For the dashboard, we laser cut a piece of wood with our logo in the pattern. Since we used a laser cutter, we could extract the needed geometry from the CAD model of our car and get a good fit. Cardboard painted blue was placed underneath the wood. It was also fitted with a display. The dashboard can be seen in Figure 101. We discovered in London that the display can't be seen when there is a strong sun. During the competition, we had to improvise a sunscreen for the display made of cardboard. Next year's team should either make a proper sunscreen or a new dashboard where the display is placed in such a way that sunlight won't be a problem.

The rules state that luggage must be in the vehicle. The luggage is a rectangular solid box with dimensions of 500 x 400 x 200 mm (L x H x W). It must be held in place by a floor and sidewalls when the car is moving. We had placed our luggage on the right side of the driver. The spot does not meet the requirements, so we had to make a luggage holder. This was also made of varnished wood and fastened to the body. It can be seen in Figure 100. The luggage itself was made a previous year. We just painted our logo on it.



Figure 100: Luggage holder



Figure 101: Interior

12 Other subsystems

12.1 Door mechanism

The door needs a hinge and a locking mechanism. It must be simple and fast to unlock and open, as the driver must be able to exit the car within 10 seconds. It was preferred to situate the hinge on the inside of the car of both aesthetic and aerodynamic reasons. Also, in a closed position, the door should be totally flush with the chassis; meaning no gaps. A simple hinge with rotation about one axis could therefore not be used, as the parts would crash into each other not allowing the movement. A design with multiple joints or sliding mechanisms were needed, but the interactions needed from the driver to open/close the door should be just one step, so the door opens conveniently. Different design ideas were often complicated and required the use of springs and similar to aid the mechanism. It was decided to go for a “4 bar linkage”, which gives a rigid travel path of the door without any need of springs. The door comes clear of the door opening in a movement where it stays parallel to the car, giving it an unusual and cool way of functioning. The longest part of the “4-bar linkages” was made of a laser cut MDF plate for good stiffness, while the rest of the parts were suited to be 3D-printed.

For no additional air drag, we wanted to eliminate the door handle. This was done by using a “push to open” mechanism meant for small cupboard. A “push to open” sticker was placed on the outside of the door to indicate where to push.-

12.2 Compartment cover



Figure 102: Motor compartment cover mechanism

Due to the curved geometry of the motor compartment cover, the best placement for a hinge was in the rear. It was far easier to get the cover to close on the flanges of the body. Wedges are placed on the sides of the cover to press on the body when closed, reducing the gaps between the two. Magnets are also fastened at different locations near the top. These measures ensure that the cover sits well enough, and it will not be opened by wind at our speeds. The cover is double hinged to ensure correct movement when closing/opening.

Quick release pins are used to make it easier for one person to remove the cover. The hinges are 3D-printed.

12.3 Head and rear lights

The casings for the lights were 3D-printed. Letting us make them perfectly shaped to fit the chassis, and giving a large gluing surface between the chassis and the casing. The combinations of thin walled design and plastic with quite low density made the casings very light-weight.

12.4 Electronics

The electrical system is essential for a working car, and many pages could have been written about the system. However, as earlier mentioned, it is not in the focus of this report and will not be explained in detail. Nevertheless, an overview of the electrical system will be described in this section to give a better understanding of the vehicle system.

The subsystems of the electrical system are:

- Motor controller
- Battery management system (BMS)
- Electronics of the front, back, brake, and indicator lights
- Steering wheel buttons and step-less accelerator
- LCD screen with information, e.g. speed
- Window wiper stepper motor and controller

The electrical system is module based using the universal module system (UM) made by Guldahl (2010), which is using the robust CAN protocol for communication. These modules make it very convenient to attach and remove electrical subsystems, as they only need to be hooked onto the host less network with an Ethernet cable.

The BMS is a safety system for the batteries. It makes sure the power is cut if there is overcurrent or the battery cells are too hot.

The motor controllers use power MOSFET to control the motors, where the power control is done with pulse width modulation (PWM). Initially, it was believed that the motor controller for brushed DC motor would be a fairly easy task to make, as only a direct current is being controlled without the need of timing etc. However, the voltage and power in this system was higher than anyone had prior experience with, which seem to complicate the system. The electrical team were successful in building working prototypes, but had struggles building a viable motor controller. Over time, components as diodes, the power MOSET or capacitors would fail.

For the interested reader, the documentation for the BMS and the motor controller can be found in the Appendix C: Motor datasheets.

13 Conclusion

13.1 SEM Summarized

13.1.1 Arrival and technical inspection

We arrived in London on Monday May 22nd. In the afternoon, we held a presentation about the project in the London office of DNV GL. We drove to Queen Elizabeth park and unloaded from the van into the paddock in the evening. After unloading, and the entire Tuesday was used working on the electronics such that we could pass the technical inspection. One issue we had was that we didn't get our horn to work. Luckily one team was kind enough to give us a horn they had as a spare. The work on the electronics continued Wednesday. In the afternoon, we decided to get in line for the technical inspection, even though the electronics wasn't finished. We passed the posts that did not involve any of the cars electronic systems that day. On the Thursday, we finished the electronics on the car and passed the final post 15 minutes before the technical inspection closed. Several teams did not make it in that time, so Shell decided to keep the technical inspection open the Friday as well. The horn we got was measured to 86 dBA. The requirement was 85 dBA. On the electrical post, the Shell engineer measured a voltage on one of our rear suspensions, which our multimeter where unable to measure. After troubleshooting, we found that the Hall effect sensor we had installed to measure our speed induced the voltage. We believe we couldn't measure it because it was a fluctuating voltage, and the multimeter Shell used could measure an average value over a shorter time period than ours. We removed the Hall effect sensor.

13.1.2 Competition day 1

Friday May 26th was the first day of competitive attempts. We were allowed maximum four attempts during SEM. The track was open for the UrbanConcept vehicles in two 2-hour periods, from 10:00-12:00 and 14:00-16:00. Last start was 39 minutes before the track closed. The morning was used to work on the electrics and we just managed to start an attempt before 11:21.

Attempt 1

The car failed after 50 m on the first attempt with a repeating punching sound occurring. The nylon pulley had loosened from the hub. It had been assumed that press fit would be good enough to hold the pulley in place. This turned out not to be the case due to the lower friction of nylon. We fixed the problem by installing bolt through the pulley and hub, which was not a time-consuming task.

Attempt 2

Before the second attempt we had issues with the BMS. The overcurrent protection system kicked in when the throttle was at about 80%, and a reset was necessary. The reset is done from the steering wheel. We decided to use an attempt anyway, and the driver needed to be careful. We managed to drive around the track on the second attempt, but the driver chose to drive into the pit after one lap. One of the mirrors had fallen off during the attempt, which he knew would cause the lap to be invalidated. The adhesive had melted in the heat, probably due to the two-component araldite used had not been mixed together well enough. The driver also saw on his clock that his speed wasn't high enough. The lap time was over the average lap time needed to get within the time limit, and he couldn't go faster. This was later confirmed by the official tracking.

After the attempt, we were optimistic that we would be able to get a valid attempt the following day. We returned to the test track. While standing still at the end of the track, another UrbanConcept vehicle rear ended us. Their speed was such that the rear of our car was lifted. Apart from some scratches on our car, there were no visible damages. The incident was reported to the track marshal, but we don't know if there were any consequences for the other team. Our car needed to go faster around the track, so we decided to increase the top speed by changing the gear ratio. On the RE50 motor we went from 200/14 to 200/16 (teeth on tyre/motor gear), and from 200/20 to 200/21 on the RE65 motor.

13.1.3 Competition day 2

On Saturday May 27th, the time slots for the UrbanConcept competition were 09:00-11:00 and 14:00-16:00.

Attempt 3

While driving on the test track, the MOSFET on the motor controller to the RE65 got fried. The RE65 was powering the right rear wheel. We were not able to fix the motor controller before the time slot for attempt 3 was over.

Attempt 4

A new motor controller was built identical to the working one. Now the motor thrust regulation (PWM) was unstable on the RE65 motor. We switched the RE65 to a RE50, and to a 16-toothed gear, to have identical set-ups on both sides. The problem was still there, which we found strange since everything were supposedly identical. We did not have time to do more troubleshooting if we were to reach making a final attempt. When the car left the start line, there was a loud slam noise. The right motor had produced a large torque force, most likely because of the motor controller giving 100% PWM. The torque was so powerful that the freewheel bearing in the pulley hub was destroyed. The car managed to get to the hill, but not up it due to loosing half the power.

13.2 Travel advises

- If you are driving to SEM yourself you need an ATA-carnet. This is a document of the items in your car and must be presented to the customs when you leave and enter Norway.
- Book flights early. Preferably once the exam dates are confirmed, such that the team members can decide if they want to travel to SEM. Remember that flight tickets must be done through NTNU. NTNU also has a partner for car rental. We did not have to book our van through this company as we drove outside Norway, but you should make sure that this rule still applies.
- Be aware that hotels in London gets fully booked early, if SEM still takes place there. You should try to find a place near the track, or at least near a metro station. Shell offers a free campsite with regular shuttle buses. It takes 30 minutes to get there. We do not currently have camping equipment for DNV GL Fuel Fighter.
- We parked the rental van in the camping area for the duration of SEM. The parking was free here.
- You should bring shelves you can put up in the paddock for better storage. We also advise that everything you bring has an assigned place in a box. Quality boxes should be used to ease storage, transport and control

13.3 Project management

Management have this year been divided by the project manager (PM) and the technical manager. The technical manager has been responsible for the systems of the car, and been the person with the best overview of the cars technical aspects. The PM was responsible for the for the overall project. Examples of responsibilities are finances, registration phases for SEM, contact with DNV GL, recruitment and interaction with the institute. A person responsible for logistics was recruited in January to help plan the trip to London. Listed are some of the experiences from this year.

- Slack was chosen as communication tool this year. It functions as a discussion arena and message board. Both private and group chats can be conducted with Slack. There are channels for different discussions. Examples of channels we had were mechanical, marketing, general and important. Slack was chosen as many use time to answer e-mail and we wanted to keep work discussions away from Facebook. The use of Slack was successful.
- As formerly mentioned, there should be a deputy PM in the team. Preferably not a master student, as they should focus on the vehicle.
- The tasks of the persons responsible for logistics could be transferred to the PM and the deputy to speed up the process.
- Again, a systems engineer should be involved from day one.
- Every week we had a meeting with management, the group leaders and marketing. Knut Aasland was also present when available. We did a recap of the previous

week, discussed major decisions and informed the other of the groups plans for the week(s) ahead. It is crucial to have this meeting.

- There should be regular meetings for the full team, and should be organized by the deputy PM. It was rarely done this year as the management did not have the time.
- The mechanical and electrical group had to produce an A3-sheet every week of their recent work every week. It said what had been finished, what was in progress, and what was to be done the next week. They were the responsibility of the group leaders and were hung up in the office for the team to read. They worked just ok for their intended purpose, but was a great aid for the PM when writing the regular status reports to DNV GL.

13.4 Vehicle improvements

To improve the current car, the highest focus should be on the electrical system. Particularly getting a working and efficient motor controller. Extensive research should be done, and we also recommend buying commercial motor controllers to study the circuits. Circuit diagrams for high voltage motor controllers are very hard to find online or in books. A commercial BMS should also be bought, such that the focus can be on designing the motor controller. A 24V system can be considered, as there exist many more commercial motor controllers at this voltage. The electrical team should seek help from people in the industry or at the electrical departments at NTNU. More universal modules should be in stock. There should not be a risk of going to SEM without backups. It is possible to get e.g. Chinese providers to fully assemble the circuit boards, saving time and reducing risk of circuit errors. They should try to improve the horn, and to get a precise speed measure. The electronic systems should be working in the winter, such that the spring can be used for testing and deciding a driving strategy optimized for the car.

The mechanical team should focus on reducing the weight of systems in the car. Figure 103 shows the weight of systems in the car. The weight of the monocoque is rounded. Our strongest recommendation is to make new rims. The tyres on the rims amounts to almost 20% of the weight of the car. At least one of the master students should focus on making new light-weight rims. They should also look into other tyres that adhere to the rules, as the current type of tyres will no longer be sold in the SEM e-shop. A new brake system should be implemented. Our brake callipers and discs weighs 3.9 kg. The hydraulic brake tubes also amount to considerable weight. At the technical inspection, we were told that our brakes were the best they have had, but the system is over dimensioned. Bicycle brakes should be modified to fit 3 mm brake discs. The suspensions should be adjusted to be in an optimized position. New windows should be made of tinted Lexan, and the side windows should be 1 mm thick. Proper mirrors should also be installed. The team should try to get access to the wind tunnel. This may be easier if a teacher is willing to have studies of the car as a part of a relevant course. The concept of turbulent flow, illustrated in Figure 104, would be interesting to test for. To check if sandpaper on the nose of the car would improve the aerodynamics. Add attachments to the front wheel wells to improve aerodynamics.

Considerable weight could be saved by producing the monocoque, with just a slightly modified design, in prepreg. This takes a lot of time, and requires a large motivated team, strong finances and an autoclave that is available. It is not something we would recommend the team of 2018 to do.

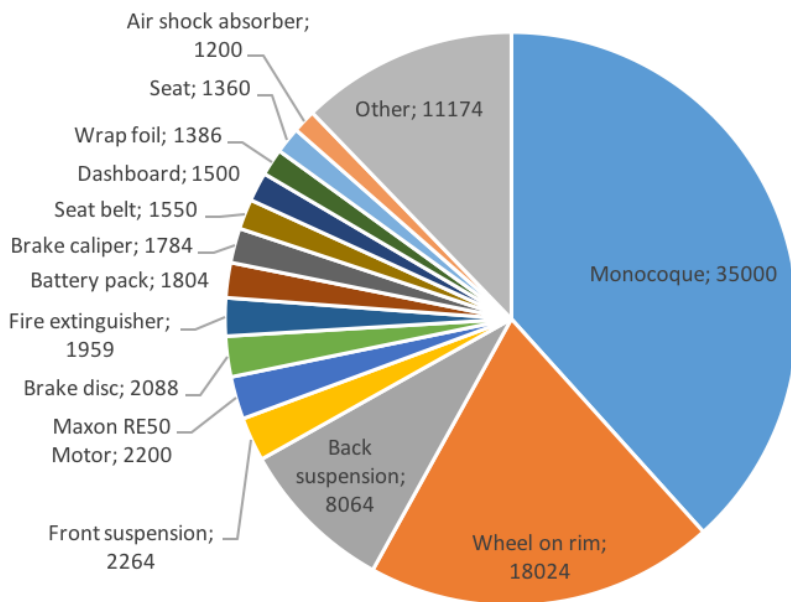


Figure 103: Weight of vehicle components

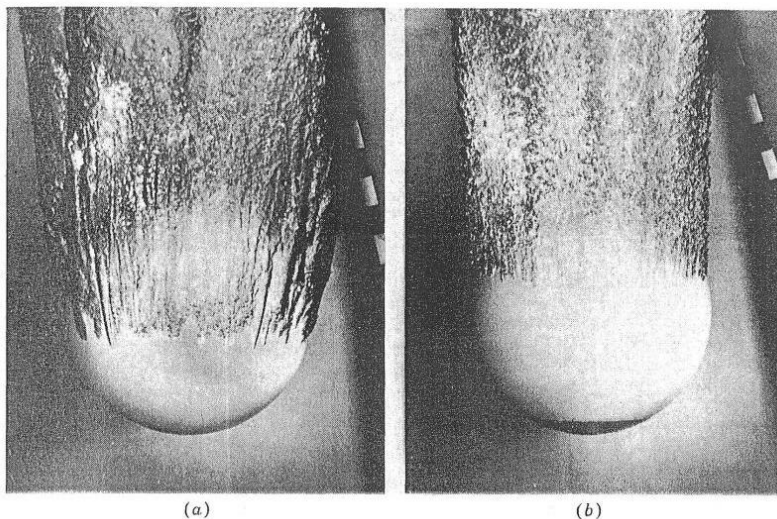


Figure 10.11. Shift in point of separation on 8.5-in-diameter bowling ball at a velocity of approximately 25 fps in water. (a) Smooth sphere—laminar boundary layer. (b) Sphere with 4-in-diameter patch of sand grains cemented to nose—turbulent boundary layer. Reynolds numbers are the same. (Photographs by U.S. Naval Ordnance Test Station, Pasadena Annex.)

Figure 104: Laminar vs turbulent flow

13.5 Final remarks

The team was of course disappointed with not getting a track result at SEM. We knew we were ambitious, but it turned out that a fresh team with all new members, building a fully-new car maybe was too ambitious. From the start, the intention was not to build an optimal car. We were fully aware that it would not be possible in one year, and focused on a car that could serve as a base for improvement. The team entire team has faced new challenges and learned a lot. Some of the knowledge the team gained was about the practice of working with carbon fibre and how much time it can take from a part is designed until it is produced. To participate in and experience SEM was also of great value to those who travelled.

The revealing of the car took place on May 4th and was held in the cafeteria “Hangaren”. The location is good, as it has AV-equipment installed and many students are already there when the revealing is scheduled.

The finances of our project were good, and we stayed well within budget. This is partially due to a focus on cost when designing the car. One example is that we spent NOK 170 000 making the monocoque, while the previous monocoque cost NOK 280 000. Enova are likely to sponsor again and should be contacted early. The principal’s office should also be asked for funding early. We applied for NOK 30 000, but we believe there are possibilities for being awarded a larger sum.

We did not get the time to test we had planned, partly due to production of parts taking more time than anticipated. Future teams should have in mind that the workshop is also heavily used by the “bicycle-project”, which reduces the access to machinery and staff. The testing we did was conducted in the area around the building. The powertrain jig was used to test the motors and is a useful tool for future teams.

We bring positives back from London as well. We were nominated for the Communications Award. Due to not getting a valid attempt we were ineligible to win the Design Award, but we were noticed and got some good feedback while there. Many people were very interested in our car. Some students said: “We have to steal that idea for next year”. And before we went on the track for an attempt, a quote from one steward was: “This is my favourite!”.

14 References

- AKOVALI, G. 2001. *Handbook of Composite Fabrication*, Shrewsbury, UNITED STATES, iSmithers Rapra Publishing.
- DASSAULT-SYSTÈMES 2014. Abaqus theory guide 6.14.
- GULDAHL, A. L. 2010. Styre- og overvåkningssystem for Shell Eco-marathon kjøretøy.
- LAMBOURN, R. F. & WESLEY, A. 2010. Motorcycle Tire/Road Friction. SAE International.
- LEE, S.-Y. & PARK, D.-Y. 2007. Buckling analysis of laminated composite plates containing delaminations using the enhanced assumed strain solid element. *International Journal of Solids and Structures*, 44, 8006-8027.
- LONGHURST, C. 2017. *FRONT SUSPENSION - INDEPENDENT SYSTEMS* [Online]. Available: http://www.carbibles.com/suspension_bible.html [Accessed 05.06.2017 2017].
- MEYWERK, M. 2015. *Vehicle Dynamics*, Somerset, UNKNOWN, John Wiley & Sons, Incorporated.
- SABIC 2015. LEXAN SHEET PROCESSING GUIDE.
- SANTIN, J. J. 2007. *The World's Most Fuel Efficient Vehicle: Design and Development of Pac Car II*, vdf Hochschulverlag AG an der ETH Zürich.
- SHELL. 2016. *About Shell Eco-marathon* [Online]. Available: <http://www.shell.com/energy-and-innovation/shell-ecomarathon/about.html> [Accessed December 08 2016].
- TITUS, J. 2012. *Careful designers get the most from brushless DC motors* [Online]. Available: <https://www.ecnmag.com/article/2012/08/careful-designers-get-most-brushless-dc-motors> [Accessed 21.06 2017].
- VAN PAEPEGEM, W. 2014. *Vacuum Infusion - The Equipment and Process of Resin Infusion* [Online]. Home Made Composites, . Available: http://www.composites.ugent.be/home_made_composites/documentation/FibreGlast_Vacuum_infusion_process.pdf [Accessed June 11. 2017].

15 Appendix

15.1 Appendix A: Steering optimization

15.1.1 Racket error optimization

```
%% Steering Geometry optimization
% Written for DNV GL Fuel Fighter NTNU - Shell Eco Marathon 2017
% Author: Håvard Vestad feb.2017
% Co-author: Odin J. Oma

clear;
clf
close all
%%Car Parameters:

width=1010; %front wheel turning points
length_aa=1548.5; %axel-axel
racket_l=179;%half joint-to-joint center
centerTwheel=width/2;
placement= 120;%distance racket from wheel center
height= 0; %placement height from steering arm
r1=95; %steering arm length

ackerman_temp=atand((width/2)/length_aa);
asyRoll_temp=atand((width/2)/(length_aa/2));

%% Course Geometry (Load and treat):
%addpath('C:\Users\H?vard\Documents\MATLAB\FuelFighter\Simulation'); %Load path of
simulation data

if exist('x0','var') == 0
    filename = 'track17.xlsx';
    sheet = 1;
    x0 = transpose(xlsread(filename,sheet,'A2:A1661'));
    y0 = transpose(xlsread(filename,sheet,'B2:B1661'));
    z0 = transpose(xlsread(filename,sheet,'C2:C1661'));

    t=30;
    x=smooth(x0,t,'lowess');
    y=smooth(y0,t,'lowess');
    z=smooth(z0,3*t,'lowess');
end
K =turningR(x,y); %Track curvature

%% Iterating over the course

step_size=0.1;
radiuses =K; %Track curvature
```

```

%radiuses=[6,7,8,9,10,15,20,25,30,35,40,45,50];
n=1:length(radiuses);
l=(ackerman_temp-4):step_size:asyRoll_temp;

p=1;
for plass=0:1:140
    s=1;
    placement=plass;
    a_aks=0:step_size:(asyRoll_temp+40);

for a_ak=0:step_size:(asyRoll_temp+40)
    r1_x0=cosd(90-a_ak)*r1;
    r1_y0=sind(90-a_ak)*r1;
    l_tieRod= sqrt(((centerTwheel-r1_x0-racket_l)^2+height^2)+(r1_y0-placement)^2);
%total tie rod length

error=0;
for b=1:length(radiuses)

    r=radiuses(b)*1000;
    if r<5000 %Too small raduis = noise in data -> ignore
        r=1000000;
    end
    if r>150000 %Too High raduis = Actually straight road -> ignore
        error =[error;0];
    else

a_st=[-asind(length_aa/r); (atand(length_aa/(sqrt(r^2-length_aa^2)-width)))]);

%One side:
    r1_x1=cosd(90-a_ak-a_st(1))*r1;
    r1_y1=sind(90-a_ak-a_st(1))*r1;

    %l_sTop =sqrt(l_tieRod^2-height^2);%tie rod projection
    l_sFront =sqrt(l_tieRod^2-(r1_y1-placement)^2);%tie rod projection

    U=sqrt(l_sFront^2-height^2);% x distance steering arm to racket
    travel(1,1)=centerTwheel-U-r1_x1-racket_l;
%Other side:
    r1_x2=cosd(90-a_ak-a_st(2))*r1;
    r1_y2=sind(90-a_ak-a_st(2))*r1;

    %l_sTop =sqrt(l_tieRod^2-height^2);%tie rod projection
    l_sFront =sqrt(l_tieRod^2-(r1_y2-placement)^2);%tie rod projection

    U=sqrt(l_sFront^2-height^2);% x distance steering arm to racket
    travel(2,1)=centerTwheel-U-r1_x2-racket_l;

    error =[error;(abs(travel(1,1)+travel(2,1)))/abs(travel(1,1))];
end
% find the rack travel for max steer angle for setup:
r=5900; %6m with some safety factor

```

```

%a_st(2)=(atand(length_aa/(sqrt(r^2-length_aa^2)-width)));
a_st=[-asind(length_aa/r); (atand(length_aa/(sqrt(r^2-length_aa^2)-width)))]);
r1_x2=cosd(90-a_ak-a_st(2))*r1;
r1_y2=sind(90-a_ak-a_st(2))*r1;

```

```

%l_sTop =sqrt(l_tieRod^2-height^2);%tie rod projection
l_sFront =sqrt(l_tieRod^2-(r1_y2-placement)^2);%tie rod projection

```

```

U=sqrt(l_sFront^2-height^2);% x distance steering arm to racket
steer1=abs(centerTwheel-U-r1_x2-racket_l);

```

```

r1_x1=cosd(90-a_ak-a_st(1))*r1;
r1_y1=sind(90-a_ak-a_st(1))*r1;

```

```

%l_sTop =sqrt(l_tieRod^2-height^2);%tie rod projection
l_sFront =sqrt(l_tieRod^2-(r1_y1-placement)^2);%tie rod projection

```

```

U=sqrt(l_sFront^2-height^2);% x distance steering arm to racket
steer2=abs(centerTwheel-U-r1_x1-racket_l);

```

```

steer(s,p)= (steer1+steer2)/2;

```

```

end

```

```

error_tot(s,p)=mean(error);
s=s+1;

```

```

end

```

```

p=p+1;
end

```

```

for p=1:14

```

```

    plot3(a_aks(1:600),p.*ones(600),(error_tot(1:600,p)));
    hold on

```

```

end

```

```

%% Plot Data

```

```

figure(2);mesh(error_tot(1:600,:).*100);
yticklabels(0:20:60);
xticklabels(0:50:150);
title('Racket error [%] - mean value track 2017 London')
xlabel('Racket of-set[mm]');
ylabel('Ackerman angles [degrees]');
zlabel('');

```

```

%%

```

```

steer2= abs(steer);
steer2(steer2 > 25)=0;
figure(3);
mesh(abs(steer(1:600,:)));

```

```

yticklabels(0:20:60);
xticklabels(0:50:150);
title('Rack travel [mm] required for min. turning radius')
xlabel('Racket of-set');
ylabel('Ackerman angles [degrees]');
zlabel('Rack travel');

az = 0;
el = 90;
view(az, el);

%%
figure(4)
title('Total mean error in racket movement for ideal inner wheel turning angle over whole
2017 track with cut-of for unrealistic racket travel')
xlabel('Racket of-set from wheel turning axis [mm]');
ylabel('Ackerman angles [degrees]');
zlabel('Mean course error [ % ]');

```

15.1.2 Racket error plotting

```

%% Steering Geometry optimization - plotting
% Written for DNV GL Fuel Fighter NTNU - Shel Eco Marathon 2017
% Author: Odin J. Oma
%%
st = abs(steer);
er = error_tot;

st(st>25)=0;
st(st>0)=1;
er = st .* er;
%%
figure(6);mesh(er(1:600,:).*100);
yticklabels(0:20:60);
xticklabels(0:50:150);
title('Mean racket error [%]')
xlabel('Racket of-set [mm]');
ylabel('Ackerman angles [degrees]');
zlabel('');
%%
figure(7)
x=1:600;x=x*60/600;
y=1:141;y=y*150/141;
[D,h]=contourf(y,x(1:1*length(x)),er(1:600,:).*100,[0.05 0.1 0:0.2:1 2]);
title('Mean racket movement error [%]');
xlabel('Racket of-set [mm]');
ylabel('Ackerman angle [degrees]');
clabel(D,h,'manual');

%%
figure(8)
x=1:600;x=x*60/600;

```

```

y=1:141;y=y*150/141;
[D2,h2]=contourf(y,x(1:1*length(x)),steer(1:600,:),0:5:50);
title('Mean racket movement error [%]');
xlabel('Racket of-set [mm]');
ylabel('Ackerman angle [degrees]');
clabel(D2,h2);

```

15.1.3 Ideal turning angles

```

%% Ideal turning angles
% Written for DNV GL Fuel Fighter NTNU - Shell Eco Marathon 2017
% Author: Odin J. Oma

```

```

B = 1010 / 1000;
x = 95 / 1000;
p = 179 / 1000;
r = 35 / 1000;
d = 130 / 1000;
beta = 24;

```

```

beta = deg2rad(beta);
a1v = 1:20;
a1v = deg2rad(a1v);

```

```

y = sqrt(( ( B-(p+2*r))/2 - x*sin(beta))^2 + (d-x*cos(beta))^2);
for i = 1:20
syms a0 q
a1=a1v(i);
eq1 = y^2 == ( B/2 - (p/2+r+q) + x*sin(a0-beta) )^2 + (d-x*cos(a0-beta) )^2;

```

```

eq2 = y^2 == ( B/2 - (p/2+r-q) - x*sin(a1+beta) )^2 + (d-x*cos(a1+beta) )^2;

```

```

sol = solve([eq1 eq2],[a0 q]);
a0 =real(rad2deg( double(sol.a0)));
a00(i) = min(a0(a0>=0));

```

```

end
%%
figure(1)

```

```

L=1549;
t=1010;
a1v = 1:20;
a0i = acotd(cotd(a1v)+t/L);
%plot(a1v,a0i,'--')
hold on
plot(a1v,a00)

```

figure (2)

```

plot(a1v,a00-a0i)
hold on

```

15.2 Appendix B: Motor efficiency plots

```
%% Motor efficiency  
% Written for DNV GL Fuel Fighter NTNU - Shel Eco Marathon 2017  
% Author: Odin J. Oma
```

```
motor = 'RE65';  
rated_voltage = 48;  
plot_pos = 2;
```

```
switch motor  
case 'RE50'  
    switch rated_voltage  
        case 48  
  
            Ct = 93.4; % mNm/A  
            Kn = 102; % rpm/V  
            Kt = 0.666; % rpm/mNm  
  
            ax1 = subplot(1,2,plot_pos);  
            tit = 'Maxon RE50 - 48V';  
            xlab = 'Torque [mNm] / I [A]';  
            ylab = 'RPM';
```

```
        case 70
```

```
            Ct = 242; % mNm/A  
            Kn = 39.5; % rpm/V  
            Kt = 0.638; % rpm/mNm  
  
            ax1 = subplot(1,2,plot_pos);  
            tit = 'Maxon RE50 - 70V';  
            xlab = 'Torque [mNm] / I [A]';  
            ylab = 'RPM';
```

```
        otherwise  
            return
```

```
    end  
    tw = 71;  
    rated_eff = 0.94;  
    r=5;
```

```
case 'RE65'  
    switch rated_voltage  
        case 36  
            Ct = 84.4; % mNm/A  
            Kn = 113; % rpm/V
```



```
Kt = 0.234; % rpm/mNm
```

```
ax1 = subplot(1,2,plot_pos);  
tit = 'Maxon RE50 - 36V';  
xlab = 'Torque [mNm] / I [A]';  
ylab = 'RPM';
```

```
case 48
```

```
Ct = 123; % 94.4; % mNm/A  
Kn = 77.8; % 102; % rpm/V  
Kt = 0.231; % 0.666; % rpm/mNm
```

```
ax1 = subplot(1,2,plot_pos);  
tit = 'Maxon RE65 - 48V';  
xlab = 'Torque [mNm] / I [A]';  
ylab = 'RPM';
```

```
case 60
```

```
Ct = 153; % mNm/A  
Kn = 62.3; % rpm/V  
Kt = 0.231; % rpm/mNm
```

```
ax1 = subplot(1,2,plot_pos);  
tit = 'Maxon RE65 - 60V';  
xlab = 'Torque [mNm] / I [A]';  
ylab = 'RPM';
```

```
end
```

```
tw = 123; %71.7;  
rated_eff = 0.88;
```

```
r=15;
```

```
otherwise
```

```
return
```

```
end
```

```
rpm = 0:5:4900;
```

```
t = 0:5:1500;
```

```
rpm_size =ones(1,length(rpm));
```

```
t_size =ones(1,length(t));
```

```
V = ( ( rpm_size.*t )*Kt + rpm.*t_size )/Kn;
```

```
I = t/Ct;
```

```
incr=.005;
```

```
max_eff = rated_eff-0.02;
```

```
rpm_loss=0.95;
```

```
while abs(max_eff-rated_eff)>incr
```

```

if max_eff > rated_eff
    rpm_loss=rpm_loss-incr;
else
    rpm_loss=rpm_loss+incr;
end

```

```

P_out=( transpose(rpm_loss*rpm)* pi/30 ) * (t-r)/1000;
P_out(P_out<0)=0;

```

```

%T= (rpm_size.' * I);

```

```

P_in = V .* (rpm_size.' * I);

```

```

ef = P_out ./ P_in ;
max_eff = max(ef(:))
end

```

```

levels=[0:0.2:0.6...
        0.7:0.05:0.85...
        0.86:0.01:0.95];

```

```

hold off
[C,h] = contour(t,rpm,ef,levels);
clabel(C,h);

```

```

map=[255,1,0; 255,3,0; 255,4,0; 255,5,0; 255,7,0; 255,8,0; 255,9,0; 255,11,0; 255,12,0;
255,13,0; 255,15,0; 255,16,0; 255,17,0; 255,19,0; 255,20,0; 255,21,0; 255,23,0; 255,24,0;
255,26,0; 255,27,0; 255,28,0; 255,30,0; 255,31,0; 255,32,0; 255,34,0; 255,38,0; 255,42,0;
255,46,0; 255,50,0; 255,53,0; 255,57,0; 255,61,0; 255,65,0; 255,69,0; 255,73,0; 255,76,0;
255,80,0; 255,84,0; 255,88,0; 255,92,0; 255,96,0; 255,99,0; 255,103,0; 255,107,0;
255,111,0; 255,115,0; 255,119,0; 255,123,0; 255,126,0; 255,131,0; 255,136,0; 255,141,0;
255,146,0; 255,151,0; 255,157,0; 255,162,0; 255,167,0; 255,172,0; 255,177,0; 255,182,0;
255,188,0; 255,193,0; 255,198,0; 255,203,0; 255,208,0; 255,213,0; 255,218,0; 255,224,0;
255,229,0; 255,234,0; 255,239,0; 255,244,0; 255,249,0; 255,254,0; 248,255,8;
238,255,18; 227,255,28; 217,255,39; 207,255,49; 196,255,59; 186,255,69; 176,255,80;
165,255,90; 155,255,100; 145,255,110; 134,255,121; 124,255,131; 114,255,141;
103,255,152; 93,255,162; 83,255,172; 72,255,182; 62,255,193; 52,255,203; 41,255,213;
31,255,223; 21,255,234; 10,255,244; 0,255,254];

```

```

map=map/255;
brighten(0.999)
colormap(ax1,map);
max_eff
rpm_loss
a=floor(length(t)/2);

```

```

title(tit)
ylabel(ylab)

```

```

hold on
offset=10;

for ii=8:8:48
V_=ii;
RPM_ = Kn * V_ - Kt .* t;
axis([0 1500 0 4900])
plot(t,RPM_,'b:');
str = [num2str(V_), ' V'];
text(t(a)+offset,RPM_(a)+offset,str,'FontSize',10,'color','b');

end
%plot(t,P_out(length(rpm),:))
%%
a1Pos = get(gca,'Position');

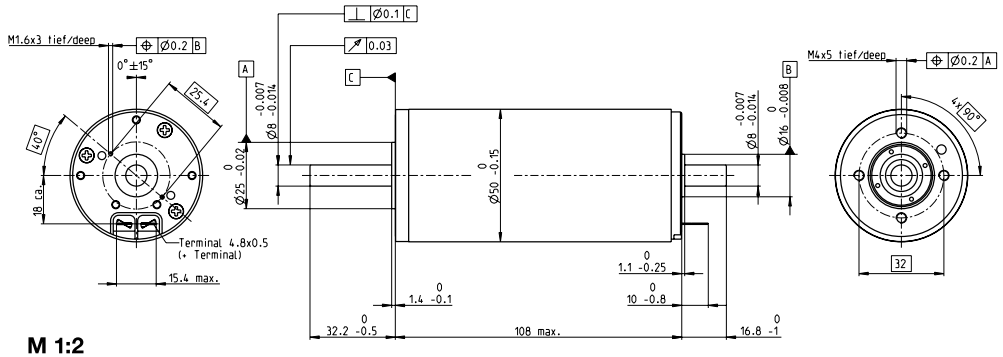
%// Place axis 2 below the 1st.
ax2 = axes('Position',[a1Pos(1) a1Pos(2)-.03 a1Pos(3)
a1Pos(4)],'Color','none','YTick',[],'YTickLabel',[]);
xlabel(xlab)
%// Adjust limits
xlim([min(I(:)) max(I(:))])

```

15.3 Appendix C: Motor datasheets

15.3.1 Maxon RE50

RE 50 Ø50 mm, Graphite Brushes, 200 Watt



- Stock program
- Standard program
- Special program (on request)

Part Numbers

Industrial Version IP54*

Motor Data

Values at nominal voltage

		370354	370355	370356	370357
		389089	389090	389091	389092
1 Nominal voltage	V	24	36	48	70
2 No load speed	rpm	5950	5680	4900	2760
3 No load current	mA	236	147	88.4	27.4
4 Nominal speed	rpm	5680	5420	4620	2470
5 Nominal torque (max. continuous torque)	mNm	405	418	420	452
6 Nominal current (max. continuous current)	A	10.8	7.07	4.58	1.89
7 Stall torque	mNm	8920	8920	7370	4340
8 Stall current	A	232	148	78.9	17.9
9 Max. efficiency	%	94	94	94	92

Characteristics

10 Terminal resistance	Ω	0.103	0.244	0.608	3.9
11 Terminal inductance	mH	0.072	0.177	0.423	2.83
12 Torque constant	mNm/A	38.5	60.4	93.4	242
13 Speed constant	rpm/V	248	158	102	39.5
14 Speed / torque gradient	rpm/mNm	0.668	0.638	0.666	0.638
15 Mechanical time constant	ms	3.75	3.74	3.78	3.74
16 Rotor inertia	gcm ²	536	560	542	560

Specifications

Thermal data

17 Thermal resistance housing-ambient	3.8 K/W
18 Thermal resistance winding-housing	1.2 K/W
19 Thermal time constant winding	71.7 s
20 Thermal time constant motor	1370 s
21 Ambient temperature	-30...+100°C
22 Max. winding temperature	+125°C

Mechanical data (preloaded ball bearings)

23 Max. speed	9500 rpm
24 Axial play at axial load < 11.5 N	0 mm
24 Axial play at axial load > 11.5 N	0.1 mm
25 Radial play	preloaded
26 Max. axial load (dynamic)	30 N
27 Max. force for press fits (static)	150 N
27 Max. force for press fits (static)	6000 N
28 Max. radial load, 15 mm from flange	110 N

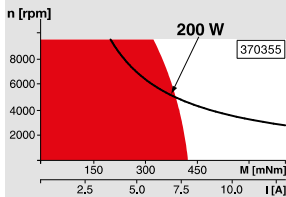
Other specifications

29 Number of pole pairs	1
30 Number of commutator segments	15
31 Weight of motor	1100 g

Values listed in the table are nominal. Explanation of the figures on page 64.

- * Industrial version with radial shaft seal ring (resulting in increased no load current). IP54 protection only if mounted on brush side, in compliance with maxon modular system.

Operating Range



Comments

Continuous operation
In observation of above listed thermal resistance (lines 17 and 18) the maximum permissible winding temperature will be reached during continuous operation at 25°C ambient. = Thermal limit.

Short term operation
The motor may be briefly overloaded (recurring).

— Assigned power rating

maxon Modular System

Planetary Gearhead

Ø52 mm
4 - 30 Nm
Page 350

Planetary Gearhead

Ø62 mm
8 - 50 Nm
Page 352



Recommended Electronics:

Notes Page 30

ESCON Mod. 50/5	427
ESCON 50/5	428
ESCON 70/10	428
EPOS2 50/5	435
EPOS2 70/10	435
EPOS4 Module/CB 50/5	442
EPOS4 Module 50/8	443
EPOS4 Comp. 50/8 CAN	443
EPOS4 Module 50/15	444
EPOS4 Comp. 50/15 CAN	444
MAXPOS 50/5	447

Overview on page 28–36

Encoder HEDS 5540
500 CPT,
3 channels
Page 414

Encoder HEDL 5540
500 CPT,
3 channels
Page 416

Industrial Version IP54*
Encoder HEDL 9140
Page 420

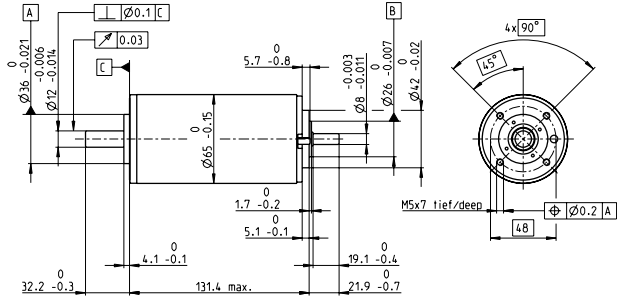
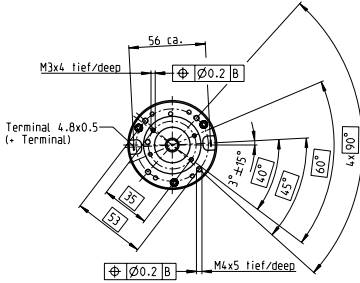
Brake AB 44
Page 462

End cap
Page 463

15.3.2 Maxon RE65

RE 65 Ø65 mm, Graphite Brushes, 250 Watt

maxon RE motor



M 1:4

- Stock program
- Standard program
- Special program (on request)

Part Numbers

353294	353295	353296	353297	353298	353299	353300	353301
388984	388985	388986	388987	388988	388989	388990	388991

Industrial Version IP54*

Motor Data

Values at nominal voltage

1 Nominal voltage	V	18	24	36	48	60	70	70	70
2 No load speed	rpm	3520	4090	3970	3670	3680	3440	3190	2690
3 No load current	mA	755	697	437	289	231	179	160	125
4 Nominal speed	rpm	3250	3810	3700	3420	3450	3220	2960	2470
5 Nominal torque (max. continuous torque)	mNm	427	501	751	800	813	832	839	888
6 Nominal current (max. continuous current)	A	10	10	9.32	6.8	5.53	4.51	4.21	3.74
7 Stall torque	mNm	13600	15700	17400	16100	16200	15100	13700	12200
8 Stall current	A	295	292	207	131	106	78.6	66.1	49.7
9 Max. efficiency	%	81	83	87	88	89	89	89	89

Characteristics

10 Terminal resistance	Ω	0.0609	0.0821	0.174	0.365	0.568	0.891	1.06	1.41
11 Terminal inductance	mH	0.023	0.031	0.076	0.161	0.251	0.393	0.458	0.644
12 Torque constant	mNm/A	46	53.7	84.4	123	153	192	207	245
13 Speed constant	rpm/V	208	178	113	77.8	62.3	49.8	46.1	38.9
14 Speed / torque gradient	rpm/mNm	0.275	0.272	0.234	0.231	0.231	0.231	0.236	0.223
15 Mechanical time constant	ms	3.98	3.68	3.38	3.25	3.19	3.16	3.16	3.13
16 Rotor inertia	gcm ²	1380	1290	1380	1340	1320	1310	1280	1340

Specifications

- Thermal data**
- 17 Thermal resistance housing-ambient 1.3 K/W
 - 18 Thermal resistance winding-housing 1.85 K/W
 - 19 Thermal time constant winding 123 s
 - 20 Thermal time constant motor 1060 s
 - 21 Ambient temperature -30...+100°C
 - 22 Max. winding temperature +125°C

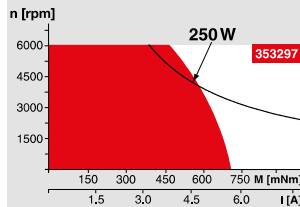
- Mechanical data (preloaded ball bearings)**
- 23 Max. speed 5500 rpm
 - 24 Axial play at axial load < 25 N 0 mm
 - > 25 N 0.1 mm
 - 25 Radial play preloaded
 - 26 Max. axial load (dynamic) 70 N
 - 27 Max. force for press fits (static) (static, shaft supported) 420 N
 - 28 Max. radial load, 15 mm from flange 12000 N
 - 350 N

- Other specifications**
- 29 Number of pole pairs 2
 - 30 Number of commutator segments 26
 - 31 Weight of motor 2100 g

Values listed in the table are nominal.
Explanation of the figures on page 64.

- * Industrial version with radial shaft seal ring (resulting in increased no load current).
IP54 protection only if mounted on brush side, in compliance with maxon modular system.

Operating Range



Comments

- **Continuous operation**
In observation of above listed thermal resistance (lines 17 and 18) the maximum permissible winding temperature will be reached during continuous operation at 25°C ambient.
= Thermal limit.
- Short term operation**
The motor may be briefly overloaded (recurring).
- **Assigned power rating**

maxon Modular System

Overview on page 28–36

Planetary Gearhead
Ø81 mm
20 - 120 Nm
Page 353



Recommended Electronics:

Notes	Page 30
ESCON Mod. 50/5	427
ESCON 50/5	428
ESCON 70/10	428
EPOS2 50/5	435
EPOS2 70/10	435
EPOS4 Module 50/8	443
EPOS4 Comp. 50/8 CAN	443
EPOS4 Module 50/15	444
EPOS4 Comp. 50/15 CAN	444
MAXPOS 50/5	447

- Encoder HEDS 5540**
500 CPT,
3 channels
Page 414
- Encoder HEDL 5540**
500 CPT,
3 channels
Page 416
- Industrial Version IP54***
- Encoder HEDL 9140**
Page 420
- Brake AB 44**
Page 462
- End cap**
Page 463

15.3.3 BMS documentation

Documentation for Battery and BMS

The DNV GL Fuel Fighter 2017 battery is an integrated module supplying both 48V nominal power for the motor controllers, and 12V regulated power for the auxiliary systems on the car, through an on-PCB DC/DC converter. The battery contains a BMS, taking measurements of voltages, temperatures and current, and providing safeguards against overvoltage, undervoltage, overcurrent, overtemperature, and other error-conditions. The charger is bought, and provides overvoltage protection and balancing during charging.

Battery summary

- 7000mAh capacity
- 48V nominal voltage
- 2100g total mass
- 12 cells in series
- Max 30A current draw from 48V
- Max 8.3A current draw from 12V

BMS summary

- Provides measurements of
 - Cell voltages
 - Temperature
 - Output voltage
 - Total current
- Interfaces the commercial batteries without modification
- Communicates over CAN bus
- Hardwired stop loop

List of components

Lines marked with a * has attached datasheets

- Battery assembly
 - 2x Tattu 7000mAh 22.2V 25C 6S1P Lipo Battery*
 - 1x Bronto LiPo-Safe - Lade/transport Bag (M) (Modified)
 - 2x Thermistor assembly
 - 2x muRata NTC Thermistors*
 - 1x 3 pin header
 - 2x Battery terminal extension
 - 1x Amass XT60 Regulatorside Plug w. Cover
 - 1x Amass XT60 Batteryside Plug w. Cover
 - 2x Amass Silicone Cable 12AWG
 - 1x Battery Management System
 - 1x BMS Casing (3D printed)
 - 1x 30mm Fan*
 - 1x Universal Module
 - 1x AT90CAN128 microcontroller
 - CAN interface
 - 12V-5V-3.3V buck converter

- 1x BMS Extension card
 - 1x 2 pin phoenix connector* (J7)
 - 1x 4 pin phoenix connector* (J9)
 - 2x Amass XT60 Regulatorside Plug (J5, J6)
 - 1x Amass XT60 Batteryside Plug (J8)
 - 2x Panasonic CN-M RELAY* (Rel4, Rel5)
 - 1x SENSOR CURRENT HALL 50A AC/DC* (CS1)
 - 1x Murata ULS-12/8.3-D48 Isolated DC/DC* (DCDC1)
 - 1x LTC6804-1 Battery Stack Monitor (U3)
 - 2x Blade chip fuses
 - Circuitry for controlling the stop loop
 - Circuitry for measurement of the output voltage
 - Circuitry for precharging the motor-controllers
 - Circuitry for cell balancing
- Charging setup
 - SkyRC Ultimate Duo 30A / 1400W Balance charger
 - SkyRC Power Supply 50A / 1200W

Protection during use

During driving, the battery pack is connected to the motor-controllers through the BMS. The BMS routes the power through two normally open relays (Rel4 and Rel5), one for each pole of the battery.

The BMS takes most measurements using the LTC6804-1 battery monitor from Linear Technologies. This chip measures the cell voltages of all 12 cells, as well as the temperature of four thermistors distributed among the cells, and the current in the cells. These values are communicated back to the AT90CAN218 microcontroller using an SPI bus, with a checksum to avoid noise causing erroneous data. If any of the measured values is out of range, or if communication to the LTC6804-1 is lost, the BMS will enter an unrecoverable error-state, where both of the mentioned relays are held open. A full restart of the system is required to reset any of these error-flags. The limits and error flags are as follows:

Measurement	Nominal	Minimum	Maximum	Associated error flag
Cell voltage	3800mV	3200mV	4200mV	Undervoltage / Overvoltage
Current	0-20A	-30A	30A	Overcurrent
Temperature	21°C	-	60°C	Overtemperature
Lost packages	0	-	0	LTC6804 Loss of Signal

The 12V DC/DC is galvanically isolated and is connected to the battery-cells inside the main relays, but outside the main fuse and current sensor. The DC/DC has built in undervoltage and overcurrent protection, and will not draw more than 2.26A.

In addition to the active protection, there is a 30A main fuse connected in direct series with the cells, a 10A fuse connected in series with the 12V output, and 1A fuses connected in series with the cell measurement wires.

Protection during charging

To charge the battery, the cells are disconnected from the custom PCB, and connected instead to the commercial charger. This charger then implements overvoltage protection and balancing. The battery pack remains assembled, with the cells protected inside the charging bag.

Tattu 7000mAh 6S1P 25C 22.2V Lipo Battery Pack with XT60 plug

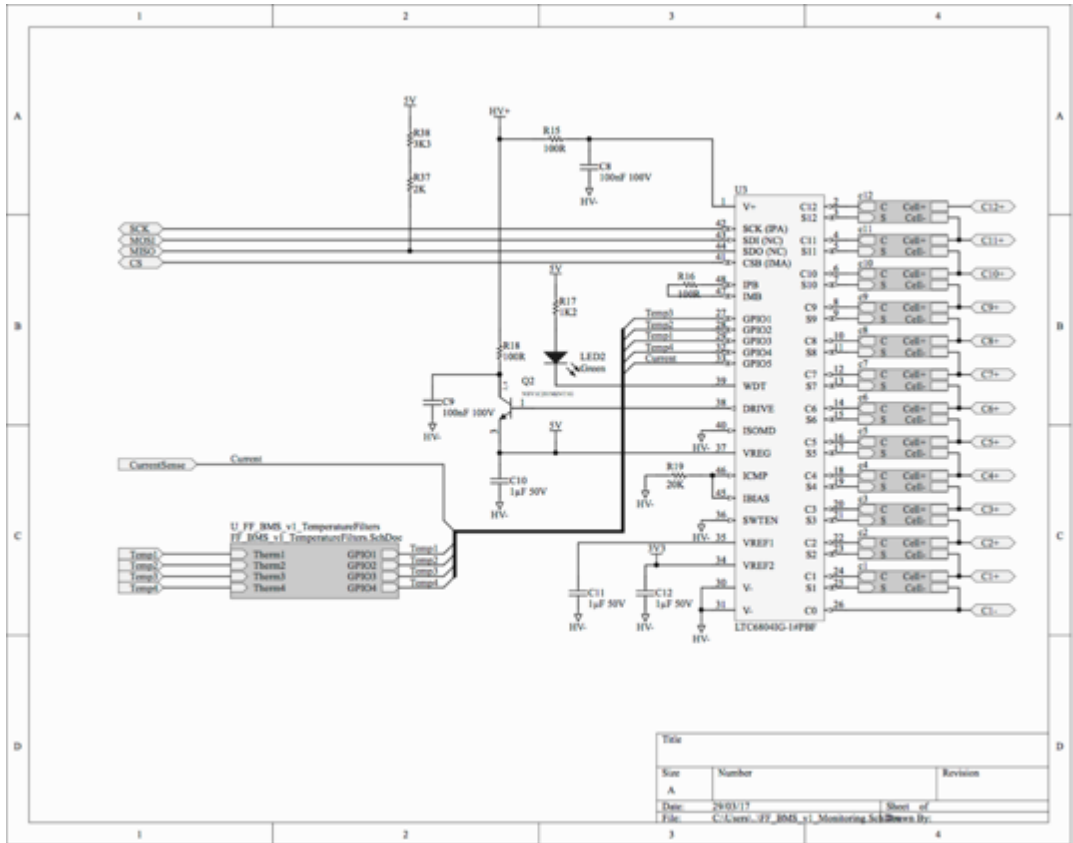
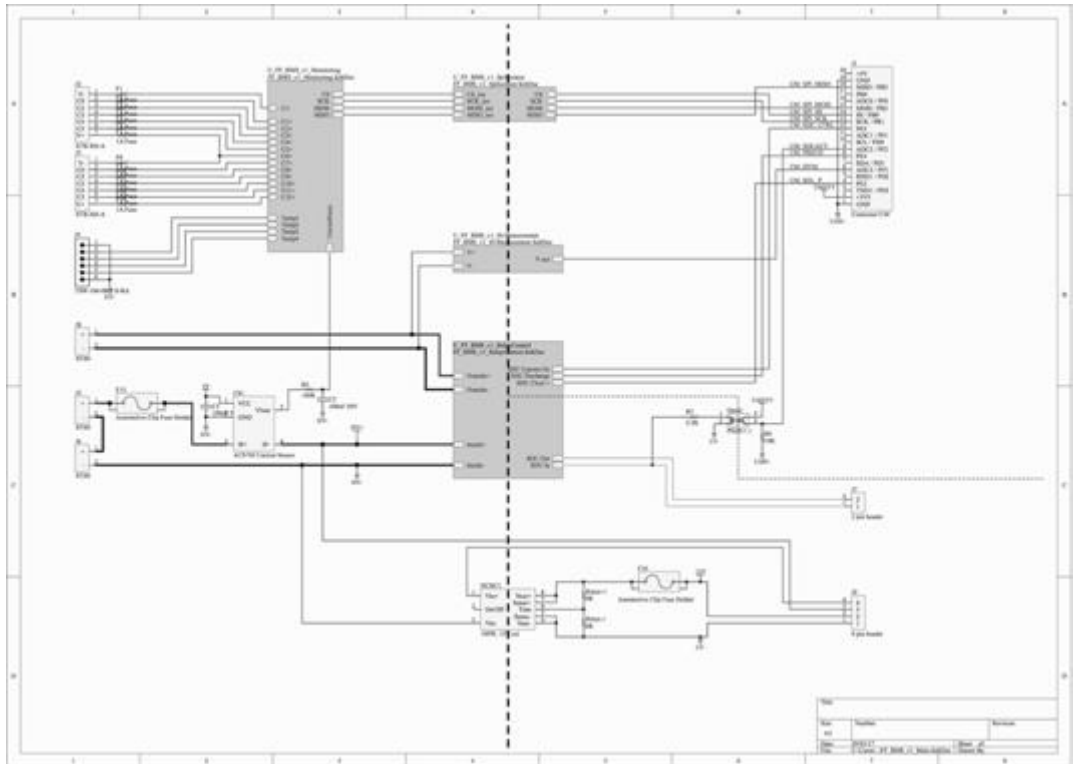
Unofficial datasheet by Sondre Ninive Andersen

Information sourced from:

<http://www.genstattu.com/tattu-7000mah-6s1p-25c-22-2v-lipo-battery-pack-with-xt60-plug.html>



Brand	Tattu
Capacity(mAh)	7000
Voltage(V)	22.2
Discharge Rate (C)	25
Max Burst discharge Rate (C)	50
Configuration	6S1P
Net Weight(± 20 g)	870
Length(± 5 mm)	138
Width(± 2 mm)	42
Height(± 2 mm)	65
Connector Type	XT-60
Wire Gauge	AWG10#
Wire Length(mm)	120
Balancer Connector Type	JST-XHR



15.3.4 Motor controller documentation

Motor Controller

Description:

The Motor controller is divided into a low voltage 3.3v area and a 15v/battery-voltage area. These areas are galvanically isolated. Control signals crosses this isolation through optocouplers. The current sensor works on the hall effect principle and is isolated internally.

The 3.3v side of the motor controller pcb is connected to a Universal Module through a 20pin header contact. The Universal Module is built around an Atmel AT90CAN128/32 microcontroller, which handles the pid control, current measurements, communication with the rest of the car and other support functions.

Power Stage:

The power stage of the motor controller is built around a single power mosfet controlling the voltage over the motor by pulse-width-modulation. This limits us to only one direction of travel, but that is of no consequence. The power mosfet is supplied with a 15 volt pwm-signal into gate, this 15v is stepped down from the propulsion battery voltage by a dc/dc converter on the motor controller pcb board. The 15v pwm signal is again generated by a CMOS Optocoupler. In series with the positive voltage trace on the pcb we have put a current sensor.

The power stage also includes a circuitry to turn the 15 volt dc/dc on/off and a simple circuit for controlling a fan. There is also a flyback diode and four 560uF smoothing capacitors.

Speed control:

The brushed DC motors unloaded rotation speed is determined by voltage that is applied to it while the direction of the rotation is determined by the polarity of that voltage. The magnitude and polarity of the output voltage is controlled by sending the motors a standard servo-style PWM signal.

Dead man switch:

The left paddle must at all times be pressed or else the motor controller will not be able to set a new duty point. If you let go of the paddle it will automatically recoil and the motor controller will set PWM duty at its lowest.

Operating modes:

The fuel fighter motor control is a state machine consisting of five operating modes: precharge, brake, normal mode, cruise control mode and torque control mode:

- Precharge
 - *When turning on the 48V voltage the four 560uF capacitors will be charged by the battery. At this stage the motor controller will turn off the DCDC.*
- Brake
 - *When braking the PWM-signal will be set to its lowest and the motors will not be able to run*
- Normal mode
 - *This mode has to be set manually in the code.*
 - *The maximum PWM-signal is adjusted relative to the rpm at the wheel. This is done to prevent overcurrent to the motors. If any overcurrents are sensed by the current sensor the motor controller will instantly set PWM duty at its lowest.*
- Cruise control mode
 - *This mode has to be set manually on the steering wheel.*
 - *When toggling the CC-button at the steering wheel the motor controller will enter a cruise control state whereas the PWM signal to the motors are based on a rpm PID-algorithm.*
- Torque control mode
 - *This mode has to be set manually in the code.*
 - *The two motors has a unique ID. Each motor-ID has a different range of torque.*
 - *The motor controllers will set PWM duty in ordinance with the maximum allowed current for a particular operating point.*

Features

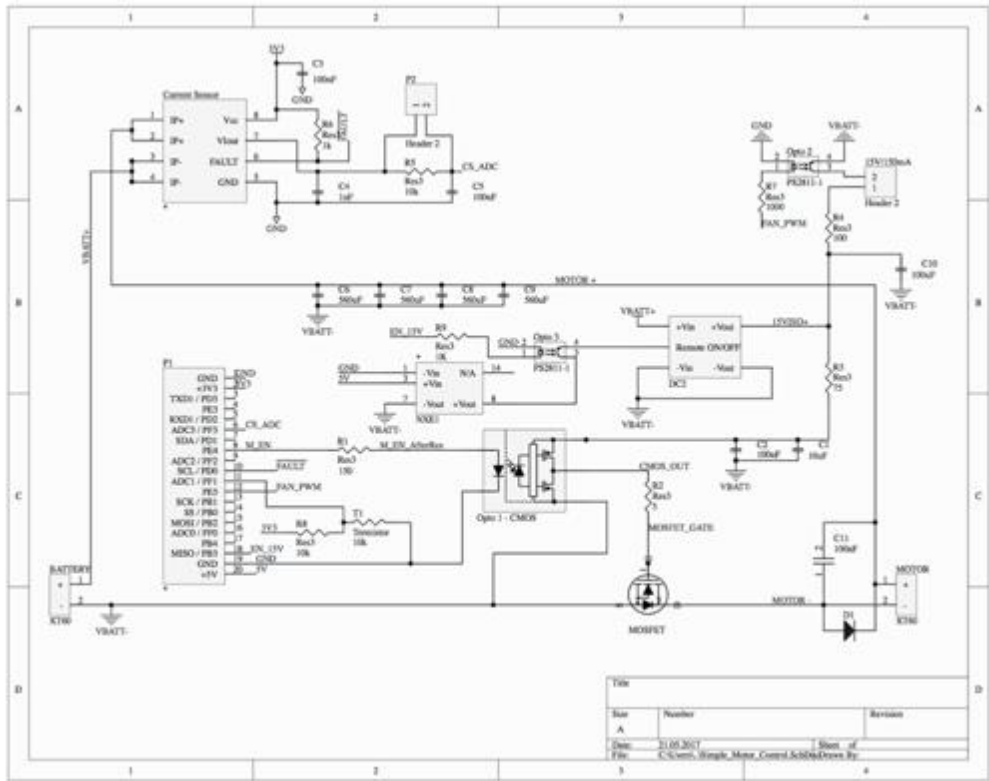
- *Overcurrent protection*
- *Calibration*
- *Integrated cable retention for PWM port*
- *RGB status LED*

Specifications

- *Continuous Current: 4-5A*
- *Peak Current: 12.5A*
- *Output PWM Frequency: 10KHz*
- *Output Voltage Range: 0V – 50V*
- *Maximum Output Voltage: 50V*

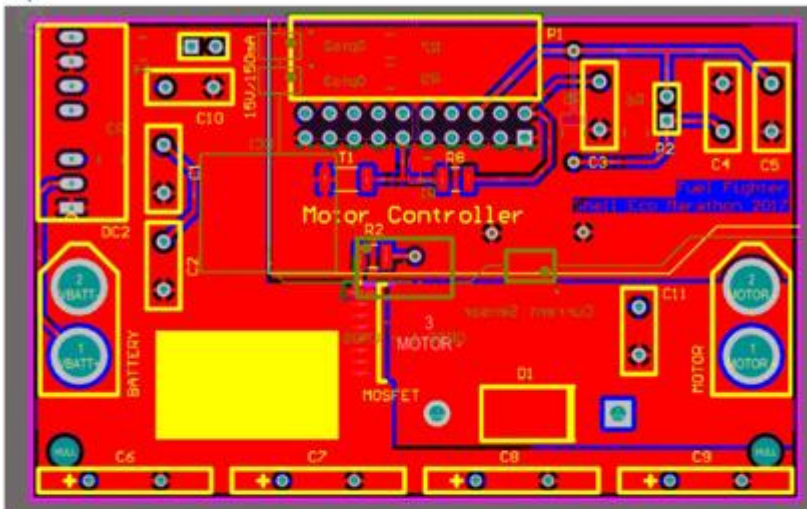
Major Components

PCB Designator	Component	Purpose	Manufacturer
Mosfet	IPT012M08N5	Switching the voltage over the propulsion motor	Infineon
Opto 1 – CMOS	FOD3182	Transmitting pwm signal through galvanic isolation. Slave side is a 15v pwm signal	Fairchild
Opto 2	PS2811	Transmitting pwm signal through galvanic isolation. Slave side is a 15v pwm signal	Renesas
Opto 3	P2811	Transmitting a simple on/off signal to the 15v dc/dc	Renesas
DC1	NXE1	5v to 5v galvanic isolated dc/dc. Used together with Opto 3 to turn off DC2	Murata
DC2	IZ4812SA	Battery to 15v dc/dc used for powering the gate of the Mosfet and Fan	XP Power
Current Sensor	ACS711	+/- 12.5A Current Sensor. Isolated. Hall Effect.	Allegro

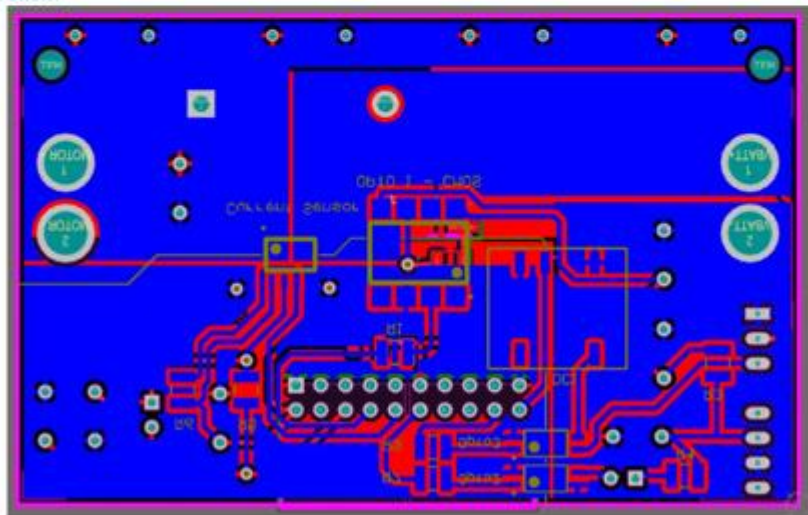


PCB-layout:

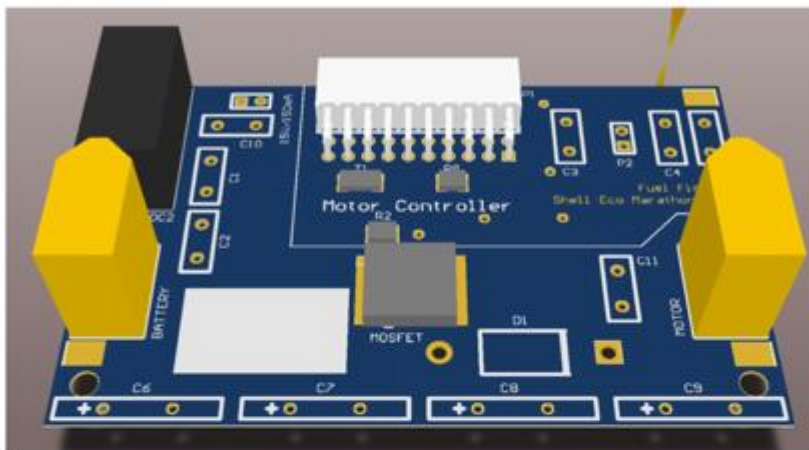
Top:



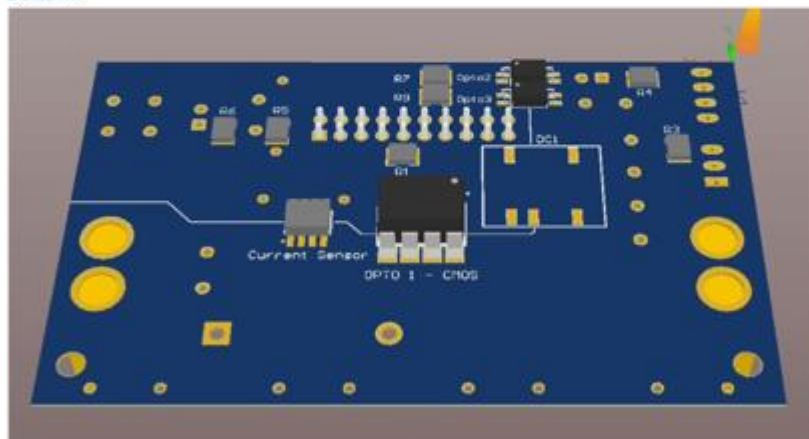
Bottom



Layout:
3D model:



Top:
Bottom:



15.4 Appendix D: Off-track award applications

15.4.1 Design award application



DESIGN AWARD APPLICATION

Design Idea

The vehicle in this application is registered in SEM for the first time in SEM Europe 2017 . In early October, we decided to build a new car instead of improving our existing car. The main reason was to have greater chance of success in the competition as our current car was quite heavy. But we were also determined that our car should look classic, cool and sporty. To market energy-efficiency to the people, it also has to appeal to them aesthetically. We started with a design workshop where the entire team came up with ideas. The inspiration came from collaboration and research on cars we liked.



Early design ideas



CAD models



3D-printed scale models

Design iterations

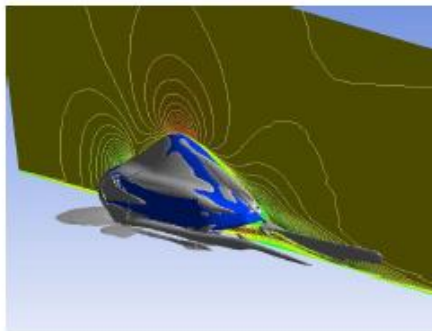
From the drawings, we 3D-modelled some of the concepts. A couple was also 3D-printed in a small scale to get a “feel” of the design.

Since a good result on the track is important to us, we chose to make the car out of carbon fibre due to its high strength-to-weight ratio. We therefore had to iterate our design so it was practical to produce. One example is no overhang in the moulds where we lay the carbon fibre.

By doing CFD-analyses we managed to reduce our drag coefficient to 0.14 from 0.24 of our first version. CFD-analyses was done in ANSYS Workbench while strength simulations were done in Abaqus or Siemens NX.

Some design choices we made were:

- **Mount the rear suspension into bulkhead.** The inner wall already needs to be strong. By mounting the rear suspension into it we could remove the rear wheel arches that would have been heavy due to strength requirements. It also made the geometry more aerodynamic and easier to make.
- **Curved floor.** By designing the floor as an arch, we created a tunnel for the air under the car. That gives the car lift. An arched floor also distributes the load from the driver better than a flat floor. Thus we could save weight on materials there compared to a flat floor.



Team structure

Management – Coordinates the team and give input to the work done. Management aim to facilitate the groups more than control them.

Support – The group where we have people working with PR, marketing, logistics and systems engineering.

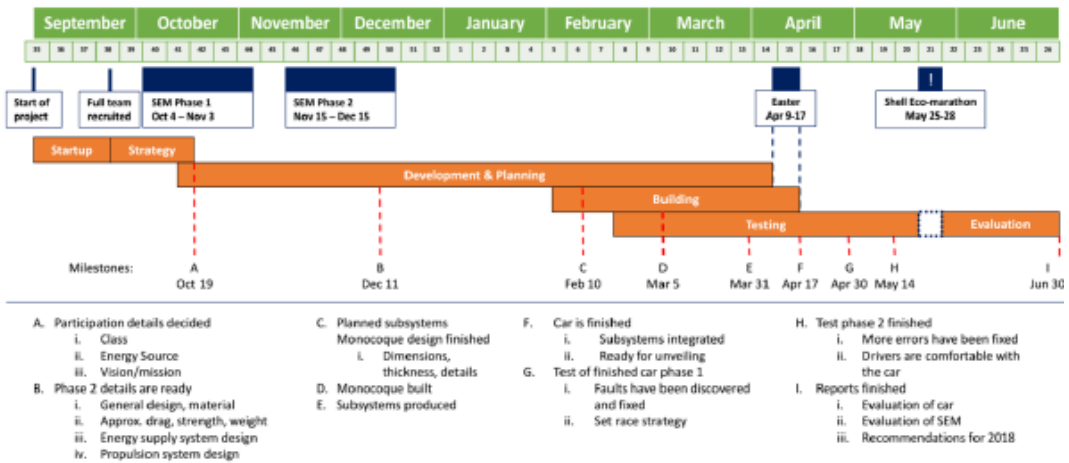
Mechanical – Were responsible for all mechanical work. They conducted the iterations of the design. The sub-groups (mechanical & electrical) had both direct contact with companies we were interested in working with. They got knowledge from that which they used in the work.

Electrical – Makes the decisions and work connected to all electrical components. They decided which motors to use.

Timeline

The following timeline was made in the autumn.

Timeline DNV GL Fuel Fighter 2017



Some remarks to this timeline:

- The production of the carbon fibre monocoque started in mid-February.
- As expected we ran into some issues during production. We had test phase 1 as a buffer for this and the car was ready to our unveiling May 4th.

Ergonomics

We chose to improve the seat used last year. The holes for the seat belts ensures that the driver is secured tightly to the seat with little room for wobbling. Despite the seat's size, it is still lightweight due to its foam and carbon fibre sandwich construction. By using foam inside a single layer carbon fibre shell, we accomplished a low-density construction (milled foam pieces are shown below).



We made the beams of the car quite thin. To get a safe strength it required more layers of carbon fibre, but it gave us better visibility. That way the driver doesn't have to move his head a lot to see things. This makes it both safer and more comfortable for the driver.

Production

Because we focused on production while designing the vehicle we managed to get the number of moulds down to three from eleven with the previous car. That saved us almost 12000 euro. A challenge we faced during production was that epoxy gathered in the small radius in the wheel arches. Our car ended up weighing 85 kg.

Details

In our interior, we have several elements made of wood. An eco-friendly material which we have used in such a way that it combines classic and sporty. By using a laser cutter, we have put our logo as details on the console and wheel. Our logo also appears on the seat, wheel covers and dashboard.



Pictures





15.4.2 Design award application



COMMUNICATION PLAN

We decided early on that the most important parts of the marketing is creating a new graphic profile, focusing on the unveiling of the car, the trip and competition in London. The goal is to let everyone take part in our journey towards the Shell Eco-marathon: through appropriate social media, blog posts and news outlets.

Graphic Profile

Last year's graphic profile was unfocused and we wanted something that ensured that everything looked coherent, as we believe the overall design is a very important part of our identity as a team. Our design is the first thing people notice about us and as such it needs to be memorable.

Grand Reveal

The reveal of the car is one of the most important events and we spent most of our budget and time planning it. We marketed it quite heavily in social media, with posters and we hid small blue cars around our campus for students to find, as a guerilla marketing stunt. Finding one of the cars would mean you were eligible to win a prize after the unveiling. In addition we created a promo video focusing on who we are as a team and why we are doing this project.

Trip to London

We will follow both the car as it is driven across Europe and the team as we fly out in groups. This will be done with pictures and text on Facebook, Instagram[stories] and the app Gobi where we have our own filter. We will also share what we do in London: Visiting our main sponsor, what we do on and off track. In addition the team members will change their profile pictures to their team headshots, and share their experience tagging everything with #Fuelfighters on their social media accounts.

Phase One: New Team (August to December)

- Website:
 - Update (1): with the new team information
 - Include the new team's headshots and group picture.
- Social Media:
 - Introduce the new team on Facebook and Instagram (group picture and text posts)
- Other:
 - Getting a student in an appropriate field to create and design new graphic profile.

Phase Two: New Look (January to April)

- Website:
 - February: Update (2): Photo album, blog.
 - April: Update (3): New graphic profile.
 - Blog post(s) relevant to what we are doing.
- Social Media:
 - Implementing new graphic profile.
- Other:
 - New jackets
 - Designing the cars wrap
 - Planning the unveiling of the car:
 - Preparing images for the press release
 - Contacting students to create a promo video + a shorter video we can use before the unveiling.

Phase Three: New Experiences (May)

Unveiling:

- Website:
 - Early May: Update Website (4): Pictures of the new car
 - Blog posts - About unveiling.
- Social Media:
 - Market the unveiling during and after.
 - Post both videos that have been created
 - Share the news articles we have been featured in.
 - Other:
 - Contact national and regional media.

London:

- Website:
 - Blog posts: trip to London, during London, after the competition is finished.
- Social Media:
 - Updates on the car and the team.
- Other:
 - Contact national and regional media.
 - Hang up posters (60) around campus.

IMPACT ANALYSIS

We have chosen not to focus too much on getting new subscribers, rather working on creating quality content that is both interesting, informative and of interest both to our fellow students here at NTNU, the family and friends that follow us, something for the team members to show others, and off course hopefully reaching outside of this sphere. We have made adjustments when needed to reach as many people as possible, an example of this is when our first blog post got few link engagements from Facebook we changed the way we shared the post. So, instead of linking to our general blog page, we shared the direct link to the blog post, making the link more visible (as Facebook does when sharing a direct link). The results were amazing, we more than doubled the link clicks from 19 to 41.

Our goal was to have an increase in followers on Facebook and Instagram, while also working on getting as many people as we could to the unveiling of the car and getting media attention both in that context and during/after the competition in London.

Facebook

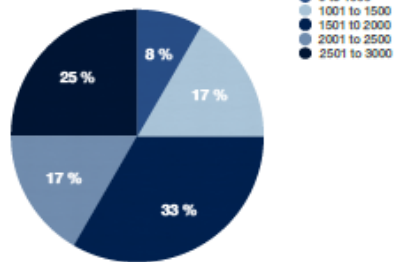
Key notes:

- Followers: 2720.
- We gained about 200 followers during the month of May when we started our focused marketing.
- The promo video for the reveal reached 2563 individuals and had 829 views.
- The first ride for the car reached 2738 individuals and had 709 views.
- The full promo video reached 3510 individuals and had 1100 views, but it was posted today (18th May) and we imagine it will reach further in the next couple of days.
- On Facebook we have posted a mix between pictures, text posts and shared all our blog posts on our Facebook site, charts show how they did:

Facebook Post Reach:

POST REACH	POSTS
0 to 1000	1
1001 to 1500	2
1501 to 2000	4
2001 to 2500	2
2501 to 3000	3
3001 to 3500	1

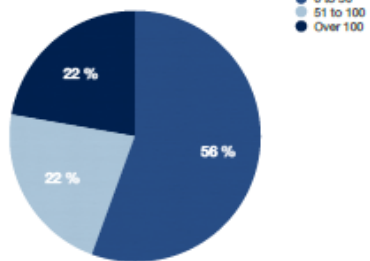
Facebook Post Reach



Likes, Views and Link Clicks

AMOUNT	POSTS
0 to 50	5
51 to 100	2
Over 100	2

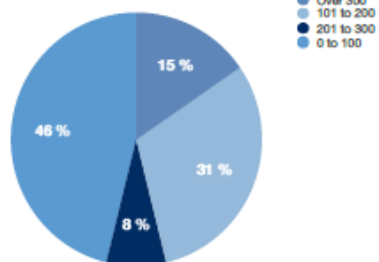
Likes, Views and Link Clicks



Engagements on Facebook

ENGAGEMENTS	POSTS
0 to 100	6
101 to 200	4
201 to 300	1
Over 300	2

Engagements



Instagram

- Followers: 138
- Post likes: 11 to 29 (13 posts)
- Video views: 100 to 170 (3 posts)

The Grand Unveiling

Around 100 people attended the event, based on the food we handed out.

Facebook Event

- Attending: 72
- Interested: 95
- Invited: 235

(pre) Promo Video on Facebook

- Reach: 2563
- Watched: 827
- Engagements: 59

Facebook album from the unveiling

- Reach: 2641
- Engagements: 2061
- Photo Views: 1859

News Outlets

We have been featured in eight different regional newspapers and one technical magazine all in connection to the car unveiling and in the days that followed.

The newspapers we were featured in were with the amount of readers in (): Adresseavisen (55.000), BergensAvisen (12.000), Haugesunds Avis (18.000), Ranablad (7500), Stjørdal Bladet (5500), Sogn Avis (8500), Sunnmørsposten (22.000), Akers Avis/Groruddalen (11.500) and TekniskUkeblad (130.000).

Marketing in and before London

We can't share any numbers of facts about how it will go in the coming two weeks, but as we have had an increase in followers and engagements on especially Facebook we imagine it will go just as well if not better than previous posts. Introducing the Gobi app to our marketing will be interesting, and it is something new!

CAMPAIGN PORTFOLIO

We have picked out different posts from our Facebook, Instagram and website, to illustrate how we have marketed the team throughout the year. We have sorted them in the same phases as we have in the communication plan, doing so we are trying to show how we actually have done what we have explained in the earlier parts of this document.

Phase One: New Team



DNV GL Fuel Fighter
Published by Renate Molvik · 19 · October 20, 2016 · €

Etter noen hektiske uker så er det nye laget endelig kommet på plass. Vi har startet arbeidet for fullt med å planlegge fram mot Shell Eco Marathon i London 2017! // After a couple of busy weeks the new team is in full work mode and we are looking forward to the Shell Eco Marathon in London 2017!

527 people reached Boost Post

Lika Comment Share

Doris Isel, Mikko Indumi and 19 others Chronological

Tor Erling Amosen Det er godt nytt både for NTNU og Shell. Jeg kommer og heier 🙌🏻👍🏻👍🏻

Like · Reply · Message · 1 · October 20, 2016 at 5:44pm



@dnvgfuelfighter · Follow

20 likes · 20 views

dnvgfuelfighter This is @tor, our project manager! Fun fact - he was got it by a monkey🐒 @dnvgfuel @dnvg @shellcomarathon2017 @shellcomarathon @dnvgmarathon @dnvgmarathon #dnvg #shellcomarathon #ntnulaife

Like · Reply · Comment · 1 · October 20, 2016 at 5:44pm



DNV GL Fuel Fighter with Renate Molvik and 10 others.
Published by Anne-Maren Karlberg · 71 · November 10, 2016 · €

Here is the new team! You will get to know each of us individually on our Instagram account @dnvgfuelfighter, so we urge you to follow us there! #NTNU #DNVGL #Shellcomarathon #ntnulaife @dnvgfuel @ntnu



3,108 people reached Boost Post

Lika Comment Share

Leif Arne Piter Nygård, Heidi Linneud and 39 others Chronological

Ronny Krogh Kule saker Ødred Carlsen

Like · Reply · Message · May 7 at 10:32pm

Phase Two: New Look

DNV GL Fuel Fighter
Published by Anne-Maren Karlberg · February 2 · 🌐

Our first blog post is up on www.fuelfighter.no/blog 🌱 Go check it out! DNV GL



2,325 people reached Boost Post

Like Comment Share

Jørgen Jackwitz, Renate Møvik and 13 others

1 share

DNV GL Fuel Fighter with Kjell Sværre and 3 others
Published by Anne-Maren Karlberg · February 8 · 🌐

Thank you Cecilia Haskins for giving us an informative and interesting presentation about Systems Engineering! DNV GL




1,835 people reached Boost Post

Like Comment Share

Moon-Hongsik, Coero/Ino Y Hachizo and 16 others

DNV GL Fuel Fighter
Published by Anne-Maren Karlberg · February 28 · 🌐

We asked some of our team members why they decided to join the DNV GL Fuel Fighter team. Here is what Geir, Amund, Josefine, Mirko and Rishate answered!



Different, but similar, the team reflects upon why we joined DNV GL Fuel Fighter

There are quite a few reasons to why someone would decide to spend a hour-a-week working to build a car without being paid for it. All of us here at DNV GL...
FUELIGHTER.NO

2,036 people reached Boost Post

Like Comment Share

Solveig Haugom-Nesset, Isahil Silwana Neteleand and 23 others

DNV GL Fuel Fighter
Published by Anne-Maren Karlberg · February 19 · 🌐

Read our new blogpost on why we switched over to battery in this years Shell Eco-marathon, DNV GL



Battery or Hydrogen, that's the question

People who have followed us for the last ten years know that we've been using hydrogen fuel cells for most of the Shell Eco-Marathon competitions we have attended. So when we decided to switch over to battery for this years race it...
FUELIGHTER.NO

1,608 people reached Boost Post

Like Comment Share

Jonas Runtjar, DNV GL and 20 others

HOW COOL IS 3D PRINTING?



165 vanlige

DNV Fuel Fighter (@dnvfuelfighter) posted a 3D model of our car @dnvfuelfighter · dnv.no · 2017

👍 165 likes · Comment · Share

DNV GL Fuel Fighter added an event.
April 28 at 9:41pm · 0%

Efter måneder med hardt arbeid er endelig bilen vår klar til avduking. Kom til Hangaren 4. mai for å få med deg bilen som skal konkurrere i Shell Eco-marathon i London. Håper å se deg der!

PS: Hvis du finner en liten blå bil et eller annet sted på Campus, ta den med til avdukingen så kan du vinne en flott premie!

///

After months of hard work, our car is finally ready. Come to Hangaren at the 4th of May to join us in the unveiling of the car we are going to compete with at the Shell Eco-marathon in London. Hope to see you there!

PS: If you find a tiny blue car somewhere on Campus, bring it to Hangaren for the reveal and you might win a prize!




GRAND REVEAL

MAY 4 **Avduking DNV GL Fuel Fighter**
Thu 11:45 AM · Hangaren, NTNU Oslohaugen · Trondheim, Renate and 13 friends · [Going](#)

Phase Three: New Experiences

DNV GL Fuel Fighter
Published by Anne-Maren Karlsberg · April 29 at 11:02am · 0%

Thank you to Benni Solli, who made our new logo! #shellessmarathon DNV GL



New car deserves new logo!

It isn't every year we turn left! So this year we have worked hard not only to make this the best car yet, but to update our looks. We have a brand new logo which, if we can say it ourselves, is quite cool. We have changed quite a lot this year, we...

[PHOTOGRAPH](#)

1119 people reached [Boost Post](#)

[Like](#) [Comment](#) [Share](#)

[Bjorn Solli](#), [Kinga Zolnicka](#) and 9 others

DNV GL Fuel Fighter
Published by Anne-Maren Karlsberg · May 3 at 10:10pm · 0%

Her er en liten smakebit for avdukingen i morgen. Vi sees i Hangaren 11.45!



2,563 people reached [Boost Post](#)

832 Views

[Like](#) [Comment](#) [Share](#)

[Anne May Hegde](#), [Kristin Vikso Sjenstad](#) and 20 others

Pre-promovideo post.

DNV GL Fuel Fighter added 10 new photos to the album **Unveiling 2017** — with Thomas Hardballe Hybertsen and 8 others at **Høgskolen, NTNU Gleshaugen**.
Published by Anne-Maren Karberg · 11 · May 13 at 4:04pm · ©

Her er bildene fra den fantastiske avsløringen vår!
//
Here are the photos from our amazing unveiling!



2,841 people reached Boost Post

DNV GL Fuel Fighter
Published by Anne-Maren Karberg · 11 · May 16 at 8:04pm · ©

First ride! DNV GL – Careers Norway #shellecomarathon #sem2017



2,753 people reached Boost Post

714 Views

Like Comment Share

Håkon Svebak, Peter Jacob Jacobsen and 14 others

3 shares

DNV GL Fuel Fighter
Published by Anne-Maren Karberg · 11 · 8 Hrs · ©

For those of you who couldn't make it to our unveiling 4th May, here is our promo video! DNV GL – Careers Norway #Shellecomarathon #SEM2017



3,085 people reached Boost Unavailable

936 Views

Like Comment Share

Erik Flåtten Dølan, Renate Melvik and 18 others

14 shares




dnvgluefighter
Følger

38 liker 1 u

dnvgluefighter Verdens største
 Ahlgrens bil? 🚗 #shelcomarathon
 #sem2017 #ntnu @dnvgnorge @ntnu
 @ahlgrens_bilar
 vinclecodrive 🙌


 Legg til en kommentar ...

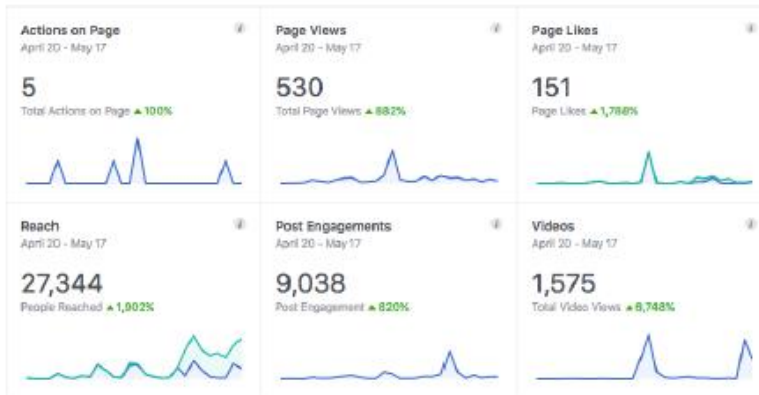



dnvgluefighter
Følger

128 visninger 1 u

dnvgluefighter Tada!
 #shelcomarathon #sem2017
 @dnvgnorge #ntnu


 Legg til en kommentar ...



Facebook Insights from April 20 - May 17

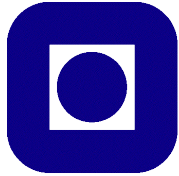


The pictures of this page is depicting the hidden cars from our guerrilla marketing stunt where we hid several small blue cars around campus, which we shared on Facebook, Instagram and had a dedicated page on our website. The students who found the cars were told to bring them to the unveiling and they would be in a lottery to win prizes. The text is in Norwegian as it wasn't something important to anyone outside of campus.



Here is the poster for the unveiling. This too is in Norwegian, as the event would both be held at campus and be in Norwegian.

15.5 Appendix E: Project paper



NTNU
Norwegian University of
Science and Technology

Specialization project

DNV GL Fuel Fighter towards Shell Eco-marathon 2017

By: Bård Carlsen & Odin Oma

Submission date: December 2016, Trondheim

Supervisor: Knut Einar Aasland, IPM

Norwegian University of Science and Technology,
Faculty of Engineering Science and Technology,
Department of Engineering Design and Materials

PROJECT WORK FALL 2016
FOR
STUD.TECHN. BÅRD CARLSEN

DEVELOPMENT OF CARS FOR SHELL ECO-MARATHON

Utvikling av biler for Shell Eco-marathon

Shell Eco-marathon is a competition between student groups to develop, build and run the most energy-efficient vehicle. The competition runs annually in Europe in May/June, and it has now been going for over 25 years. Last year there were over 200 participating teams. NTNU has participated the last 9 years and has achieved very good results in the class "urban concept". Some years ago we also participated in the prototype class with mixed results.

Last year we participated with a car for urban concept class. This was powered by a hydrogen fuel cell. We were unable to get any valid result with this car. A prototype car was developed for the 2014 season, and with it we got a decent result, but it is far from the best in class. We should therefore concentrate our efforts this year to get the one or the other or both cars to work well and to get better results.

The project is a collaboration between a number of students from various departments at NTNU, and in addition to the technical work it also includes sponsorship work, work with the documents that are required to enroll in the car to the competition as well as organizing the work and taking part in the race in the spring of 2017.

In this project, much authority and responsibility is entrusted to the project team. If the cars are to be modified much or improved where necessary, if it should be run on battery electric drive or fuel cell or whether we should switch to something else, is up to the project group. Anyway, there is much that needs to be developed. Therefore there are a number of problem areas that need to be explored and where important decisions must be made:

- which class to compete in and whether we improve on one of our existing cars or we build a new one
- energy source (fuel cell, batteries, other solutions)
- electric motor solution, inclusive motor control
- suspension
- steering and front wheel geometry
- user interface and ergonomics
- driving style – which strategy yields the best results?
- possibly body – aerodynamics, driving style and door solution

We emphasize good project management.

It is not possible to work on this project independently of the others: It is the totality - the resulting vehicle and the driving of it – that counts.

A project plan and a distribution of tasks and responsibilities between project participants must be made early in the project. This also determines the content of the project report to the individual as well as group report.

Formal requirements:

Students are required to submit an A3 page describing the planned work three weeks after the project start as a pdf-file via "IPM DropIT" (<http://129.241.88.67:8080/Default.aspx>). A template can be found on IPM's web-page (<https://www.ntnu.edu/ipm/project-and-specialization>).

Performing a risk assessment is mandatory for any experimental work. Known main activities must be risk assessed before they start, and the form must be handed in within 3 weeks after you receive the problem text. The form must be signed by your supervisor. Risk assessment is an ongoing activity, and must be carried out before starting any activity that might cause injuries or damage materials/equipment or the external environment. Copies of the signed risk assessments have to be put in the appendix of the project report.

No later than 1 week before the deadline of the final project report, you are required to submit an updated A3 page summarizing and illustrating the results obtained in the project work.

Official deadline for the delivery of the report is 13 December 2016 at 2 p.m. The final report has to be delivered at the Department's reception (1 paper version) and via "IPM DropIT".

When evaluating the project, we take into consideration how clearly the problem is presented, the thoroughness of the report, and to which extent the student gives an independent presentation of the topic using his/her own assessments.

The report must include the signed problem text, and be written as a scientific report with summary of important findings, conclusion, literature references, table of contents, etc. Specific problems to be addressed in the project are to be stated in the beginning of the report and briefly discussed. The report should not exceed thirty pages including illustrations and sketches.

Additional tables, drawings, detailed sketches, photographs, etc. can be included in an appendix at the end of the thirty page report. References to the appendix must be specified. The report should be presented so that it can be fully understood without referencing the Appendix. Figures and tables must be presented with explanations. Literature references should be indicated by means of a number in brackets in the text, and each reference should be further specified at the end of the report in a reference list. References should be specified with name of author(s) and book, title and year of publication, and page number.

Contact persons:

At the department : Jan Magnus Farstad, Nils Petter Vedvik
From the industry : Kristina Dahlberg, DNV GL



Knut Aasland
Supervisor



NTNU
Norges teknisk-
naturvitenskapelige universitet
Institutt for produktutvikling
og materialer

Preface

This project paper describes the start-up of this year's project, and the work done by the Fuel Fighter team in the autumn semester 2016. This paper gives the background information and the discussion leading towards the decisions made in this first phase of the project.

The team of 2017 will participate in the UrbanConcept class of Shell Eco-marathon with a new car running on batteries.

We want to thank the people at IPM making this project possible:

Knut E. Aasland, Per-Erik Heksem, Børge Hølen, Nils Petter Vedvik,

The rest of the team,

And finally, we want to especially thank our main sponsor DNV GL and Kristina Dahlberg.

The authors of this paper have had Advanced Product Development as their specialization course.

Bård Carlsen, Product Development and Materials Engineering

Odin Oma, Product Development and Materials Engineering

Contents

1	Introduction	9
1.1	About Shell Eco-marathon	9
2	The team	10
2.1	Start	10
2.2	Recruitment	10
2.3	Reflection on methods of recruitment	11
2.4	Interview	11
2.5	Full team	12
3	Key decisions	14
3.1	Vision, mission and goals	14
3.2	Class	16
3.3	New or current car	17
3.4	Energy source	18
3.4.1	Hydrogen	18
3.4.2	Batteries	21
3.4.3	Decision	21
4	Timeline	22
5	Design of the car	24
5.1	Restrictions by Shell Eco-marathon	24
5.2	Design process	25
5.2.1	Sketching	25
5.2.2	Computer aided design (CAD)	26
5.2.3	CFD guided designing	27
5.2.4	Small scale model	28
5.3	Fabrication of the chassis and choice of materials	31
5.4	Preparations for production	34
5.5	Requirement specification	36
6	Calculations	37
6.1	Force calculations	37
6.2	Force on rear suspension	38

6.3	Energy calculations	39
7	Subsystems	48
7.1	Drivetrain	48
7.1.1	1WD	51
7.1.2	Differential	52
7.1.3	Belt or gears	52
7.1.4	Internal gears	52
7.1.5	Multiple gears ratios and motors	52
7.1.6	Conclusion	54
7.2	Suspension	55
7.2.1	Front suspension	55
7.2.2	Rear suspension	59
7.3	Requirement specification	62
7.4	Other subsystems	63
7.4.1	Steering	63
7.4.2	Interior	63
7.4.3	Electrical system	63
8	References	64
9	Appendix	65
9.1	Track simulations	65
9.2	The influence of the combined efficiency (see Table 3) and the Cr parameter. Cd=0,138 and mass=90kg	70
9.3	Fuel efficiency for car mass of 60 to 110 kg, and Cd of 01 to 0.3.	71
9.4	Recruitment mail	72
9.5	Off-track awards	74
9.6	Horizon fuel cell	76
9.7	Energy supply system	77
9.8	Sketches	79

Table of figures

Figure 1 Track in London 2017.....	9
Figure 2: Recruitment poster	11
Figure 3: Off-track awards	14
Figure 4: Prototype and UrbanConcept with 2015 design.....	16
Figure 5: A selection of Prototype and UrbanConcept cars in 2016	16
Figure 6: Hydrogen stack in lab	18
Figure 7: Visualized dimensions, top view	24
Figure 8: Visualized dimension, side view.....	24
Figure 9: Sketches of initial car ideas.....	26
Figure 10: Dimension reference car	26
Figure 11: 3D-printed models.....	28
Figure 12: Design alternatives.....	29
Figure 13: CFD simulations	30
Figure 14: Strength vs density of engineering materials	32
Figure 15: The monocoque.....	33
Figure 16: Modified wheel well	34
Figure 17: Body split for the moulds.....	35
Figure 18: Forces on rear suspension when braking	38
Figure 19: free body diagram	40
Figure 20: lateral force vs normal force vs slip angle for race cars.....	40
Figure 21: Power required to climb the steepest hill in 15 km/h for different car weights to the left, and power required on flat road in different speeds with car weight of 90 kg to the right.	41
Figure 22: Cd value's effect on aerodynamic drag	42
Figure 23: Simulation of the track with Cd = 0,138, A = 0,883 m ² corresponding to geometry of current car. Elev.= elevation, v=the car's speed, a=acceleration, P = motor power, Ft = force by centripetal acceleration. $F = \sum F$ acting on the car.....	44
Figure 24: Driving profile for a car with Cd=0,25 m=110 kg	45
Figure 25: Simulating fuel efficiency for car mass of 60 to 110 kg, and Cd of 01 to 0.3. A larger plot with all the data can be found in the appendix.....	46
Figure 26: The influence of the combined efficiency (see Table 3) and the Cr parameter. Cd=0,138 and mass=90kg	47
Figure 27: Belt drive and gears.....	48
Figure 28: Lateral force caused by 1WD.....	51
Figure 29: Motor efficiency contour plots.....	53
Figure 30: Old suspension system	55
Figure 31: Old suspension system with bent and fractured rods.	56
Figure 32: Lower A-arm of welded rods	56
Figure 33: MacPherson strut (left) and double wishbone suspension (right).....	57
Figure 34: Illustration of camber	58
Figure 35: Shows inner walls behind bulkhead to mount suspension on.	59

Figure 36: Trailing arm on wheel	59
Figure 37: Constraints and loads	60
Figure 38: Displacement with inner struts.....	61
Figure 39: Displace without inner struts.....	61
Figure 40: Seat made in 2016	63

Table of tables

Table 1: Current vs new car	17
Table 2: Cd results from CFD analysis.....	28
Table 3: Parameters of the fuel efficiency performance of a car	39

1 Introduction

1.1 About Shell Eco-marathon

Shell Eco-marathon (SEM) is a unique competition that challenges students around the world to design, build and drive the most energy-efficient car. With three annual events in Asia, Americas and Europe, student teams take to the track to see who goes further on the least amount of fuel (Shell, 2016a).

SEM is split into two categories; Prototype and UrbanConcept. These are again split into groups by energy type; petrol, diesel, ethanol, GtL, CNG, hydrogen and battery electric. Maximum efficiency is the focus in the Prototype class, which is where the most extreme design is found. The UrbanConcept class is for vehicles with a more practical design that may inspire people to choose a greener car in their personal life. This class therefore have some additional regulations: e.g. the need for luggage room and a window wiper. UrbanConcept vehicles have larger dimensions than the Prototype cars. The regulations the cars need to follow are stated in the SEM rulebook. In addition to the awards for most efficient vehicle, there are off-track awards, e.g. the design or the safety award. The European version will in 2017 take place in Queen Elizabeth Olympic Park, London, UK from May 25-28. DNV GL Fuel Fighter will participate in this competition in the UrbanConcept class. The car must drive around a 1659 m track ten times in less than 39 minutes, and include a full stop at every lap.



Figure 105 Track in London 2017

2 The team

2.1 Start

2017 will mark the 10th time a team from NTNU has participated in Shell Eco-marathon, first in 2008. The project is initiated at the Department of Engineering Design and Materials (IPM) as an opportunity for students to choose as their specialization project and master thesis. The department has a role as a “silent owner”. All decisions, logistics, recruitment and financial funding is the responsibility of the team. This year’s project started on August 25th with four team members in their fifth-year mechanical study, who were to write their specialization paper. Two of them left in the starting weeks to work on other projects. The remaining members were Bård Carlsen and Odin Oma.

2.2 Recruitment

After setting into a new office, the first objective of the team was recruiting new team members. The specifics of the project were not yet decided, and it was felt that these decisions should be based on the competence and motivation of a full team. We identified a need to recruit in the following areas:

- Mechanical
- Electrical
- PR & Marketing
- Hydrogen²

The means we used to inform students that we were recruiting were:

- **E-mail³**. We wrote an e-mail informing about the recruitment and got the study advisors from relevant studies to send to wanted students. This was also sent to other schools than NTNU.
- **Post on Facebook and our website**. We put up a post and changed the cover picture on Facebook.
- **Stand**. Over several days, we had a stand in the Electrical building or at Stripa. These were the areas we identified as best to reach the students we wanted. The prototype car from previous years was brought along to gain people’s attention. Interested could also sign up to receive an e-mail with more information.
- **Lecture talk**. We went to the lectures where we could reach the largest audience or were for students we had a particular interest in. After the lecture break, we showed a short movie and talked about why they should apply.
- **Posters**. Posters were printed and put up around the campus.

² Later decided not to be used as means of energy.

³ Text can be seen in appendix

2.3 Reflection on methods of recruitment

At the interviews, we asked how the applicants had heard about us. The most successful method was the stand in the Electrical building. To bring the prototype car worked well to start a conversation with people. The stand at Stripa was not so successful. It is an area where there often are a lot of stands, which many people are accustomed to and tired of. Therefore, they aren't that interested in stopping at our stand. The lecture talks were also a success, and is an efficient way to get many people aware of us. The e-mail we sent out and the Facebook post also worked, but to a lesser extent than the former mentioned. A large portion of our applicants also heard about us from a friend. Thus, it is important to be aware of that even though the person you talk to aren't interested in joining, they may know someone who could be interested and tell them about it. Some people were made aware by our posters, but not many.



Figure 106: Recruitment poster

2.4 Interview

Generally, few students have any prior experience developing a car. Therefore, the aim of the interviews was to get to know the applicants and assess their personal qualities. We did not ask for transcript of records or resume. One of the objectives of the project is that students get to mix theoretical and practical work. The applicants had to show an interest to learn and give us the impression that they were a person who could work well in this team. Experience was not a prerequisite, but it was beneficial with more theoretical knowledge. Some of what we asked them about were:

- Their motivation for being a part of DNV GL Fuel Fighter.
- What they were interested in working on.
- Their expectations for time spent on the project.
- Their experience with and ability to work in a team.

We had not set a specific number of team members we wanted. The decision was based on the numbers of last year's team (they were 17 in the spring) and which persons we felt would be an asset to DNV GL Fuel Fighter. The team now consists of 18 people from different studies and nationalities.



2.5 Full team

MANAGEMENT



Project Manager

Bård Carlsen

✉ leder@fuelfighter.no

☎ +47 977 72 906

Product Development and Materials Engineering, 5th year

Hometown: Bergen



Technical Manager

Odin J. Oma

✉ odin@fuelfighter.no

☎ +47 919 92 121

Product Development and Materials Engineering, 5th year

Hometown: Tønsberg



Public relations, race driver

Anne-Maren Karlberg

Creative Marketing Communication,

2nd year

Hometown: Bjerka



Public relations

Renate Molvik

Media Com. and Information

technology, 4th year

Hometown: Steinkjer

MECHANICAL



Head of Mechanical team

Kjell Sverre Høyvik Bergum

Product Development and Materials

Engineering, 3rd year

Hometown: Leikanger



CFD mono-coque

Espen Halvorsen Verpe

Energy, Process and Flow

Engineering, 4th year

Hometown: Haugesund



Mono-coque

Espen Braastad

Product Development and Materials

Engineering, 5th year

Hometown: Oslo



Suspension

Mirko Indumi

Mechanical Engineering, 3rd year

EPFL University, Lausanne

Hometown: Bern



Molding process

Josefine Caroline Stokke Haugom

Product Development and Materials

Engineering, 4th year

Hometown: Oslo



Steering

Augustin Rigal

Mechanical Engineering, 3rd year

SIGMA, Clermont-Ferrand

Hometown: Chambéry



Interior, driver interaction

Thomas Hybertsen

Energy, Process and Flow

Engineering, 3rd year

Hometown: Trondheim



Drivetrain, race driver

Sivert Rød Hatletveit

Product Development and Materials

Engineering, 4th year

Hometown: Molde

ELECTRICAL



Head of Electrical team
Jørgen Jackwitz
Industrial Cybernetics, 5th year
Hometown: Holmestrand



Motor controller
Kristoffer Rakstad Solberg
Marine Technology, 3rd year
Hometown: Lørenskog



Motor controller
Marius Strand Ødven
Cybernetics and Robotics, 4th year
Hometown: Ålesund



Motor controller
Ole Sivert Otterholm
Cybernetics and Robotics, 4th year
Hometown: Ålesund



Electrical system
Oia Lium
Computer Science, 2nd year
Hometown: Malvik



Electrical system
Jan Fijalkowski
Cybernetics and Robotics, 1st year
Hometown: Kolbotn

3 Key decisions

There were several decisions that needed to be clear before the project could take off. The entire team was gathered to discuss their motivation and ambitions. We felt that they should take part in these key decisions to create a sense of ownership over the project.

The areas we identified as important to decide on were:

- Which class we should compete in – UrbanConcept, Prototype or both.
- If should continue with our current car(s) or build a new one.
- Which kind of energy type we should choose.
- Our vision, mission and goals.

3.1 Vision, mission and goals

Last year’s car was made to win the design award. A requirement to win an off-track award is that the car get a valid attempt. It hasn’t happened in the two years the car has participated, and thusly not been qualified to be up for consideration for an award. The purpose of SEM, to have the most energy-efficient car, determines who wins the on-track awards. The team who use the least amount of energy wins. The prizes are awarded in three energy categories in both Prototype and UrbanConcept; Internal combustion, Hydrogen Fuel Cell and Battery Electric. In addition, teams can win the off-track awards in Figure 107. These have to be applied for, and a team can apply for maximum two; or three if one of them are the Safety Award. The objectives of the awards can be seen in appendix 9.5.

SHELL ECO-MARATHON OFF-TRACK AWARD	ASIA/AMERICAS	EUROPE
Communications Award	\$3,000	€2,500
Vehicle Design Award Prototype	\$3,000	€2,500
Vehicle Design Award UrbanConcept	\$3,000	€2,500
Technical Innovation Award	\$3,000	€2,500
Safety Award	\$3,000	€2,500
Perseverance and Spirit of the event Award	\$3,000	€2,500

Figure 107: Off-track awards

The team chose to focus on the on-track award. We wanted to stick to the objective of SEM and have a car which could compete in going the furthest. We also prioritized to get a valid result this year, and not fail for the third time in a row. From the off-track awards, we decided to go for the Communication Award and the Vehicle Design Award, but these were of a lower priority.

We had a workshop with brainstorming to decide:

- Our vision – what we want to achieve
- Our mission – what we want to do

Derived from the objective of SEM, from previously used vision and our own take on it, we decided on:

OUR VISION IS:

To focus on innovation towards a sustainable future -
To learn, improve and challenge how we perceive
today's transportation possibilities.

OUR MISSION IS:

To develop and build an ultra-energy-efficient car and
demonstrate its performance in the Shell Eco
Marathon.

3.2 Class



Figure 108: Prototype and UrbanConcept with 2015 design

It was decided to just work on one car since there aren't enough team members to have the capacity to work on two. That would also require greater financial resources, which would be an extra challenge to acquire. When it came to the choice between a Prototype or an UrbanConcept car, the entire team preferred UrbanConcept. It was felt that there wasn't much work we could do to improve our Prototype car. A new one would be almost identical to the competitors. In this class, where you are allowed to lay flat inside the vehicle, the designs have converged to be long and droplet-shaped. UrbanConcept was seen as a more exciting task, where we could challenge ourselves more and have greater freedom in our engineering.



Figure 109: A selection of Prototype and UrbanConcept cars in 2016

3.3 New or current car

After it was decided that we would compete in the UrbanConcept class, we had to decide if we were going to improve our current car or build a new one. The current car was made to win the design award, and is unnecessary big and heavy. It was not designed to have a low drag or weight. It weighs in at 113 kg, 41% more than the winner of the UrbanConcept Hydrogen class at 80 kg. A clear disadvantage for us in the competition and an important element in our decision. We also thought about the cost of the project. Making a new car is much more expensive than improving the old one. That requires more from us in getting funds from sponsors, or get work and materials at a reduced cost or free. It will also take much more work in developing an entire new car. With our current car, the problems are known to us and can be addressed now. With a new car, new and unexpected problems will occur.

Table 21: Current vs new car



	CURRENT CAR	NEW CAR
Cost	LESS +	MORE -
Possibilities to: <ul style="list-style-type: none"> • Shed weight • Improve aerodynamics • Change design 	LIMITED -	OPEN +
Work	LESS +	MORE -
Problem areas	KNOWN +	UNKNOWN -

We felt a new car had to be made to match our ambitions of a good result, even though it is a higher risk associated with it. The team had the motivation to put in the work required to make a new car and were ready to face the challenges that comes with it. We assessed that a new car also fitted our goals better. Since we chose to go for a new car, we were also conscious about not making it too complicated for our self. We follow the KISS philosophy – “Keep It Simple Stupid”. We will not spend time on areas where we can achieve small improvements, but focus our effort on what will get us to the finish line. The car is meant to be a groundwork for the teams in following years to improve upon.

3.4 Energy source

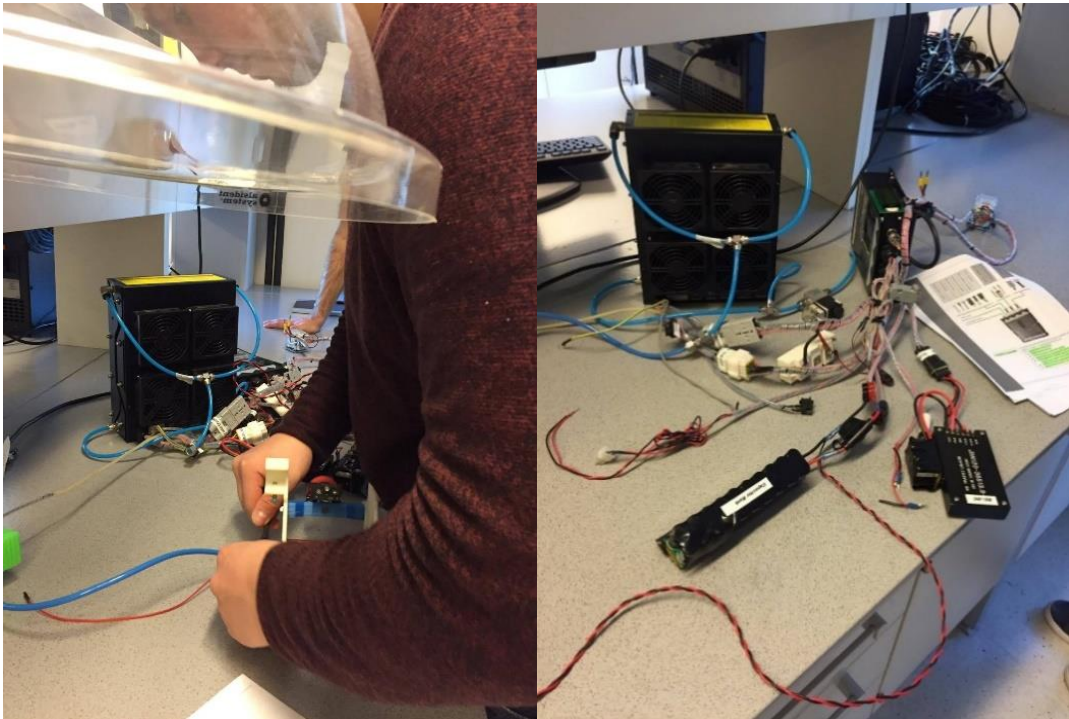
The last two years, DNV GL Fuel Fighter has competed with an UrbanConcept car running on hydrogen. We had to decide if we were going to continue using hydrogen. We knew we wanted to have an emission-free car, so our alternatives were hydrogen or batteries.

3.4.1 Hydrogen

If we wanted to go for hydrogen this year, we had four possibilities:

1. Use current system.

The hydrogen system we were in possession of was Horizon 1000XP (See appendix 9.6). We wanted to know the condition of this system. The hydrogen group took a safety course to get access to the lab and we got an area to perform testing at SINTEF. The hydrogen stack was flushed with distilled water to prevent it becoming too dry, and set up in the lab at SINTEF.



With this system, we could ask last year's team for help and build on their experiences. Some of what they told us were:

Figure 110: Hydrogen stack in lab

- The control unit had once stopped working and had to be sent to Horizon in Shanghai. The team never got to know what the problem was. If the control box were to fail during the competition, there is nothing we can do to fix it.
- We won't be able to modify the system.
- They got the fuel cell software from Horizon but could not get it to work.
- The stack could not deliver the needed power to climb the hill on the track.
- The stacks from Horizon have a high hydrogen leakage before they warm up. They had no problem passing technical inspection when they ran it for about ten minutes first.
- It would be a good idea to add capacitor to be able to accumulate energy and run the fuel cell at its best efficiency point. Hard to optimize.
- Ventilation should be better to cool the stack.

Pros and cons of current fuel cell system:

+ Known problems	- Can't be modified
+ In possession of system – Cheap	- Uncertainty about power output
+ Old know system and can help	- Unreliable
	- Problematic software

2. Buy a new system.

Since our current system is a couple of years old, newer and more efficient models exist. This would be an advantage in the competition. We did not have the track information at the time we had to make a decision though. It was therefore not possible to calculate the power we required from a stack. That would make the choice more difficult and risky. The hydrogen team looked at the options that exist, and estimated that the cost of a new system would be 100 000 – 150 000 NOK.

Pros and cons of buying a new fuel cell system:

+ Can be bought after wanted specs	- Expensive
+ State of the art system	- Unknown requirements
	- Unreliable

3. Buy a new stack and build control unit.

This option involved only buying a new stack and build our own system around it. This would give us the possibility to modify it the way we wanted. We estimated the cost of a new stack alone to be 50 000 – 100 000 NOK. In addition comes the cost of building the system. We had an offer to borrow a stack from the Swedish company PowerCell for one year, free of charge. The stack they could offer was too heavy and didn't have the power

output we wanted. It would be a disadvantage against our competitors. The problem with not knowing the track was an issue in this alternative also. We have no one in the team with any knowledge of how to build such a system, so the task would pose a major challenge.

Pros and cons of buying a new stack:

- | | |
|------------------------------------|--|
| + Can be bought after wanted specs | - Unknown requirements |
| + State of the art stack | - Expensive if bought |
| + Control over system | - If free stack – heavy and less efficient |
| | - Difficult to build |

4. Build our own system.

Would be a major project, and since we didn't have any members with any experience this didn't seem like a feasible task. Although the guys at SINTEF found the idea exiting, they made it clear how much work this was, that it would not be as efficient as a commercial one and advised us not to do it. The idea was quickly dropped.

Pros and cons of building our own system:

- | | |
|--------------------|-----------------------|
| + Complete control | - Time consuming |
| | - Low efficiency |
| | - Extremely difficult |

General for hydrogen

We considered alternative 4 as too complicated and alternative 2 as too expensive. We continued with alternatives 1 and 3, to compare them with batteries. They share some positive and negative features. As hydrogen cars are not as common as battery cars, it's more likely that it would attract attention from media. That would be a selling point to potential sponsors.

Pros and cons of hydrogen:

- | | |
|----------------------|--------------------------------------|
| + More exotic | - Needs ventilation |
| + SINTEF are helpful | - Strict hydrogen transfer procedure |

3.4.2 Batteries

Batteries as an energy source in cars is now a mature technology. Hence a lot of resources for us to use exist. If we were to choose batteries, the rules states that we have to make motor controllers and PCBs purpose-built for SEM. We are also restricted to two motors.

Pros and cons of batteries:

- + Cheap components
- + More resources online
- + Takes less room
- Have to make a motor controller

3.4.3 Decision

We wanted to include most people in deciding which type of energy we should use, especially the hydrogen and electrical group since they are most affected by our choice. We excluded our current fuel cell on account of its reliability. Our main objective is to finish, and when they have not been able to do so in the last two years using it, we didn't feel we could trust it. Our tests supported our concern. With the choice of going for batteries or a new stack, we had to make a controller nevertheless. Tasks which we had not much more knowledge about one over the other, and there are more resources online about motor controllers than about controllers for hydrogen fuel cells. A new hydrogen stack is also much more expensive than batteries. We did not want to use the option of borrowing a stack which was not optimized for our purpose. A reason for choosing hydrogen is the gimmick. It is an exciting technology that attracts attention. With these considerations, there was a consensus that we should choose batteries. The people who were in the hydrogen group were initially more motivated to still using hydrogen than to switch to batteries. They got to be involved in our decision and thought that we had made the correct choice switching to batteries.

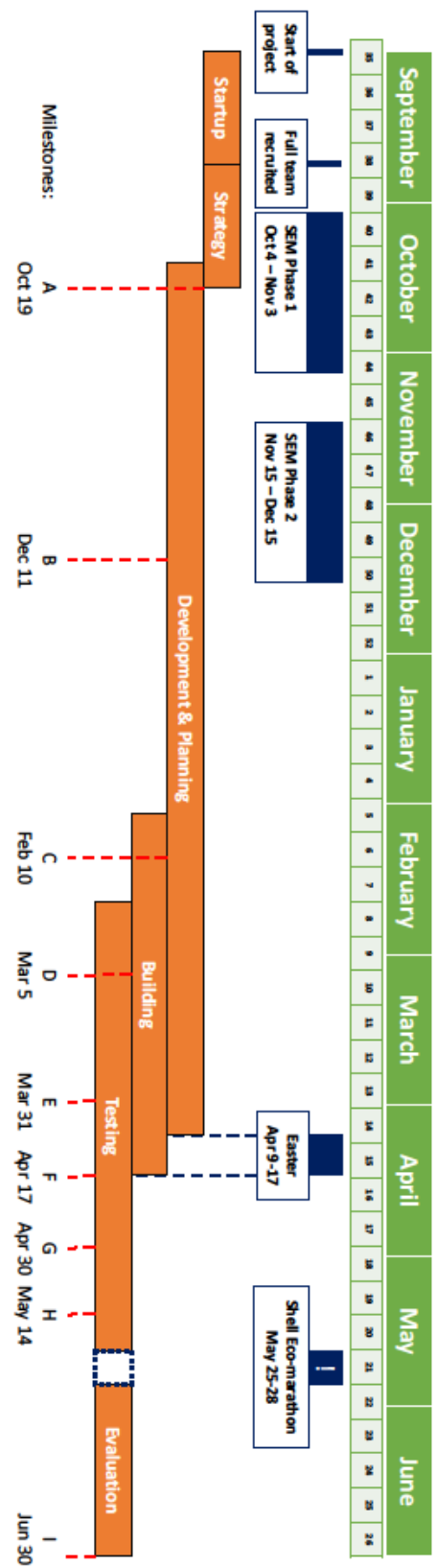
4 Timeline

To facilitate better project management and have a plan of our work, a timeline was created. With the timeline, all team members know our schedule and when different milestones need to be completed. It also informs about when the different phases of our project are, how they overlap and what we should be working on.

The different phases are:

- Startup – Knowledge transfer, recruitment, etc.
- Strategy – Define what our project will be.
- Development and planning – Engineering of the technical solutions, logistics of travel.
- Building – Manufacturing of subsystems and assembly of vehicle.
- Testing – Check that both subsystems and the entire vehicle works.
- Shell Eco-marathon – Competition.
- Evaluation – Define what went well/bad. Create a report with recommendations for next year's project.

Timeline DNV GL Fuel Fighter 2017



- A. Participation details decided
 - i. Class
 - ii. Energy Source
 - iii. Vision/mission
- B. Phase 2 details are ready
 - i. General design, material
 - ii. Approx. drag, strength, weight
 - iii. Energy supply system design
 - iv. Propulsion system design
- C. Planned subsystems Monocoque design finished
 - i. Dimensions, thickness, details
- D. Monocoque built
- E. Subsystems produced
- F. Car's finished
 - i. Subsystems integrated
 - ii. Ready for unvelling
- G. Test of finished car phase 1
 - i. Faults have been discovered and fixed
 - ii. Set race strategy
- H. Test phase 2 finished
 - i. More errors have been fixed
 - ii. Drivers are comfortable with the car
 - iii. Reports finished
 - iv. Evaluation of SEM
 - v. Recommendations for 2018

5 Design of the car

5.1 Restrictions by Shell Eco-marathon

To be allowed to participate in the competition, vehicles must fulfil Shell's dimension specifications, stated in the Eco-marathon rulebook (Shell, 2016b). To give us an overview and guide us in the design of the car, we visualized all dimension requirements, shown in Figure 112 and Figure 111.

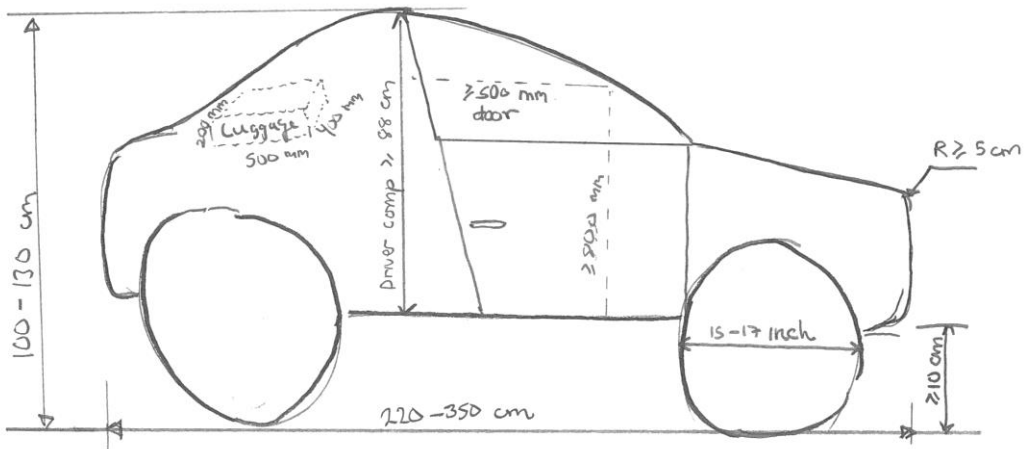


Figure 112: Visualized dimension, side view

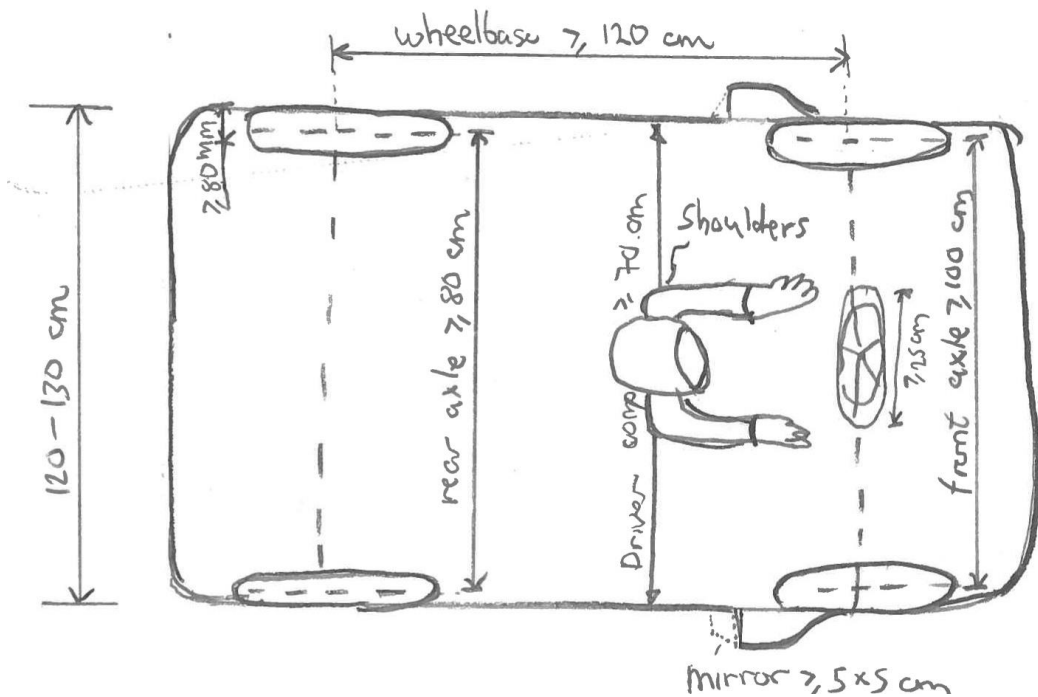


Figure 111: Visualized dimensions, top view

Another important requirement from the rules affecting the design of the car is:

“The body must cover all mechanical parts whether the vehicle is viewed from the front, the rear, the sides or from above. However, the wheels and suspension must be fully covered by the body when seen from above and up to the axle centre line when seen from front or rear. The covering for the wheels and suspension must be a rigid integral part of the vehicle body.”(Shell, 2016b)

This takes away design ideas with open regions through the car or the wheels being outside the main body. From a radical innovation point of view, this requirement is a bit disappointing as it reduced the solution space and restricts to car to look similar to today’s cars. As there is a requirement to have a certain sized luggage room, our opinion is that this requirement is enough to make the car functional for the city.

5.2 Design process

5.2.1 Sketching

In the beginning of the project we had a workshop to “kick-start” the project. At this workshop, we had a sketching session where we urged the team to draw vehicle designs without any restrictions or pre-sets. The idea was to embrace full creativity, even though many of the design proposals would be off the requirements. More sketches can be found in appendix 9.8.

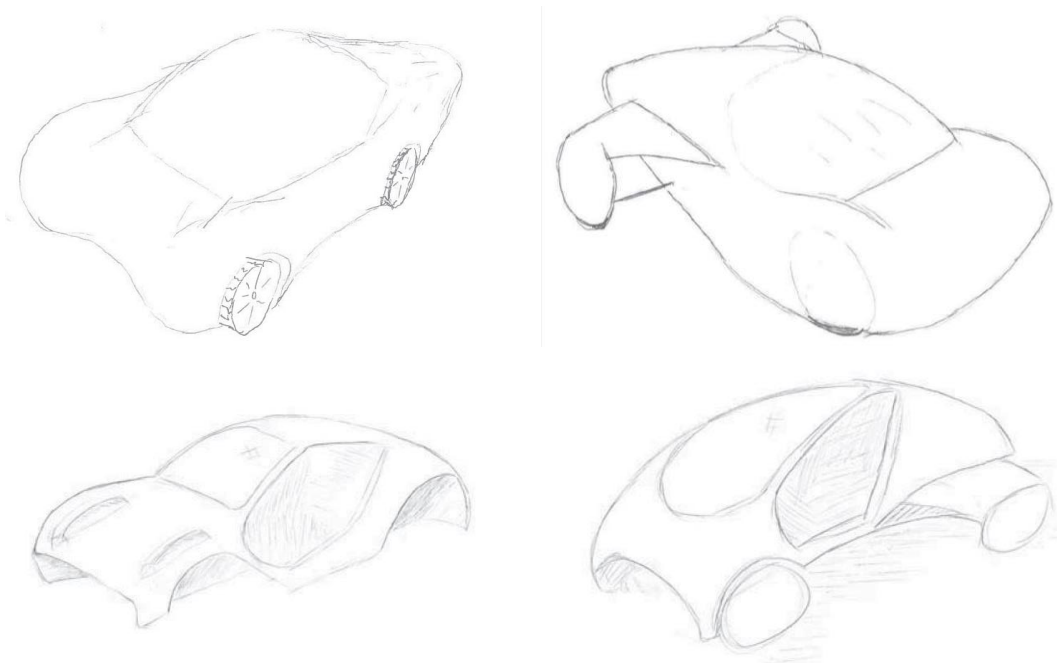


Figure 113: Sketches of initial car ideas

5.2.2 Computer aided design (CAD)

NX Siemens was the chosen CAD-system, as it is the preferred software by most team members. Car design were made with inspiration from the sketches, as well as production and concept car on the list of car with lowest drag coefficient. To guide and restrain the models, a reference car was made (Figure 114). If a proposed car design is able to fit this reference model inside itself, it will be within the dimension requirements.

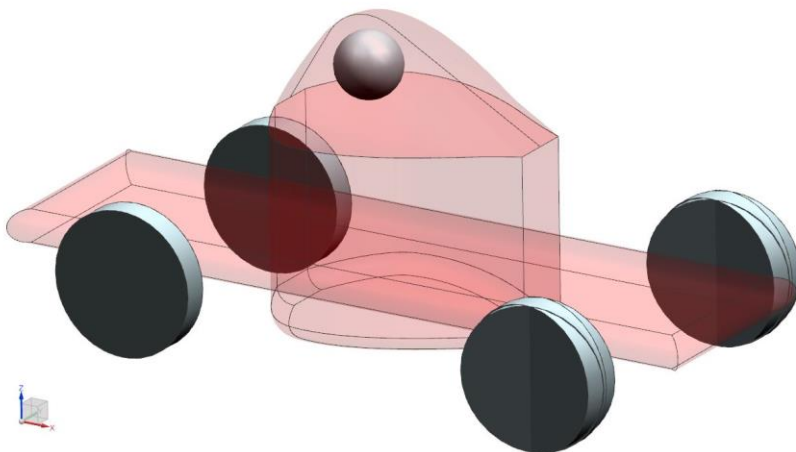


Figure 114: Dimension reference car

This reference model further reduces the minimal size of the car required. This model fully accounts for:

- The driver compartments must be 70 cm wide, measured at the driver's shoulders.
- The vehicle must have a height of 100 cm, which is fulfilled if the highest point is 100 cm above the ground. However, the driver must have 5 cm clearance from his head to the roof/wall in all directions.

5.2.3 CFD guided designing

Reducing the aerodynamic drag on the car is highly important factor to get a fuel-efficient car, as discussed in the energy section. Thus, we had a focus on pushing the designs to be as aerodynamic as possible. We have actively used CFD to guide the progress of making the design more aerodynamic. Car design were analysed in the CFD Software Fluent. Some of the results leading us to the final car design are presented in Table 22. These results are all from simulations where the calculation model has become stable, with a commonly used *residual convergence value of 10^{-6}* . To get a reference of the minimum drag coefficient (C_d) we could produce, a test model was made. The shape of the car was design with a low complexity, and resemble a long droplet, a highly aerodynamic shape (Çengel and Cimbala, 2010).

Important findings:

- The car body should have a round, oval front to nicely cut the air. Thereafter, the body should be as straight as possible, toward a middle point in the back of the car. Sidewalls curving inwards, to reduce volume of the car, will have a negative impact on the C_d .
- A tunnel under the car will reduce the frontal area and slightly reduce the C_d . However, the tunnel must have a constant cross section. If not, pressure differences will arise in the flow under the car, and result with the C_d becoming worse.

Table 22: Cd results from CFD analysis

Model	Iteration	Frontal area [m ²]	C _d	Comment
Design A	1	0,859	0,270	Sidewall curves in
Design B	1	0,885	0,282	Sidewall curves in
Design B	2	0,885	0,276	
Design C	1	0,915	0,16901	Test design
Design C	2	0,866	0,140	Test design, added tunnel
Design B	3	0,896	0,1421	More straight surfaces
Design B	4	0,882	0,138	Added tunnel

5.2.4 Small scale model

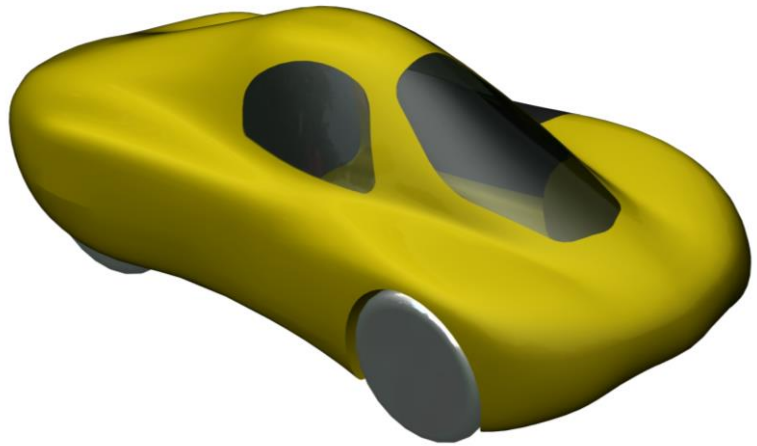
Designs were 3D-printed to get a better feel of the shape. Also, the initial plan was to test the small models in the wind tunnel to compare with the CFD-results. Our CFD-team calculated that to scale our smallest models to the same Reynolds number (Re), the wind speed had to be extremely high – around 350 km/h. It is possible to get acceptable results with a lower Re as long it can be assured the flow over the car is turbulent. However, with the maximum speed of the wind tunnel, the models would be in the transition area between laminar and turbulent flow, and would yield bad results. Making models at least twice the size, and an overall scale of 20%, would yield a Re within the turbulent area. Unfortunately we did not get access to use the wind tunnel lab at NTNU.



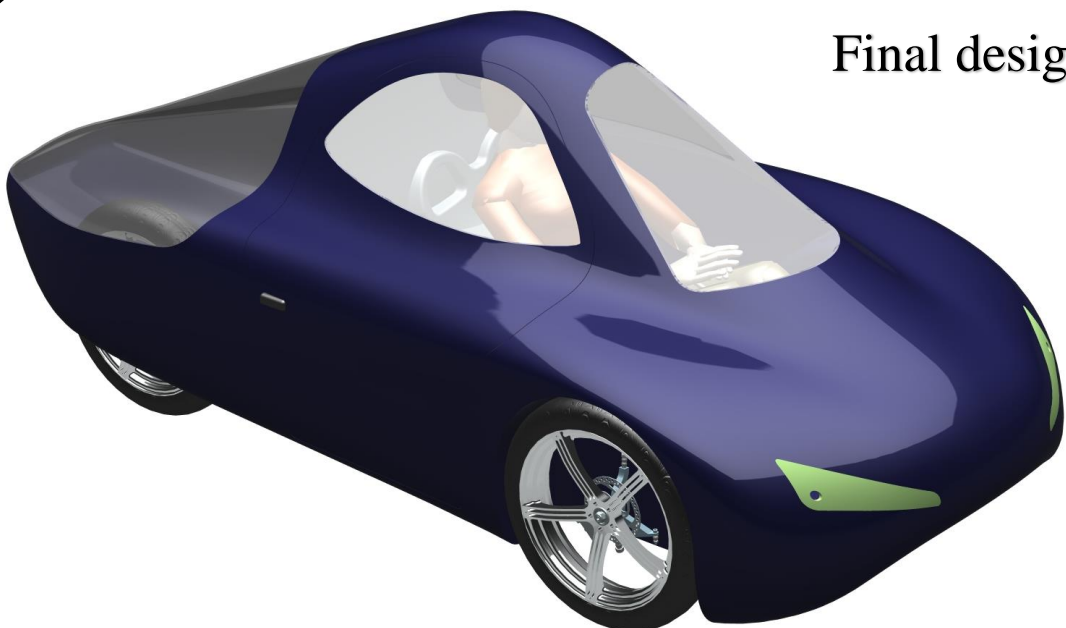
Figure 115: 3D-printed models



Design A



Design B



Final design

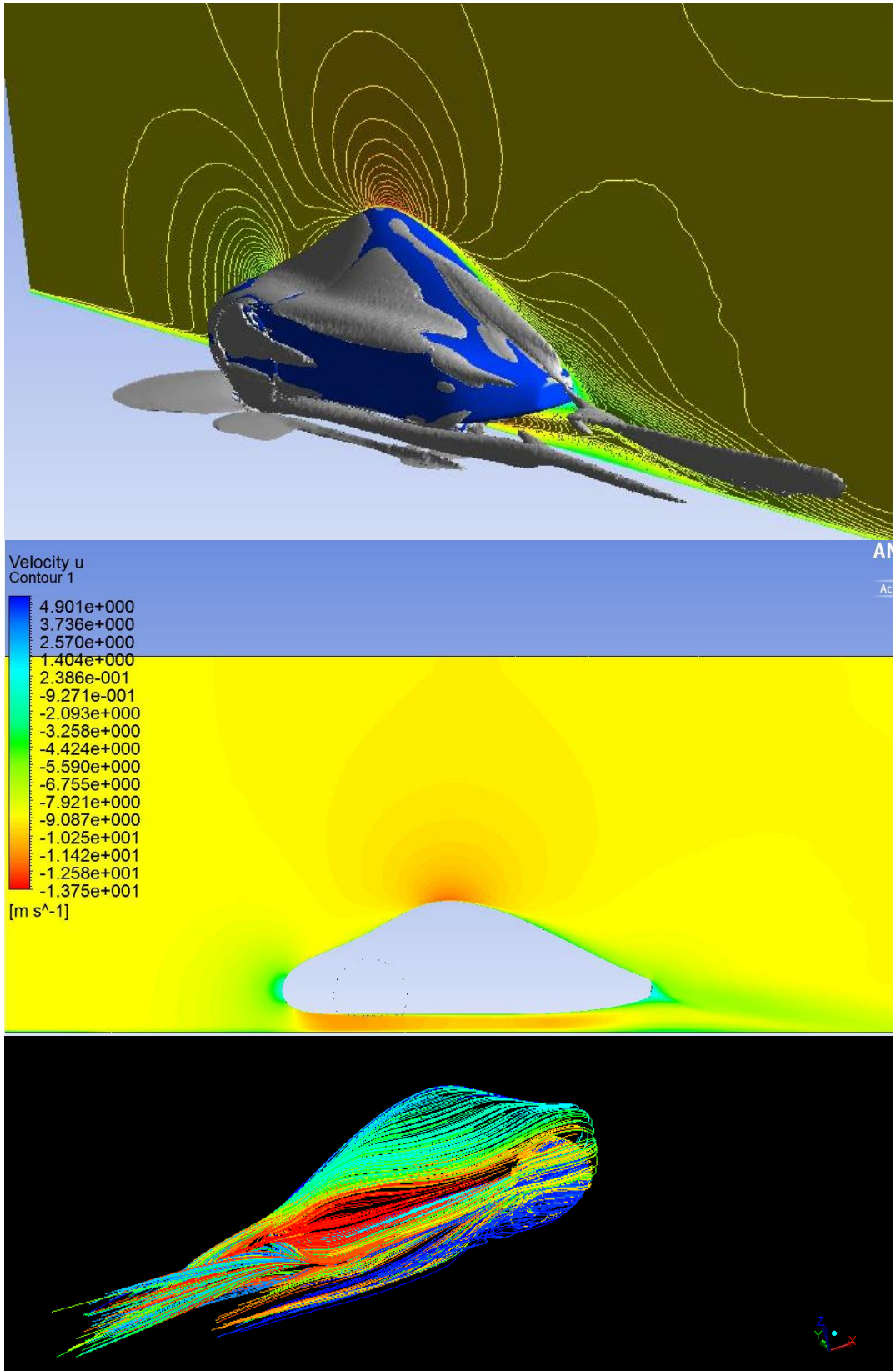
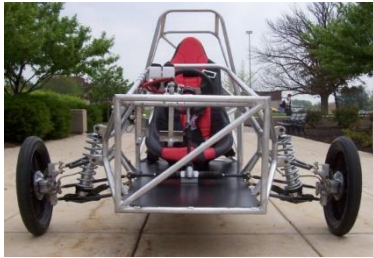


Figure 117: CFD simulations

5.3 Fabrication of the chassis and choice of materials



	Steel	Aluminium	Carbon fibre	Bamboo
Affordable	■■■□□	■■□□□	■□□□□	■■■■□
Lightweight	■□□□□	■■□□□	■■■■□	■■■■■
Strength	■■■■□	■■■□□	■■■■■	■□□□□
Specific strength	■■■□□	■■■■□	■■■■■	■■■□□
Life cycle	■■■□□	■■■■□	■□□□□	■■■■■
Machinability	■■■■□	■■■■■	■□□□□	■■□□□
Availability	■■■■■	■■■■■	■□□□□	■□□□□

There are two initial decisions to take regarding the chassis.

1. Material selection
2. Frame or monocoque

Carbon fiber composite is the only applicable material for monocoque among our alternatives. Which means it is either that, or have frame structure. The chassis should be as light as possible, while being able to withstand the static and dynamic forces acting on it.

Steel and aluminium

Steel is the heaviest among the alternatives. However, there exist high strength steels with incredible tensile strength, which makes it possible to make a thin tubed frame. These are expensive and special skills are needed to weld them. Aluminium is a lightweight metal, but the tensile strength is lower. There are high strength aluminium alloys, where again welding is a problem.

Bamboo

Building the car with a proper eco-material would be a new, interesting twist. Bamboo is much stronger and lighter compared to other timber, and would be suitable as a frame material. Obviously, the mechanical properties would not be able to match the other alternatives. However, this material choice would have scored many points in the design award, for use of eco-friendly material and new-thinking. The same applies to the interest and media coverage of our project. Bamboo beams are not easily available in Norway. This alternative would also be substantially risky material-wise, as we have no experience with the material.

Carbon fibre

This composite material has a considerable advantage compared to the other materials. When comparing to typical steels and aluminium, its specific strength is by far the highest of our alternatives. However, it is the least recyclable and difficult to mass produce.

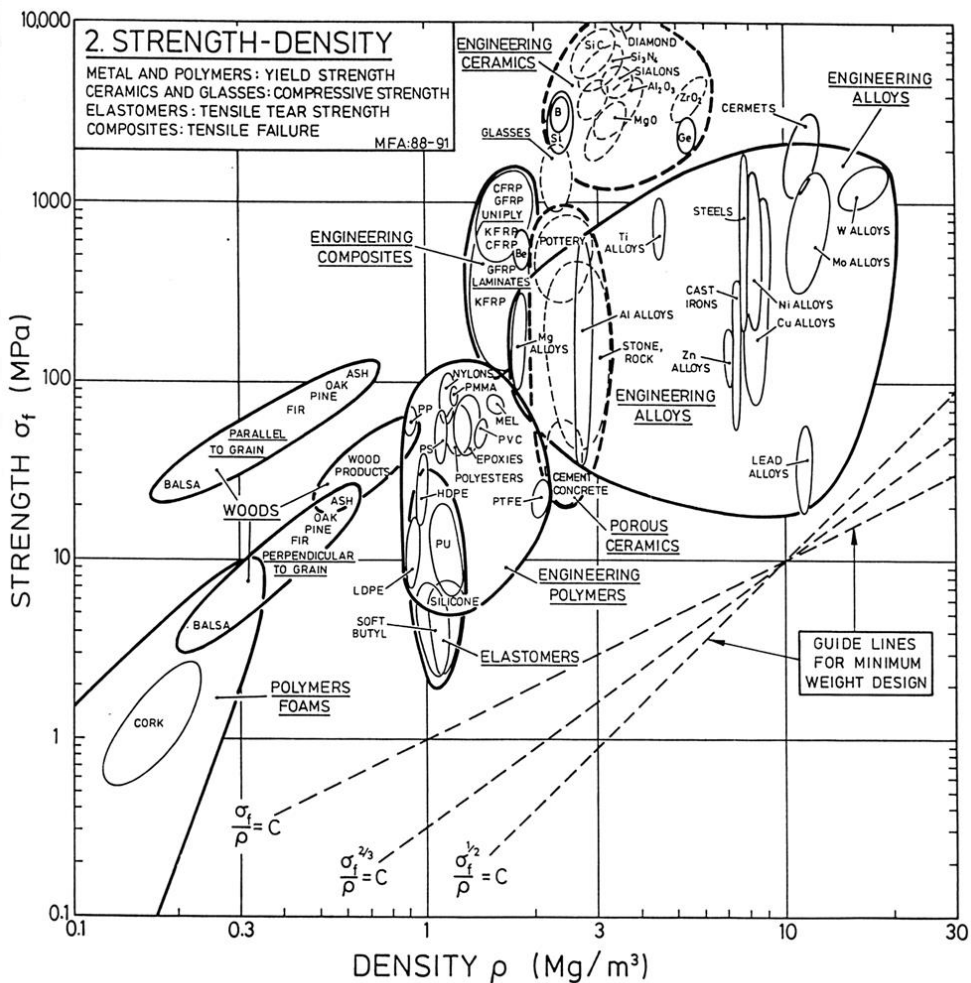


Figure 118: Strength vs density of engineering materials

A monocoque combines the frame and the body, whereas the other solutions would need body panels increasing the weight of the car. Our curved body shape, means that these panels would require a moulding process, which would be just as complex as for a monocoque. The conclusion is that carbon fiber composite is the best material choice for our car, if we are to be able to make a highly aerodynamic design with the lowest weight possible.

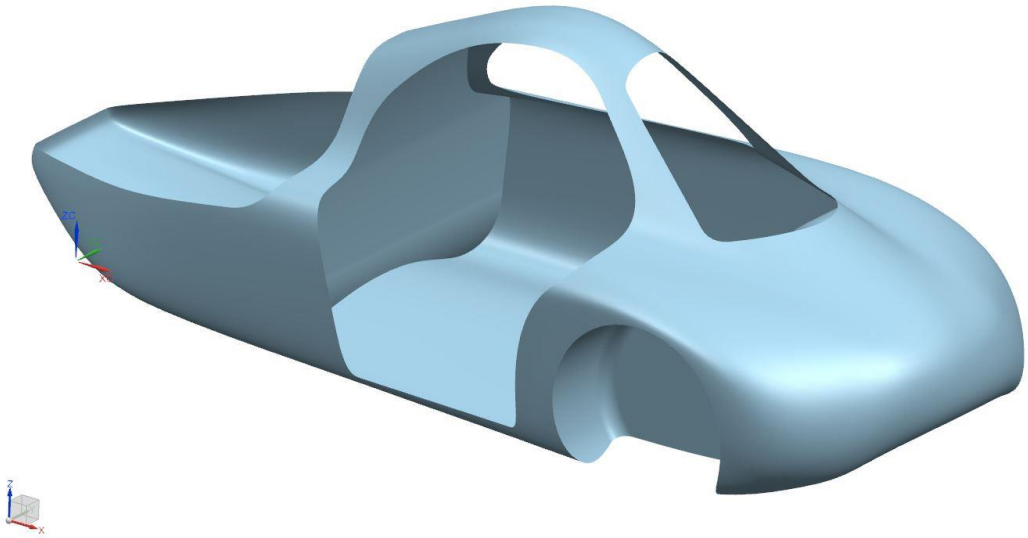


Figure 119: The monocoque

5.4 Preparations for production

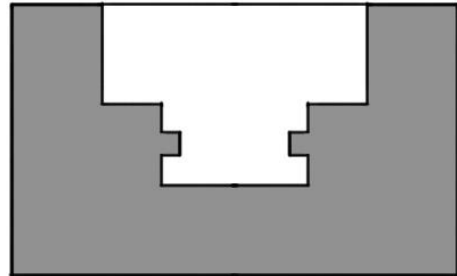
Our sponsor partner SHAPE will mill the monocoque moulds. The moulds produced will be of the negative type.

Modification of the design

There had to be done some minor changes to the design to make it possible to mould the car.

No undercut

There cannot be any parts sticking out in the mould, or the mould must be destroyed to get the casting out. This is not an option as we need to keep the mould intact to manufacture the windows and the door.



Slip angle of 1°

The angle is the offset from the vertical plan. Without this angle, the casting may be impossible to get out. The friction forces simply become too big, and the only option again is to destroy the mould.

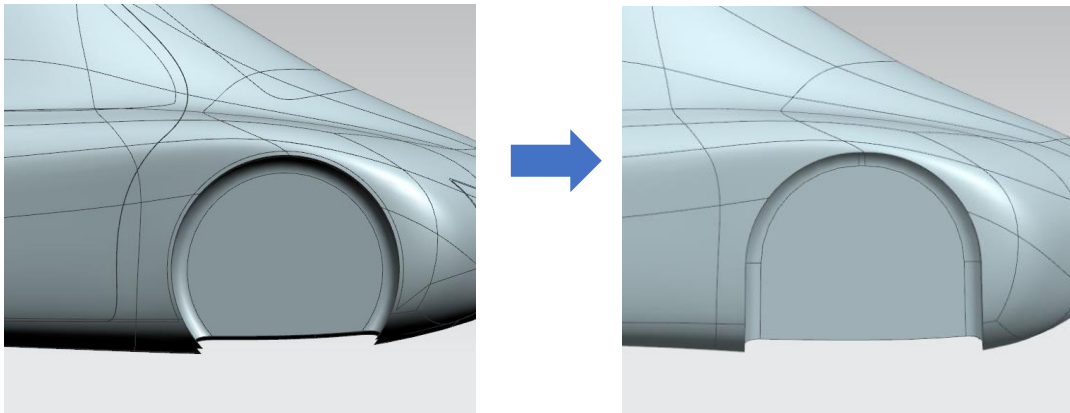


Figure 120: Modified wheel well

The wheel well had to be modified for moulding. We consider to build the removed part at NTNU, as the original well looks better and provides better aerodynamic flow around the wheels. To create the moulds, the model of the car was split using the isocline tool in NX. This splits the model in half exactly where the body is parallel to the vertical plane. Thus there are no undercut in the moulds. The wheel wells are attached, as whole, to the bottom

part. This because the bearing forces attack the wheel wells and they will handle the stresses better as whole parts without splices.

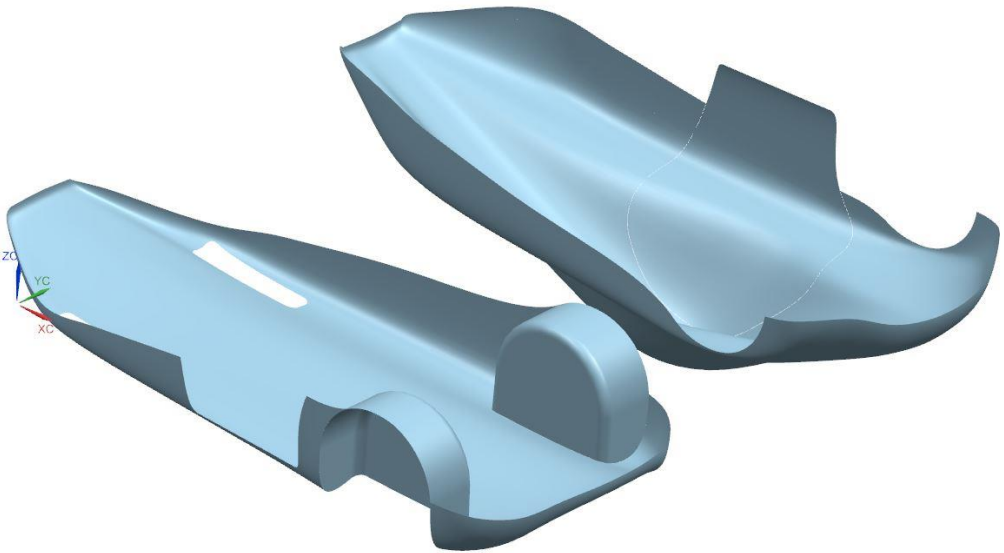


Figure 121: Body split for the moulds

5.5 Requirement specification

Product requirement – monocoque

		Must	Should
1	Production requirement		
	Complexity		
1.1	Number of parts/moulds	<20	<10
1.2	Manufacturing time		<30 hours
	Cost		
1.3	Maximum total cost	<300 000 NOK	<250 000 NOK
2	Functional requirements		
	<i>Instant performance</i>		
2.1	Max displacement	5 mm	
2.2	Coefficient of drag (Cd)	<0.30	<0.15
2.3	Field of view at driver position	180 degrees	
2.4	Wheel size fitting in wheel well	17 inches	
2.5	Wheel well depth	>300 mm	
2.6	Load on wheel wells	1000 N	1500 N
2.7	Load on roof	700 N	
	<i>Long-time performance</i>		
2.8	Fatigue life under load	100 hours	10 000 hours
3	Physical properties		
3.1	Height	>1000 mm	1020 mm
3.2	Width	1200-1300 mm	1220 mm
3.3	Weight	<150 kg	<85 kg
3.4	Length	2200-3500 mm	
3.5	Fixed roof	Yes	
3.6	Mass	<70 kg	<50 kg
3.7	Door size	800x500mm	
4	Requirements from surroundings		
4.1	Operational temperatures	0-50°C	
4.2	Waterproof	IP44	

6 Calculations

6.1 Force calculations

Symbol	Value	Unit	Description
m_c	90	kg	Mass of car.
m_d	70	kg	Mass of driver.
v_{corner}	6	m/s	Velocity through corner.
r_{corner}	6	m	Radius of corner. Required turning radius in SEM rules.
a	2.6	m/s^2	Acceleration from still.
a_B	9.81	m/s^2	Deceleration when braking. Assumption that value is similar to production cars, and set to equal 1G.
g	9.81	m/s^2	Gravitational acceleration.

To dimension the car, we need to estimate the forces it may be subjected to. The calculations below are based on simple assumptions we find to be realistic, and is multiplied with a safety factor.

When the driver is inside the vehicle, the vertical force is calculated to be:

$$F_{static} = (m_d + m_c)g * 1.5 = 2354.4 N$$

When the driver enters or exits a car, an impulse occurs. It may also be from a bump in the road. To simplify the calculation of the force which acts on the car, the safety factor has been increased.

$$F_i = (m_d + m_c)g * 2.5 = 3924 N$$

The roll cage must withstand a static load applied in all directions. This is defined in the SEM rules to be 700N.

$$F_{roll} = 700 N$$

During braking, the mass of the driver will act with a force on the seatbelt. This is calculated to be:

$$F_{belt} = m_d a_B * 2 = 1373.4 N$$

Acceleration force from still:

$$F_{acc} = (m_d + m_c)a * 2 = 832 \text{ N}$$

The force when braking:

$$F_B = (m_d + m_c)a_B * 2 = 3139.2 \text{ N}$$

Force driving through a corner.

$$F_{turn} = (m_d + m_c) \frac{v_{corner}^2}{r_{corner}} * 1.5 = 1440 \text{ N}$$

6.2 Force on rear suspension

The forces calculated in this section is used in section 0. To calculate the force acting upon one of the rear suspension, we assume that the total braking force is divided equally on all four wheels. During heavy braking, more force acts upon the front wheels than the rear wheels. We chose to divide equally to get an extra safety.

Therefore, the braking force on one wheel:

$$F_b = \frac{F_B}{4}$$

Our tyres have a radius, l_b , of 27 cm.

The brake disks have a radius, l_d , of 8 cm. The force, F_d , acting upon our rear suspension will therefore be:

$$\begin{aligned} \sum M &= 0 \\ F_b l_b - F_d l_d &= 0 \\ F_d &= \frac{F_b l_b}{l_d} \\ F_d &= 2648.7 \text{ N} \end{aligned}$$

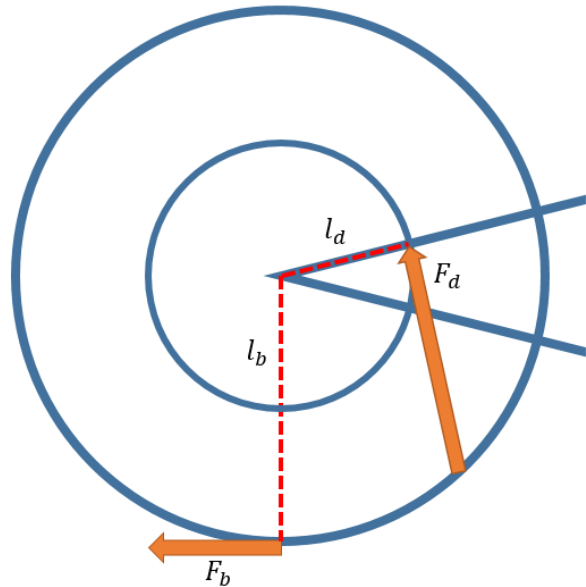


Figure 122: Forces on rear suspension when braking

6.3 Energy calculations

In this section, the energy consumption of the car will be discussed.

The parameters influencing the car's energy use are:

Table 23: Parameters of the fuel efficiency performance of a car

Parameter	Typical range	Value for initial calculation
Motor efficiency	0.5 – 0.95	0.85
Motor controller efficiency	0.85 – 0.99	0.95
Drivetrain efficiency	0.75 – 0.95	0.90
Mass of the car	70 – 110 kg	90 kg
Coefficient of rolling resistance (C_r)	0.003 – 0.006	0.004
Coefficient of drag (C_d)	0.10 - 0.30	0.20

How much power must the motor deliver, and how are the parameters affecting the efficiency of the car? To investigate this, the car is drawn in a free-body-diagram.

Drag forces on the vehicle:

Aerodynamic drag	$F_d = \frac{1}{2} C_d \rho v^2 A$
-------------------------	------------------------------------

Gravitational drag	$F_g = mg$
---------------------------	------------

Rolling drag	$F_r = C_r N$
---------------------	---------------

Acceleration drag	$F_a = ma$
--------------------------	------------

(Cornering force)	-
--------------------------	---

Motor force	$F_m = \frac{P_m}{v}$
--------------------	-----------------------

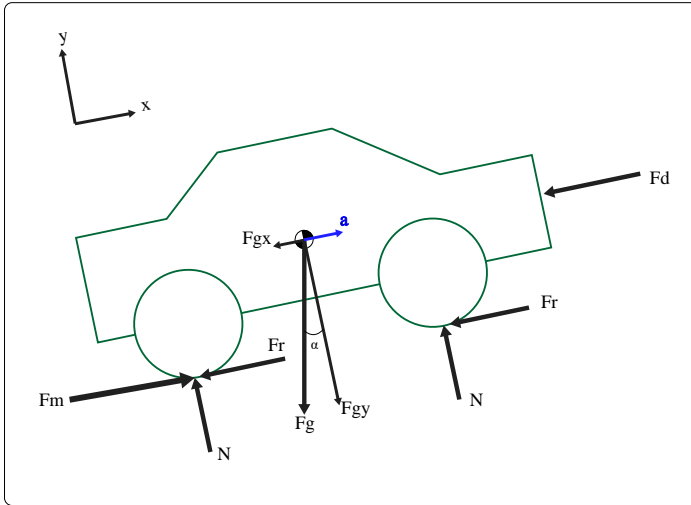


Figure 123: free body diagram

The wheels will generate a cornering force with a component in the negative travel direction when turning, because of slip angle. Tires are made of elastic rubber, which deforms in cornering manoeuvres. The consequence is that the direction of the wheel will be different than the travel direction, where the difference is the slip angle. However, this deformation and force is only prominent for race cars, with high speed and forces while cornering. We use very stiff tires to reduce the rolling resistance, and the slip angle will be lower compared to race cars. Figure 124 shows that the even with a 400kg car (~4000 N normal force) with race car tires, the slip angle will be below $0,5^\circ$ using a lateral force of 900 N. In the simulation results later in this section, the maximum combined lateral force on all 4 wheels are 900 N. Thus, the slip angle and the resulting force from it will be neglectable in our case.

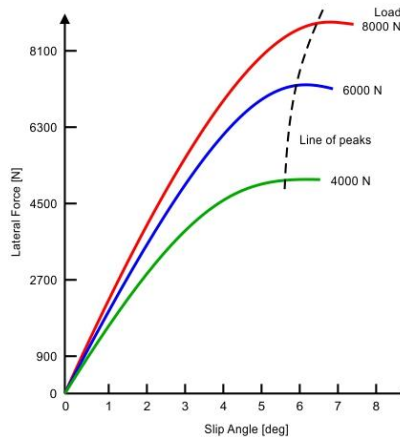


Figure 124: lateral force vs normal force vs slip angle for race cars

Initially, to have a look at the required power for an eco-marathon car, calculations are done for two scenarios; the steepest hill at the London track (5,5% gradient), and driving on a flat road. The initial parameters in Table 23 is used. When climbing the hill, the gravitational force will be dominant. There is a linear relationship between the power and the mass of the car. In the scenario where the car is driving on flat ground, there will not be any contribution from the gravitational force and the needed power is around a third compared to the hill. In the speed range presented, F_d and F_r have each a share of around 50% of the total power. Looking closer, F_d becomes a greater share of the total power as the speed increased. The reason for this that the aerodynamic force formula is exponential. At 40 km/h the share will be 28% ,72% for F_r , F_d respectively.

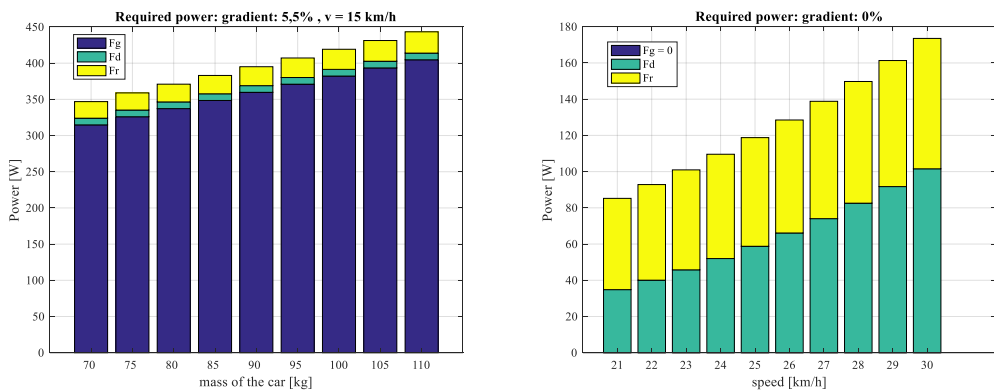


Figure 125: Power required to climb the steepest hill in 15 km/h for different car weights to the left, and power required on flat road in different speeds with car weight of 90 kg to the right.

The Shell eco-marathon race is at low speed compared to speeds with commercial cars. To get a valid result, the average speed must be above 25 km/h. Required motor power caused by aerodynamic drag is shown for different C_d -values over speed range from 15-40 km/h in Figure 126. Even though the race is a relatively low speed, this shows that aerodynamic shape of the vehicle greatly influences the fuel efficiency of the car. It is highly likely that our car must drive slower than the average speed when climbing the hills, which must be balanced by other parts of the track being driven at higher speed – with expendably higher aerodynamic force.

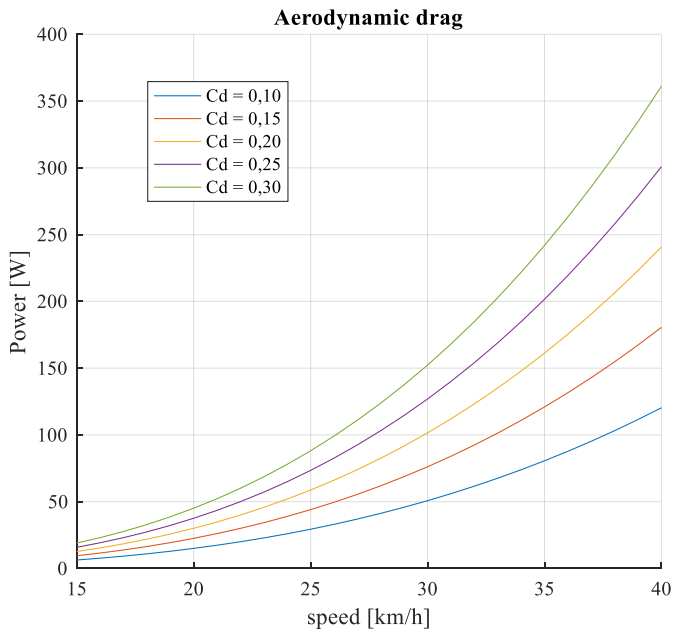
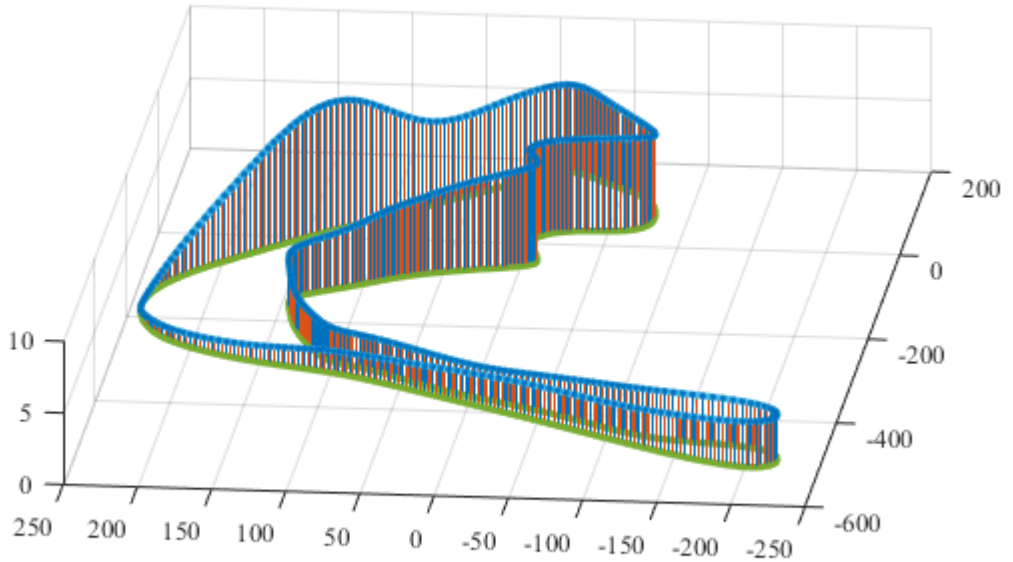


Figure 126: Cd value's effect on aerodynamic drag

To further investigate how the parameters will influence the overall fuel efficiency, a simulator was programmed in MATLAB. Coordinates of the 2016 track are available, with a total of 43 points through the track. The points were interpolated to make a smooth track. Properties of the track were calculated:

- Length per increment.
- Total length.
- Curvature at each increment.
- Gradient at each increment.

The 2017 track was released mid-December, too late to be included in this report. However, much of the track is the same as last year, including the hill. The results will likely be similar.



At each increment of the track, the acting forces on the car can be calculated. Beginning at the start point, Newton's 2 law of motion yields the cars acceleration,

$$\begin{aligned} \sum F &= ma \\ \Rightarrow a &= \frac{\sum F}{m} = \frac{F_m - F_g - F_d - F_r}{m} \end{aligned}$$

where F_m is the force provided by the motors. The car's speed in the next increment can now be calculated with Torricelli's equation,

$$v_1 = \sqrt{v_0^2 + 2a \cdot \Delta d}$$

where Δd = is the length of the increment. This gives the framework of the simulator for calculating the physics.

Control system

The simulator has been implemented with a powertrain system which is planned for the real car: one low-power motor and one high-power motor. How these motors should be controlled is an optimization problem with endless possibilities, which can be extremely complicated. Fortunately, the motor setup with low and high power have shown to give a stable speed profile with a not too complicated controller. Decision making in the motor controller are as following:

When activated, the motors always run on 80% of max power, which is in the region where electrical motors are most efficient.

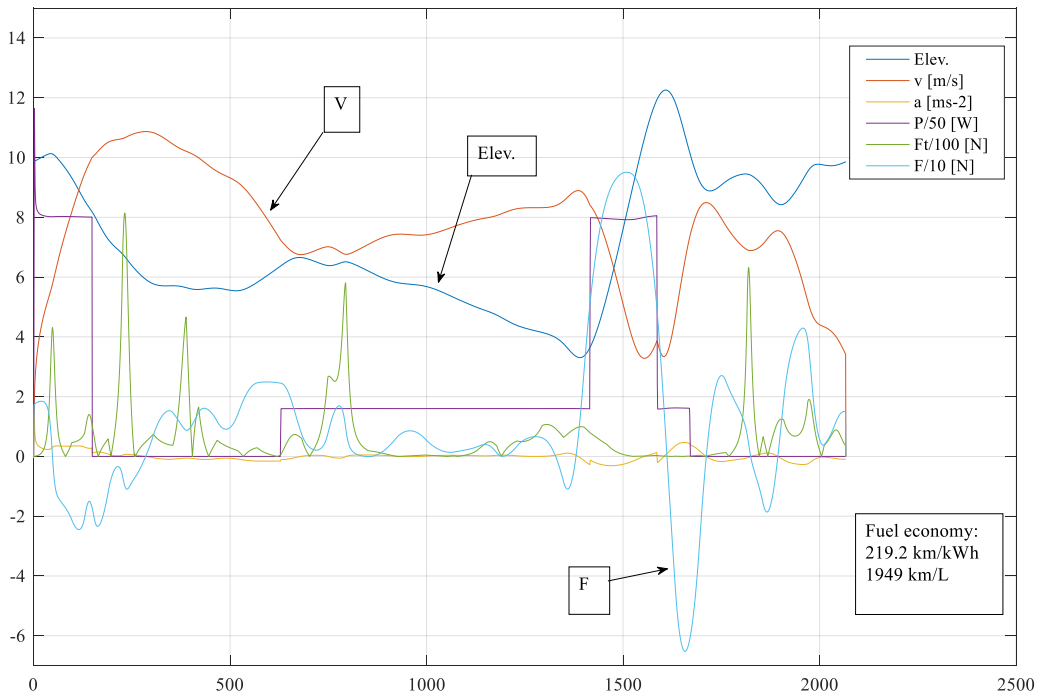
Use the high-power motor if:

- Total drag force is above a threshold (50 N)
- Initial launch to get speed

Else use the low-power motor.

Turn off motors (coast) if:

- Speed is above a threshold (36 km/h)
- There is a turn ahead with a radius below a threshold (15 m) and speed is above a threshold (6 m/s)
- Pit stop in a certain distance ahead (Coast to the pit stop)



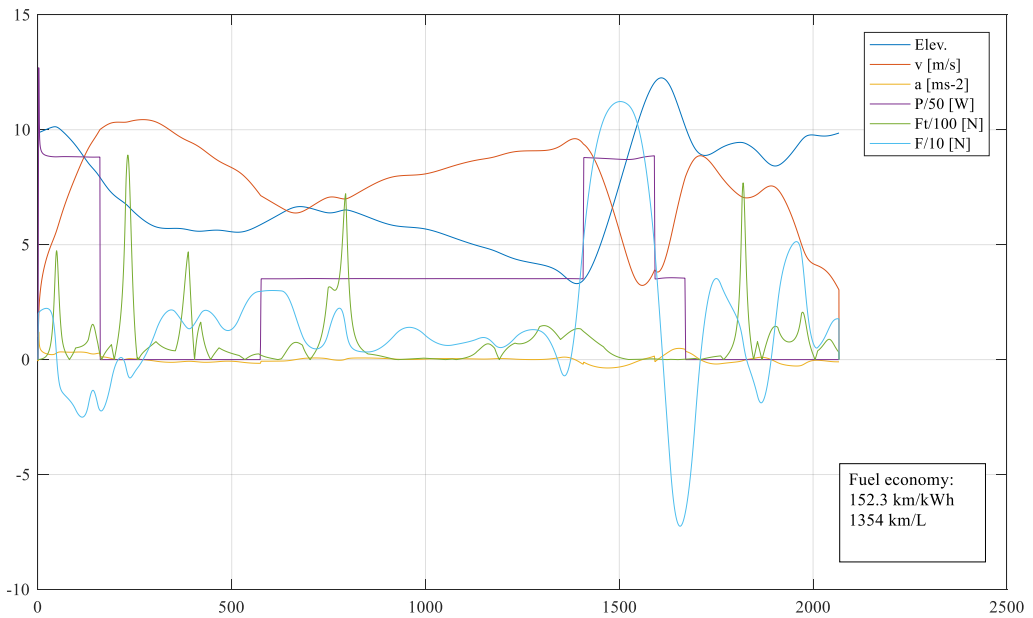
Cd	Mass of car	High-power motor	Low-power motor
0,138	90 kg	500 W	120 W

Figure

127:

Simulation of the track with $Cd = 0,138$, $A = 0,883$ m² corresponding to geometry of current car. Elev.= elevation, v=the car's speed, a=acceleration, P = motor power, Ft = force by centripetal acceleration. $F = \sum F$ acting on the car.

The race simulation with the C_d and frontal area of our latest car and otherwise the average parameters from Table 23, is shown in Figure 127. The speed profile in orange shows that the car quickly gains speed from the beginning, using the high-power motor. Next, the car is coasting downhill followed by using the low-power motor before the steepest hill. In this hill, the high-power motor is activated again. As this hill is relatively steep, the speed will decrease steadily to match the max power of the motor. Entering the hill at a speed of 9 m/s, and the speed is gradually reduced to 3 m/s. Simulation of a 110kg car with a C_d of 0,25 is shown in Figure 128. The fuel efficiency is dropped by 32%.



Cd	Mass of car	High-power motor	Low-power motor
0,25	110 kg	650W	150W

Figure 128: Driving profile for a car with $C_d=0,25$ $m=110$ kg

Of course, a lot more optimization can be done to the driving strategy to yield a higher fuel efficiency. However, it will probably be small margins. We believe the current simulator gives a good estimate of the fuel efficiency.

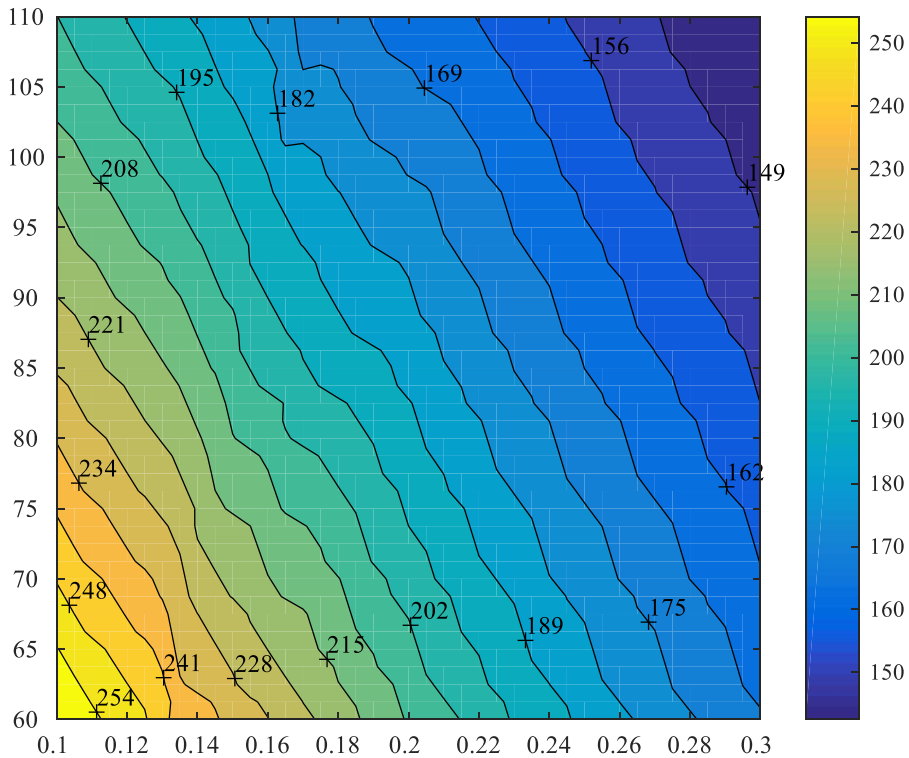


Figure 129: Simulating fuel efficiency for car mass of 60 to 110 kg, and C_d of 0.1 to 0.3. A larger plot with all the data can be found in the appendix.

To examine the influence of car mass and C_d , simulations of car mass in the range 60 to 110 kg and C_d in the range 0.10 to 0.30 were done. At each combination of car mass and C_d the simulator would iterate until the average speed is between 25-26 km/h (Completing the race just in time). The result is shown in Figure 129. The contours show accomplished fuel efficiency [km/kWh], with variation of C_d on the x-axis and car mass on the y-axis. The whole dataset diagram can be found in appendix 9.3. The results clearly illustrate the importance of the C_d -parameter. There are some variations, but roughly anywhere on the plot a 0.02 reduction in C_d is equivalent to shedding 10 kg off the car.

Two of the reasons why the aerodynamic shape of the car is so important:

- The aerodynamic drag force is 100% loss of energy. Gravitational drag force used to climb a hill, is partly recovered when rolling down the other side of hill (Conservation of potential energy).
- A good aerodynamic shape will make the car coast faster and longer down hills without using motor power.

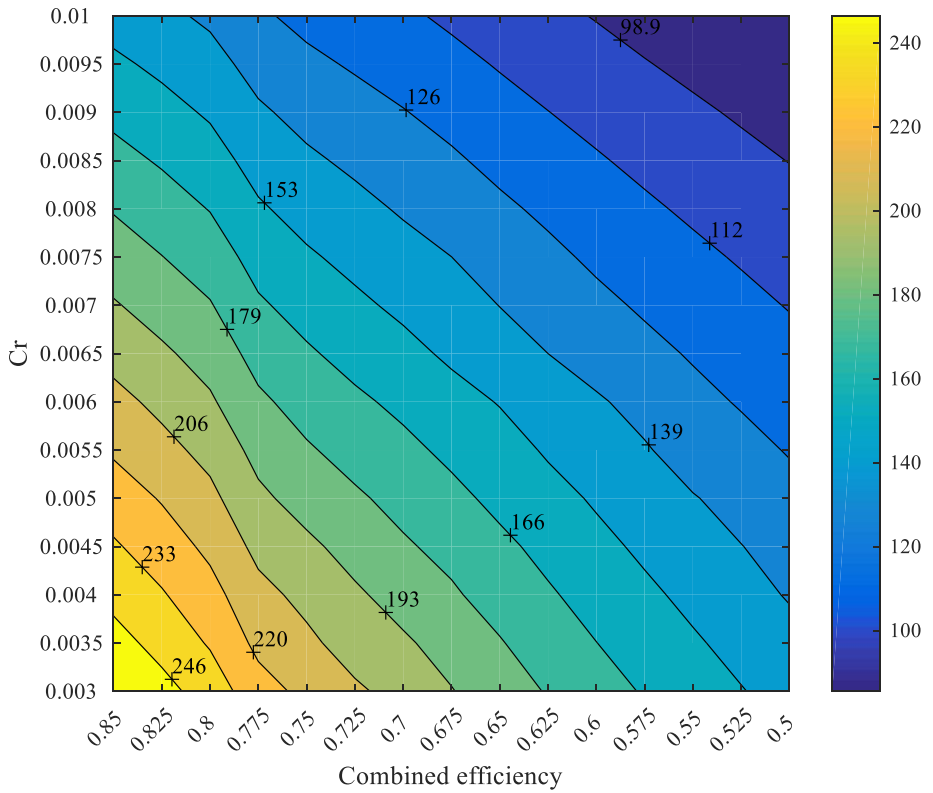


Figure 130: The influence of the combined efficiency (see Table 23) and the C_r parameter. $C_d=0,138$ and $mass=90kg$

Figure 130 shows the effect C_r and the combined efficiency of the components in the powertrain has on fuel efficiency.

7 Subsystems

7.1 Drivetrain

The drivetrain system are the components that contributes to deliver power to the wheels.

Ten different concepts have been considered for the car's drivetrain, illustrated on the next page.

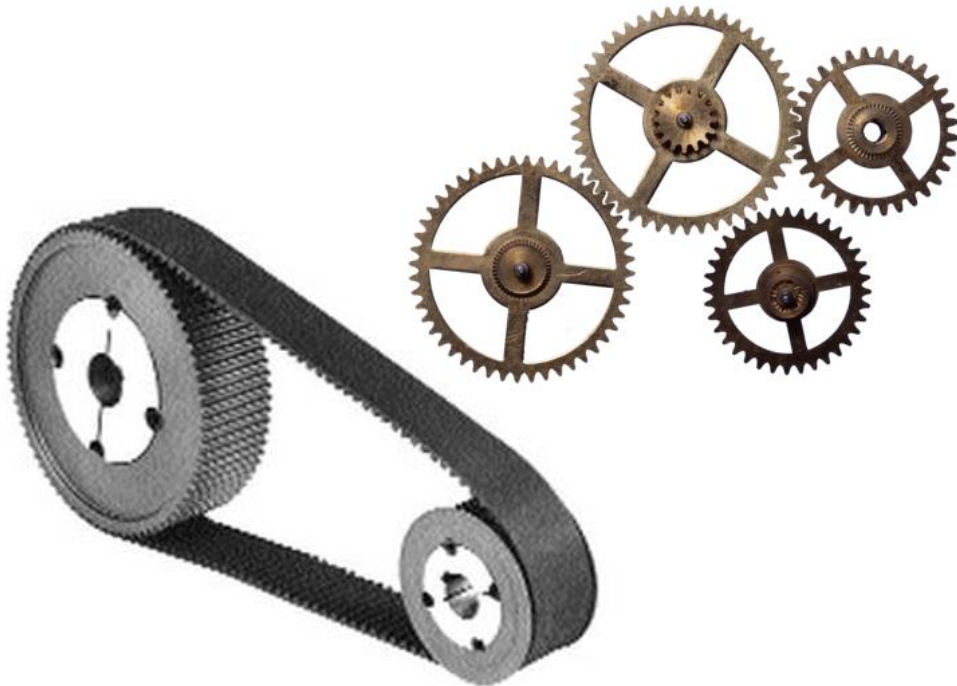
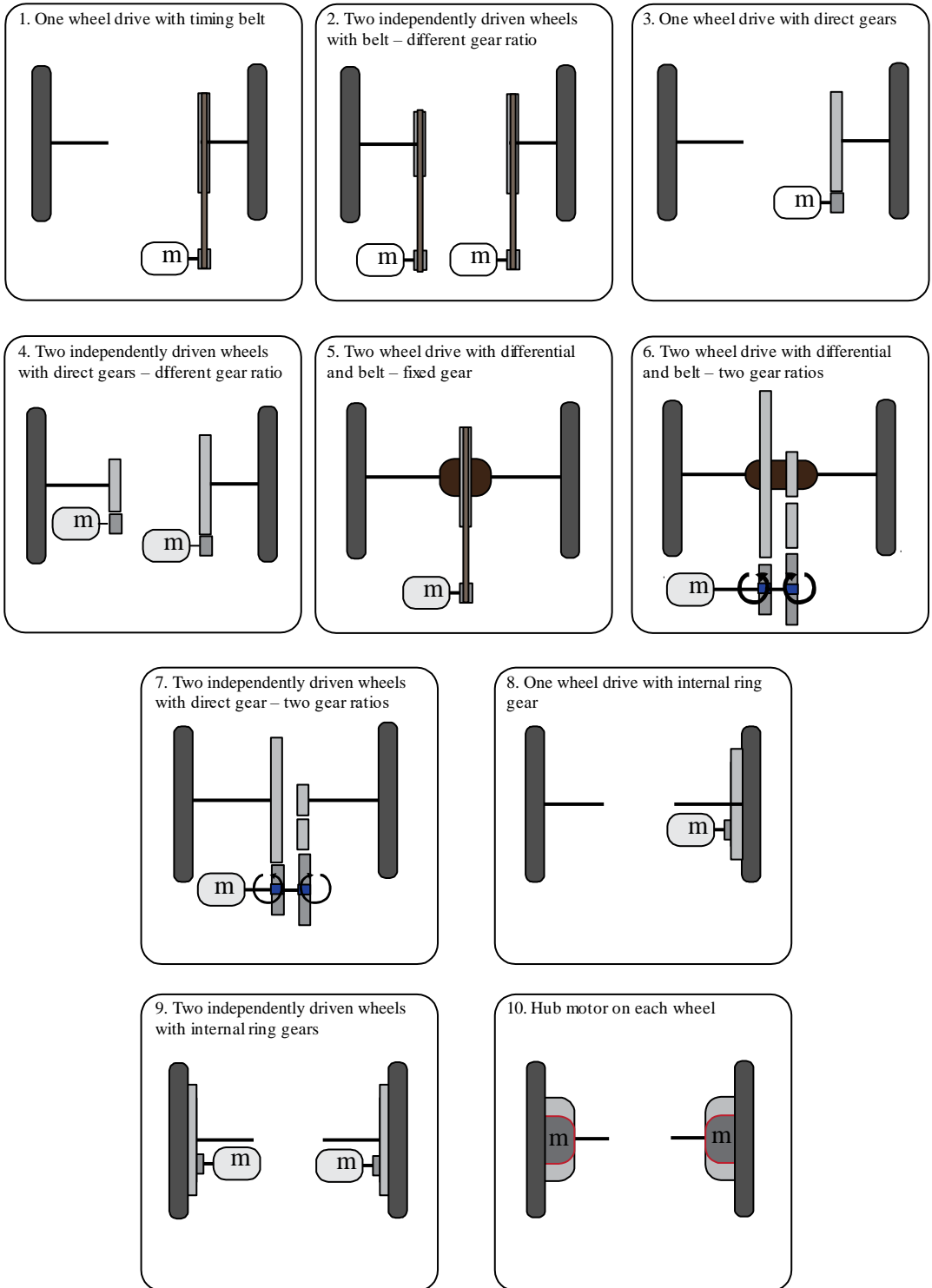


Figure 131: Belt drive and gears

DRIVETRAIN CONCEPTS



1. One wheel drive with timing belt

Simple solution. One wheel drive (1WD) been used on earlier NTNU eco-marathon cars with good results.

2. Two independently driven wheels with belt – different gear ratio

As above, applied to both wheels. One high geared and high-power motor to be able to climb the hills, and the other lower geared and low-power motor for flat terrain in higher speeds.

3. One wheel drive with direct gears

As #1, but with direct spur gears.

4. Two independently driven wheels with direct gears – different gear ratio

As #2, but with direct spur gears.

5. Two-wheel drive with differential and belt – fixed gear

As #1, but with differential to distribute the motor force to both wheels.

6. Two-wheel drive with differential and belt – two gear ratios

Similar to #5, but with two gear ratios. Two transmissions to same axle are accomplish without a clutch and gearbox. There are two spur gears on the motor axle, each mounted with a freewheel/ratchet. The freewheels have opposite open rotation directions. With the motor in the initial rotation direction, the first gear is activated and the other gear is free. Switching the motor to rotate in the opposite direction, and the second wheel will engage while the first gear is free.

7. Two independently driven wheels with direct gear – two gear ratios

Similar to above, but without a differential. Initial motor direction activates the first transmission and the first wheel, and the opposite motor direction activates the second transmission and wheel.

8. One wheel drive with wheel mounted gear

This design is principally equal to #3, but with an internal ring gear that can be mounted on the wheel rim.

9. Two independently driven wheels with wheel mounted gears

The principle above, on both wheel.

10. Hub motor on each wheel.

Motors directly inside the wheel hub, integrated with gears. Commercial product for i.e. electric bikes.

The drivetrain concepts can be categorized followingly:

- 1) Independent motor power on one wheel - 1,2,3,4,7,8,9, (10)
- 2) Distributed power with a differential - 5,6
- 3) Belt drive – 1,2,5
- 4) Gear drive- 3,4,6,7,8,9
 - a) External gear – 3,4,6,7
 - b) Internal ring gear – 8,9
 - c) Integrated hub gear (planetary, commercial product) – 10
- 5) Two motors – 2,4,9,10

7.1.1 1WD

To address any undesirable forces caused by a 1WD drivetrain system, consider the free-body diagram in Figure 132.

$$\sum M_{cg} = (F_{ll} + F_{lr}) \cdot \frac{W}{2} - F_m \cdot \frac{T}{2} = 0$$

Assume $F_{ll} = F_{lr}$

$$\Rightarrow F_{ll} = F_{lr} = F_m \cdot \frac{T}{W}$$

Track simulation with a 110 kg car, estimates a max $F_m = 100N$. With our car geometry, this yields:

$$F_{l_{max}} = 100 N \cdot \frac{800}{2 \cdot 1550} = 25,8 N$$

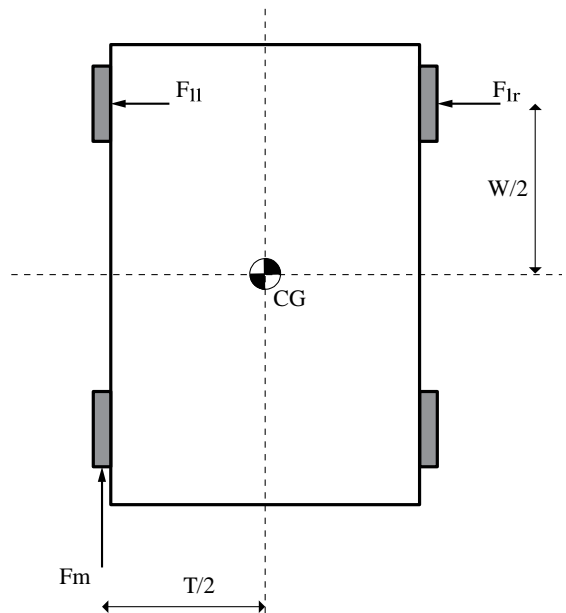


Figure 132: Lateral force caused by 1WD

We believe this has neglectable effected on the car handling and rolling efficiency, as the deformation of the tire is close to zero with this force. Additionally, previous eco-marathon teams from NTNU have had 1WD, with good results. Another consideration is road traction. The race is on smooth asphalt, and there are low speeds and accelerations. As long as there are not layers of sand or ice on the road, we will not have any problems with traction. We can assume these criteria will be met.

7.1.2 Differential

The advantages of implementing a differential is distribution of the motor force to both wheels, enhancing car handling. The disadvantage is the extra weight it will add. The part is also complicated, and it is an additional “risk of failure” element.

7.1.3 Belt or gears

Direct spur gears have efficiency of over 99% when working properly (Petry-Johnson et al., 2008). Synchronous belts, when perfectly assembled, have an efficiency up to 98-99% (CORP, 2014). Concerning the efficiency, spur gears are therefore slightly more favourable.

Direct gears transfer the force from “tooth-to-tooth”, and consequently must be built in tougher materials than timing pulleys (the gears for belt drive), where the force is distributed over a section of teeth from the belt. This implies that a direct gear system will be heavier than a belt system. The gear system will also be more exposed to vibrations if the motor is not running smoothly. Addition to being an annoyance, this increase the risk of fatigue cracking. High tolerances will reduce the problem. The belt system will be better at handling irregularities from the motor. The elasticity of a belt reduced the transmission of vibrations. Because of the large gear ratio, the belt system will need an additional pulley to prevent slip. This may reduce the efficiency of the system slightly.

7.1.4 Internal gears

In concept 8 and 9, internal gear is mounted directly on the wheel rim. This system will be competitive in weight to the belt system. If the gears acquired are built in a strong material with high tolerances, this will be the best solution regarding efficiency, simplicity, and weight. If we are not able to obtain the gears within the requirements, the belt drive system will be our safest bet.

7.1.5 Multiple gears ratios and motors

The last consideration is whether to have fixed gear or two gears, and whether to have one or two motors. The motor power needed to climb the steepest hill of the London track is obviously much higher than what is needed for a steady pace over the otherwise flat track. Efficiency curves of electric motors shows that they are not equally efficient for all loads and RPMs. An area with centre around 60% of rated RPM and 40% of rated torque (multiplies to 80% of rated power), is where most motors have the highest efficiency (Figure 133). We want our motor to run optimal in all the power conditions that will occur in the race, i.e.:

- High power and low speed when climbing the hill.
- High speed with low power on flat parts.

With one motor, the engine must be powerful enough to climb the hill. At the flat parts, the utilisation of the motor will be too low to yield the best efficiency, even with an additional gear. To gain the best overall efficiency, two motor with individual gear ratios will be best. Combined they give a larger range of RPM and torque that will be in the high efficiency area.

Including one more motor and gear train means added weight. It must be certain that the gained motor efficiency outweighs the negative impact of a higher weight. This can be investigated with our track simulator, but the exact efficiency plots for the motors must be known. Electrical motor manufactures rarely include efficiency plots in their product specification. We have requested this from some manufactures without any luck yet. Ultimately, we should test our motors ourselves, to verify the manufactures specification. The plan is to build a test rig for this purpose in the start of the next semester. Several motors will be ordered, as motors are not too expensive. After conclusive tests, the best suited motor(s) can be chosen.

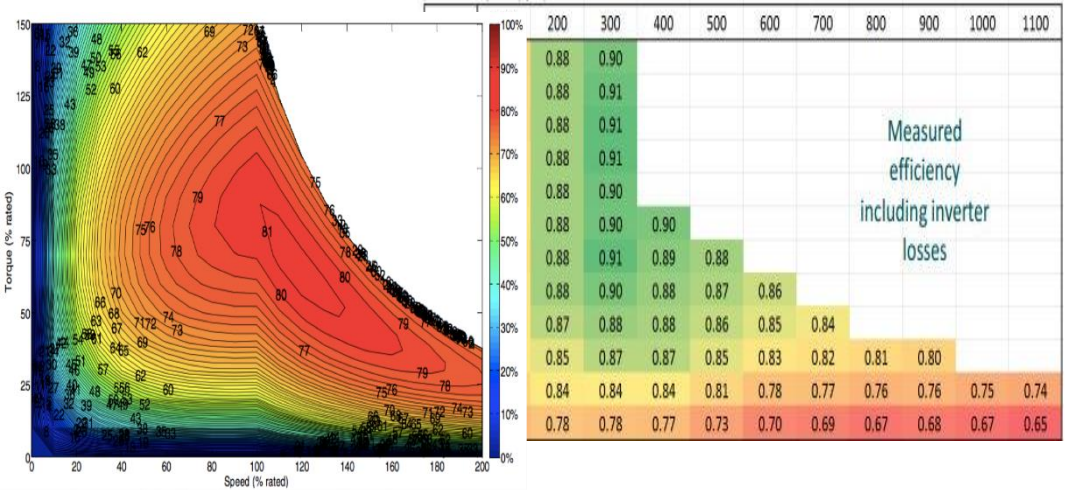


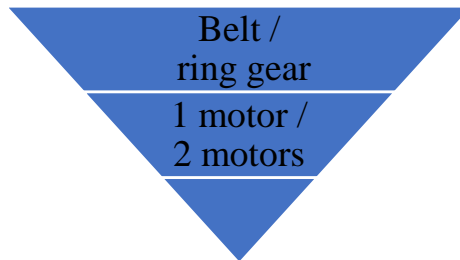
Figure 133: Motor efficiency contour plots

7.1.6 Conclusion

We have decided that there is no need for a differential. 1WD will be sufficient and saves weight. The decision between one or two motors depends on the motor specifications, which can only be fully obtained with testing in the lab. The top choice for the gear train is *internal gear ring*, but it depends on finding a supplier that can deliver it within the requirements. If it is found impossible, we will go for the second best: *belt drive*. This converges the set of solutions to concept 1,2,8, and 9.

	BELT DRIVE	INTERNAL GEAR
1 MOTOR	Concept 1	Concept 8
2 MOTORS	Concept 2	Concept 9

The layout of the engine compartment and rear suspension allows all 4 concepts to be implemented. The 2-motor-alternatives is basically duplicating its 1-motor-alternative. Meaning going from 1 to 2 motors is a matter of scaling, with some minor adaption for fitting different gear size and motor power. The order of convergence to the final design will be as follows:



7.2 Suspension

With a new car, there is also the need to look at the suspension system. We are currently in the process of choosing how we will solve it. Our progress so far is described below.

7.2.1 Front suspension

Before it was decided that we were building a new car, the old team advised us get a new suspension system. The old one can be seen in Figure 134. The lower wishbone is asymmetrical and the upper rods hinder each other in having the wanted freedom.

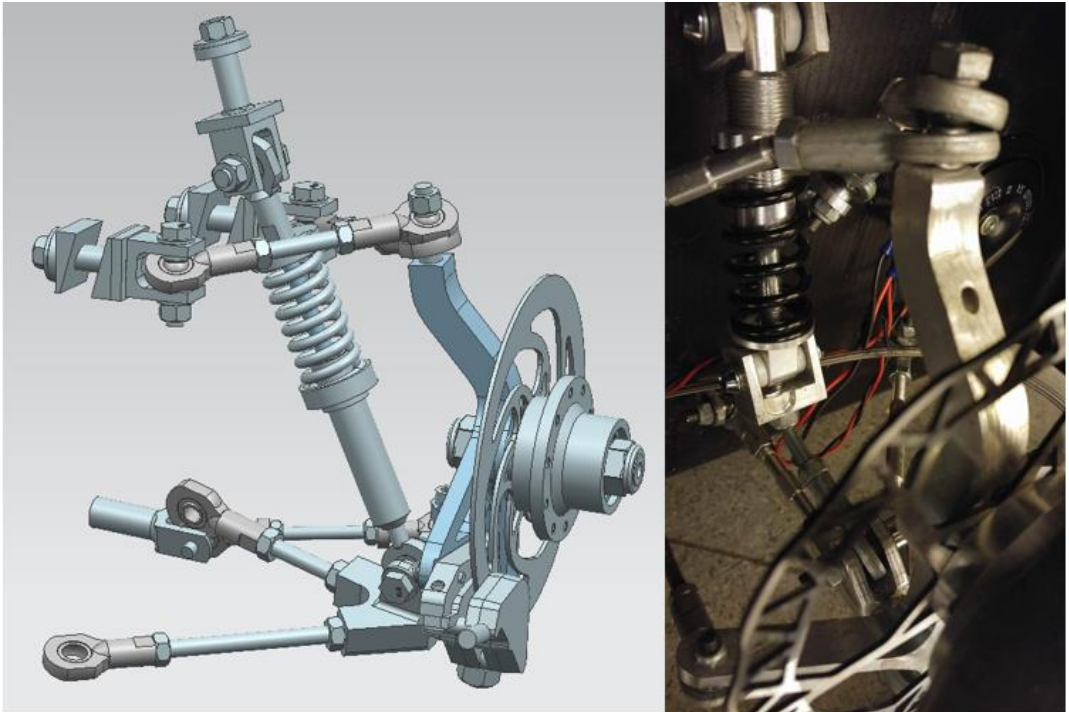


Figure 134: Old suspension system

During SEM 2016 the team had misunderstood one of the rules. The ground clearance was not high enough when the driver was in the car. They therefore had to remove the shock absorber and insert a stiff rod to pass the technical inspection. On the track the new rod suffered a fracture and one of the upper rods was bent. See Figure 135. It was clear that the entire suspension system should be reworked – a task we are currently working on. Since the car has rear-wheeled drive, we don't have to accommodate the front suspension for a drivetrain.

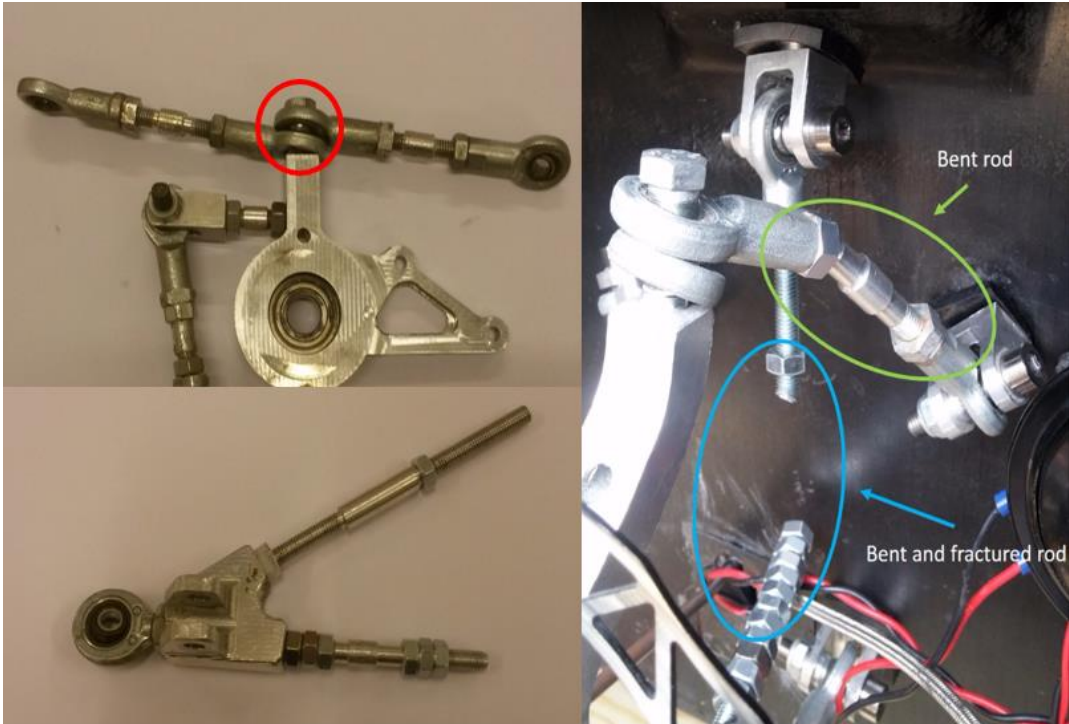


Figure 135: Old suspension system with bent and fractured rods.

After looking at several types of suspensions, we are now considering to use either a double wishbone suspension, like earlier teams, or a MacPherson strut. Regardless of the choice, the suspension will be redesigned. The old team used two rods with ball bearings on top of the upright which hinder each other's movement. The lower wishbone was asymmetrical and made up of rods as well. Both the upper and lower solution will be replaced by an A-arm. That also may require a new upright. To make the A-arms we are considering a plate which is CNC-machined or rods which are welded. The plate we are considering is a 20-mm aluminium alloy 7075-T6, which has high tensile and yield strength. This is the same plate which we are planning to use to make the rear suspension (to be described later), and would be cost effective. This alloy is not suitable to be welded and another alloy should be chosen if we are going for the solution with the rods.

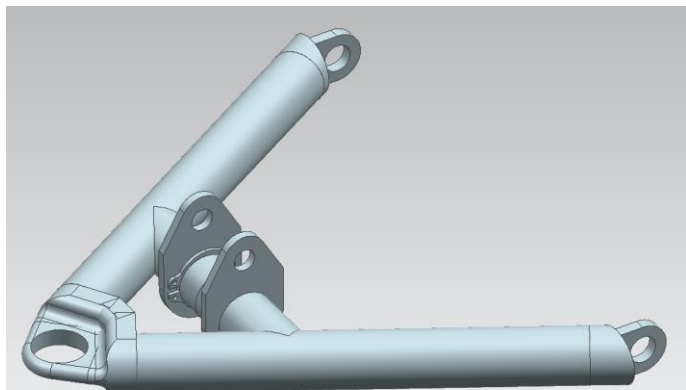


Figure 136: Lower A-arm of welded rods



Figure 137: MacPherson strut (left) and double wishbone suspension (right)

Feature	MacPherson struts	Double wishbone suspension
Strength in monocoque structure	Floor edge and top of wheel well	Inner wall of wheel well
Saves space	Horizontally	Vertically
Number of components	Fewer	More
Camber	<ul style="list-style-type: none"> • No camber gain • Less freedom 	<ul style="list-style-type: none"> • Camber gain • More freedom

The choice of suspension will affect the design of the car. We have to dimension the monocoque differently with the two types of suspension. They have different mounting points on the body, and consequently different areas need to be strengthened to handle the forces. With a double wishbone, we need to reinforce the inner wall of the wheel well which the wishbones are connected to. The wall also need an area to be angled where the spring comes in, to better handle the forces and make it easier to connect. With a MacPherson, the force comes through the spring into the top of the wheel well. That would have to be the strong area, together with the lower area where the suspension is mounted.

One of the reasons that MacPherson suspension is commonly used, is that it's compact in a horizontal direction. This gives more space on the inside of the vehicle, often as legroom. By the SEM rules, the distance between the midpoints of the front wheels must be minimum 100 cm. We want to minimize our frontal area and won't have a wider car than that. The inner width will increase in the front of our car, but it's not actually needed. The driver has enough legroom anyway, there are not any batteries or motors in front. MacPherson is often used in cars with front wheel drive, as it has good space for a driveshaft. Compared to double wishbone, a MacPherson suspension will increase the height. This is not desirable as it increases the frontal area.

A MacPherson strut consists of fewer components than a double wishbone suspension. That saves both weight and cost. As with the A-arms in the double suspension, we could make the lower arm to the MacPherson suspension out of the same aluminium we are considering buying to the rear suspension.

Comparing the two suspensions, there are also differences in camber, the angle between the vertical axis of the tyre and the road. A negative camber improves grip when cornering as it gives more contact area. This only applies to the outer tyre, which is the one that has a larger force on it in a corner. Due to the vertical movement of a MacPherson strut, it hasn't camber gain. So when a car has body roll during cornering, positive camber will occur and it will lose grip. Double wishbone can instead create negative camber in a corner with an upper A-arm which is shorter than the lower. Thus, the grip in corners is better. There is also more freedom to engineer the double wishbone into the set-up that is wanted. The camber is more adjustable than with the MacPherson, where it is normally fixed.

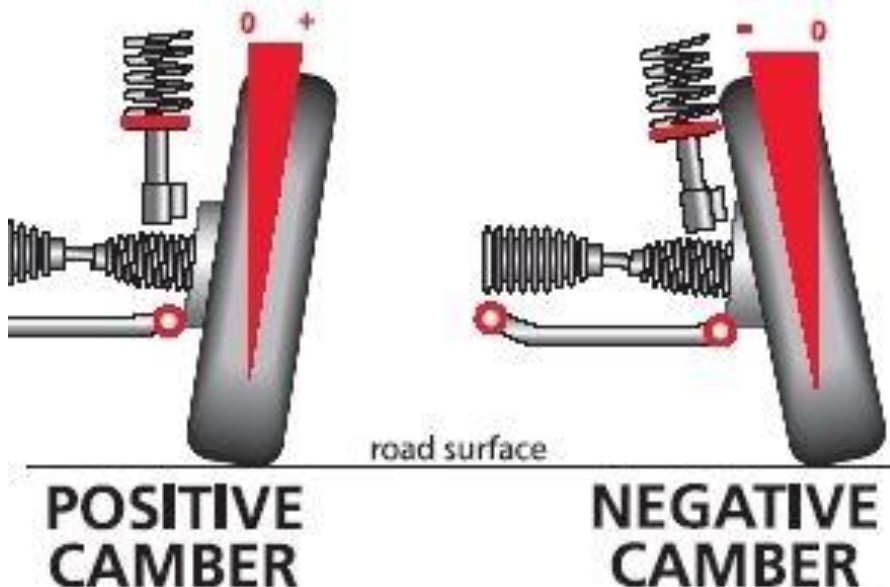


Figure 138: Illustration of camber

7.2.2 Rear suspension

Our initial idea was to have a double wishbone suspension in the rear. A MacPherson suspension would be a challenge since we want the walls to cover the back wheels. With a double wishbone suspension, there is needed an inner walls behind the bulkhead for them to be mounted on.

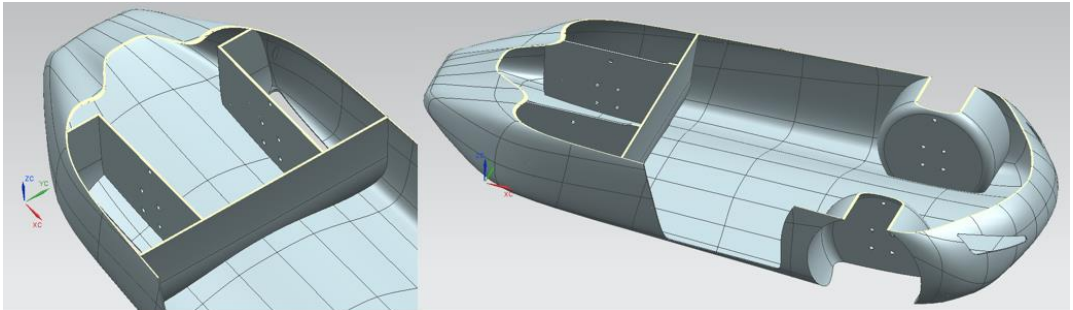


Figure 139: Shows inner walls behind bulkhead to mount suspension on.

We then chose to look at trailing suspension in the rear (see Figure 140). In this solution, the arm is fastened on both sides of the wheel. The other end is on a hinge connected to the bulkhead. A shock absorber goes from the arm at an angle up to the bulkhead, which should have an angled fastening area. When the wheel needs to be removed, it is loosened from the arm and lifted up. By mounting the suspension on the bulkhead, the need for the inner walls vanishes. The floor behind the bulkhead also, doesn't need the same strength. These eliminations reduce both weight and cost. Without the inner walls, the monocoque is also easier to manufacture. With this design, the plan is to mount the motors on the side of the arm such that they can follow the movement of the wheel.



Figure 140: Trailing arm on wheel

We have done a rough analysis on this preliminary design of the control arm. We wanted to see the effects of the force occurring from braking. The arm has pinned constraints where the hinge and shock absorber should be and bearing forces upwards from the wheel. A small distance out on the arm is where the force from the brake clamp will act upon the arm. The

forces that have been applied is from the calculations in section 6.2. On the side where the brake is located, inner struts have been inserted. The purpose is that the force from the brake should be absorbed as compression, and thus reduce displacement and bending. The struts are not necessary on the side without the braking force. The sides of the arms are intended to be machined from the aforementioned aluminium plate. The design of the bridge connection the profiles, have not yet been optimized.

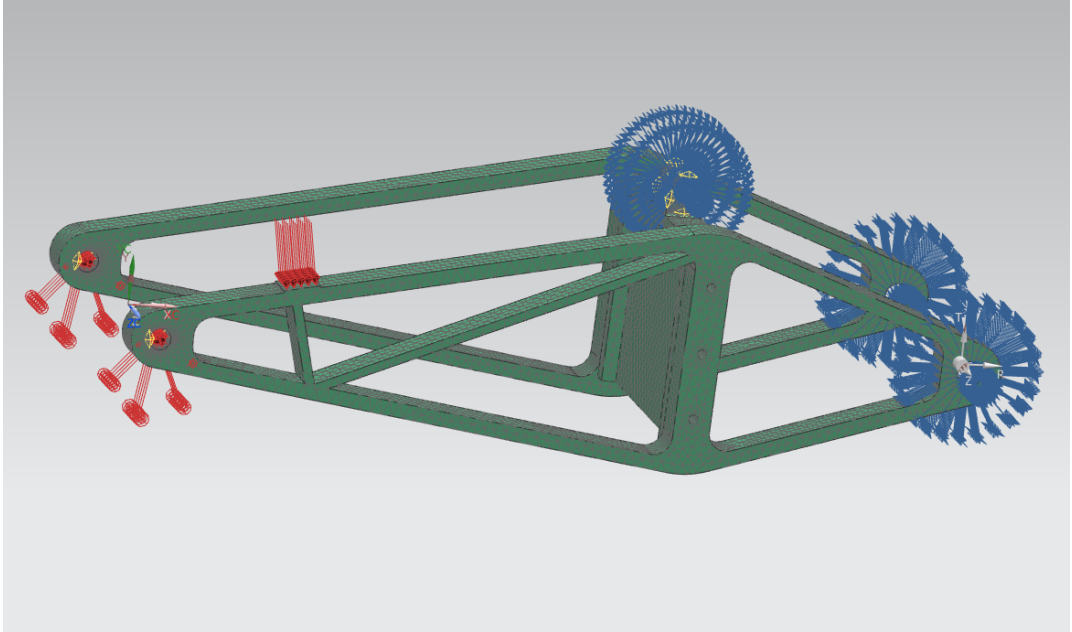


Figure 141: Constraints and loads

The result can be seen in Figure 142. This was a quick analysis on an aluminium alloy with lower tensile and yield strength than intended 7075-T6. Our intended material would give even smaller displacements.

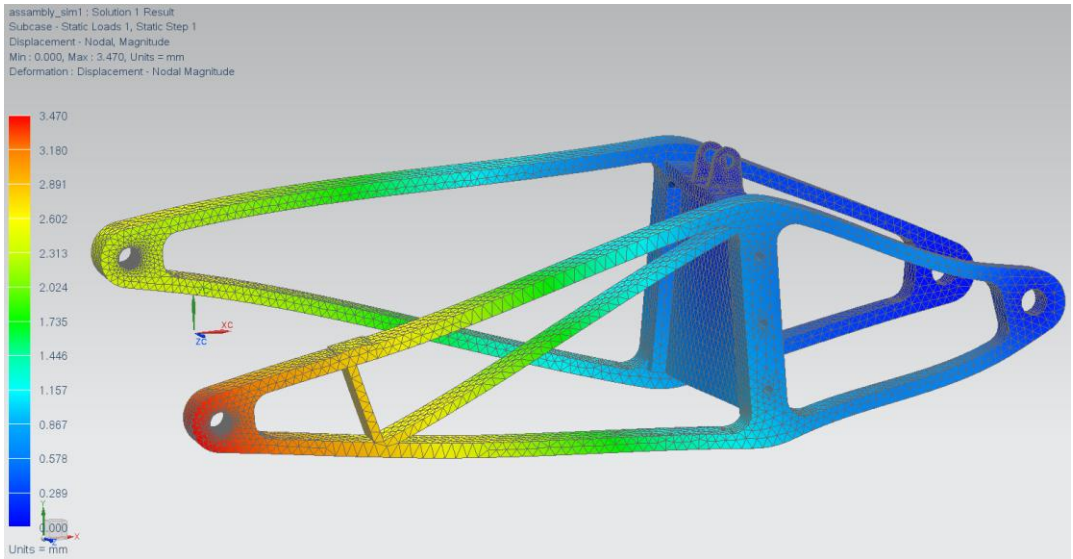


Figure 142: Displacement with inner struts

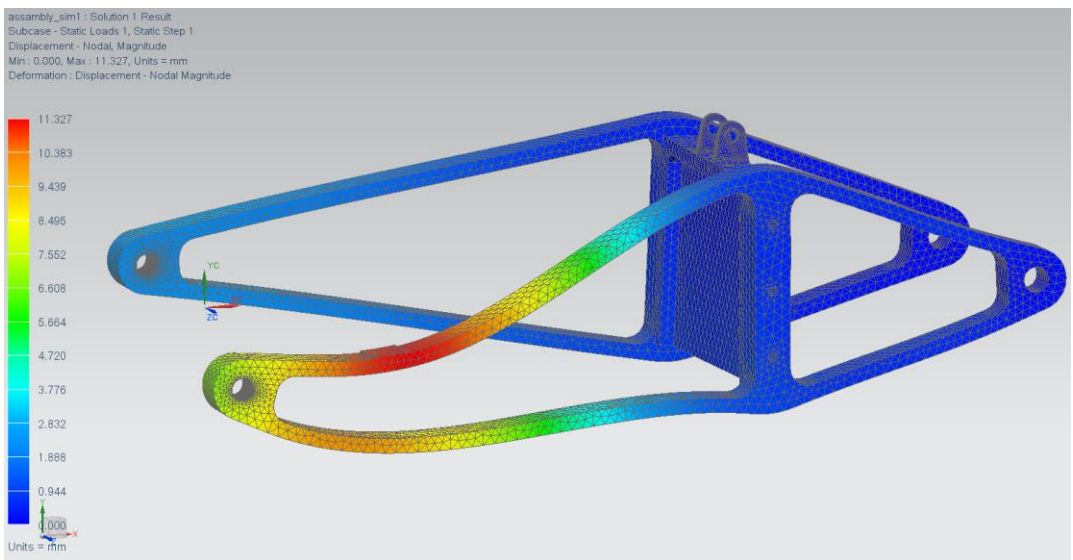


Figure 143: Displace without inner struts

The difference in displacement with and without the inner struts when braking force is applied can be seen in Figure 142 and Figure 143. The maximum displacement is 11.3 mm without them, and 3.5 mm with them. Other points on the suspension are have almost equal displacement, but the colours are different because of the scale.

7.3 Requirement specification

Product requirement – suspension system

		Must	Should
1	Production requirement		
1.1	Number of parts – front	< 30	< 20
1.2	Number of parts - rear	< 25	< 18
1.3	Cost	20 000 NOK	10 000 NOK
2	Functional requirements		
2.1	Ground clearance with driver inside	≥ 10 cm	
2.2	Endure braking force – single suspension	> 2000 N	> 3000 N
2.3	Endure vertical load – total system	> 3700 N	> 4500 N
2.4	Endure lateral load – single suspension	> 500 N	> 675 N
2.5	Allow turning radius	< 6 m	< 5 m
2.6	Fatigue life at normal use	> 100 h	> 500 h
2.7	Facilitate drivetrain – rear suspension	✓	
2.8	Scrub radius	< 20 mm	< 10 mm
2.9	Camber angle	< $\pm 1^\circ$	0°
2.10	Change in camber angle during vertical travel	< $\pm 2^\circ$	< $\pm 1^\circ$
2.11	Vibration reduction	✓	
2.12	Damping/travel during race	± 2 cm < X $\leq \pm 3$	± 1 cm < X $\leq \pm 2$
2.13	Toe-in	cm	cm
2.14	Adjustable camber	< $\pm 1^\circ$	0° ✓
3	Physical properties		
3.1	Mass of single front suspension	< 3.5 kg	< 2 kg
3.2	Mass of single rear suspension	< 4 kg	< 2.5 kg

7.4 Other subsystems

Several subsystems in the vehicle have we chosen not to focus on in this report as they consist of reused components, or the development process has not progressed far enough.

7.4.1 Steering

The steering system from the old car will be reused for the 2017 model. It is made from carbon fiber rods, so it has a low weight and it is strong. It has proved it works well.

7.4.2 Interior

The 2016 team put much effort in making a seat, and we will be reusing this. It is lightweight and needs small modifications to fit in our car. A new steering wheel will be designed, but this has not been addressed yet as it is not a major task.

7.4.3 Electrical system

We have chosen to leave out the details on the electrical system, as we feel it is outside the scope of our specialization paper. The architecture of the energy supply from battery to motor is ready. We will not elaborate on it, but a diagram of it can be found in appendix 9.7 along with a description. Many of the universal modules from earlier teams will be adapted and reused.



Figure 144: Seat made in 2016

8 References

- ÇENGEL, Y. A. & CIMBALA, J. M. 2010. *Fluid mechanics : fundamentals and applications*, Boston; Mexico City, McGraw-Hill.
- CORP, G. 2014. *ENERGY SAVINGS FROM SYNCHRONOUS BELTS* [Online]. Available: <http://designcenter.gates.com/wp-content/uploads/2015/05/Gates-Energy-Saving-from-Synchronous-Belt-Drives-White-Paper.pdf> [Accessed 15.12 2016].
- PETRY-JOHNSON, T. T., KAHRAMAN, A., ANDERSON, N. E. & CHASE, D. R. 2008. An Experimental Investigation of Spur Gear Efficiency. *Journal of Mechanical Design*, 130, 062601-062601.
- SHELL. 2016a. *About Shell Eco-marathon* [Online]. Available: <http://www.shell.com/energy-and-innovation/shell-ecomarathon/about.html> [Accessed December 08 2016].
- SHELL. 2016b. *Shell Eco-marathon 2017 Rules - Chapter 1* [Online]. Available: http://www.shell.com/promos/download-the-shell-eco-marathon-global-rules/_jcr_content.stream/1472744744388/7b204129356de26d47c9f21e2c8f58e07f3e2e4f266ae7714c8e6b17bb7051e1/sem-2017-rules-chapter-1.pdf [Accessed 15.09 2016].

9 Appendix

9.1 Track simulations

```
%      Energy simulation Eco Marathon
%      Fuel Fighter, NTNU
%      Author: Odin Oma
%      December, 2016

%  Variables

car_weight = 90;
Cd = 0.138;
Cd_6 = 0.153;
C_rolling = 0.004;

front_A = 0.882;

%Power of motors. Always running on 80% (highest efficiency)

Pm1 = 500*0.8; % Motor #1
Pm2 = 120*0.8; % Motor #2

inertia = 30; % damper on rate of power increase/decrease.

interpolation_factor = 1000;

%  Efficiency

eff_motor = 0.85;
eff_drivetrain = 0.90;
eff_motorcontroller = 0.95;
eff = eff_motor * eff_drivetrain * eff_motorcontroller;

%  Constants

air_density = 1.2754;
g = 9.81;
m = 70 + car_weight;

%  Import gps data if not already loaded

if exist('x','var') == 0
    filename = 'energy_sim_data.xlsx';
    sheet = 1;
    x = xlsread(filename,sheet,'C6:C48');
    y = xlsread(filename,sheet,'D6:D48');
    z = xlsread(filename,sheet,'I6:I48');
```

```

% Interpolation

i = 1:43;
ii = 1:1/interpolation_factor:43;
x = interp1(i,x,ii,'spline');
y = interp1(i,y,ii,'spline');
z = interp1(i,z,ii,'spline');
%v= interp1(i,v,ii,'spline');
x(1)=[];y(1)=[];z(1)=[];ii(1)=[]; %remove duplicates
end

% Movement vectors, distance and time

Vx = x - circshift(x,1);
Vy = y - circshift(y,1);
dd = sqrt(Vx.*Vx + Vy.*Vy);

d = cumsum(dd); % Total distance at each step

d_z = z - circshift(z,1); % height change
gradient = d_z ./ dd*100;

K =turningR(x,y); %Track curvature

f_rolling = m*g*C_rolling; %Constant

fg =
zeros(1,length(ii));fd=fg;fa=fd;a=fd;t=a;F=a;P=a;P_b=a;ft=a;v=a;Fms=a;Fm_rec=a;

v(1)=1; %Inital speed cannot be zero..

sw=0; %Motor off switch

Fms = zeros(1,inertia); %Motot power damper

iii=length(ii);

for i=2:iii-1

% Iterations through track

v(i)=sqrt(v(i-1)^2+ 2*a(i)*dd(i)); %New speed

% Force calc

fa(i) = m * a(i);
fg(i) = m*g*d_z(i)/dd(i);
fd(i) = 0.5 * air_density * v(i)^2 * Cd * front_A;
F(i) = f_rolling + fg(i) + fd(i);% + fa(i);

```

```

ft(i) = m*v(i)^2 /k(i); %Centripetal force

% Available force from motors at current speed
Fm1= Pm1*eff/v(i);

Fm2 = Pm2*eff/v(i);

% Motor controller
if v(i)>10 || sw || i >iii*0.8 || (k(i+4000)<15 && v(i)>6) %Coasting

    Fms=[0 Fms(1:inertia-1)];
    Fm = mean(Fms);
    Fmm(i)=Fm1;
    sw=1;

    Fmss(i+1)=10; % Record motor state. 10=off,20=small motor,30=big motor

    if v(i)<7.25 %Stop coasting
        sw = 0;
    end

else
    if F(i)>50 || i < iii*0.2 %Big motor
        Fms=[Fm1 Fms(1:inertia-1)];
        Fm = mean(Fms);
        Fmss(i+1)=30;
    else
        Fms=[Fm2 Fms(1:inertia-1)]; %Small motor
        Fm = mean(Fms);
        Fmss(i+1)=20;
    end

end

t(i) = dd(i)/v(i); %Duration in section

a(i+1)= (Fm-F(i))/m/1.02; % <- 1,02 = damper on acceleration to prevent
simulator from becoming unstable

P(i) = Fm * v(i);
Fm_rec(i)= Fm;

if P(i)<0 %Zero power if negative power. No re-generation
    P(i)=0;
end

P_b(i) = P(i)/eff;

```

```
end
```

```
%      Power and energy
```

```
lap_time = sum(t);  
lap_distance = sum(dd)/1000; %km  
avg_v2 = 1000*lap_distance/lap_time*3.6
```

```
e = P_b .* t;  
E = sum(e);  
bensin = 32010*1000; %j/l  
bf=E/bensin;
```

```
E_kwh = E/3600000;  
Economy = lap_distance/E_kwh % km/kwh  
Eco_b = lap_distance/bf
```

```
% Plotting
```

```
q=0;  
q=q+1;  
figure(q)  
clf
```

```
plot(d,P_b,d,Fm_rec,d,F)  
legend('P_b','Fmotor','Fresistance')  
grid on
```

```
q=q+1;  
figure(q)  
clf
```

```
plot(d,z,d,v,d,a,d,P_b/50,d,ft/100,d,F/10)  
legend('Elev.','v [m/s]','a [ms-2]','P/50 [w]','Ft/100 [N]','F/10 [N]')  
grid on
```

```
q=q+1;  
figure(q)  
clf
```

```
semilogy(d,K)
```

```
q=q+1;  
figure(q)  
clf  
hold off
```

```
plot(x,y)
axis equal
hold on
pp = find(k<20);
scatter(x(pp),y(pp))
pp2 = find(gradient>2);
scatter(x(pp2),y(pp2),'+')
pp2 = find(gradient>2);
scatter(x(pp2),y(pp2),'+')
```


9.2 The influence of the combined efficiency (see Table 3) and the Cr parameter. Cd=0,138 and mass=90kg

Efficiency	Cr															
	0	0,003	0,0035	0,004	0,0045	0,005	0,0055	0,006	0,0065	0,007	0,0075	0,008	0,0085	0,009	0,0095	0,01
0,85	259,9	250,6	240,8	224,7	216,4	208,2	201,8	193,4	187,7	185,7	178,5	171,9	164,9	159,2	153,2	148,2
0,825	251,2	242,2	231,7	216,5	208,9	200,8	194,7	187,8	180,3	172,5	166,1	160,2	154,0	148,9	143,6	
0,8	242,8	234,2	224,2	210,1	202,7	194,8	187,7	181,1	174,0	167,5	161,3	154,9	149,7	144,1	138,1	
0,775	234,6	226,3	216,7	202,7	195,6	188,0	181,0	175,7	168,8	162,5	155,8	150,4	144,7	139,4	135,0	
0,75	226,7	218,7	209,5	195,6	187,5	181,3	175,5	169,3	162,8	156,8	151,1	145,3	139,8	135,3	129,5	
0,725	217,9	210,3	202,3	188,6	180,8	174,8	169,2	163,2	157,7	151,2	145,8	140,2	134,1	129,5	125,0	
0,7	210,3	202,9	194,6	181,8	174,3	168,4	163,0	157,2	151,9	145,7	140,6	135,3	129,1	124,8	120,7	
0,675	202,0	195,0	187,7	174,6	167,7	161,6	156,4	150,4	144,8	139,2	133,9	128,7	124,1	120,2	116,2	
0,65	194,0	187,2	180,3	167,8	161,0	155,1	149,9	144,8	139,0	133,6	128,7	124,1	119,9	115,7	111,7	
0,625	186,1	179,7	173,0	161,0	154,3	149,0	143,7	139,2	133,7	128,6	123,6	119,3	115,1	111,1	107,4	
0,6	178,5	172,3	165,5	154,2	147,8	142,8	137,8	133,3	128,1	123,3	118,6	114,4	110,3	106,5	103,0	
0,575	170,5	164,6	158,1	147,6	141,4	136,7	132,0	127,6	122,4	117,8	113,6	109,4	105,6	102,0	98,6	
0,55	162,7	157,1	151,0	141,1	135,1	130,6	126,3	121,7	116,9	112,5	108,4	104,5	100,9	97,5	94,4	
0,525	155,1	149,7	144,0	134,3	128,6	124,4	120,3	115,9	111,4	107,1	103,2	99,5	96,1	93,0	90,0	
0,5	147,3	142,2	136,8	127,7	122,2	118,2	114,4	110,1	105,8	101,8	98,3	94,7	91,5	88,5	85,5	

[km/kWh]

9.4 Recruitment mail

FOR ENGLISH VERSION, SEE BELOW

Hei,

DNV GL Fuel Fighter skal ta opp nye medlemmer. Vi trenger engasjerte studenter til å bli med å utvikle og bygge en bil som skal delta i Shell Eco-marathon i London neste år. Shell Eco-marathon er en konkurranse hvor studenter konkurrerer om å bygge den mest energieffektive bilen. Konkurransen deles inn i forskjellige energiklasser, blant annet naturgass, hydrogen og batteridrevet. Fjorårets DNV GL Fuel Fighter kjørte på hydrogen.

Det er stor variasjon i arbeidet som må til for å lage en miljøvennlig bil, og vi har forskjellige og spennende utfordringer for alle fagfelt. Eksempler på fagområder er mekanikk, design, programmering, mekanisk arbeid, el-systemer, brenselceller/batterier, PR, økonomi og mer.

Det er ingen krav til forkunnskap og årstrinn. Alle studenter som ønsker å oppleve teori i praksis oppfordres til å søke.

Har du lyst til å jobbe med et spennende og praktisk prosjekt for å skape et bærekraftig og fremtidsrettet produkt? Da er DNV GL Fuel Fighter noe for deg! Du kan også få prosjektet godkjent som 7,5 stp

Send en kort søknad hvor du forteller litt om deg selv og hvorfor du vil bli med til fuelfighter.ntnu@gmail.com⁴. Søknadsfrist er 14.09 kl. 23.59.

Ta gjerne kontakt dersom du har spørsmål!

Vennlig hilsen

DNV GL Fuel Fighter team 2017



Sjekk gjerne ut vår facebookside: <https://www.facebook.com/DnvGLFuelFighter/> og vår nettside: <http://www.fuel-fighter.com/>

⁴ No longer in use

ENGLISH VERSION

Hi,

DNV GL Fuel Fighter are recruiting new team members. We want motivated students to join in the development and building of a car to participate in Shell Eco-marathon in London next summer.

Shell Eco-marathon is a competition where students compete in building the most energy-efficient car. The competition is split in multiple energy classes, i.e. natural gas, hydrogen and battery. Last year DNV GL Fuel Fighter ran on hydrogen.

There is great variation in the work needed to make an environmentally friendly car, and we have varied and exciting challenges within different fields. For example engineering, design, programming, mechanical work, electric systems, fuel cells / batteries, PR, economy and more.

No prior knowledge is required . All students who wish to combine theory with practical work are encouraged to apply.

Do you want to work on an exiting and practical project to create a sustainable and provident product? If so, DNV GL Fuel Fighter is the right thing for you! You can also get the project approved as 7.5 units of credit.

Send a short application where you tell a bit about yourself and why you want to join to fuelfighter.ntnu@gmail.com. The deadline is 14.09 at 23.59.

You are welcome to contact us if you have any questions.

Best regards,
DNV GL Fuel Fighter team 2017

We welcome you to check out our facebook page: <https://www.facebook.com/DnvGLFuelFighter/> and our website: <http://www.fuel-fighter.com/>

9.5 Off-track awards

FROM SEM RULES:

COMMUNICATIONS AWARD

Objective:

To run the most impactful and successful integrated Communications campaign showing the efforts to promote the team ahead of the Shell Eco-marathon competition in 2017. The winner will be the team that demonstrates best the continuous communicational and promotional activities of the team on the road to the Shell Eco-marathon (SEM) competition.

VEHICLE DESIGN AWARD

Objective:

This prize recognises innovative design research and execution and will be awarded to the team, which presents the most original and coherent vehicle in terms of aesthetics, ergonomics, technical feasibility, choice of materials and eco-friendliness. Each of these five criteria will be weighted equally in the Jury's decision. Due to their non-comparable designs there will be one award each for the Prototype and UrbanConcept categories.

TECHNICAL INNOVATION AWARD

Objective

This award is presented to the Team which demonstrates outstanding technical ingenuity along with optimal use of new materials, components and inventions in their drive train, chassis, body, instrumentation and tyres.

SAFETY AWARD

Objective

This award aims to highlight the importance of structural, process and behavioural safety in the Shell Eco-marathon programme and encourages all participating teams to actively consider and implement safe practices in their daily work. It challenges all team to review established practices, inspect tools and equipment as well review their procedures in order to implement changes which lead to higher safety standards.

PERSEVERANCE AND SPIRIT OF THE EVENT AWARD

This Award is presented to the team which, in the opinion of the Organisers, symbolises best the spirit and values of Shell Eco-marathon through their actions, which can involve but are not restricted to:

- Overcoming great obstacles in order to attend Shell Eco-marathon;
- Mastering exceptional challenges while participating in Shell Eco-marathon;
- Supporting other participants to help them overcoming significant challenges or obstacles;
- Keeping high spirits, showing outstanding resilience, resolve and resourcefulness; and
- Teams cannot apply for this award.

H-1000XP

Designed for Efficiency



Built to win.
Lightweight, efficient, easy to use.



CONCEPT CATEGORY

www.horizonfuelcells.com

H-1000XP

Competition-grade 1KW fuel cell

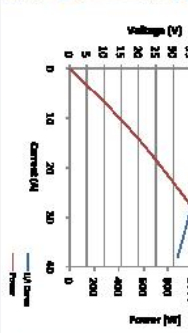


NEW!
SERIAL PORT MONITOR (OPTIONAL)
The newly designed serial ports monitor will provide real time data from the system to your computer in a newly designed user interface.

- Produces greatly reduced H2 fuel consumption
- Plug & play, easy to integrate!
- Lower weight, smaller size - new materials...
- Compliant with new Eco-nurture rules

Type of fuel cell	PEM
Number of cells	50
Rated power	1000W
Rated performance	30V@35.5A
Reactants	Hydrogen and Air
External temperature	5 - 35°C
Max stack temperature	65°C
Composition	99.99% dry H2
H2 pressure	7.2 - 9.4 PSI
Humidification	Self-Humidified
Cooling	Air
Weight	5.9kg
Dimensions	205mm x 304mm x 264mm
Flow rate at rated output	12 SL/min
Peak efficiency of stack	59%

www.horizonfuelcells.com



- H-1000 stack with blower
- hydrogen supply valve
- hydrogen purging valve
- fuel cell controller
- manual
- PU tube
- over current protection
- low voltage protection
- over temperature protection
- hydrogen sensor (25% LFL) safety emergency shut down switch
- self-audible function

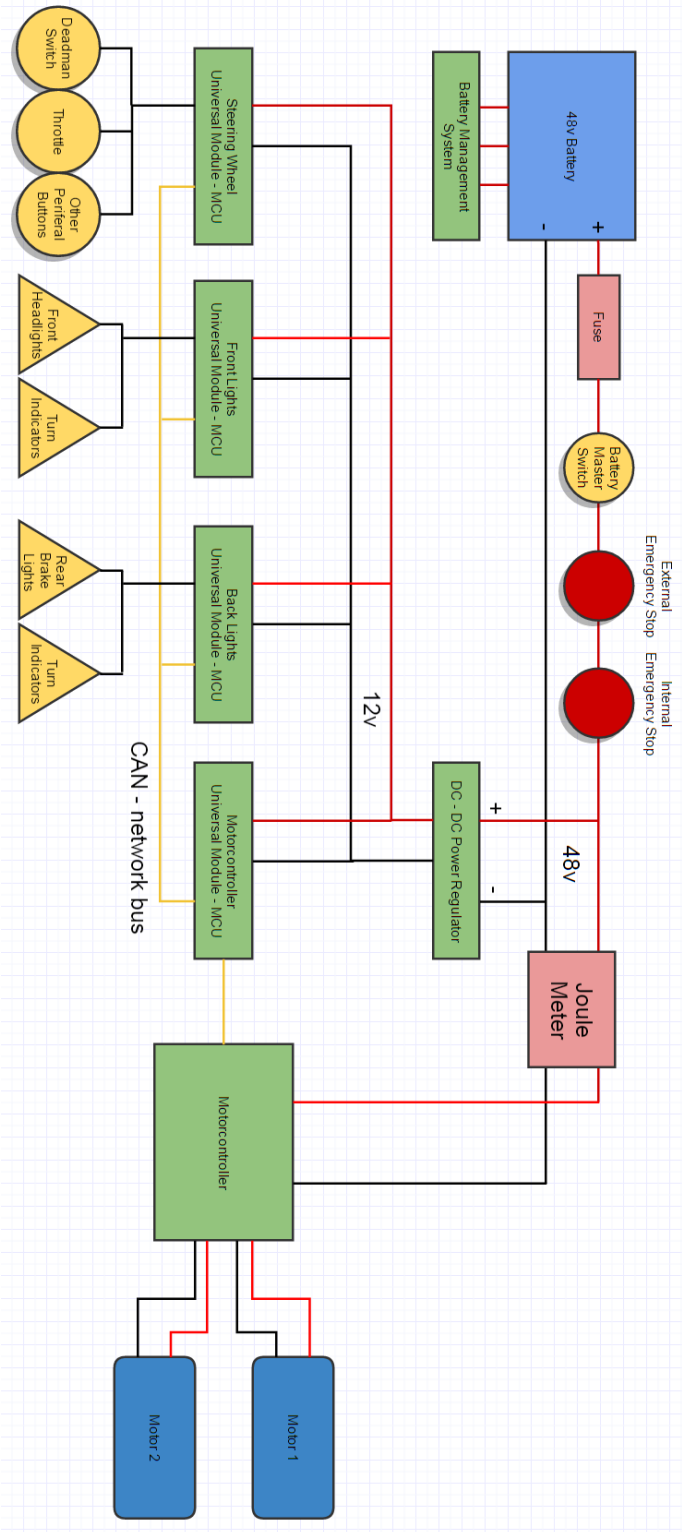
Safety

The new H-1000 XP also offers savings on parts such as DC-DC converters, hydrogen sensors, data acquisition systems and computers.

User friendly - standard to develop the fuel cell controller for the field of performance vehicles and performance applications!



9.7 Energy supply system



The Electrical Supply will be described from the positive connection of the battery to the negative connection. The components will appear in this sequence

Battery

The propulsion battery for our car will be a 48v Lithium-Ion based battery. We have not chosen the battery yet, but we are aware of the requirements stated in Article 57 about BMS, charging and maximum capacity. We will most likely acquire a commercial product.

Fuse

A fuse will be connected close to the positive connection of the battery. Since the specifics of our battery and motors has not been finalized we do not have a specification for this fuse yet.

Battery Master Switch

This is the master switch for the whole circuit, when this is off all components are powerless.

Emergency Stop

There are two Emergency Stop buttons. One for the driver and one external emergency switch mounted easily accessible on the outside. The emergency switches will be normal push and rotate switches. The one in the cockpit will be connected to a Normally Open relay mounted in series on the 48v line. All according to Article 37.

Junction

A junction to connect the DC-DC power regulator. The DC-DC regulator will provide a 12v 1A DC current for the telemetry equipment as well as 21v for our own peripheral equipment.

Joule meter

Supplied by SEM. Connected in series on the 48v line.

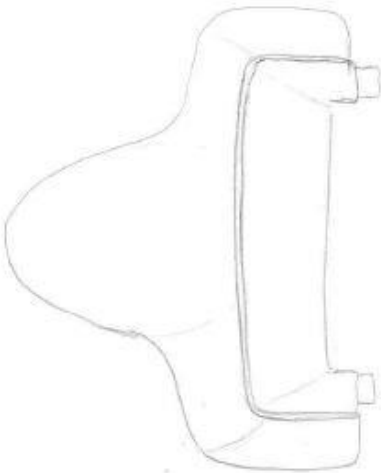
Motor controller

We will create a motor controller especially for SEM. At this date we are looking at using Brushed DC motors. And will thus need a DC motor controller.

Motors

We will use two brushed DC motors. One on each rear wheel. No motor has been specified at this time.

9.8 Sketches



Hand-drawn sketch of a mechanical component, possibly a handle or a bracket, shown in a perspective view. It features a curved top surface and a rectangular base with two small protrusions on the right side.

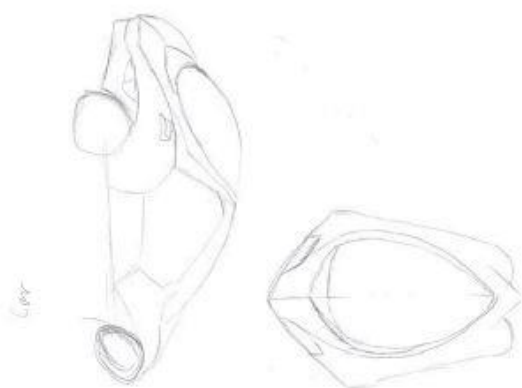
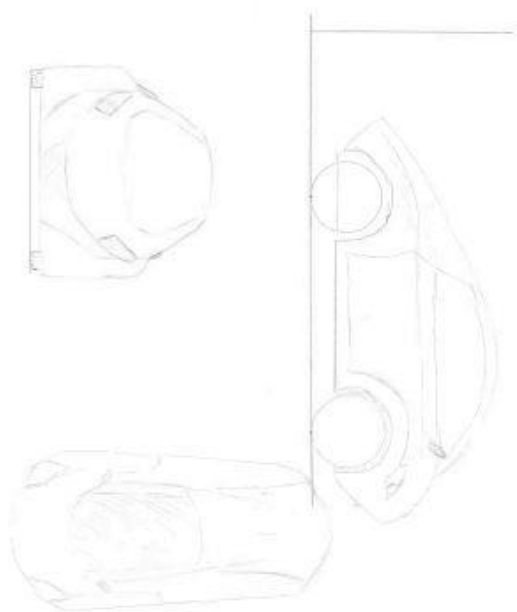


Hand-drawn sketch of a mechanical component, possibly a handle or a bracket, shown in a perspective view. It features a curved top surface and a rectangular base with two small protrusions on the right side.



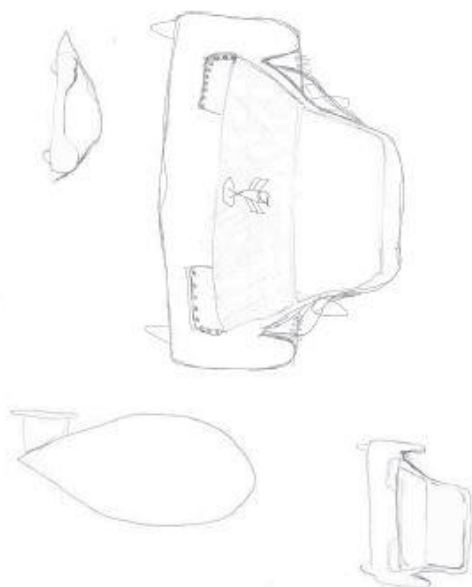
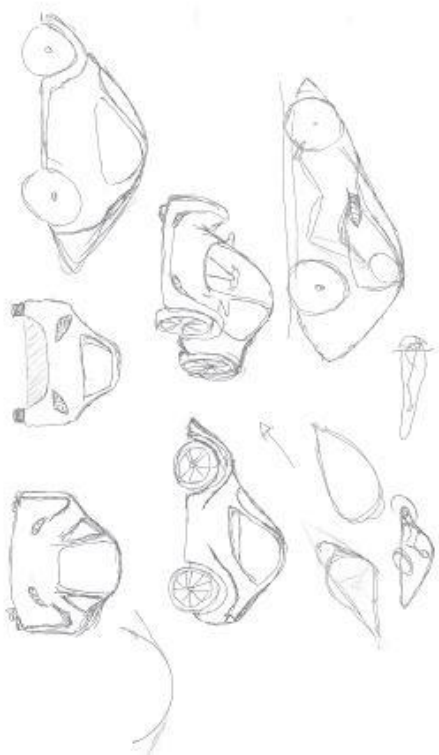
Hand-drawn sketch of a mechanical component, possibly a handle or a bracket, shown in a perspective view. It features a curved top surface and a rectangular base with two small protrusions on the right side.

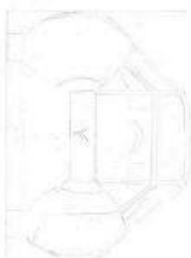
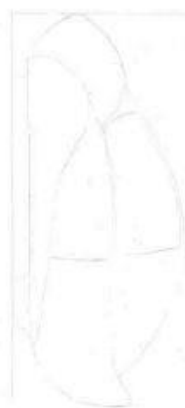
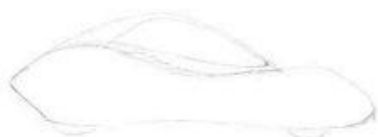
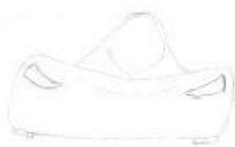
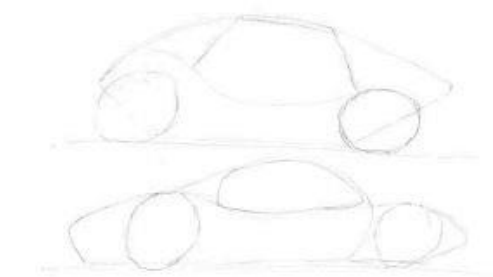




Car

CLASS'S





K3

